

Role of the antagonistic histone methylation marks H3K4me3 and H3K27me3 in the cold stress response of *Arabidopsis thaliana*

A dissertation

Submitted in Partial Fulfillment of the requirements for the Degree of
Doctor rerum naturalium (Dr. rer. nat.)

to the Department of Biology, Chemistry, Pharmacy
of Freie Universität Berlin

by

Léa Andrée Charlotte Faivre

From Besançon, France

Berlin, 2022

The investigations described in the following thesis were performed under the supervision of Prof. Dr. Daniel Schubert in the group of Plant Epigenetics at the Institute of Biology of the Freie Universität Berlin (01.2017 – 01.2022).

1st reviewer: Prof. Dr. Daniel Schubert

2nd reviewer: Prof. Dr. Reinhard Kunze

Date of defense: 27.04.2022

Herewith I certify that I have prepared and written my thesis independently and that I have not used any sources and aids other than those indicated by me.

Berlin,

31st of January, 2022

Léa Faivre

TABLE OF CONTENTS

List of Figures	IV
List of Tables	V
List of Abbreviations	VI
Summary	IX
Zusammenfassung	X
1 Introduction	1
1.1 Mechanisms of the cold response	1
1.1.1 Cold-induced damages and the necessity of cold acclimation	1
1.1.2 Cold sensing and signalling	3
1.1.2.1 Perception of low temperatures	3
1.1.2.2 Cold signal transduction by secondary messengers	5
1.1.2.3 Establishment of defences by the cold-regulated genes	7
1.1.2.4 The ICE-CBF regulon.....	8
1.1.2.5 CBF-independent pathways	9
1.1.3 Deacclimation and memory: the importance of controlling the stress response	10
1.1.3.1 Cold deacclimation.....	10
1.1.3.2 Priming and cold stress memory	11
1.1.3.3 Stress memory is associated with transcriptional trainability	12
1.1.4 The central role of transcriptional regulation in the stress response	13
1.2 Chromatin structure and its impact on transcription.....	14
1.2.1 The basic structure of chromatin	14
1.2.1 Histone post-translational modifications	15
1.2.1.1 The high diversity of histone post-translational modifications	15
1.2.1.2 Histone writers and erasers antagonistically regulate transcription	17
1.2.2 Histone variants: another layer in the chromatin diversity	18
1.2.3 Chromatin states and bivalency.....	19
1.2.4 Regulation of transcription by the chromatin environment.....	21
1.3 The role of chromatin regulation in the response to abiotic stress.....	22
1.3.1 Chromatin-mediated regulation of the cold stress response	23
1.3.2 Cold stress memory might be encoded at the chromatin level	25
1.3.2.1 Chromatin modification plays a key role in abiotic stress memory.....	25
1.3.2.2 Cold memory: the example of vernalization	27
1.4 Aims of this study	28

2	Material and Methods	30
2.1	Plant material	30
2.2	Electrolyte leakage	30
2.3	Transcriptomics	31
2.3.1	RNA extraction and RT-qPCR	31
2.3.2	RNA-seq	32
2.4	Western Blot	32
2.5	Epigenomics	34
2.5.1	Chromatin immunoprecipitation	34
2.5.2	ChIP-seq	35
2.5.3	Re-ChIP	36
2.6	Bioinformatic analyses	36
2.6.1	RNA-seq analysis	37
2.6.2	ChIP-seq analysis	37
2.6.3	Gene ontology analysis	39
2.6.4	Chromatin state analysis	39
2.6.4.1	Chromatin state analysis at the gene level	39
2.6.4.2	Chromatin state analysis at the binding site level (DEK2 and hDEK)	40
2.6.5	Chromatin accessibility	40
2.6.6	ChromDB	40
2.6.7	Multiple sequence alignment	41
2.6.8	Statistics and data visualization	41
3	Results	42
3.1	Bivalency poises stress inducible genes for transcriptional changes	42
3.1.1	Cold-regulated genes are enriched in bivalent targets	42
3.1.2	Bivalency is a common feature of stress-regulated genes	45
3.1.3	H3K4me3 and H3K27me3 co-occur on S2 genes	47
3.1.4	Towards the identification of bivalent domains <i>in planta</i>	49
3.1.5	Bivalency prepares genes for changes in expression upon stress exposure	51
3.1.6	Identification of potential bivalency readers	54
3.2	Cold exposure triggers changes in histone methylation	59
3.2.1	Cold-triggered changes in methylation	59
3.2.1.1	Global changes of methylation upon cold exposure	59
3.2.1.2	H3K4me3 and H3K27me3 differential methylations target separate sets of genes	65

3.2.1.3	Bivalency is not resolved to monovalency upon cold exposure	71
3.2.1.4	Bivalent genes are not more likely to undergo differential methylation	73
3.2.1.5	Differential methylation partially correlates with changes in expression	74
3.2.1.6	Differential methylation is not caused by a change in nucleosome density ..	81
3.2.2	Identifying the actors involved in cold-triggered histone methylation dynamics	83
3.2.2.1	Cold affects the transcription and splicing of many chromatin regulators	83
3.2.2.2	Role of H3K4me3 methyltransferases and H3K27me3 demethylases in the cold response	85
3.3	Persisting H3K27me3 losses might be responsible for cold stress memory.....	88
3.3.1	Plants can remember cold stress	88
3.3.2	ELF6 is necessary for cold stress memory	90
3.3.3	Cold-induced differential methylation persistence and transcriptional memory	92
4	Discussion	95
4.1	Bivalency poises cold-inducible genes	95
4.1.1	Bivalency is involved in plant stress response.....	95
4.1.2	The H3K4me3 profile of bivalent genes suggests its mitotic stability	97
4.1.3	Bivalency might poise genes through enhanced accessibility	98
4.1.4	EBS, SHL and DEK2 are putative bivalency readers	100
4.1.5	Bivalency or bistability?	102
4.2	Cold-induced dynamics of histone methylation.....	104
4.2.1	Cold triggers changes in H3K4me3 and H3K27me3	104
4.2.2	Differential methylation partially correlates with differential expression.....	107
4.2.3	Differential methylation affects stress responsive and developmental genes.	108
4.2.4	Mechanisms of the differential methylation.....	109
4.3	Cold stress memory is encoded at the chromatin level	111
4.3.1	Persisting chromatin changes correlate with transcriptional memory.....	111
4.3.2	H3K27me3 loss as a support of cold stress memory	114
4.4	H3K4me3 and H3K27me3 play distinct roles in the control of <i>COR</i> genes transcription	116
4.5	On the importance of considering the whole chromatin status	118
4.6	Conclusion and perspectives	119
5	References.....	123
6	Appendix.....	146
	Acknowledgements.....	160
	List of publications	160

LIST OF FIGURES

Figure 1: Schematic representation of cold signalling in <i>Arabidopsis thaliana</i>	4
Figure 2: Cold stress memory at the physiological and transcriptional level.....	12
Figure 3: The expression of cold-inducible genes is tightly regulated at every step	14
Figure 4: Major histone marks and chromatin modifiers	15
Figure 5: Bivalency is a common characteristic of stress inducible genes.....	44
Figure 6: GO term enrichment analysis of S2 genes	46
Figure 7: Many S2 genes appear to be bivalent in vivo	48
Figure 8: GO biological process term enrichment analysis of bivalent genes	49
Figure 9: Validation of the in silico bivalency using Re-ChIP	50
Figure 10: Characterization of bivalent gene.....	52
Figure 11: Role of the putative bivalency readers SHL and EBS in the cold response.....	55
Figure 12: Role of the putative bivalency reader DEK2 in the cold response	57
Figure 13: Impact of cold treatment on the global levels of H3K4me3 and H3K27me3.....	60
Figure 14: Global changes of H3K27me3 and H3K4me3 upon cold exposure.....	62
Figure 15: Characterization of differentially methylated regions	63
Figure 16: Characterization of differentially methylated genes	66
Figure 17: GO biological process term enrichment analysis of genes showing differential H3K4me3 methylation	69
Figure 18: GO biological process term enrichment analysis of genes showing differential H3K27me3 methylation	70
Figure 19: Cold-triggered changes in bivalency	72
Figure 20: Fate of bivalent genes during cold exposure	74
Figure 21: Changes of methylation levels on differentially expressed genes	75
Figure 22: Correlation between the changes in methylation and the changes in expression	77
Figure 23: Identification of differentially methylated and differentially expressed genes.....	79
Figure 24: Genome browser views at differentially methylated genes	80
Figure 25: Changes of H3 levels upon cold exposure.....	82
Figure 26: Cold regulation of the expression and splicing of chromatin actors	84
Figure 27: Freezing tolerance of histone modifier mutants	86
Figure 28: H3K4me3 and H3K37me3 levels in histone modifier mutants on two cold-induced genes	87
Figure 29: Different priming schemes can lead to cold memory	89
Figure 30: ELF6 is required for cold memory	91
Figure 31: Some cold-triggered methylation changes persist after return to ambient temperature	93
Figure 32: Influence of the chromatin methylation status on the transcriptional activity of COR genes.....	121
Suppl. Figure 1: Impact of the promoter size on the chromatin state analysis	147
Suppl. Figure 2: Characterization of H3K4me3 and H3K27me3 domains	147
Suppl. Figure 3: Role of the putative bivalency readers DEK2 and DEK3 in the cold response	148
Suppl. Figure 4: H3K4me4 and H3K27me3 levels on selected cold inducible genes	149

Suppl. Figure 5: GO biological process term enrichment analysis of genes showing both a gain and a loss of H3K27me3 upon cold exposure	150
Suppl. Figure 6: GO biological process term enrichment analysis of genes showing differential expression during cold exposure	151
Suppl. Figure 7: GO biological process term enrichment analysis of genes gaining or losing bivalency upon cold exposure	152
Suppl. Figure 8: Genome browser views at genes used as controls in the ChIP-qPCR.....	153
Suppl. Figure 9: Validation of the differential methylation analysis	154
Suppl. Figure 10: Complete results of the priming screening assays	155
Suppl. Figure 11: Cold-triggered changes in the expression of histone variants	156

LIST OF TABLES

Table 1: Transgenic lines used in this study	30
Table 2: qPCR reaction mix for one sample.....	31
Table 3: qPCR program	31
Table 4: Read counts of the RNA-seq samples.	32
Table 5: Composition of the buffers used in the extraction of chromatin enriched proteins ...	33
Table 6: Composition of the buffers used in the SDS-PAGE and Western Blot.....	33
Table 7: Composition of the SDS gels	33
Table 8: Antibodies used for Western Blot and chromatin immunoprecipitation	34
Table 9: Reads count of the ChIP-seq samples.....	35
Suppl. Table 1: Genotyping primers.....	157
Suppl. Table 2: RT-qPCR primers.....	157
Suppl. Table 3: ChIP and ReChIP-qPCR primers.....	158
Suppl. Table 4: Softwares	158
Suppl. Table 5: R packages	159
Suppl. Table 6: Sources of reference data.....	159

LIST OF ABBREVIATIONS

ABA: Abscisic Acid
ABF: ABRE Binding Factors
ABRE: ABA Responsive Element
ac: acetylation
AFP: Antifreeze Protein
ATAC-seq: Assay for Transposase-Accessible Chromatin sequencing
BAH: Bromo-Adjacent Homology domain
bp: base pair
BR: brassinosteroid
CaM: Calmodulin
CAMTA: Calmodulin-Binding Transcription Activator
CBF: C-repeat Binding Factor
CBL: Calcineurin B-Like calcium sensor
cDNA: complementary Deoxyribonucleic Acid
CDPK: Calcium-Dependant Protein Kinase
ChIP: Chromatin immunoprecipitation
ChIP-seq: ChIP DNA sequencing
CIPK: CBL-Interacting Protein Kinase
CLK: CDC-like kinases
CRLK: Calcium/Calmodulin-regulated Receptor-Like Kinase
CRT: C-Repeat
Col-0: Columbia 0
COR: Cold-Regulated
CSP: Cold Shock Protein
Ct: Threshold Cycle
DAS: Differentially Spliced
DE: Differentially Expressed
DM: Differentially Methylated
DNA: Deoxyribonucleic Acid
DRE: Drought Responsive Element
DREB: Drought Responsive Element Binding factor
E(z): Enhancer of zest
ERD: Early Dehydration inducible
ERF: Ethylen Responsive Factor
FAIRE-seq: Formaldehyde-Assisted Isolation of Regulatory Elements sequencing

Flg: Flagellin
FPKM: Fragment Per Kilobase per Million mapped reads
GA: Gibberellic Acid
GO: Gene Ontology
GOI: Gene Of Interest
HAT: Histone Acetyltransferase
HDAC: Histone Deacetylase
hDEK: human DEK
HK: Housekeeping Gene
HOS: High expression of Osmotically responsive genes
HSP: Heat Shock Protein
ICE: Inducer of CBF Expression
IDR: Irreproducible Discovery Rate
IgG: Immunoglobulin G
IP: immunoprecipitation
JA: Jasmonic Acid
JMJ: Jumonji
K: lysine
kb: kilobase
KIN: cold inducible
log₂FC: log₂ Fold Change
LSD: Lysine Specific Demethylase
LT₅₀: Temperature of 50% electrolyte leakage
LTI: Low Temperature Induced
MAPK(K)(K): Mitogen-Activated Protein Kinase (Kinase) (Kinase)
me: methylation
mRNA: messenger Ribonucleic Acid
N: Naïve (plants)
P: Primed (plants)
PcG: Polycomb Group
PCR: Polymerase Chain Reaction
Pd: Primed for three days
Ph: Primed for three hours
PHD: Plant Homeo Domain
pho: phosphorylation
PIF: Phytochrome Interacting Factor
PL: Primed and Lagged (plants)

PLT: Primed and Triggered (plants)
PRC1/2: Polycomb Repressive Complex 1/2
PSII: Photosystem II
PTM: Post-Translational Modification
qm: *elf6-ref6-jmj30-jmj32* quadruple mutant
qPCR: quantitative Polymerase Chain Reaction
RD: Responsive to Desiccation
Re-ChIP: sequential ChIP
RNA: Ribonucleic Acid
RNA-seq: RNA sequencing
ROS: Reactive Oxygen Species
RPKM: Reads Per Kilobase per Million mapped reads
RT: Reverse Transcription
S2: State 2
SA: Salicylic Acid
SDS(-PAGE): Sodium Dodecyl Sulphate (-Polyacrylamide Gel Electrophoresis)
sem: standard error of the mean
SR: Serine/Threonine Rich
T: Triggered (plants)
TES: Transcription End Site
TrxG: Trithorax
TSS: Transcription Start Site
Ub: ubiquitination
UTR: Untranslated Region
WB: Western Blot
Wt: wild-type
YFP: Yellow Fluorescent Protein
ZAT: salt tolerant zinc-finger

SUMMARY

As sessile organisms, plants need to adapt to their changing environment, including temperature fluctuations. As low temperatures can have major noxious consequences on their development and survival, plants need to establish the proper defences in order to endure the stress. This requires a massive and very fast transcriptome reprogramming involving, among others, the induction of hundreds of cold-responsive (*COR*) genes. Following the immediate response to chilling stress, plants are also able to memorize cold spells, leading to an improved survival during a second stress episode. This process is associated with a revised transcriptomic response also called transcriptional memory. Overall, both the response to cold and the memory of this stress rely on the tight transcriptional regulation of the *COR* genes. While numerous transcription factors necessary for their induction were already identified, the role of chromatin modifications in this process remains largely undiscovered. As the combination of chromatin modifications (the “chromatin state”) is a key determinant of gene expression, this study aimed at uncovering the potential role of histone modifications in the transcriptional regulation of *COR* genes before, during and after a cold episode. First, a comprehensive *in silico* analysis of the chromatin state of *COR* genes prior to any cold occurrence revealed that a majority of those genes carry both the activating mark H3K4me3 and the silencing mark H3K27me3, forming a specific chromatin state called bivalency. The *in vivo* characterization of bivalent genes revealed that this chromatin state decorates not only cold-inducible genes but numerous reversibly silenced stress-responsive genes and might poise them for expression by maintaining them in an open chromatin conformation. Furthermore, the putative bivalency reader DEK2 was shown to prevent the over-induction of bivalent *COR* genes during a cold episode, suggesting that bivalency can also participate in transcriptional regulation *in trans* through the action of specific readers. In a second stage, the dynamics of H3K4me3 and H3K27me3 during a cold stress were analysed using genome-wide approaches, revealing that both marks underwent intensive redistribution already after three hours of low temperature. Those changes partially correlated with expression changes: in particular, the induction of *COR* genes was associated with a loss of the repressive mark H3K27me3 or a gain of the activating mark H3K4me3. However, each mark displayed different targets and dynamics, suggesting that they hold distinct roles in the cold response: H3K4me3 associated with immediate stress responses while H3K27me3 rather correlated with longer-term adaptation. Upon return to ambient temperature, the cold-induced variations reverted at a different pace depending on the gene and some changes were maintained for up to seven days. Both the maintenance of H3K4me3 and H3K27me3 changes were linked to transcriptional memory: higher levels of H3K4me3 were associated with sustained induction while lower levels of H3K27me3 were correlated with a faster re-induction during a second stress exposure. Finally, the H3K27me3 demethylase ELF6 was shown to be essential for cold stress memory. This led to the hypothesis that cold stress memory might rely on the maintained loss of H3K27me3 on specific *COR* genes, allowing a faster re-establishment of defences during a second stress episode. In conclusion, this study demonstrates that the antagonistic marks H3K4me3 and H3K27me3 jointly participate to the transcriptional regulation of *COR* genes and reveals a new role of bivalency in the plant cold stress response and memory.

ZUSAMMENFASSUNG

Da Pflanzen an ihren Standort gebunden sind, müssen sie sich ständig an veränderte Umweltbedingungen anpassen. Kälte kann schädliche Folgen für die Pflanzenentwicklung und sogar zum Absterben von Pflanzen führen. Daher müssen Pflanzen auf diesen Stress reagieren, indem sie eine geeignete Abwehr zum Überleben aufbauen. Dies erfordert eine erhebliche Umprogrammierung des Transkriptoms, welche die Induktion von zahlreichen kälteempfindlichen (*COR*) Genen enthält. Nach einer direkten Stressantwort sind Pflanzen in der Lage ein Kältegedächtnis aufzubauen, wodurch sie eine zweite Kälteepisode besser überstehen. Dieser Prozess ist mit massiven Änderungen auf Genexpressionsebene verbunden, die auch „transkriptionelles Gedächtnis“ genannt wird. Sowohl die unmittelbare Reaktion auf, als auch das Bilden eines längerfristigen Gedächtnisses an Kälte, sind auf eine präzise Transkriptionsregulation von *COR* Genen angewiesen. Obwohl der Chromatinzustand ein bestimmender Faktor für Genexpression ist, ist die Rolle von Chromatinmodifikationen in der Induktion von *COR* Genen noch weitgehend unbekannt. Deshalb war es das Ziel dieser Arbeit, die Rolle von Histonmodifikationen in der Transkriptionsregulation von *COR* Genen vor, während, und nach Kältestress zu analysieren. Zunächst offenbarte eine umfassende *in silico* Analyse des Chromatinzustands von *COR* Genen vor einem Kälteereignis, dass die Mehrheit dieser Gene sowohl die aktivierende Modifikation H3K4me3 als auch die repressive Modifikation H3K27me3 tragen. Dieser Chromatinzustand wird auch als bivalent bezeichnet. Die *in vivo* Charakterisierung bivalenter Gene zeigte, dass besonders stillgelegte, induzierbare Gene durch einen bivalenten Chromatinzustand markiert sind. Diese könnten dadurch für eine eventuelle Expression vorbereitet sein, indem diese Genbereiche in einer offenen Chromatin-Konformation verbleiben. Der vermeintliche Bivalenz-Leser DEK2 verhinderte die Überinduktion von bivalenten Genen während einer Kälteepisode. Dies weist darauf hin, dass Bivalenz auch an der Transkriptionsregulation *in trans* durch die Aktion von bestimmten Reader-Proteinen Anteil nehmen kann. Die Analyse der H3K4me3 und H3K27me3 Dynamik mittels genomweiter Methoden zeigte, dass bei niedrigen Temperaturen eine intensive Neuverteilung beider Modifikationen stattfindet, die teilweise mit Expressionsvariationen korrelierte. Insbesondere war die Induktion von *COR* Genen mit einem Verlust der repressiven Modifikation H3K27me3 oder einer Zunahme der aktivierenden Modifikation H3K4me3 assoziiert. Die Modifikationen haben jedoch distinkte Rollen in der Kälteantwort. H3K4me3 war mit der unmittelbaren Stressantwort assoziiert, während H3K27me3 eher mit Langzeitadaptation korreliert war. Nach der Rückkehr zu ambienter Umgebungstemperatur kehrte das Chromatin zu seinem Ausgangszustand in unterschiedlichem Tempo abhängig vom Gen zurück, wobei manche Veränderungen bis zu sieben Tage beibehalten wurden. Die Aufrechterhaltung von sowohl H3K4me3 als auch H3K27me3 Variationen waren mit transkriptionellem Gedächtnis assoziiert: höhere H3K4me3 Mengen korrelierten mit beständiger Induktion und niedrigere H3K27me3 Mengen waren mit einer schnelleren Re-Induktion während einer zweiten Kälteepisode assoziiert. Schließlich wurde gezeigt, dass die H3K27me3 Demethylase ELF6 unabdingbar für das Kältestressgedächtnis ist. Der fortbestehende Verlust von H3K27me3 auf spezifischen Genen könnte daher die molekulare Basis für das Kältestressgedächtnis sein, indem ein schnellerer Wiederaufbau der Abwehr während einer zweiten Stressepisode ermöglicht wird. Insgesamt zeigt diese Studie, dass die antagonistischen Modifikationen H3K4me3 und H3K27me3 gemeinsam an der Transkriptionsregulation von *COR* Genen teilhaben, und offenbart eine neue Rolle der Bivalenz bei der Kältestressreaktion von Pflanzen.

1 INTRODUCTION

During the entirety of its life cycle, a plant must constantly adjust to its changing environment and tightly balance its resources between growth and stress response to achieve successful reproduction. Temperature is a major contributor to these fluctuations in environmental cues, as it undergoes not only diurnal but also seasonal changes, and it can have noxious consequences on the development and survival of plants. Getting a deep understanding of how the plants respond to temperature is crucial especially in the context of climate change, as it will not only lead to increased average temperatures but also to a higher frequency of extreme weather events, including cold spells (Petoukhov & Semenov, 2010; Seneviratne et al., 2012). In the coming decades, temperature variations will therefore increase in magnitude and frequency, which could have dramatic consequences on crop yields. According to this rationale, this study aims at dissecting the role of chromatin regulation in cold stress tolerance and memory.

1.1 MECHANISMS OF THE COLD RESPONSE

1.1.1 Cold-induced damages and the necessity of cold acclimation

Plants growing in temperate regions have to face episodes of colder weather, which can be categorized into chilling stress, when the temperature is under the optimal range for plant growth (varying depending on the plant species and ecotype) but remains above 0°C, and freezing stress, when the temperature drops below 0°C. For the model plant *Arabidopsis thaliana*, chilling stress is considered to start at temperatures lower than 14°C (Zarka et al., 2003). Both chilling and freezing temperatures can be harmful to the plants. Cold lowers the fluidity of lipid membranes, which in turn slows down cytoplasmic streaming, increases the ion permeability of the membrane, inhibits electron transport and decreases the activity of membrane enzymes (Kawamura & Uemura, 2013; Lyons, 1973; Nishida & Murata, 1996). Chilling temperatures also affect the activity of soluble enzymes and lead to the formation of RNA secondary structures (McWilliam, 1983; Ruelland et al., 2009). If not counteracted by the plants, all of these events might lead to metabolic imbalance, an accumulation of toxic metabolites and reactive oxygen species (ROS) as well as photoinhibition, which altogether may trigger irreversible cellular and tissue damage such as chlorosis or even plant death (Allen & Ort, 2001; Levitt, 1980a). In addition to the damages described above, temperatures below 0°C cause further injuries to the plants, not only by exacerbating cold-triggered enzyme inactivation but also due to water freezing (Kawamura & Uemura, 2013; Ruelland et al., 2009; Zrobek-Sokolnik, 2012). As intracellular freezing always leads to cell death, plants devised ways to ensure that freezing mostly occurs in extracellular spaces (Levitt, 1980b, 1980c). However, extracellular freezing also has noxious consequences as it causes mechanical stress on the protoplast due to the pressure exerted by the ice on the plasma membrane, as well as dehydration (Kawamura & Uemura, 2013). Dehydration leads to increased cytoplasmic concentrations of solutes such as salts, which in turn decrease enzymatic activity and cause protein denaturation (Zrobek-Sokolnik, 2012). Moreover, plants can suffer from additional injuries after the freezing episode has passed, when the ice crystals thaw. This leads to a quick rehydration of the cells, whose plasma membranes might then rupture (Zrobek-Sokolnik,

2012). Overall, lower temperatures can potentially cause a multitude of damages to plants, highlighting their need to detect and respond to temperature variations in order to survive.

As cold could be harmful for living organisms in multiple ways as described above, plants evolved mechanisms allowing them to avoid potential damages. Indeed, in *Arabidopsis thaliana*, the rigidification of membranes is counteracted by changes in their compositions, such as an accumulation of phospholipids and loss of cerebrosides in the plasma membrane (Uemura et al., 1995). The membranes are further protected through the action of dehydrins, a group of hydrophilic proteins characterized by the presence of a K-segment and potentially other conserved sequences such as Y- and S-segments (Ruelland et al., 2009). The genome of *Arabidopsis thaliana* encodes several dehydrins such as *LOW TEMPERATURE INDUCED (LTI) 29*, *LTI30*, *COLD-REGULATED (COR) 47* and *RAB GTPASE HOMOLOG B18 (RAB18)*, which were shown to improve freezing tolerance through the stabilization of membranes (Eriksson et al., 2011; Puhakainen et al., 2004). The accumulation of ROS triggered by cold is counterbalanced by the activation of scavenging systems (catalases, superoxide dismutases) as well as the production of antioxidant compounds (ascorbate, glutathione, tocopherol) (Ruelland et al., 2009). To adapt to reduced energy demands and photoinhibition, non-photochemical quenching as well as photosystem II (PSII) reaction centre quenching are increased in cold-exposed plants (Ruelland et al., 2009; Sane et al., 2003). Additionally, chilling induces the accumulation of cold shock proteins such as AtCSP1 and AtCSP3, which act as RNA chaperones and prevent the formation of undesirable RNA secondary structures (Juntawong et al., 2013; M.-H. Kim et al., 2009). Plants are also able to cope with sub-zero temperatures by preventing ice formation and adapting to freezing-induced damages such as dehydration (Ruelland et al., 2009). Ice formation itself can be avoided by the production of antifreeze proteins (AFPs), which lower the temperature at which leaves would freeze (Griffith et al., 2005). In *Arabidopsis thaliana*, KIN1 and KIN2 were identified as potential AFPs due to their homology with the AFPs of arctic flounder (Kurkela & Borg-Franck, 1992; Kurkela & Franck, 1990). Besides AFPs, ice formation can be counteracted by an accumulation of sugars leading to super-cooling and ice spreading is avoided by reducing the size of cell wall pores, as was shown in suspension-cultured cells of *Vitis* spp and *Malus domestica* (Rajashekar & Lafta, 1996; Reyes-Díaz et al., 2006; Ruelland et al., 2009). However, it is not possible to completely avoid the formation of ice in the plant, so the consequences of freezing have to be managed as well. As described previously, one of those consequences is cell dehydration, which is counteracted by a cytoplasmic accumulation of sugars such as sucrose, fructose, glucose and raffinose (Zuther et al., 2019). This process increases the osmotic potential of the cell, thus preventing the loss of water induced by extracellular freezing (Ruelland et al., 2009). This readjustment of the osmotic pressure between cytoplasm and apoplast might be reinforced through the accumulation of other compatible solutes such as proline, glycine betaine and polyamines (Jenks & Hasegawa, 2013). However, the role of those compounds is not completely elucidated yet and they might also help stabilizing proteins and membranes (Ruelland et al., 2009). Extracellular freezing, through dehydration, leads to the reduction of the volume of the cells and therefore cell deformation, underlining the important role played by the cell wall during a freezing episode (Rajashekar & Lafta, 1996). In *Arabidopsis thaliana*, the total amount of cell wall is increased during cold exposure and its composition and structure are modified, which might lead to an increase of the resistance of cells against deformation (Takahashi et al., 2019). All in all, plants have developed numerous mechanisms allowing them

to cope with cold episodes, but those have to be tightly regulated and coordinated so that they do not interfere with plant growth during warmer periods where they are not required.

1.1.2 Cold sensing and signalling

Most of the plants growing in temperate regions are chilling tolerant, as they often face episodes of low but non-freezing temperatures (Levitt, 1980a). This tolerance is not entirely constitutive and is improved when the plant faces low temperatures (Jan et al., 2009). Additionally, in temperate regions, moderately low temperatures often precede periods of freezing cold, such as the drop in temperature in autumn announcing the imminent arrival of winter. Therefore, when experiencing chilling temperatures, plants do not only respond to the current stress but also undergo a process named cold acclimation, through which they increase their freezing tolerance in preparation for potential colder days (Gilmour et al., 1988). The improvement of the chilling and freezing tolerance are both triggered by the exposure to low temperatures, which sets off a massive reprogramming of the transcriptome through both differential expression and differential alternative splicing, affecting several thousands of genes (Calixto et al., 2018). In the past years, tremendous progress has been made in the elucidation of the pathways leading to this reprogramming, which are recapitulated below and in Figure 1.

1.1.2.1 Perception of low temperatures

In order to respond to cold, plants need to first perceive the change in temperature. While the exact cold-sensing mechanism remains unclear, many hypotheses emerged in recent years and temperature sensing is believed to be achieved by a multitude of systems. One of the most supported ideas is the role of membrane fluidity as the main “plant thermometer”. Indeed, as previously explained, low temperatures trigger a rigidification of membranes, which could set off the cold signalling cascade: several studies showed that inducing membrane rigidification at warmer temperatures led to the transcriptional activation of cold-inducible genes, while maintaining membrane fluidity in cold-treated plants prevented it (Örvar et al., 2000; Sangwan et al., 2001). Wang et al. (2020) suggested that the signal could then be amplified and translated to the downstream actors through the cytoskeleton. Indeed, cold treatment destabilizes microtubules and actin filaments and stabilizing them at lower temperatures prevented the expression of cold-induced genes (Örvar et al., 2000; Pokorná et al., 2004; Sangwan et al., 2001). Plants exposed to low temperatures show a sharp cytosolic Ca^{2+} influx mere seconds after the transition to cold, suggesting a role for calcium signalling in the cold response (H. Knight et al., 1996; M. R. Knight et al., 1991). Inhibiting this calcium influx or chelating the cytosolic Ca^{2+} prevented the induction of cold-responsive genes during cold exposure while an artificial calcium influx led to their induction at ambient temperature, demonstrating the role of Ca^{2+} as an upstream signalling agent of the cold response pathway (H. Knight et al., 1996; Monroy & Dhindsa, 1995; Sangwan et al., 2001). Furthermore, the cold-induced Ca^{2+} influx was inhibited both by membrane and microtubule stabilizers, suggesting that membrane fluidization and cytoskeleton destabilization might lead to the activation of transmembrane calcium channels through the perception of changes in mechanical forces (Örvar et al., 2000; L. Wang et al., 2020). Five families of calcium channels were identified in *Arabidopsis thaliana*, tallying around 60 members in total but only two of those, MID1-COMPLEMENTING ACTIVITY (MCA) 1 and 2, are mechanosensitive channels (Kudla et al.,

2018). Recent work proved that MCA1 and MCA2 are involved in the cold-triggered Ca^{2+} influx and are necessary for cold tolerance (Mori et al., 2018). Altogether, it is possible that cold is sensed through changes in the membranes which then activate MCA1 and MCA2, leading to an influx of Ca^{2+} that triggers downstream signalling cascades, which will be described in more details below (Figure 1).

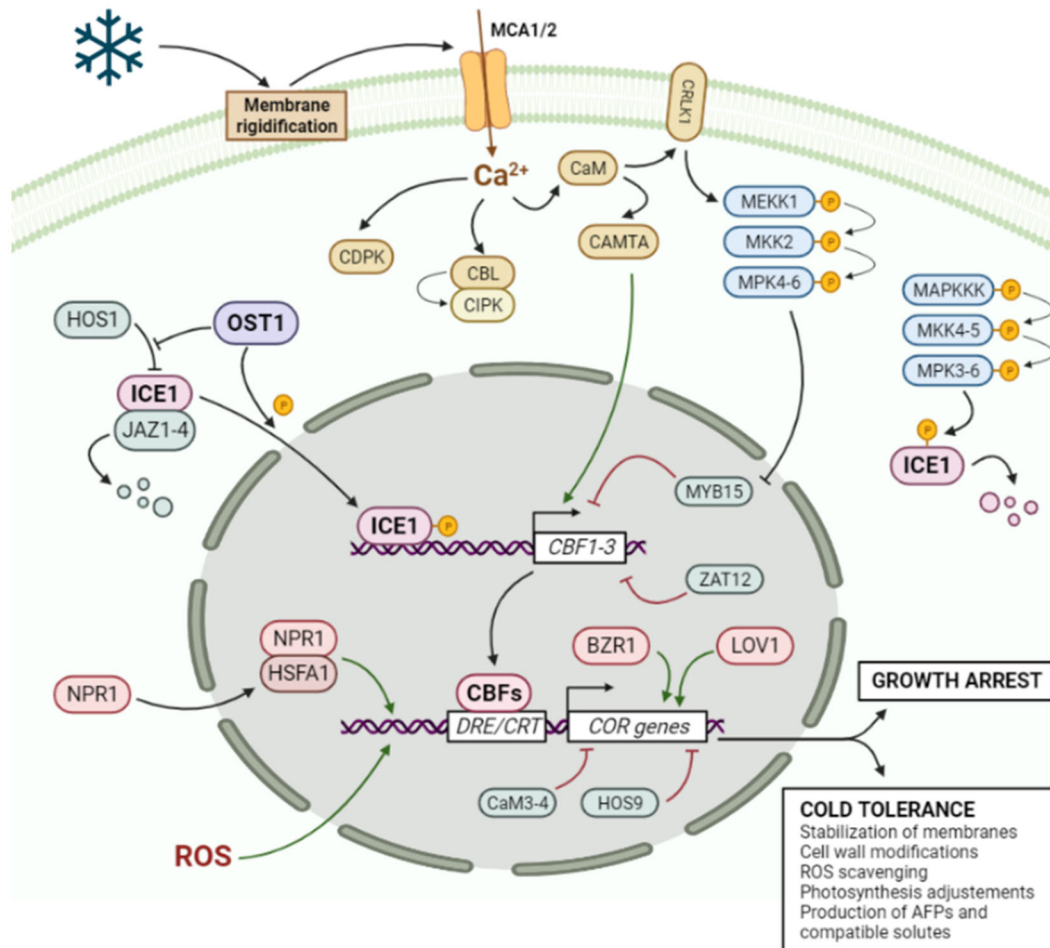


Figure 1: Schematic representation of cold signalling in *Arabidopsis thaliana*. Cold is perceived through membrane rigidification, resulting in the activation of the mechanosensitive calcium channels MCA1/MCA2. The increased cytosolic calcium concentration activates many calcium-dependant proteins such as CDPK, CBL, CIPK and CaM. In turn, CaM can activate CRLK1, triggering the MAPK phosphorylation cascade. In parallel, OST1 is activated and phosphorylate ICE1. It also prevents the degradation of ICE1 by HOS1. Being liberated from JAZ1-4, the phosphorylated ICE1 is free to bind to CBFs promoters, activating their transcription. CBFs transcription is also positively regulated by CAMTA and negatively regulated by transcription factors such as MYC15 and ZAT12. CBFs bind to the DRE/CRT element in the promoter of COR genes, leading to their transcriptional activation. COR genes are also transcriptionally activated through the action of BZR1, LOV1 and NPR1 bound to transcription factors such as HSF1, while negative regulators such as HOS9 and CaM3-4 limit their expression. COR genes expression is also activated through ROS signalling. The induction of COR genes finally leads to growth arrest and the establishment of cold tolerance. Green arrows indicate positive transcriptional regulation while red arrows show negative transcriptional regulation.

However, this membrane-cytoskeleton- Ca^{2+} system might not be the only module through which plants sense cold. Indeed, recent studies showed that temperature can induce changes

in the state or activity of certain proteins. For example, the reversion rate of the phytochrome B photoreceptor as well as its binding to its targets is affected by temperature, suggesting it as a potential thermosensor (Jung et al., 2016; Legris et al., 2016). The transcriptional regulator EARLY FLOWERING 3 (ELF3) is also inactivated by warmer temperatures, through phase transition driven by its prion-like domain: upon heat exposure, ELF3 forms speckles, preventing it from binding to its targets (Jung et al., 2020). While these studies unfortunately focused on warmer temperatures, one cannot exclude the possibility of similar mechanisms being involved in cold detection. Work in human and mouse showed that the activity of CDC-like kinases (CLKs) is temperature-dependant due to a temperature-triggered conformational change (Haltenhof et al., 2020). As CLKs phosphorylate Serine and Arginine-rich (SR) proteins, these changes in activity allow the control of alternative splicing in a temperature-dependant manner. *Arabidopsis thaliana* possesses three CLK homologs (ARABIDOPSIS FUS-COMPLEMENTING (AFC) 1, 2 and 3) and the key residues involved in the temperature-triggered conformational change are conserved, suggesting a potential role of AFCs as plant thermosensors (Lin et al., 2020). Finally, as mentioned previously, temperature can also act on RNA structure: the transcript of *PHYTOCHROME INTERACTING FACTOR 7 (PIF7)* forms a RNA hairpin on its 5' extremity when exposed to warmth, leading to an enhanced translation and therefore higher protein levels, which trigger the signalling cascade involved in the response to heat (Chung et al., 2020). One can therefore imagine that cold could also be “perceived” by some transcripts through their structure, in an analogue manner to the detection of heat by *PIF7* mRNA.

1.1.2.2 Cold signal transduction by secondary messengers

Once the plant detects a change in temperature, this signal needs to be transduced in order to activate the necessary defence responses. As previously mentioned, cold exposure leads to an influx of Ca^{2+} in the cytosol. Calcium is a well-known secondary messenger in plants, whose importance and plurality of roles were highlighted in a recent review (Kudla et al., 2018), it is therefore not surprising that it also plays a major role in cold signal transduction. Calcium modulates the activity of numerous proteins, which usually requires Ca^{2+} -binding to be active, such as calmodulins (CaMs) (Kudla et al., 2018). The inhibition of CaMs prevented cold acclimation and proper induction of the cold-induced *KIN* genes, while their overexpression inhibited the expression of *COR* genes which are essential for cold tolerance (see section 1.1.2.3 for details), suggesting that they play an important role in fine-tuning the response to cold (Tähtiharju et al., 1997; Townley & Knight, 2002). Calmodulins can bind a multitude of target proteins with highly diverse functions, such as protein kinases, catalase, Ca^{2+} -ATPases or transcription factors, and can therefore impact cold tolerance through numerous mechanisms, explaining their plurality of impact (Ruelland et al., 2009). One of those mechanisms is the activation of the calmodulin-binding transcription activators (CAMTAs), which positively regulate cold tolerance by inducing the expression of *C-REPEAT BINDING FACTOR (CBF) 1, 2 and 3*, three major components of the cold response whose role will be described in greater details ulteriorly (section 1.1.2.4) (Yanglin Ding et al., 2019). CaMs also activate the Ca^{2+} /CaM-regulated receptor-like kinases (CRLK). CRLK1 in particular is a positive regulator of the cold response: after being activated by CaM and Ca^{2+} , CRLK1 induces the expression of *CBF* and *COR* genes (P. Yuan et al., 2018). Calcium can also be detected by the calcineurin B-like calcium sensors (CBL), that in turn can bind to and activate the CBL-

interacting protein kinases (CIPK) (Kudla et al., 2018). Together, they regulate parts of the cold response: for example, CBL1 activates CIPK7, leading to the induction of cold-responsive genes and therefore the establishment of cold tolerance (P. Yuan et al., 2018). Some protein kinases can be directly activated by calcium, such as the Calcium-Dependant Protein Kinases (CDPK): upon calcium binding, those proteins undergo a conformational change toward an active form (Liese & Romeis, 2013). Several studies in *Oryza sativa* have proven that certain CDPKs (OsCPK27, OsCPK17 and OsCPK7) act as positive regulators of cold tolerance (Saijo et al., 2000; P. Yuan et al., 2018).

Another important part of signal transduction in plants is the Mitogen-Activated Protein Kinase (MAPK) cascade (Figure 1). This pathway is involved in the response to a multitude of stresses and consists of at least three levels of protein kinases that activate their downstream targets through phosphorylation: the MAPKKKs activate the MAPKKs which then activate the MAPKs (Cvetkovska et al., 2005). The MAPK module is involved in the cold response and is connected to calcium signalling. As described in the review from Yuan et al. (2018), CRLK1 activates the MAPKKK MEKK1, which then phosphorylates MKK2, which in turn activates MPK4 and MPK6. In the absence of MKK2, MPK4 and MPK6 are not activated by cold, preventing the establishment of cold resistance (Teige et al., 2004). On the other hand, MPK3 and MPK6, which are activated by MKK4 and MKK5, were recently shown to be negative regulators of INDUCER OF CBF EXPRESSION 1 (ICE1), whose key role in the induction of *COR* genes will be detailed in a later section (1.1.2.4) (C. Zhao et al., 2017). *Arabidopsis thaliana* possesses at least 23 MAPKs, 10 MAPKKs and 60 MAPKKKs, highlighting the possibility of numerous MAPKKK-MAPKK-MAPK being involved in the cold response and having antagonistic effects (Cvetkovska et al., 2005).

Other secondary messengers have been shown to be involved in the transduction of the cold signal. For instance, as previously mentioned, low temperatures lead to the accumulation of ROS, which then act as signalling molecules (Mittler, 2017). They have been described as feeding back into the Ca²⁺ signalling, but might also directly act on transcription as some cold-induced genes possess ROS response elements in their promoters (H. Cheng et al., 2020; L. Wang et al., 2020). These ROS response elements are bound by several transcription factors whose binding affinity is affected by the presence of H₂O₂ (H. Cheng et al., 2020). While this particular study did not examine cold, it raises the possibility of ROS playing a part in the transcriptional response to cold through these response elements and the action of H₂O₂.

Finally, numerous phytohormones participate in the signalling and regulation of the cold response. Abscisic acid (ABA) is one of the most investigated phytohormones in this context. Indeed, the endogenous levels of ABA increase slightly in response to chilling or freezing temperatures and many cold-induced genes are also induced by ABA (H. Knight et al., 2004; Lång et al., 1994; Seki et al., 2002). Furthermore, ABA insensitive and ABA deficient mutants are not able to fully cold acclimate, proving the essential role of ABA for a successful cold response (Mantyla et al., 1995). Many *COR* genes also have an ABA Responsive Element (ABRE) in their promoter, which can be bound by ABRE Binding Factors (ABFs) transcription factors to induce their expression (Roychoudhury et al., 2013; Ruelland et al., 2009). The brassinosteroids (BRs) are also positive regulators of the cold response: plants treated with exogenous brassinosteroid showed a higher induction of *COR* genes (Kagale et al., 2007). Furthermore, BR signalling deficient mutants showed a lower basal and acquired freezing tolerance, while mutants with a constitutively active BR signalling displayed an improved cold

response (Eremina et al., 2016). Jasmonate (JA) is required for proper cold response, as plant deficient in jasmonate biosynthesis or signalling have a lower basal and acquired freezing tolerance, while treating plants with exogenous jasmonate improves their cold response (Yanru Hu et al., 2013). Upon cold exposure, the bioavailable levels of gibberellic acid (GA) decrease due to the activation of the GA2 oxidase (Achard et al., 2008). This leads to an accumulation of the DELLA proteins, which slow down growth and promote freezing tolerance. Salicylic acid (SA) is also involved in the inhibition of growth triggered by low temperatures and the cold-induced accumulation of SA limits the induction of *COR* genes (Miura & Ohta, 2010; Scott et al., 2004). Finally, cold is known to inhibit the root basipetal transport of auxin by preventing the relocalization of PIN-FORMED (PIN) transmembrane efflux carriers, which leads to an arrested root growth (Shibasaki et al., 2009). It is therefore possible that auxin participates in the inhibition of plant growth induced by cold. Deciphering the individual role of each phytohormone in the cold response is however not trivial due to substantial cross-talks between the different pathways (Yanru Hu et al., 2017). Still, it is evident that phytohormones are major constituents of low-temperature signalling, as they coordinate the stress and developmental responses.

1.1.2.3 Establishment of defences by the cold-regulated genes

The different upstream cold signalling pathways eventually lead to the differential expression of thousands of genes, including the induction of several thousand *COLD-REGULATED (COR)* genes (Calixto et al., 2018; Shi et al., 2018). *COR* genes were first identified in 1985 and were since then repeatedly shown to be essential for freezing tolerance (Guy et al., 1985; Thomashow, 1999; D. Z. Wang et al., 2017). They are divided into five major families: cold-regulated (also called COR), low-temperature induced (LTI), responsive to desiccation (RD), early dehydration-inducible (ERD) and cold-inducible (KIN) (Shi et al., 2018). They are often also induced by dehydration stress or ABA (D. Z. Wang et al., 2017). *COR* genes code for a variety of proteins such as chaperones, antifreeze proteins, osmolytes, transcription factors, LATE EMBRYOGENESIS ABUNDANT (LEA) proteins or enzymes involved in respiration or the metabolism of antioxidants, phenylpropanoids and lipids (Yanglin Ding et al., 2019; D. Z. Wang et al., 2017). For example, one of the most well-known *COR* gene is *COR15A* (Cold Regulated 15A) which encodes for a protein localized in the stroma of chloroplasts (Thomashow et al., 1997). *COR15A* is essential for freezing tolerance as it improves the cryostability of the chloroplast inner membrane and stabilizes freeze-labile chloroplastic enzymes (Nakayama et al., 2007; Steponkus et al., 1998). *LTI30* is a cold-induced dehydrin involved in the stabilization of membranes during cold exposure: this protein is able to lower the temperature of the lipid phase transition of membranes, leading to freezing tolerance (Eriksson et al., 2011; Gupta et al., 2019; Puhakainen et al., 2004). Cold also induces the transcription of many of the *GOLS* genes, such as *GOLS3*, which encode galactinol synthases (Calixto et al., 2018; Kwon et al., 2009). As galactinol is an osmoprotectant and antioxidant, the induction of *GOLS* genes might protect the plants from the cold-triggered accumulation of ROS (Nishizawa et al., 2008). Finally, *COR* genes can encode for transcription factors and even chromatin modifiers. SALT TOLERANCE ZINC FINGER 10 (*ZAT10*) is a transcription factor induced by cold which also acts as a positive regulator of osmotic stress tolerance through the promotion of ROS detoxification processes (Nguyen et al., 2016; Rossel et al., 2007; van Buer et al., 2016). *TOLERANT TO CHILLING AND FREEZING 1 (TCF1)* regulates

the expression of certain cold-responsive genes through the modulation of their chromatin state, in particular the levels of H3K4me3 and H3K27me3, and acts as a negative regulator of freezing tolerance (Ji et al., 2015). While the expression of *COR* genes is essential to cold and freezing tolerance, the tight control of the timing and magnitude of their transcriptional induction is critical to ensure proper plant development and survival.

1.1.2.4 The ICE-CBF regulon

A major hub controlling the induction of *COR* genes is the ICE-CBF pathway: it regulates the expression of 10 to 25% of all *COR* genes (Shi et al., 2018). This regulon is a cascade composed of three components: the INDUCER OF CBF EXPRESSION (ICE) induces the expression of the C-REPEAT BINDING FACTOR (CBF) transcription factors which in turn leads to the transcriptional activation of the *COR* genes (D. Z. Wang et al., 2017) (Figure 1). Two *ICE* genes are encoded in the genome of *Arabidopsis thaliana*, *ICE1* and *ICE2*, which are MYC-like bHLH transcription factors (D. Z. Wang et al., 2017). It has been reported that *ice1* mutant plants are more sensitive to freezing and prolonged chilling treatments than wild type plants, while plants overexpressing *ICE1* are more freezing-tolerant (Chinnusamy et al., 2003). *ICE1* was therefore identified as a positive regulator of the cold response: it can bind to the promoter of *CBF3* and promotes its transcription. *ICE2* also acts as a positive regulator of the cold response, but by promoting the transcription of *CBF1* (Fursova et al., 2009). *ICE1* is constitutively expressed but is only active after cold exposure, suggesting that post-translational modifications play a key role in the regulation of its activity (Chinnusamy et al., 2003). In the absence of cold, *ICE1* activity as a transcription factor is hindered by its physical interaction with the jasmonate-zim-domain proteins JAZ1 and JAZ4 and by its ubiquitination by the E3 ubiquitin-ligase HIGH EXPRESSION OF OSMOTICALLY RESPONSIVE GENES 1 (HOS1) which targets it for degradation (C. H. Dong et al., 2006; Yanru Hu et al., 2013). Upon cold exposure, the jasmonic acid signalling pathway targets JAZ1 and JAZ4 for degradation and *ICE1* is activated through phosphorylation by the Ser/Thr protein kinase OPEN STOMATA 1 (OST1) (Yanglin Ding et al., 2015). This phosphorylation stabilizes *ICE1* as it prevents its targeting by HOS1, finally leading to the induction of the *CBF* genes. However, *ICE1* can also be phosphorylated by MPK3 and MPK6 in cold-treated plants, which targets the protein for degradation (Hui Li, Ding, et al., 2017; C. Zhao et al., 2017).

When active, ICEs lead to the transcription of the *CBF* genes. *Arabidopsis thaliana* possesses four *CBF* genes, *CBF1-4*, that belong to the APETALA 2/ETHYLENE-RESPONSIVE FACTOR family of transcription factors (Ruelland et al., 2009). *CBF1*, *CBF2* and *CBF3* are encoded in a tandem on chromosome 4 and show a high sequence similarity (D. Z. Wang et al., 2017). The three of them are induced by low temperatures, partially through the binding of *ICE1* to the MYC-binding sites present in their promoters (Chinnusamy et al., 2003; Medina et al., 1999). They are essential for cold and freezing tolerance: *cbfs* triple mutant plants are not able to properly cold-acclimate while plants overexpressing *CBFs* are more freezing tolerant before and after cold acclimation (Gilmour et al., 2004; Jia et al., 2016; C. Zhao et al., 2016). Contrary to the other three, *CBF4* is not cold-induced and has not been shown to be involved in cold tolerance (D. Z. Wang et al., 2017). *CBFs* mostly act as transcriptional activators by binding to the CCGAC motif, called Drought Responsive Element (DRE) or C-repeat (CRT), present in the promoter of many *COR* genes (Medina et al., 1999; Yamaguchi-Shinozaki & Shinozaki, 1994). A recent study by Song et al. (2021) identified 146 *COR* genes that are directly bound

and regulated by the CBFs, but the transcript levels of several hundreds of genes are directly and indirectly affected by those transcription factors. Similarly to ICE1, the activity of the CBFs is tightly regulated, especially at the transcriptional level. In addition to ICE1, the transcription of *CBFs* is induced by the CAMTA proteins that bind to the CMT2 motif present in their promoters (Doherty et al., 2009; Y. Kim et al., 2013). RNA-DIRECTED DNA METHYLATION 4 (RDM4) enhances the binding of RNA Pol II to the *CBFs* promoters, leading to an increased transcription (Chan et al., 2016). On the other hand, *CBFs* are targeted by many repressors. Firstly, the CBFs act as repressors for one another: CBF2 prevents the transcription of *CBF1* and *CBF3*, while CBF1 and CBF3 repress *CBF2* (Novillo et al., 2004; C. Zhao et al., 2016). MYB DOMAIN PROTEIN 15 (MYB15), a MYB transcription factor, represses the cold-induction of *CBFs* by binding to the type II Myb recognition sequence in their promoters (Agarwal et al., 2006). The transcription of the *CBFs* is also repressed by the C2H2 transcription factor ZAT12, the cold shock proteins CSP2 and CSP4, and the Phytochrome-Interacting Factors PIF3, PIF4 and PIF7 (B. Jiang et al., 2017; Kidokoro et al., 2009; Sasaki et al., 2013; Vogel et al., 2005).

1.1.2.5 CBF-independent pathways

Despite its major impact on cold tolerance, the induction of the majority of *COR* genes is not controlled by the ICE-CBF regulon, suggesting the existence of alternative pathways coordinating the expression of these non-CBF target genes. NON EXPRESSOR OF PR GENES 1 (NPR1) is part of one of these pathways and acts as a positive regulator of both basal and acquired freezing tolerance (Olate et al., 2018). Upon cold exposure, NPR1 is monomerized and translocates to the nucleus, where it can bind to transcription factors such as HEAT SHOCK FACTOR 1 (HSFA1s), inducing the expression of certain *COR* genes. NPR1 does not act on the *CBFs* nor is itself regulated by them, proving that it functions independently of the ICE-CBF regulon. Another CBF-independent regulon is controlled by BRASSINAZOLE-RESISTANT 1 (BZR1): prior to the cold exposure, BZR1 is phosphorylated by BRASSINOSTEROID INSENSITIVE 2 (BIN2), which targets it for nuclear export and proteasomal degradation. Upon cold exposure, the activation of the BR pathway leads to the dephosphorylation of BZR1, which can then induce the expression not only of *CBFs* but also of some CBF-independent *COR* genes (Hui Li, Ye, et al., 2017). Finally, LOCUS ORCHESTRATING VICTORIN EFFECTS1 (LOV1) is a positive regulator of both basal and acquired freezing tolerance: it induces the expression of certain *COR* genes in a CBF-independent manner (Yoo et al., 2007). CBF-independent pathways can also act as repressors of the cold-responsive genes. For example, the calmodulin CaM4 prevents the over-induction of certain *COR* genes independently of the CBFs as their expression was not affected in *cam4* mutants (Chu et al., 2018). CaM3 is also a negative regulator of the induction of *COR* genes (Townley & Knight, 2002). While the expression of *CBFs* was not investigated in this study, it is possible that CaM3 also acts independently of CBFs, like CaM4. The transcription factor HIGH EXPRESSION OF OSMOTICALLY RESPONSIVE GENES 9 (HOS9) was also proposed to work in a CBF-independent manner to prevent the over-induction of certain *COR* genes (J. Zhu et al., 2004). Contrary to CaM4, HOS9 is a positive regulator of basal and acquired freezing tolerance (Chu et al., 2018; J. Zhu et al., 2004). This suggests that either the expression of *COR* genes is detrimental to freezing tolerance above a certain threshold or that HOS9 also acts as an activator for other *COR* genes.

1.1.3 Deacclimation and memory: the importance of controlling the stress response

1.1.3.1 Cold deacclimation

While it is crucial for plants to induce the appropriate stress responses when exposed to cold, it is equally critical for them to inhibit those defences when the temperature is favourable. Indeed, a constant activation of the cold response has adverse consequences on plant fitness and development. Overexpression of *CBFs*, which leads to a constitutively high freezing tolerance and an increased accumulation of cryoprotectants even in the absence of cold, causes the plants to grow slower, bolt later and produce less seeds (Gilmour et al., 2004; S. Park et al., 2015; Zhen et al., 2011). This was confirmed in the meta-analysis conducted by Dong et al. (2018), which showed that the overexpression of *DRE Binding (DREB)* genes leads to a significantly reduced plant height. In general, inducible defences are thought to be favoured by plants over constitutive ones for three main reasons: i) constitutive defences have allocation costs since they divert energy and resources from growth and reproductive processes, ii) they might be directly incompatible with growth and iii) constitutive defence against one stressor might confer susceptibility to another (Agrawal & Karban, 1999; Cipollini et al., 2017). This explains why, while cold exposure triggers a myriad of defence responses so that the plant is able to survive the stress episode, those defences are quickly lost upon return to ambient temperature, following a process called cold deacclimation (Kalberer et al., 2006). In *Arabidopsis thaliana*, deacclimation could already be seen 24 h after the return to ambient temperature as the freezing tolerance acquired during cold acclimation was significantly reduced (Oono et al., 2006; Zuther et al., 2015). The exact time required for full deacclimation depends on the length of the acclimation period and the ecotype of the plant. Oono et al. (2006) showed that 24 h at 22°C were sufficient to lose the freezing tolerance acquired during a week of cold treatment, while Zuther et al. (2015) still observed a higher freezing tolerance in plants that were cold acclimated for two weeks and placed back at 20°C for three days compared to non-acclimated plants. As described previously, cold acclimation involves an extensive reprogramming of the transcriptome and the metabolome. The changes of the transcriptome were shown to be reverted very quickly upon return to ambient temperature: two hours at 20°C were sufficient to trigger detectable changes in gene expression and the transcriptome of deacclimated plants was virtually indistinguishable from naïve plants after 24 h (Pagter et al., 2017). The metabolome recovers at a slower pace, as 24 h of deacclimation are not sufficient to return to a pre-acclimation state (Pagter et al., 2017). Indeed, the accumulation of compatible solutes such as proline and several sugars, although quickly decreasing upon return to ambient temperature, required three days to return to naïve levels in plants that were previously cold acclimated for two weeks (Zuther et al., 2015). Deacclimation does not only involve the reversal of defences built during the cold exposure, it also entails recovery from potential damages caused by the stress as well as the reactivation of photosynthesis and growth (Oono et al., 2006). Just as cold acclimation, deacclimation therefore relies on well-coordinated transcriptomic changes. A return to ambient temperatures triggers the repression of genes that were induced by the cold exposure, such as *COR* genes, genes involved in secondary metabolism as well as transcription factors and kinases involved in cold signalling (Byun et al., 2014; Pagter et al., 2017). On the other hand, it induces the expression of genes linked to photosynthesis, detoxification, cell wall biogenesis, lipid

degradation and phytohormones biosynthesis (Byun et al., 2014; Oono et al., 2006; Pagter et al., 2017).

1.1.3.2 Priming and cold stress memory

However, while deacclimation is essential for plants to resume growth once favourable environmental conditions return, it can be noxious if it occurs prematurely. In spring for example, warm spells may precede periods of colder weather, meaning that deacclimated plants might need to re-acclimate. This re-acclimation has a cost for the plant, due to the potential damages done by the stress in the time it takes to re-establish all necessary defences (Cipollini et al., 2003). A potential solution to edge this cost might be priming, a mechanism through which plants can memorise past stressful events (Hilker et al., 2015). This memory maintains the primed plants in a “pre-active” state, which leads to a more efficient re-acclimation and therefore an improved survival to a potential second stress episode. While the word priming has been used to describe many different and sometimes conflicting concepts, in this study, it will refer to the definition offered by Hilker et al. (2015): when a plant experiences a stress that might reoccur, it stores the information about this first stressful episode, also called priming event (P) (Figure 2). This information is then remembered over a stress-free period, called lag phase (PL). If the plant experiences a second stress episode, named triggering event (T), this memory of the priming will allow the plant to react more efficiently than an individual that did not experience the priming event, through a stronger, faster, earlier and/or more sensitive response. In this definition, it is important to note that the information is retained over a period where the stress disappeared and the plant underwent deacclimation, meaning that the benefit from priming is not simply due to a persisting acclimation response to the first stress but to the actual memory of it. As priming is associated with low costs compared to a constant acclimation, it provides a profitable strategy for plants to respond to frequently reoccurring stresses such as temperature variations (Douma et al., 2017). Priming has already been described for various biotic and abiotic stresses, including cold (Brzezinka et al., 2016; Byun et al., 2014; Yong Ding, Fromm, et al., 2012; Hilker et al., 2015; Lämke et al., 2016; Sani et al., 2013; Zuther et al., 2019). Indeed, Byun et al. (2014) demonstrated that *Arabidopsis thaliana* plants primed at 0°C for 24 h and deacclimated for 72 h had a higher freezing tolerance than non-primed plants upon triggering (Figure 2). Similarly, Zuther et al. (2019) showed that plants primed at 4°C for three days before being returned to ambient temperature for a week also performed better than non-primed plants upon re-exposure to 4°C, confirming that plants can remember cold stress. While the exact mechanisms encoding cold stress memory remain undiscovered, a few studies provided precious insight. Indeed, upon triggering, previously primed plants accumulate higher levels of specific lipids such as arabidopsides and compatible solutes (proline, sucrose, raffinose) than their non-primed counterparts (Zuther et al., 2019). Cold priming also results in an increased PSII activity and photochemical quenching, while non-photochemical quenching is reduced (van Buer et al., 2016). This suggests that cold memory leads to an improved response of many systems involved in cold and freezing tolerance, such as membrane protection, avoidance of intracellular freezing or photosynthesis, which ultimately contributes to the enhanced survival of primed plants compared to their non-primed counterparts.

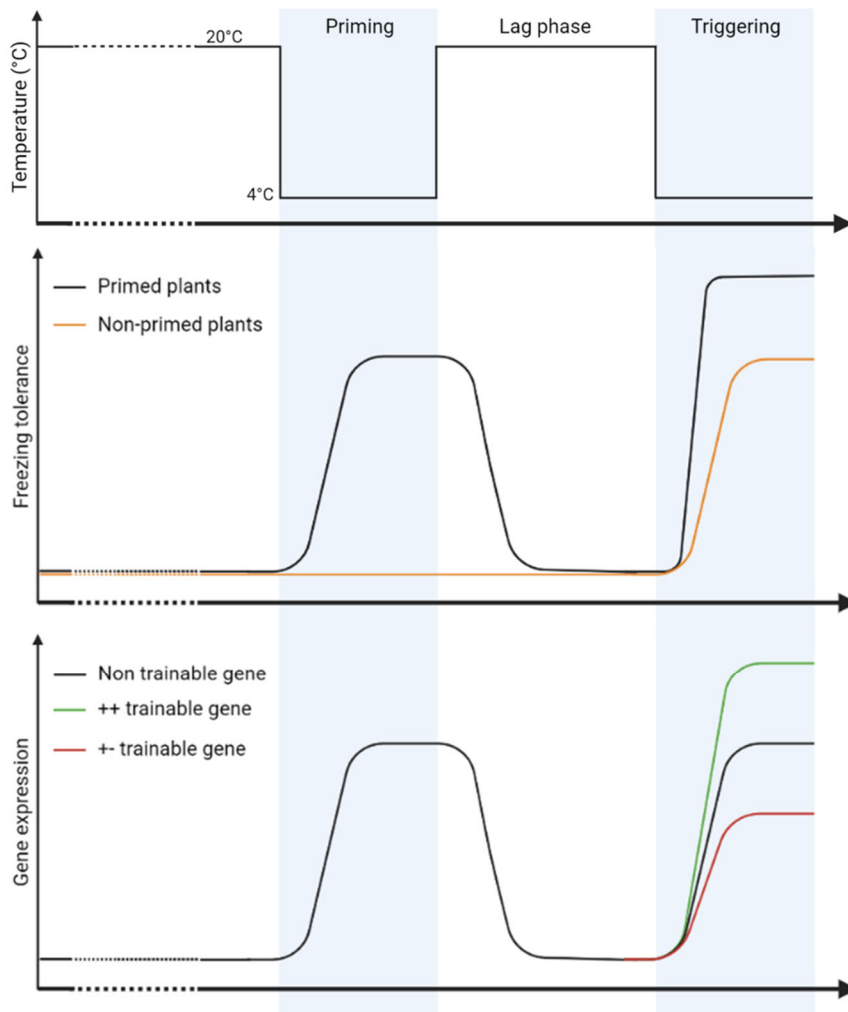


Figure 2: Cold stress memory at the physiological and transcriptional level. Schematic views of the temperature (upper panel), freezing tolerance (middle panel) and expression of cold-inducible genes (lower panel) during a priming and triggering scheme. Primed plants acquire a higher freezing tolerance than non-primed plants upon a triggering cold treatment. This altered physiological response is associated with a refined transcriptomic response: while some cold-inducible genes are expressed at the same level during the first and second cold event, some are trainable, meaning that they are induced to a higher (++) or lower (+-) level during triggering.

1.1.3.3 Stress memory is associated with transcriptional trainability

While cold priming is associated to the enhanced response of several cold defence systems, transcriptomic analyses showed that the higher freezing tolerance in primed-and-triggered (PLT) plants compared to triggered-only plants (T) is not simply due to a stronger expression of the cold-responsive genes. On the opposite, some genes are not re-induced during the triggering stress while other are newly induced (Byun et al., 2014; Zuther et al., 2019). This revised transcriptional response upon a second stressful episode is not unique to cold. Investigations of the memory of other abiotic stresses such as drought or heat revealed that a priming event might affect the transcriptional activity of a gene, either during the lag phase or the triggering stress (Yong Ding et al., 2013; H. Liu et al., 2018). This phenomenon is called transcriptional memory and can be categorized into two types: sustained induction and revised response, also coined trainability (Friedrich et al., 2018). Sustained induction refers to the persisting transcription of stress-inducible genes even after the stress has passed and has

been observed for drought and heat stress memory (Lämke et al., 2016; N. Liu et al., 2014). Trainable genes are genes whose magnitude of induction (resp. repression) differs during the triggering event compared to the priming one. Transcriptomic analyses of plants that faced repeated drought stresses identified four categories of trainable genes: induced genes that are induced to a higher (++) or lower (+-) level during a subsequent stress and repressed genes that are more (--) or less (-+) repressed during the triggering stress (Yong Ding et al., 2013). Trainability has also been observed in heat stress memory and systemic acquired resistance (Jaskiewicz et al., 2011; H. Liu et al., 2018; Mozgová et al., 2015) as well as during cold priming. For example, van Buer et al. (2016) identified *COR15A*, *PHE AMMONIA LYASE (PAL1)* and *CHALCONE SYNTHASE (CHS)* as being induced to a higher level in primed plants (++ trainable) and *ZAT10* and *BON ASSOCIATED PROTEIN 1 (BAP1)* as being less induced (+- trainable). This suggests that cold priming, similarly to other abiotic and biotic stresses memory, relies on a refined transcriptomic response rather than simply on the over-induction of all *COR* genes, which improves the overall response to cold and survival chances of the plant (Figure 2). How the trainability of *COR* genes is encoded remains so far unelucidated but investigations of other abiotic stresses memory highlighted the key role played by chromatin modifications in this process (see section 1.3.2.1 for more details), suggesting that similar mechanisms could be involved and opening an interesting avenue for deeper investigations of cold stress memory.

1.1.4 The central role of transcriptional regulation in the stress response

As detailed in the previous sections, the tight control of gene expression is a key aspect of the cold response (Figure 3). Prior to cold exposure, the *COR* genes need to be repressed to allow proper growth. However, upon cold exposure, this repression has to be rapidly lifted, following a precise cascade: the signalling actors (kinases, transcription factors) are induced first, followed by the genes directly involved in the defence against cold (dehydrins, cryoprotectants) (Byun et al., 2014; Calixto et al., 2018). The vast number of negative regulators of the ICE-CBF-COR regulon underlines the importance of preventing an over-induction of those genes also during a cold episode, meaning that the transcriptional activity is maintained within a tight range. It is interesting to note that this regulation does not only target the *COR* genes: many of their activators and repressors are themselves induced or repressed by cold. Once the warmer weather returns, all those changes have to be reverted and the *COR* genes are once again repressed to allow growth to resume. Finally, should the plant experience cold again, the defences must be re-established. This requires not only the re-induction of the *COR* genes but a refining of the transcriptomic response: some genes are induced to a higher magnitude, others to a lower one, while others are not re-induced at all. Altogether, this demonstrates the essential role of the precise control of gene expression in the cold response and memory. This is not unique to the response to low temperatures: indeed, the adaptation to any adverse condition relies on the transcriptional induction of thousands of genes (Garcia-Molina et al., 2020; Kreps et al., 2002). While some genes are specifically involved in the response to one particular stressor, others can be induced by several types of adverse conditions (Kreps et al., 2002; Swindell, 2006). Garcia-Molina et al. (2020) for example identified 456 genes, including 41 transcription factors, which can be induced by heat, cold and high-light stress. Irrelevant of which stress they are induced by, all stress-responsive genes follow the same pattern described previously, where they are tightly repressed in naïve conditions and induced

according to a precise timing and magnitude upon stress exposure, underlining the central role of transcriptional regulation in all stress responses. The induction of stress-responsive genes is achieved by the coordinated action of multiple transcription factors, which have been the object of intensive investigation in the last decade. To execute their functions, these transcription factors need to have access to the DNA, underlining the essential role played by chromatin accessibility in this process. Furthermore, chromatin modifications are known to contribute to the recruitment of transcription factors to their target loci (B. Li et al., 2007). Despite the key role of the chromatin status in the control of gene expression and the adding evidence of the key role of chromatin regulation in the response to stress (Asensi-Fabado et al., 2017), this aspect was only very rarely addressed in studies investigating *COR* genes.

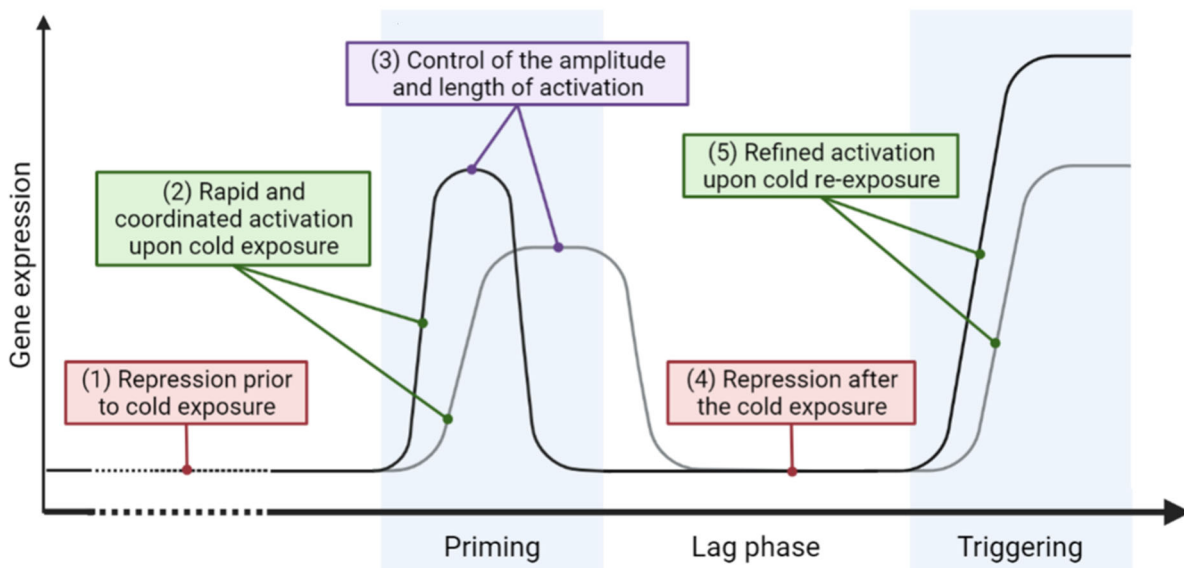


Figure 3: The expression of cold-inducible genes is tightly regulated at every step. When the plant is not exposed to cold, the cold-inducible genes are repressed (1). Lower temperatures trigger their rapid and coordinated activation (2) and the magnitude of this induction is also controlled (3). Once the cold subsides, the genes are once again repressed (4). Finally, if the plant re-experiences cold, the activation of cold-inducible genes is refined compared to the first stress (5). The black line represents a gene induced early in the cold response, while the grey line represents a gene induced later. The blue boxes show episodes of cold.

1.2 CHROMATIN STRUCTURE AND ITS IMPACT ON TRANSCRIPTION

For all eukaryotic organisms, most of the information necessary to life is encoded in the nuclear DNA. In order to fit inside this small organelle, the long DNA molecules have to be tightly packaged while remaining accessible for processes such as transcription, replication and repair. This fragile equilibrium is achieved through the association of DNA with a various set of proteins that together form the chromatin. The chromatin is a place of dynamic and reversible changes that impact, among others, the accessibility of genes to the transcriptional machinery, making it a crucial level of control of gene expression.

1.2.1 The basic structure of chromatin

The chromatin is essentially a polymer of repeated units called nucleosomes. A nucleosome is formed by an octamer of histones, consisting of two H2A-H2B-H3-H4 tetramers, around

which is wrapped a 147 bp-long segment of DNA (Kornberg, 1977; Luger et al., 1997). Two nucleosomes are separated from one another by the linker DNA, whose length varies between 20 and 80 bp depending on the organism and cell type (Bednar et al., 1998). This leads to the basic “beads on a string” structure, which is the first level of chromatin compaction. The chromatin is further condensed through the binding of the linker histone H1 to the nucleosome and linker DNA, which bring the nucleosomes closer to one another (Bednar et al., 1998). However, nucleosomes are not regularly distributed along the DNA molecules: certain sections are packed more tightly than others. Chromatin is often categorized into two different types depending on its degree of compaction. Euchromatin refers to the decondensed chromatin found at actively transcribed or poised genes while the more tightly packed heterochromatin is associated with silenced loci (Blakey & Litt, 2015). Heterochromatin is itself divided into constitutive heterochromatin, found on pericentromeric and telomeric regions as well as repetitive elements, and facultative heterochromatin that marks genes that are currently silenced but might need to be transcribed at an ulterior stage. Indeed, facultative heterochromatin retains the potential to switch to an euchromatic state (Trojer & Reinberg, 2007). At the molecular level, these different chromatin environments are characterized by the presence of distinctive histone marks and histone variants that dictate their structure and accessibility (Figure 4).

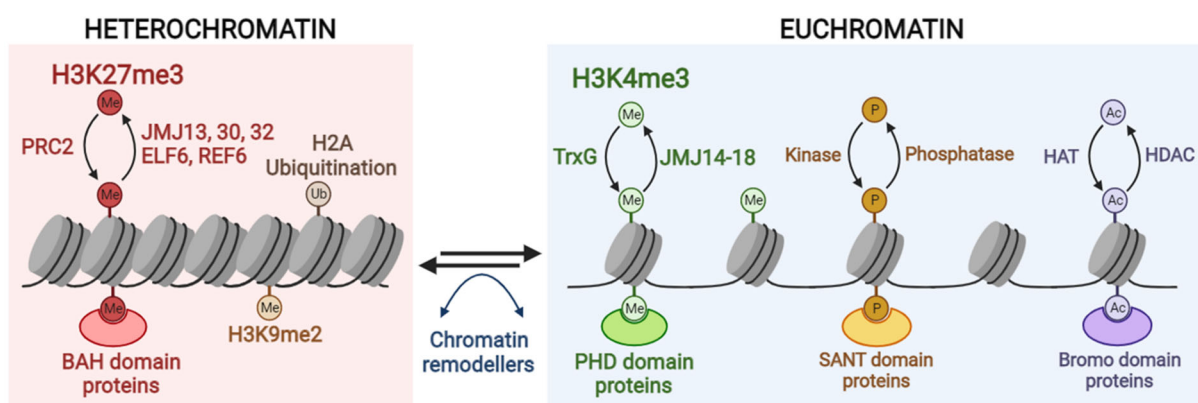


Figure 4: Major histone marks and chromatin modifiers. Heterochromatin is tightly packed and characterized by the presence of H3K27me3, H3K9me2 and H2AUb. Euchromatin is more loose and characterized by the presence of H3K4me3, phosphorylation and acetylation. Modifications are added by histone writers such as the PRC2 complex, the TrxG proteins, kinases, HAT and removed by histone erasers such as the JMJ demethylases, phosphatases and HDAC (upper part). They are read by proteins containing specific domains such as BAH, PHD, SANT or Bromo (lower part). The structure of chromatin is also dictated by the action of chromatin remodellers that slide nucleosomes along the DNA or evict them.

1.2.1 Histone post-translational modifications

1.2.1.1 The high diversity of histone post-translational modifications

The core histones (H2, H3 and H4) all share a similar structure, composed of a globular domain and a protruding histone tail (or two in the case of H2). This tail is formed by the terminal part of the amino acid sequence (N-terminal part for H3 and H4) and represents around 25% of the histone mass (Luger & Richmond, 1998). The tails contain numerous lysine and arginine

residues, making them highly basic, and are the site of numerous post-translational modifications (PTMs). These histone PTMs are very diverse and include for example phosphorylation (pho), methylation (me), acetylation (ac), ubiquitination (Ub), sumoylation or ADP-ribosylation (Y. Zhao & Garcia, 2015). They occur on specific residues that are often conserved across a wide range of eukaryotic organisms and while efforts have been directed towards the documentation of the full array of modifications and their localization, the function of many remains undiscovered. Indeed, the histone PTMs can affect the compaction and accessibility of chromatin by (i) *cis* effects: the modification induces changes in the physical properties of the histone tail and therefore the strength of DNA-histone interaction and/or nucleosome spacing or (ii) *trans* effects: the modification is recognized by a specific binding protein, called reader, which can recruit a complete protein complex and in turn alter the chromatin structure or simply prevent the binding of the transcriptional machinery (Blakey & Litt, 2015). Depending on the effect of those modifications on transcription, histone PTMs are categorized as active (favouring transcription) or repressive (inhibiting or limiting transcription).

The most investigated modifications are acetylation, phosphorylation and methylation (Figure 4). Histone acetylation happens on lysine (K) residues and neutralizes their positive charge, decreasing the affinity of the histone tails for the DNA (Hong et al., 1993). This leads to a more accessible chromatin which is favourable to transcription, explaining why acetylation is commonly described as an active mark. Histone phosphorylation can occur on serine (S), threonine (T) or tyrosine (Y) residues (Y. Zhao & Garcia, 2015). As it is negatively charged, it creates repulsion between the residues and the negatively charged DNA, which results in DNA unwrapping and therefore increased chromatin accessibility (Brehove et al., 2015). On the contrary, the consequences of methylation on transcriptional activity are more nuanced. This modification can occur on arginine (R) to form mono- or dimethylated arginine, or on lysine residues, which can be mono-, di- or tri-methylated (Y. Zhao & Garcia, 2015). Histone methylation does not affect the charge of the residues but their hydrophobicity and size (Blakey & Litt, 2015). Depending on the targeted residue and the methylation state, this PTM has a different impact on the transcriptional activity of the underlying genes. In plants, lysine methylation can occur on the residues K4, K9, K23, K27, K36 and K79 of H3 and on the residue K20 of H4 (K. Cheng et al., 2020). H3K4 and H3K36 methylation are both associated with transcriptionally active chromatin but show a slightly different distribution over transcribed regions. H3K4me2 and me3 are localized in the promoters and 5' UTR regions of actively transcribed genes while H3K36me3 spans a wider section of the gene body (Roudier et al., 2011). H3K4me1 and H3K36me2 are found in the body of transcriptionally active genes, especially towards the 3' end (X. Zhang et al., 2009). To the contrary, H3K9 and H3K27 methylation are associated with silenced loci as they are mainly found in heterochromatin (K. Cheng et al., 2020). However, they hold slightly different functions depending on the methylation state. Indeed, H3K9me1 and me2, the most common methylated forms of H3K9 in plants, are found at centromeres, chromocenters, transposons and repetitive elements, which belong to the constitutive heterochromatin (Bernatavichute et al., 2008; Jackson et al., 2004). H3K9me2 in particular is associated with DNA methylation and gene silencing (Jackson et al., 2004). In plants, contrary to what is observed in mammals, H3K9me3 is located in the euchromatin and is associated with the activation of transcription (Charron et al., 2009). H3K27me1 is also found in the constitutive heterochromatin and is necessary for gene silencing and chromatin condensation, while H3K27me2 is associated both with eu- and heterochromatin (Jacob et al., 2009; Mathieu et al., 2005; Roudier et al., 2011). H3K27me3 is

also linked to silencing but is mostly located on the transcribed region of inactive genes. About 16% of all *Arabidopsis thaliana* genes carry H3K27me₃, those genes are involved in many processes ranging from tissue specification and developmental transitions to stress responses (Kleinmanns & Schubert, 2014; Lafos et al., 2011; X. Zhang et al., 2007). Of the previously described histone PTMs, H3K4me₃ and H3K27me₃ are two of the most investigated. They are generally mutually exclusive and their antagonistic regulation of gene expression is essential to cell differentiation and plant development (Kuroda et al., 2020).

1.2.1.2 Histone writers and erasers antagonistically regulate transcription

Histone PTMs are added by enzymes called histone writers while their active removal is performed by histone erasers (Figure 4). Histone acetylation is added by histone acetyltransferases (HATs) and removed by deacetylases (HDACs), while histone phosphorylation is written by kinases and erased by phosphatases. Histone methylation is performed by methyltransferases. The genome of *Arabidopsis thaliana* encodes around 50 SET domain proteins that can perform this function, which are divided into four families: Enhancer of Zeste (E(z)), ASH1, Trithorax (TrxG) and Su(var) (K. Cheng et al., 2020). The methyltransferases are usually part of bigger protein complexes which ensure their binding to their specific targets and/or coordinate the transfer of methyl groups to other activities such as chromatin remodelling (Ringrose & Paro, 2004). Su(var)3-9 proteins are mostly responsible for H3K9 methylation while the ASH1 family members di- or tri-methylate H3K36 (K. Cheng et al., 2020). To date, six H3K4me₃ methyltransferases were identified in *Arabidopsis thaliana*: ARABIDOPSIS TRITHORAX 1 (ATX1), ATX3-5, ARABIDOPSIS TRITHORAX-RELATED (ATRX) 3 and 7 (K. Cheng et al., 2020). They are members of the Trithorax (TrxG) group, which also contains ATP-dependant chromatin remodelling factors, other lysine methyltransferases and transcription factors that all together enhance chromatin accessibility and promote transcriptional activity (Ingham, 1983; Kuroda et al., 2020; Ringrose & Paro, 2004). In plants for example, the H3K4me₃ methyltransferases act in concert with other TrxG proteins such as the co-activators ULTRAPETALA1 and 2 (ULT1 and 2) and chromatin remodellers to activate gene expression (Köhler & Hennig, 2010; Monfared et al., 2013).

This activation of gene expression is counteracted by the repressive actions of Polycomb group (PcG) members (Kuroda et al., 2020). Most Polycomb proteins act as part of the complexes Polycomb Repressive Complex 1 (PRC1) or 2 (PRC2). The latter is a histone writer complex responsible for the trimethylation of H3K27. It was first identified in *Drosophila* and consist of four subunits: the methyltransferase E(z), the histone binding protein p55, Su(z)12, a zinc finger protein binding to nucleosome and the WD40-containing protein EXTRA SEX COMB (ESC) which acts as a scaffold for the whole complex (Müller et al., 2002). *Arabidopsis thaliana* possesses multiple paralogs of all PRC2 components except ESC, whose single homolog is FERTILIZATION INDEPENDENT ENDOSPERM (FIE) (Chanvivattana et al., 2004; Derkacheva & Hennig, 2014). Three H3K27me₃ methyltransferases are encoded in its genome: MEDEA (MEA), CURLY LEAF (CLF) and SWINGER (SWN) (Chanvivattana et al., 2004). MULTICOPY SUPPRESSOR OF IRA (MSI) 1-5 are homologs of p55 while EMBRYONIC FLOWER 2 (EMF2), REDUCED VERNALIZATION RESPONSE 2 (VRN2) and FERTILIZATION INDEPENDENT SEED 2 (FIS2) are homologs of Su(z)12 (Derkacheva & Hennig, 2014). This multiplicity of homologs for each subunit allows the formation of distinct PRC2 complexes which regulate different developmental processes such as gametophyte

development, flowering or vernalization (Derkacheva & Hennig, 2014; Köhler & Hennig, 2010). The repressive state initiated by PRC2 is further enhanced through the complementary action of PRC1, which is able to bind to H3K27me₃ and subsequently monoubiquitinates H2AK118/K119 (Cao et al., 2005; Molitor & Shen, 2013). PRC1 binding also prevents chromatin remodelling and binding of the transcriptional machinery (Shao et al., 1999).

Histone demethylation can be achieved either by amino-oxidase from the Lysine-Specific Demethylase (LSD) family (for mono- and dimethylated residues) or hydroxylases from the Jumonji (JMJ) family (mono-, di- and trimethylated residues). *Arabidopsis thaliana* possesses four LSD and 21 JMJ demethylases (K. Cheng et al., 2020). The LSD demethylases (FLOWERING LOCUS D (FLD), and LYSINE-SPECIFIC HISTONE DEMETHYLASE (LDL) 1-3) were found to target H3K4me₁ and me₂ while the JMJ demethylases have diverse targets (D. Jiang et al., 2007). To date, five of them were identified as demethylating H3K27me₃: EARLY FLOWERING 6 (ELF6), RELATIVE OF ELF6 (REF6), JMJ13, JMJ30 and JMJ32 (Gan et al., 2014; Lu et al., 2011; W. Yan et al., 2018). H3K4me₃ is removed by the five demethylases JMJ14-18 (Huang et al., 2019; P. Liu et al., 2019; H. Yang, Han, et al., 2012; H. Yang, Mo, et al., 2012; W. Yang et al., 2010). JMJ25, 27, 28 and 29 demethylate H3K9me₂ while JMJ20 and JMJ22 target the arginine residues H3R2me₃ and H4R3me₂ (Cho et al., 2012; Dutta et al., 2017; D. Fan et al., 2012; Hung et al., 2020, 2021). While the JMJ demethylases were shown to be involved in development and stress response, substantial work is still required for their characterization, for instance to determine how they recognize their targets (K. Cheng et al., 2020; Crevillén et al., 2014; Gan et al., 2014; Yamaguchi et al., 2021).

1.2.2 Histone variants: another layer in the chromatin diversity

The chromatin environment is further diversified through the presence of histone variants. Canonical histones are incorporated in the chromatin during DNA replication, however they can be replaced by variants outside of the S phase. The incorporation of histone variants usually requires the action of chaperones. It can occur concurrently to transcription, by replacing the core histones evicted during the elongation of transcripts, or independently from it, through the action of ATP-dependant chromatin remodellers (Gómez-Zambrano et al., 2018; B. Li et al., 2007; Schwartz & Ahmad, 2005). Histone variants might differ from the canonical ones by a few amino-acid substitutions or more substantial changes to their tail or fold (Probst et al., 2020). *Arabidopsis thaliana* possesses variants for each histone except H4. H3 is encoded by 15 *HTR* genes that can be grouped into genes coding for the canonical H3.1 (*HTR1*, *HTR2*, *HTR3*, *HTR9* and *HTR13*), the H3.3 variant (*HTR4*, *HTR5* and *HTR8*), which only differ from H3.1 by five amino acids, the atypical histone variants (*HTR6*, *HTR10*, *HTR11*, *HTR14* and *HTR15*), the centromeric cenH3 variant (*HTR12*) and the pseudogene *HTR7* (Probst et al., 2020). The H3.3 variant is found mainly in the 3' region of actively transcribed genes and mostly carries activating marks such as H3K36me₃ or acetylation (Johnson et al., 2004). On the contrary, the canonical H3.1 is usually found on loci bearing repressive marks such as H3K27me₃, showing that histone variants are preferentially associated with active or repressive chromatin states. H2A histones are encoded by 13 *HTA* genes, which can be divided into canonical H2A (*HTA1*, *HTA2*, *HTA10* and *HTA13*), H2A.Z (*HTA4*, *HTA8*, *HTA9* and *HTA11*), H2A.X (*HTA3* and *HTA5*) and H2A.W (*HTA6*, *HTA7* and *HTA12*) variants. The H2A.Z variant differs from the canonical H2A by a shorter C-terminal tail, which affects the

docking domain interacting with H3, and a longer acidic patch, which leads to higher chromatin folding *in vitro* (J. Y. Fan et al., 2004; Kawashima et al., 2015). Interestingly, this variant is located on genes but shows a different distribution depending on their transcriptional activity: highly expressed genes tend to have H2A.Z only around their transcription start site (TSS) whereas it is present over the whole gene body of lowly expressed or silenced genes (Yelagandula et al., 2014). Finally, H2B histones are encoded by 11 HTB genes and the linker histone H1 by three genes (Probst et al., 2020). It is important to note that, in addition to direct effects from an altered structure as for H2A.Z, histone variants might impact the chromatin environment by their inability to carry certain modifications. For instance, the HTR15 variant of H3 has an asparagine residue and a histidine residue instead of lysines at the positions 4 and 27 respectively, and therefore cannot be methylated at these positions (A. Yan et al., 2020). Altogether, this highlights the role of histone variants as contributors to the chromatin complexity.

1.2.3 Chromatin states and bivalency

As described above, most of the histone marks were assigned to either the activating or repressing category depending on their impact on transcription, forming the histone code (Jenuwein & Allis, 2001). However, inferring the transcriptional activity of a gene solely based on the abundance of one mark would be overly simplistic. Indeed, a single nucleosome might carry several PTMs at once and a single gene possesses a multitude of nucleosomes over its promoter and coding sequence, creating hundreds of potential combination of chromatin modifications over a gene. Furthermore, the effects of a PTM can be affected or overwritten by its combination with another modification: for instance, the phosphorylation of serine 10 (resp. 28) of H3 prevents the binding of readers on the nearby H3K9me3 (resp. H3K27me3), leading to the transcriptional activation of the underlying genes (Dormann et al., 2006; Nga leng Lau & Cheung, 2011). Histone variants add another layer to this problem, complexifying the translation of the chromatin environment into transcriptional activity. However, it was observed that certain chromatin features associate preferentially with one another, suggesting that they might act synergistically to create an active or repressive environment. For example, the H2A.Z variant and the repressive histone mark H3K27me3 were found to be associated with one another at repressed poised genes, while active loci often carry H3K4me3, H3K36me3 and H3.3 (Sequeira-Mendes et al., 2014). Therefore, numerous studies offered means of simplifying the chromatin environment into a reduced number of states by integrating information about the different layers contributing to its regulation (histone variants, histone PTMs, DNA methylation...). Chromatin states are defined by the presence of a combination of different marks and variants and can be used to predict the transcriptional activity and responsiveness of genes. Several chromatin topographies were thus established for *Arabidopsis thaliana*, ranging from the global to the very precise (Yue Liu et al., 2018; Roudier et al., 2011; Sequeira-Mendes et al., 2014). Roudier et al. (2011) used the distribution of 11 histone modifications and DNA methylation to categorize the chromatin into four states: active genes, repressed genes, silent repeat elements and intergenic regions. Liu et al. (2018) integrated more than 200 datasets (including chromatin accessibility) to define 36 chromatin states (Yue Liu et al., 2018). However, the most routinely used classification is the one established by Sequeira-Mendes et al. (2014): the authors combined 16 chromatin features (including histone PTMs, histone variants, DNA methylation and GC content) to classify the

genome into nine different states, resulting in a simple yet precise topography. Each chromatin state is preferentially found on specific genomic features and is associated with a certain transcriptional activity: States 1 and 3 are localized on the 5' UTR and gene body of active genes, while State 5 is found on silenced genes and States 8 and 9 are mainly associated to intergenic regions and transposable elements. These states can therefore be used to predict the transcriptional activity of a gene. Furthermore, this analysis revealed the existence in *Arabidopsis thaliana* of a specific state characterized by the presence of the active mark H3K4me3 and the repressive mark H3K27me3 on the same locus.

The co-occurrence of these two antagonistic modifications was first observed on the promoter of developmental genes in mouse embryonic stem cells and termed bivalency (Bernstein et al., 2006). Bivalency was later found in mammalian nonpluripotent cells as well as in plants (Sequeira-Mendes et al., 2014; Voigt et al., 2013; Zeng et al., 2019). Sequential chromatin immunoprecipitations (Re-ChIP) revealed that bivalency is due to the co-existence of the two marks on the same (or neighbouring) nucleosome(s) rather than to a mixed population where some cells would carry H3K4me3 while others display H3K27me3 at the same locus (Bernstein et al., 2006; Sequeira-Mendes et al., 2014). As the action of certain PRC2 complexes can be blocked by the presence of H3K4me3, it is unlikely that both modifications could co-occur on the same H3 tail (Schmitges et al., 2011). Later studies could indeed demonstrate that bivalent domains consist, at least partly, of asymmetrically modified nucleosomes where one H3 tail carries H4K3me3 while the other carries H3K27me3 (Voigt et al., 2012). Bivalency is considered to be a mechanism poising genes by maintaining them in a reversible silenced state that allows a rapid activation at the appropriate time point during cell differentiation. Indeed, during differentiation, most of the bivalent domains are resolved into monovalent ones through the loss of one mark and these changes are associated with transcriptional activation (for H3K4me3 monovalent domains) or silencing (for H3K27me3 monovalent domains) (Bernstein et al., 2006). The presence of repressive marks at bivalent genes is thought to prevent their untimely activation by providing robustness against noises (Voigt et al., 2013). On the other hand, H3K4me3 maintains the bivalent loci in a transcriptionally accessible state which is necessary for their potential induction (Mas et al., 2018). Additionally to this effect *in cis*, nucleosome pull down assays performed with mouse nuclear extract showed that bivalency is recognized by specific readers such as SNF2-RELATED CREBBP ACTIVATOR PROTEIN (SRCAP) and LYSINE ACETYLTRANSFERASE 6B (KAT6B) (Bryan et al., 2021). As KAT6B is necessary for proper neuronal differentiation, this suggests that the recognition of bivalency by readers is also essential to its role in gene poising and activation. Interestingly, the second bivalency reader identified by Bryan et al. (2021), SRCAP, is known to be involved in the incorporation of the H2A.Z variant (Wong et al., 2007). In embryonic stem cells, H2A.Z is present on bivalent loci and is necessary for the deposition of H3K27me3 (Ku et al., 2012; Y. Wang et al., 2018). This association between bivalency and H2A.Z seems to be conserved in plants, as the topography from Sequeira-Mendes et al. (2014) showed that the State 2 (bivalent state) is also characterized by the presence of this variant. Recently, DEK-DOMAIN CONTAINING PROTEIN 2 (DEK2) was suggested as a potential plant bivalency reader as it is able to bind to H3K4me3-H3K27me3 peptides *in vitro*, but not to H3K4me3 or H3K27me3 monovalent peptides (Rayapuram et al., 2020, personal communication). DEK2 belongs to a family of four homologs in *Arabidopsis thaliana* (DEK1-4) and DEK2, DEK3 and DEK4 were identified as H2A.Z interactors (Brestovitsky et al., 2019). Furthermore, DEK3 was suggested to mediate H2A.Z distribution and its human and fly homologs hDEK and dDEK were shown

to be histone chaperones, reminiscent of the role of SRCAP in H2A.Z incorporation (Brestovitsky et al., 2019; Sawatsubashi et al., 2010). Altogether, this raises the possibility that the bivalency reading function might be a shared feature of DEK proteins and contributes to H2A.Z deposition at those loci.

In mammals, bivalency was mainly described as being associated with cell differentiation (Voigt et al., 2013). In plants, it has been shown to be involved in development (Jeong et al., 2009; Saleh et al., 2007; Xi et al., 2020) but recent reports indicate that it might also play a role in stress responsiveness as it could be detected on stress-regulated genes (Y. Dong et al., 2021; Zeng et al., 2019). A study of bivalency in *Solanum tuberosum* tubers showed that this chromatin signature spreads over a larger region of the gene body contrary to the strict promoter location in mammalian cells and, similarly to what was observed in embryonic stem cells, bivalency coincided with a greater chromatin accessibility (Zeng et al., 2019). Furthermore, it has been found on many cold-induced or repressed genes prior to cold exposure. Altogether, these studies led to the hypothesis that bivalency might be involved in plant stress responses, maintaining stress-inducible genes in an open chromatin conformation in naïve conditions, which might facilitate the binding of transcriptional regulators during a stress episode. However, this remains a conjecture and further work is required to examine whether bivalency might also participate to the regulation of *COR* genes in *Arabidopsis thaliana*.

1.2.4 Regulation of transcription by the chromatin environment

Nucleosomes have long been described as an obstacle to transcription as they prevent binding of the RNA polymerase (Knezetic & Luse, 1986). However, a recent study has shown that chromatin is actually a better template for transcription than naked DNA, proving that it also holds a positive role in the regulation of gene expression (Nagai et al., 2017). This demonstrates that the chromatin environment is a key determinant of transcriptional activity, mainly through the regulation of its structure. Indeed, both the initiation and elongation steps of transcription require the DNA template to be accessible to the RNA polymerase as well as the numerous transcription factors and co-activators composing the transcriptional machinery. While chromatin accessibility is regulated by inherent physical properties of chromatin modifications such as histone modifications or certain histone variants (see sections 1.2.1.1 and 1.2.2), it is also affected by them in *trans*, through the action of histone modification readers.

Histone modification readers are proteins that recognize and bind to a specific histone PTM, due to specific domains for each type of modification (Figure 4). For example, acetylation is read by Bromo domains while phosphorylation is recognized by SANT and BRCT domains as well as 14-3-3 proteins (Blakey & Litt, 2015; Macdonald et al., 2005; Stucki et al., 2005). The reading of lysine methylation is achieved by a variety of domains that form an aromatic cage around the methylated residue. Some of these domains belong to the Royal family, including the Chromo domain, PWWP domain, MBT repeat domain and Tudor domain (Maurer-Stroh et al., 2003). The latter has also been found to recognize methylated arginine (Côté & Richard, 2005). The Plant Homeo Domain (PHD) and Bromo-Adjacent Homology domain (BAH) are also involved in the reading of lysine methylation: PHD domains have a particular affinity for the higher methylated forms of H3K4 while BAH has been implicated in the recognition of

H3K27 and H3K9 (Du et al., 2012; Z. Li et al., 2018; Mellor, 2006; Y. Z. Zhang et al., 2020). On the other hand, certain domains recognize unmodified residues only. A single reader often carries several histone binding domains, recognizing the same or different modifications. For example, the DNA methyltransferase CHROMOMETHYLASE3 (CMT3) possesses a Chromo domain and a BAH domain that can both bind to H3K9me2 and this dual recognition is thought to increase its affinity and specificity (Du et al., 2012). The multiple domains can also ensure that a reader is targeted towards a specific chromatin state, i.e. a combination of different marks. This is exemplified by the human reader BROMODOMAIN PHD FINGER TRANSCRIPTION FACTOR (BPTF) that possesses a PHD-Bromo domain cassette that binds to H3K4me3 and H4K16ac, ensuring its preferential targeting to bivalent H3K4me3-H4K16ac nucleosomes (Ruthenburg et al., 2011). *Arabidopsis thaliana* also possesses dual readers: EARLY BOLTING IN SHORT DAYS (EBS) and SHORT LIFE (SHL) are two paralogs that both possess a PHD domain binding H3K4me3 and a BAH domain binding H3K27me3 (Qian et al., 2018; Z. Yang et al., 2018). Histone readers often have numerous functions as they might be involved in the propagation of the mark they recognize, the cross-talk between different modifications or the modulation of the chromatin structure. The latter is achieved by chromatin remodellers, which actively change the chromatin conformation by using ATP hydrolysis to slide nucleosomes across the DNA, transiently unwrap the DNA from a nucleosome or even exchange histones (B. Li et al., 2007). Additionally to the ATPase domain, chromatin remodellers possess domains enabling them to interact with specific histone modifications, such as the Bromo domain present in the members of the SWI/SNF family, the Chromo domains of the members of the CHD family or the SANT domain of the ISWI family, targeting them to act at specific loci (Clapier et al., 2017). Chromatin remodellers have been shown to be essential actors of transcriptional initiation and elongation (Clapier & Cairns, 2009; Mizuguchi et al., 1997; Roberts & Winston, 1997).

The chromatin environment and chromatin readers can also affect transcription more directly by guiding the binding of transcription factors or even of the RNA polymerase at specific loci. For example, in *Arabidopsis thaliana*, DEK3 and DEK4 have been shown to promote the expression of flowering repressor genes by recruiting RNA polymerase II at these loci (Zong et al., 2021). Previous work had shown that these proteins can bind to H2A.Z (Brestovitsky et al., 2019), which suggest that they might recruit the transcriptional machinery at specific genes based on their chromatin state. Altogether, this demonstrates the essential role played by the chromatin environment in general and histone PTMs in particular in the regulation of gene expression, highlighting the necessity of examining the chromatin state when investigating processes involving a transcriptional response.

1.3 THE ROLE OF CHROMATIN REGULATION IN THE RESPONSE TO ABIOTIC STRESS

In recent years, many studies examined the role of chromatin regulation in the plant stress response, mainly focusing on the involvement of histone PTMs and histone variants in the induction of stress responsive genes and their findings are summarized below (Asensi-Fabado et al., 2017; Banerjee et al., 2017; J.-M. Kim et al., 2015).

1.3.1 Chromatin-mediated regulation of the cold stress response

As discussed earlier (section 1.1.4), stress responsive genes are silenced when a plant grows in optimal conditions. In the case of low temperatures, this is thought to be at least partially achieved through the repressive mark H3K27me3. Indeed, prior to cold stress, many cold-responsive genes carry H3K27me3 (Vyse et al., 2020; X. Zhang et al., 2007). Furthermore, many of them (such as *COR15A* and *KIN1*) are repressed in the absence of cold through the action of the PcG proteins EMF1 and EMF2, which directly bind to loci carrying H3K27me3 (S. Y. Kim et al., 2010, 2012; Kleinmanns & Schubert, 2014). The PcG protein MSI4/FVE also acts as a repressor of the CBF/DREB pathway: in *fve* mutants, the *COR* genes such as *COR15A* are up-regulated at ambient temperatures and over-induced during cold exposure (H. J. Kim et al., 2004). This repression is mediated by a direct binding of FVE to *COR* genes (Jeon & Kim, 2011). Moreover, the CLF-interacting protein BLISTER (BLI) is required for the repression of certain cold-inducible genes at ambient temperatures while during a cold episode, it promotes their induction and therefore chilling tolerance (Kleinmanns et al., 2017; Purdy et al., 2011). This H3K27me3-mediated repression is not unique to the cold response: indeed, the PcG protein MSI1 has been shown to be required for the repression of the drought-stress response in favourable conditions as its absence led to the up-regulation of drought-responsive genes (Alexandre et al., 2009). Interestingly, during cold exposure, the transcriptional induction of two key *COR* genes, *COR15A* and *GOLS3*, correlates with a decrease in their H3K27me3 levels which is independent from the nucleosome occupancy, suggesting that cold triggers an active H3K27me3 demethylation (Kwon et al., 2009). Whether H3K27me3 removal is necessary for the induction of those genes or a rather a consequence of the increased transcription remains unclear. Overall, these studies suggest that *COR* genes are repressed in naïve conditions at least partially through the presence of H3K27me3 and its reading by various PcG and PcG-interacting proteins. This repression might then be lifted upon cold exposure through the removal of H3K27me3, pointing to this repressive mark as a key player in the transcriptional regulation of cold-responsive genes and therefore in the stress response.

However, H3K27me3 is not the only chromatin mark affected by cold exposure. Indeed, during a cold episode, the promoters of *COR* genes gain H3 acetylation, in particular H3K9ac and H3K14ac and this accumulation is rapidly reversed when returning to ambient temperature (Lim et al., 2020; Pavangadkar et al., 2010). The cold-induced histone acetylation was also observed in crops: in *Zea mays* for example, cold triggered a switch in the chromatin status of repetitive sequences from silenced to active, as they lost H3K9me2 but gained H3K9ac, which increased chromatin accessibility (Yong Hu et al., 2012). In *Oryza sativa*, *OsDREB1* showed an accumulation of H3K9ac, H3K14ac and H3K27ac upon cold exposure that correlated with an increased presence of RNA polymerase II, an enhanced chromatin accessibility and transcriptional activation (Roy et al., 2014). In *Arabidopsis thaliana*, this acetylation is prevented in the absence of cold by the histone deacetylase HD2C which binds to *COR* promoters thanks to HOS15 and POWERDRESS (PWR) (Lim et al., 2020; J. Park et al., 2018). Upon cold exposure, HOS15 mediates the degradation of HD2C, allowing the acetylation and therefore the transcriptional activation of the *COR* genes. While several proteins involved in histone acetyltransferase complexes such as GENERAL CONTROL NON DEREPRESSIBLE 5 (GCN5) and TRANSCRIPTIONAL ADAPTR 2b (ADA2b) are necessary for a proper induction of *COR* genes, to date none of them has been identified as being responsible for the cold-induced acetylation of histones (Pavangadkar et al., 2010; Vlachonasios et al., 2003). On the

other end, deacetylation is also necessary for cold acclimation: global H3 and H4 deacetylation could be observed upon cold exposure and treating the plants with the histone deacetylase inhibitor trichostatin A hinders the proper induction of certain *COR* genes (Yong Hu et al., 2011). In accordance with these observations, the histone deacetylase HDA6 has been shown to function as a positive regulator of acquired freezing tolerance in *Arabidopsis thaliana* (To et al., 2011). Histone deacetylases were proposed to be recruited at *COR* genes through FVE, as this PcG protein has been shown to bind both *COR* genes and HDA6 (Gu et al., 2011; Jeon & Kim, 2011). This indicates that histone acetylation and H3K27me3 methylation could be involved in a cross-talk contributing to the transcriptional regulation of *COR* genes.

These changes in histone modifications coincide with variations in chromatin accessibility: Raxwal et al. (2020) showed that upon cold exposure, the chromatin of *Arabidopsis thaliana* tends to adopt a more opened conformation. In addition to the *cis* effect of histone PTMs on the structure of chromatin, recent studies reported the active role played by chromatin remodellers in this process. For example, SWITCH/SUCROSE NON FERMENTING 3C (SWI3C), a core subunit of the SWI/SNF chromatin remodeller complex, is a negative regulator of freezing tolerance (Gratkowska-Zmuda et al., 2020). SWI3C binds to the locus of several cold-induced genes such as *CBF1* and *ICE1* in a temperature-dependant manner and regulates nucleosome positioning, ultimately affecting their expression. Furthermore, the deacetylase HD2C interacts with SWI/SNF chromatin remodellers to regulate the heat response via the control of heat-responsive genes and it is involved in the cold response (Buszewicz et al., 2016; Lim et al., 2020; J. Park et al., 2018). One can therefore speculate that a cross-talk between histone acetylation and chromatin remodelling might also occur during cold episodes. A similar link could exist between chromatin remodelling and histone methylation: the chromatin remodeller PICKLE (PKL) binds preferentially loci enriched in H3K27me3 and is required for a proper cold acclimation as it regulates the induction of *CBF3* (R. Yang et al., 2019; H. Zhang et al., 2008, 2012).

Chromatin accessibility was also linked to H3K4me3-H3K27me3 bivalency in the work of Zeng et al. (2019) in *Solanum tuberosum* tubers. As mentioned earlier (section 1.2.3), the authors observed that many genes induced by cold became more accessible, and this increased accessibility was even more pronounced for previously bivalent loci. Furthermore, many genes gained bivalency during cold exposure. As the cold-opening loci identified by Raxwal et al. (2020) were enriched in H3K4me3, it is possible that *Arabidopsis thaliana* presents a similar interplay between bivalency and chromatin accessibility. At any rate, several recent reports indicate that bivalency might play a key role in the potentiation of stress responsive genes: Zeng et al. (2019) showed that genes marked with bivalency at ambient temperature were more likely to be differentially expressed in cold-treated *Solanum tuberosum* tubers. This seems to be conserved in *Arabidopsis thaliana* as Dong et al. (2021) demonstrated that the co-occurrence of H3K27me3-H3K4me3 on TARGET OF RAPAMYCIN (TOR) target genes allows them to rapidly transition between active and silenced states. While H3K27me3 was already investigated in the context of cold (see above), the potential role of H3K4me3 in the response to this stress remains undiscovered. However, it has been found to be essential for the response to other abiotic stresses: indeed, the deposition of H3K4me3 by the methyltransferase ATX1 is required for drought tolerance and the induction of drought-responsive genes (Yong Ding et al., 2011). On the other hand, the H3K4me3 demethylase JMJ17 is a negative regulator of the dehydration resistance as it prevents the over-methylation

(and therefore induction) of drought-responsive genes (Huang et al., 2019). Furthermore, JMJ17 directly controls the levels of H3K4me3 on *OST1*, a positive regulator of ICE1, suggesting that it might also play a role in the cold response. Taken together, these studies do not only suggest H3K4me3 as an interesting candidate for the transcriptional regulation of cold-responsive genes but they also once more demonstrate the importance of investigating the role of the combination of several chromatin marks in gene expression (in particular H3K4me3-H3K27me3 bivalency) instead of examining them individually.

As described previously (section 1.2.2), the chromatin environment is further diversified by the existence of a multitude of histone variants. To the best of our knowledge, their potential role in the cold stress response has not been demonstrated yet. However, a recent transcriptomic analysis of chromatin regulators revealed that numerous histone variants are induced by low temperatures or during deacclimation, suggesting that they might be involved in the response to this particular stress (Vyse et al., 2020). Additionally, several studies focusing on other abiotic stresses demonstrated the essential role of certain histone variants in the transcriptional regulation of stress-inducible genes. In particular, H2A.Z has been shown to be associated with gene responsiveness to adverse environmental conditions: the higher the level of H2A.Z on a gene, the stronger its induction during drought or heat stress exposure (Brestovitsky et al., 2019; Sura et al., 2017). Furthermore, during a heat or drought stress episode, H2A.Z is evicted from genes, leading to their induction (Cortijo et al., 2017; S. V. Kumar & Wigge, 2010; Sura et al., 2017). This variant is not the only one that has been involved in the stress response: indeed, the linker histone variant H1.3 has been shown to be necessary for the adaptation to low light and drought stress (Rutowicz et al., 2015). In its absence, the plants are not able to slow down their growth upon stress exposure. The expression of H1.3 is induced upon drought stress but also by ABA treatment (Ascenzi & Gantt, 1997). As drought and cold responses share many common regulators and numerous *COR* genes are also ABA-responsive, H1.3 might be involved in the response to low temperatures as well. So far, to the best of our knowledge, no study examined this hypothesis nor the potential involvement of any other histone variant in the cold response in general.

Altogether, while some studies revealed that cold triggers changes in the chromatin status of stress-responsive genes, whether and how those variations impact the induction of the underlying genes remains unclear. Furthermore, more chromatin features should be investigated in order to obtain a more comprehensive view of the role of the chromatin environment on the transcriptional response of *COR* genes.

1.3.2 Cold stress memory might be encoded at the chromatin level

1.3.2.1 Chromatin modification plays a key role in abiotic stress memory

In addition to their role in controlling the transcription of stress-responsive genes, chromatin modifications have been implicated in transcriptional stress memory. As described earlier, the memory of various stresses requires the higher induction of ++ trainable genes upon a second stress and/or the sustained induction of certain genes during the lag phase (see section 1.1.3.2). Since transcriptional memory can persist over several stress-free days, it was hypothesized that it might be encoded at the chromatin level (Hilker et al., 2015). Indeed, the enhanced induction of drought-responsive genes was shown to be due to an accumulation of

H3K4me3 on their promoters during the priming event, which was retained over the lag phase (Yong Ding, Fromm, et al., 2012). This was accompanied by a sustained accumulation of Ser5P RNA polymerase II, which is a marker of transcription initiation and poising. The marking of the promoters of drought-trainable genes by H3K4me3 and Ser5P RNA polymerase II could also be triggered by a JA treatment (N. Liu & Avramova, 2016). A JA treatment did not lead to the induction of those genes, proving that the deposition of the mark and the poised polymerase could also occur independently of transcription. A similar mechanism has also been observed for the memory of osmotic stresses, where the priming-induced accumulation of H3K4me3 persists for up to five days (Feng et al., 2016). Finally, the memory of heat stress also involves the maintenance of the heat-triggered trimethylation of H3K4 on certain trainable heat-shock genes, which leads to their enhanced induction during the triggering stress (Lämke et al., 2016).

However, H3K4me3 is not the only methylation mark that has been implicated in stress memory. Indeed, heat priming triggers a localized loss of the repressive mark H3K27me3 on certain heat shock genes occurring through the action of the JMJ demethylases JMJ30, JMJ32, ELF6 and REF6 (Yamaguchi et al., 2021). This loss is maintained during the lag phase and leads to the higher expression of the affected genes upon a subsequent heat stress compared to non-primed plants. Interestingly, an overlap exists between genes showing a sustained H3K27me3 loss and H3K4me3 accumulation upon heat priming, suggesting the existence of a cross-talk between the two antagonistic marks that leads to the trainable behaviour of those specific heat shock genes. Similarly, osmotic stress triggers an active removal of H3K27me3, leading to a fragmentation of the H3K27me3 islands (Sani et al., 2013). This loss is maintained for several days after the stress subsides, the exact duration varying depending on the gene considered. As the persisting low levels of H3K27me3 correlated with a higher induction of the affected gene upon a second stress episode, it was suggested that this change in the chromatin status might be the support of the osmotic stress memory observed by the authors. Interestingly, some genes that were repressed during the priming stress showed a gain of H3K27me3 that persisted after the stress subsided. Those genes were repressed to a higher magnitude during the triggering episode, indicating that this methylation mark might be involved in the fine-tuning of the response to subsequent stress episodes.

Additionally to lysine methylation, stress memory was also linked to histone acetylation. Indeed, priming plants with an initial *Pseudomonas* infection or benzothiadazole (a compound inducing disease resistance in plants) treatment led to a higher induction of certain *WRKY* transcription factors in primed and triggered plants compared to triggered-only plants (Jaskiewicz et al., 2011). This enhanced induction was linked to the persisting accumulation not only of H3K4me3 but also H3ac and H4ac. Likewise, Singh et al. (2014) showed that priming plants with abiotic stresses such as repeated heat or cold exposure could improve plant resistance to a subsequent pathogen infection thanks to the maintenance of H3K9ac and H3K14ac by the histone acetylase HAC1.

As explained previously, histone modifications and chromatin structure are tightly linked, particularly through the action of chromatin remodellers (see section 1.2.4). It is therefore not surprising that the latter were also implicated in transcriptional memory. The sustained induction of heat responsive genes is essential for heat memory and requires the action of FORGETTER1 (FGT1) (Brzezinka et al., 2016). FGT1 interacts with ISWI (CHROMATIN REMODELING FACTOR (CHR) 11 and 17) and SWI/SNF (BRAHMA (BRM)) chromatin

remodellers and recruits them to its target genes. There, they maintain a lowered nucleosome occupancy around the TSS, which is favourable to transcription. Interestingly, FGT1 possesses a PHD domain and preferentially binds to the State 2/bivalent loci described by Sequeira-Mendes et al. (2014) (see section 1.2.3) (Brzezinka et al., 2016). This suggests that FGT1 might integrate the information provided by the H3K4me3 and H3K27me3 to facilitate transcriptional activity at trainable and sustained genes. The Chromatin Assembly Factor 1 (CAF1) complex has also been implicated in the regulation of the transcriptional memory of biotic stress (Mozgová et al., 2015). Composed of FASCIATA 1 (FAS1), FAS2 and MSI1, this complex acts as a histone chaperone and is involved in the deposition of nucleosomes. The *fas* mutants are constitutively primed against biotic stresses: triggered-only *fas* mutants display an over-induction of *PR* genes that is similar to what is observed in primed and triggered wild-type plants. This over-induction is linked to a decreased nucleosome occupancy as well as an accumulation of H3K4me3 on those genes prior to the triggering stress, which are normally induced by priming in wild-type plants. CAF1 is therefore proposed to act as a negative regulator of priming, preventing the plants from being constitutively primed.

Collectively, all those studies highlight the essential role of chromatin modifications and structure in transcriptional memory. However, whether they also act in cold stress memory remains unclear. While the cold-induced loss of H3K27me3 on *COR15A* and *GOLS3* described earlier persists for several days, it does not lead to a higher or faster re-induction of the genes when the plants are re-exposed to cold (Kwon et al., 2009). Yet, many chromatin modifiers are regulated at the transcriptional and/or post transcriptional level during cold exposure and deacclimation, suggesting that they might be involved in cold stress memory (Vyse et al., 2020). Furthermore, it is already well-known that cold-triggered changes of the chromatin status of certain genes persist even after the cold subsides, affecting their transcriptional activity: additionally to its action as a stressor, cold also acts as a development cue for the plants, triggering their flowering upon return to ambient temperature. This process, called vernalization, relies on chromatin modifications and will be described in more details in the next section.

1.3.2.2 Cold memory: the example of vernalization

Vernalization refers to the acquisition of the ability to flower at ambient temperature after being exposed to cold (Chouard, 1960). Both vernalization and cold stress memory rely on the ability of the plant to memorize episodes of low temperatures, however the pathways involved in both processes are truly distinct and independent from one another (Bond et al., 2011; F. Li et al., 2021). Indeed, none of the major cold stress response regulators are involved in vernalization, and both processes are triggered by different temperatures and with distinct kinetics. In light of these differences and as vernalization is a developmental response to cold rather than a stress response, it is out of the scope of this thesis and will only be briefly summarized below as an example of how episodes of low temperatures can be memorized at the chromatin level. In *Arabidopsis thaliana*, flowering time is controlled by several pathways converging, among others, on the floral integrator FLOWERING LOCUS T (FT), which promotes flowering (Hepworth & Dean, 2015). The expression of *FT* is negatively regulated by the floral repressor FLOWERING LOCUS C (FLC). Vernalization relies on the gradual silencing of *FLC* upon cold exposure, thereby lifting the repression of *FT* and inducing flowering (Sheldon et al., 2000). When the plant is experiencing cold, H3K27me3 and H3K9me3 are progressively accumulated

at the *FLC* locus while H3K36me3 and histone acetylation are lost, which altogether create a silenced chromatin state leading to the repression of *FLC* (Bastow et al., 2004; Shindo et al., 2006; H. Yang et al., 2017). The deposition of H3K27me3 on *FLC* is achieved by a PHD-PRC2 complex composed of the PRC2 proteins VRN2, SWN, FERTILIZATION-INDEPENDENT ENDOSPERM (FIE) and MSI1 and three PHD finger proteins: VRN5, VERNALIZATION INSENSITIVE (VIN3) and VIN3-LIKE 1 (VEL1) (De Lucia et al., 2008). Among the proteins identified as vernalization actors, VIN3 is the only one whose expression is induced by cold (Sung & Amasino, 2004). VIN3 thereby acts as a thermosensor for vernalization, registering the length of the cold period and triggering the silencing of *FLC* (Antoniou-Kourouniotti et al., 2018; Hepworth et al., 2018). Upon cold exposure, the PRC2 complex is recruited by VIN3 at a specific region around the first exon of *FLC*, called the nucleation site, and deposits H3K27me3 there (Angel et al., 2011; De Lucia et al., 2008). Once the plant is returned to ambient temperature, *FLC* remains silent while H3K27me3 spreads over its whole locus (De Lucia et al., 2008). In the absence of the H3K27 tri-methyltransferase CLF and the H3K27me3-binding protein LIKE-HETEROCHROMATIN PROTEIN 1 (LHP1), H3K27me3 spreading does not occur and *FLC* expression slowly increases, proving that the transcriptional memory of cold displayed by *FLC* is encoded at the chromatin level through the sustained accumulation of H3K27me3 (H. Yang et al., 2017). This transcriptional memory is highly stable, as the trimethylation marks are retained over *FLC* for the remainder of the plant life and are only reset through active demethylation by ELF6 during embryogenesis (Crevillén et al., 2014; Sheldon et al., 2008). Vernalization therefore serves as a proof of concept that cold can be memorized at the chromatin level, impacting gene transcription even after the cold subsided. This adds weight to the hypothesis that cold stress transcriptional memory might be encoded by chromatin modifications.

1.4 AIMS OF THIS STUDY

The response of plants to cold requires a massive transcriptome reprogramming, including the rapid induction of *COR* genes. The tight regulation of the expression of those genes at every step of the plant life cycle is essential to its survival: in the absence of cold, they have to be repressed so as to avoid growth impairment but they must be rapidly up-regulated when the temperature drops in order to avoid damages (Figure 3). While they return to their silenced state when the environmental conditions are favourable again, several studies indicate that they might display a modified transcriptional response (e.g. faster or stronger induction) should the cold ever re-occur, proving that plants possess a transcriptional memory of cold. So far, investigative efforts were concentrated on the role of various transcription factors in the induction of *COR* genes, whose results are summarized in the previous sections (see 1.1.2). However, very little work has focused on a potential contribution of chromatin regulation to this process. Furthermore, the molecular mechanisms of cold memory remain undiscovered. The present study therefore aims at elucidating the potential role of chromatin modifications in the transcriptional regulation of *COR* genes, focusing around four key questions:

- (i) How are *COR* genes repressed prior to the cold exposure while being potentiated for a rapid induction? Previous work from our lab has hinted at a role of H3K27me3 in this process (Vyse et al., 2020). However, the influence of the chromatin environment onto gene expression cannot be reduced to the absence or presence of a single histone PTM as it involves cross-talks between multiple histone marks, variants and other chromatin modifier actors. A

comprehensive and unbiased *in silico* approach will therefore be used to examine the chromatin environment at *COR* genes prior to cold exposure to identify more chromatin features involved in their repression. These chromatin features will then be further characterized *in vivo*, with the aim of predicting the function and transcriptional activity of genes based on their chromatin state.

(ii) Does the chromatin environment of *COR* genes undergo changes during cold exposure, rendering these loci more favourable to transcription? The examination of other stresses such as heat and drought has demonstrated that the induction of gene expression is associated with an accumulation of the activating mark H3K4me3 (Yong Ding, Fromm, et al., 2012; Van Dijk et al., 2010). On the other hand, previous studies have shown that cold leads to the removal of the repressive mark H3K27me3 on certain *COR* genes (Kwon et al., 2009; Vyse et al., 2020). Therefore, the fate of these two antagonistic methylation marks upon cold exposure will be examined at the genome wide level and correlated with transcriptional changes.

(iii) Are those potential changes of the chromatin environment of *COR* genes necessary for their transcriptional induction? To that end, a screening of chromatin modifier mutants will be performed, in order to identify the actors responsible for those cold-induced changes. This will allow the investigation of the transcriptional activity of *COR* genes in mutant plants where the chromatin status is not altered by cold and thereby to determine whether chromatin changes are required for their induction or whether the two processes are independent.

(iv) Is the memory of cold stress encoded at the chromatin level? The transcriptomic response of plants to a second cold exposure differs from the first one, indicating that they are able to memorise this stress (Byun et al., 2014; Zuther et al., 2019). Investigations of heat and drought memory have shown that it requires stress-induced changes in certain chromatin marks such as H3K4me3 and H3K27me3 to be maintained over the lag phase, which leads to a refined transcriptomic response to a second stress (Yong Ding, Fromm, et al., 2012; Lämke et al., 2016; Sani et al., 2013; Yamaguchi et al., 2021). Thus, the persistence of cold-induced changes in H3K27me3 and H3K4me3 levels will be examined by ChIP-qPCR and correlated to changes in the transcriptional response upon cold re-exposure to examine the possibility that cold stress memory is also encoded at the chromatin level.

2 MATERIAL AND METHODS

2.1 PLANT MATERIAL

Arabidopsis thaliana seeds were stratified at 4°C in the dark for three days and grown on ½ MS media supplemented with Gamborg B5 vitamins (Duchefa) plates with 1.5% (w/v) plant agar (Duchefa) in short day conditions (8 h light, 16 h darkness) at 20°C. Cold stresses were performed at 4°C in short day conditions (8 h light, 16 h darkness). *A. thaliana* accession Columbia-0 (Col-0) was used as a wild type (Wt). The transgenic lines used in this study are described in Table 1. The oligonucleotides used for genotyping are listed in Suppl. Table 1.

Table 1: Transgenic lines used in this study

Mutant	Type of mutation	Source
<i>atx1</i>	T-DNA insertion line SALK_149002	NASC
<i>dek2</i>	T-DNA insertion line SALK_137152C	Rayapuram and Hirt, 2020, personal communication
DEK2-YFP	DEK2::DEK2-YFP complementation line	Rayapuram and Hirt, 2020, personal communication
<i>ebs</i>	T-DNA insertion line WiscDsLoxHs072_11H	Z. Li et al., 2018
<i>elf6.3</i>	T-DNA insertion line SALK_074694	NASC
<i>elf6c</i>	CRISPR line causing a 242 bp deletion	W. Yan et al., 2018
<i>jmj13</i>	CRISPR line causing a single bp deletion	W. Yan et al., 2018
<i>jmj30</i>	T-DNA insertion line SAIL_811_H12	NASC
<i>jmj32</i>	T-DNA insertion line SALK_205401	NASC
<i>jmj30-jmj32</i>	T-DNA insertion lines GABI_454C10 & SALK_003313	Gan et al., 2014
<i>qm</i>	<i>elf6-ref6-jmj30-jmj32</i> quadruple mutant (SALK_074694, SALK_001018, GABI_454C10 & SALK_003313)	Yamaguchi et al., 2021
<i>ref6c</i>	CRISPR line causing a 268 bp deletion	W. Yan et al., 2018
<i>ros1</i>	T-DNA insertion line SALK_045303	NASC
<i>shl</i>	T-DNA insertion line FLAG_546H05 (introgressed into Col-0)	Z. Li et al., 2018
<i>vin3</i>	T-DNA insertion line SALK_004766	NASC

2.2 ELECTROLYTE LEAKAGE

Plants were grown as described previously (section 2.1) for 21 days and placed at 4°C for three days. For the memory experiments, plants were then placed back at ambient temperature for another week before encountering a second 3-day cold exposure. The freezing tolerance was then measured by electrolyte leakage assay using a protocol adapted from Hinch and Zuther (2014). Three to four technical replicates were performed for each biological replicate. For each sample, five to six temperature points were measured, using a pool of shoot tissue of five to eight seedlings. The LT₅₀ was determined using the non-linear regression *log(agonist) vs response* from the GraphPad Prism version 7.0 (GraphPad Software).

2.3 TRANSCRIPTOMICS

2.3.1 RNA extraction and RT-qPCR

Samples for RNA extraction were harvested four hours after the end of the night. After grinding in pre-cooled mortars, total RNA was extracted from whole seedlings using the innuPREP Plant RNA Kit (Analytik Jena) according to the manufacturer's instructions. RNA concentrations were measured using the Nanodrop ND-1000 Spectrophotometer (Nanodrop Technologies). Samples were treated with DNaseI (Thermo Scientific) to remove any potential contamination with genomic DNA, according to the kit's instructions. cDNA was synthesized using the RevertAid Reverse Transcriptase kit (Thermo Scientific) according to the manufacturer's instructions, using oligo(dT) and 0.5 µg of DNase-treated RNA. The obtained cDNA was diluted 1:20 and subsequently used for qPCR analyses. This was performed using the KAPA SYBR FAST qPCR 2X Master Mix (KAPA Biosystems) or the ROX SYBR 2X blue Master Mix (Takyon) and the QuantStudio5 RT-qPCR system (Applied Biosystems). The composition of the qPCR mix is described in Table 2. Each reaction was performed in triplicates and the qPCR was performed according to the program shown in Table 3. All primers used in this study are listed in Suppl. Table 2.

Table 2: qPCR reaction mix for one sample

Component	Amount (µL)
SYBR master mix (2X)	5
Forward primer (10 µM)	0.2
Reverse primer (10 µM)	0.2
Template cDNA (diluted 1:20)	2
Water	0.8

Table 3: qPCR program

Step	Temperature	Time	
Initialization	95°C	3 minutes	
Denaturation	95°C	3 seconds	x40 cycles
Annealing, Elongation & Data acquisition	60°C	30 seconds	
Denaturation	95°C	15 seconds	Melt curve stage
Complete annealing	60°C	1 minute	
Dissociation curve & Data acquisition	0.05°C/s up to 95°C	-	

Data analysis was performed using the Pfaffl method (Pfaffl, 2001). Shortly, the efficiency of each primer pair was first determined. To this end, a pool of all cDNA samples was prepared and diluted 1:10 and 1:100. These three dilutions were used to plot a standard curve of the Ct value as a function of the log₁₀ of the dilution factor. A linear regression was applied to the standard curve, and the slope was used to compute the efficiency of the primer pair according to the following equation:

$$Efficiency = 10^{-\frac{1}{slope}}$$

Then, the Ct values of the technical triplicates were averaged and the relative expression of the gene of interest (GOI) compared to the housekeeping gene (HKG) was calculated using the following equation:

$$\text{Relative Expression} = \frac{\text{efficiency GOI}^{\text{Ct mean GOI}}}{\text{efficiency HKG}^{\text{Ct mean HKG}}}$$

Unless specified otherwise, *TAP42 INTERACTING PROTEIN OF 41 KDA (TIP41) (AT4G34270)* was used as the housekeeping gene. The average and standard error of the mean (sem) of at least three biological replicates were then computed.

2.3.2 RNA-seq

RNA samples were extracted and DNaseI-treated as described in the previous section (2.3.1). The library preparation and sequencing were performed by Novogene. Briefly, after mRNA library preparation by poly-A enrichment, the paired-end sequencing of the samples was performed using the NovaSeq 6000 platform (Illumina) with a read length of 150 bp. Three biological replicates were analysed for each condition and at least 20 million reads were produced for each sample. A summary of the number of reads is given in Table 4.

Table 4: Read counts of the RNA-seq samples. As sequencing was performed in a paired-end manner, the numbers here are the numbers of paired-reads.

	Reads	Mapped reads
N_1	24,779,231	23,980,916
N_2	20,826,059	20,119,503
N_3	20,562,189	19,899,195
Ph_1	21,818,003	20,879,042
Ph_2	20,378,678	19,759,227
Ph_3	21,699,737	21,031,400
Pd_1	21,777,122	21,144,600
Pd_2	21,415,128	20,678,212
Pd_3	23,612,407	22,825,901

2.4 WESTERN BLOT

For protein extraction, 100 mg of 21 day-old seedlings were harvested 4 h after the end of the night and flash-frozen in liquid nitrogen. They were grinded to a fine powder in a pre-cooled mortar and resuspended in 1 mL of buffer A (Table 5). After filtering through Miracloth (Millipore), the samples were centrifuged for 20 minutes at 4°C and 4,000 rpm. The pellets were resuspended in 0.3 mL of buffer B (Table 5) and centrifuged 10 min at 4°C and 13,000 rpm. The pellets were resuspended in 0.3 mL of buffer C and carefully layered onto 0.3 mL of fresh buffer C (Table 5). The samples were then centrifuged for 1 h at 4°C and 13,000 rpm. Pellets were finally resuspended into 100 µL of nuclear lysis buffer (Table 5).

Table 5: Composition of the buffers used in the extraction of chromatin enriched proteins

Buffer A	Buffer B	Buffer C	Nuclear Lysis buffer
0.4 M sucrose	0.25 M sucrose	1.7 M sucrose	50 mM Tris-HCl pH 8
10 mM Tris-HCl pH 8	10 mM Tris-HCl pH 8	10 mM Tris-HCl pH8	10 mM EDTA
10 mM MgCl ₂	10 mM MgCl ₂	2 mM MgCl ₂	
	1% (v/v) Triton-X	0.15% (v/v) Triton-X	1% (w/v) SDS
5 mM BME	5 mM BME	5 mM BME	
0.5 µL/mL AEBSF protease inhibitor (Thermo Scientific)	0.5 µL/mL AEBSF protease inhibitor (Thermo Scientific)	0.5 µL/mL AEBSF protease inhibitor (Thermo Scientific)	
10 µL/mL Plant Protease inhibitor Cocktail (Sigma)	10 µL/mL Plant Protease inhibitor Cocktail (Sigma)	10 µL/mL Plant Protease inhibitor Cocktail (Sigma)	10 µL/mL Plant Protease inhibitor Cocktail (Sigma)

The protein concentration was assessed using the Qubit protein assay (Thermo Fisher Scientific) according to the manufacturer's instructions, by combining 5 µL of each sample with 195 µL of working solution. The concentration of the samples was then diluted to the one of the less concentrated sample using nuclear lysis buffer and an appropriate amount of 5X SDS buffer (Table 6) was added before incubating the samples at 95°C for three minutes.

Table 6: Composition of the buffers used in the SDS-PAGE and Western Blot

5X SDS buffer (10 mL)	10X SDS Running buffer (1 L)	1X WB running buffer	1X PBS-T (pH 7.4) (1 L)
0.0025 g bromophenol blue	10 g SDS	1X SDS Running buffer	8g NaCl
0.771 g DTT	30.3 g Tris	20% (v/v) MeOH	0.2 g KCl
5 mL glycerol	144.1 g Glycin		1.42 g Na ₂ HPO ₄
1 g SDS			0.24 g KH ₂ PO ₄
2.5 mL 1 M Tris pH 6.8			1% (v/v) Tween 20

The protein separation was performed by SDS-PAGE, using a 5% stacking gel and a 15% resolving gel and 1X SDS running buffer (Table 6 and Table 7) in a Bio-Rad system. PageRuler (Thermo Fisher Scientific) was used as a protein ladder and 10 to 20 µg of proteins were loaded for each sample. The electrophoresis was ran at 50 mA for 90 minutes.

Table 7: Composition of the SDS gels

5% Stacking gel (6 mL)	15% Resolving gel (20 mL)
750 µL 40% (v/v) acrylamide mix	7.5 mL 40% (v/v) acrylamide mix
600 µL 1 M Tris pH 6.8	5 mL 1 M Tris pH 8.8
60 µL 10% (w/v) SDS	200 µL 10% (w/v) SDS
60 µL 10% (w/v) APS	200 µL 10% (w/v) APS
6 µL TEMED	20 µL TEMED

After electrophoresis, the proteins were transferred to an Immobilon-FL 0.45 µm PVDF membrane (Merck Millipore). The membrane was activated by incubation in MeOH for 20 seconds, followed by a rinsing in water for two minutes and equilibration in WB running buffer

for 30 min (Table 6). At the same time, the SDS gels were also equilibrated in WB running buffer. After equilibration, the gels were deposited onto Whatman paper (Cytiva) soaked in WB running buffer, covered with the membrane and another soaked Whatman paper. The transfer was performed in a Bio-Rad system at 4°C for 2 h at 250 mA.

After transfer, the membrane was blocked in PBS Odyssey blocking solution (Li-Cor) for 1 h at room temperature. It was then placed into PBS Odyssey blocking solution supplemented with 0.1% (v/v) Tween 20 (Sigma) and 4 µL of anti-H3K4me3 or anti-H3K27me3 antibody (Table 8). It was subsequently incubated overnight at 4°C. 2 µL of anti-H3 antibody were added and the membrane was incubated at room temperature for one hour. Afterwards, it was washed four times for five minutes in PBS-T (Table 6). The two secondary antibodies were then added (Table 8) and the membrane was incubated for 2 h in the dark at room temperature. The membrane was washed four times for five minutes in PBS-T and carefully dried for 1 h in Whatman paper (Cytiva). Finally, the imaging was performed using the Image Studio Lite software (Li-Cor, version 5.2). H3 intensity was used to normalize the intensity of H3K27me3 and H3K4me3.

Table 8: Antibodies used for Western Blot and chromatin immunoprecipitation

Antibody	Catalog number	Company	Volume used for WB	Volume used for IP	Host
Anti-H3pan	C15200011	Diagenode	2 µL	1.4 µL	Mouse
Anti-H3K4me3	C15410003	Diagenode	4 µL	0.7 µL	Rabbit
Anti-H3K27me3	C15410195	Diagenode	4 µL	0.7 µL	Rabbit
IgG Rabbit	C15410206	Diagenode	-	1 µL	Rabbit
IRDye 680 RD	-	Li-Cor	0.266 µL	-	Goat
IRDye 800 CW	-	Li-Cor	0.533 µL	-	Goat

2.5 EPIGENOMICS

2.5.1 Chromatin immunoprecipitation

For chromatin immunoprecipitation (ChIP), 0.5 g to 1 g of 21 day-old seedlings were harvested four hours after the end of the night. The cross-link reaction and the chromatin extraction were performed as previously described in Vyse et al. (2020). The antibodies and respective volumes used for the immunoprecipitation are listed in Table 8.

The quantitative PCR was performed using the reactants, device and program described previously (section 2.3). Primer sequences can be found in Suppl. Table 3 and the primer efficiencies were calculated as described in section 2.3. Each reaction was performed in triplicates, whose Ct values were averaged. The %input was computed for each sample and immunoprecipitation using the following equation:

$$\%input = 100 \times \frac{Volume_{input}}{Volume_{IP}} \times efficiency^{Ct(input) - Ct(IP)}$$

When mentioned, the %input were normalized to an appropriate control locus, depending on the analysed histone mark.

2.5.2 ChIP-seq

Chromatin immunoprecipitation was performed as described previously (section 2.5.1). The DNA was purified and concentrated using the ChIP DNA Clean and Concentrator kit according to the manufacturer's instructions (Zymo Research). Libraries were prepared using the ThruPLEX DNA-seq kit (Takara Bio) and the indexes from the SMARTer DNA HT Dual Index kit (Takara Bio) according to the manufacturer's instructions. The size selection was performed using AMPure beads (Beckman Coulter): first the bead-sample ratio was adjusted to 0.5 and after five minutes of incubation at room temperature, the supernatant was transferred to a fresh tube. This first step allowed to retain only fragments shorter than 800 bp. Beads were added to the supernatants in order to reach a bead-to-sample ratio of 1. The samples were incubated five minutes at room temperature before the supernatant was removed. The beads were then washed twice with 80% ethanol and air-dried for 2 minutes. The beads were resuspended in water, incubated at room temperature for 2 minutes before the supernatant was transferred to a fresh tube. This second size selection step removed all fragments shorter than 100 bp. The concentration of samples was then measured using the Qubit dsDNA High Sensitivity kit and the Qubit Fluorometer (ThermoFisher Scientific) and the quality of the libraries was assessed using the High Sensitivity DNA ScreenTape analysis on the TapeStation instrument (Agilent).

The sequencing was performed by Novogene on the HiSeq sequencing platform (Illumina), generating paired-end reads with a length of 150 bp. Two biological replicates were sequenced for each condition and antibody (as well as the input sample) and at least 20 million reads were produced for each sample. The number of reads of both Ph-K4me3 samples was much lower than that of the other samples so they were re-sequenced on the NovaSeq 600 platform (Illumina) and the reads from both runs were combined after mapping. A summary of the number of reads is given in Table 9.

Table 9: Reads count of the ChIP-seq samples. As sequencing was performed in a paired-end manner, the numbers here are the numbers of paired-reads. The mapped and filtered read pairs column shows the number of paired-reads pairs mapped uniquely and concordantly after PCR duplicate removal.

	Reads	Mapped and filtered read pairs
N_1_input	40,220,755	8,475,010
N_1_H3	38,343,656	11,102,013
N_1_H3K4me3	49,774,569	18,580,905
N_1_H3K27me3	42,399,491	3,665,161
N_2_input	38,205,146	5,414,344
N_2_H3	43,410,218	11,324,039
N_2_H3K4me3	41,096,474	16,753,326
N_2_H3K27me3	44,434,949	15,848,023
Ph_1_input	37,686,286	10,775,643
Ph_1_H3	44,5103,65	8,223,513
Ph_1_H3K4me3	12,745,941	3,979,429
Ph_1_H3K4me3_bis	35,651,729	5,085,906 (merged with the previous sample)
Ph_1_H3K27me3	43,838,020	14,038,316
Ph_2_input	42,866,388	4,159,083
Ph_2_H3	46,058,591	12,163,369
Ph_2_H3K4me3	25,536,052	15,047,387

Ph_2_H3K4me3_bis	11,697,037	19,076,846 (merged with the previous sample)
Ph_2_H3K27me3	36,123,231	13,308,390
Pd_1_input	42,385,426	11,086,143
Pd_1_H3	52,660,890	17,402,995
Pd_1_H3K4me3	40,293,245	16,293,577
Pd_1_H3K27me3	42,357,353	16,088,837
Pd_2_input	39,697,497	9,129,252
Pd_2_H3	45,817,504	14,771,794
Pd_2_H3K4me3	36,639,555	15,517,161
Pd_2_H3K27me3	35,465,557	14,519,115

2.5.3 Re-ChIP

For the sequential ChIP (Re-ChIP) experiment, 1 g of 21 day-old seedlings were harvested four hours after the end of the night. The cross-linking and chromatin extraction were performed as described in Vyse et al., 2020. The Re-ChIP was performed using the Re-ChIP-IT kit (Active Motif), according to the manufacturer instructions. Each sample of extracted chromatin was divided in three tubes. The first was first immunoprecipitated using an anti-H3K4me3 antibody and then an anti-H3K27me3 antibody. The second was immunoprecipitated using an anti-H3K4me3 antibody and no antibody in the second immunoprecipitation to verify whether the antibodies from the first immunoprecipitation could be carried-over in the second step. The third one was immunoprecipitated twice using the anti-IgG antibody as a specificity control. The antibodies and respective volumes used for the immunoprecipitation are listed in Table 8. After the proteinase K treatment, the DNA was purified and concentrated using the ChIP DNA Clean and Concentrator kit (Zymo Research).

The quantitative PCR was performed using the reactants, device and program described previously (section 2.3). Primer sequences can be found in Suppl. Table 3 and the primer efficiencies were calculated as described in section 2.3. Each reaction was performed in triplicates, whose Ct values were averaged. The %input was computed for each sample and immunoprecipitation (IP) using the following equation:

$$\%input = 100 \times \frac{Volume_{input}}{Volume_{IP}} \times efficiency^{Ct(input) - Ct(IP)}$$

Finally, the fold change to the H3K4me3-no antibody sample was computed using the following equation:

$$Fold\ Change = \frac{\%input\ (IP)}{\%input\ (H3K4me3 - no\ antibody)}$$

2.6 BIOINFORMATIC ANALYSES

An overview of all tools used in this study is provided in Suppl. Table 4 and Suppl. Table 5, while the source of any reference data is listed in Suppl. Table 6. All steps until the R part of the RNA-seq and ChIP-seq analyses were performed using Curta, the High Performance Computing of the Freie Universität Berlin (Bennet et al., 2020).

2.6.1 RNA-seq analysis

Quality assessment:

The quality of the reads was assessed using FastQC (version 0.11.7, Andrews S., 2010 <http://www.bioinformatics.babraham.ac.uk/projects/fastqc/>) and the results were aggregated using MultiQC (version 1.9) (Ewels et al., 2016).

Mapping:

The reads were mapped to the reference genome of *Arabidopsis thaliana* (TAIR10) using STAR (version 2.7.1) (Dobin et al., 2013). The index was generated based on the TAIR10 genomic sequence (top level, Suppl. Table 6) and the TAIR10 GTF annotation file created by converting the TAIR10 GFF3 annotation file (Suppl. Table 6) using Cufflinks *gffread* (version 2.2.1) (Trapnell et al., 2010). The `--genomeSAindexNbases` argument was set to 12 and the `-sjdbOverhang` parameter was set to 149 (read length - 1). The mapping was then performed using a minimum intron size of 60 bases and a maximum intron size of 6000 bases. The quality of the mapping was assessed with Qualimap (version 2.2.1) (García-Alcalde et al., 2012), using the GTF annotation file generated previously, in paired-end mode and `-a proportional` to include multimapping reads.

Differential expression analysis:

The counting was performed on genes using featureCounts (Subread version 2.0.1) (Liao et al., 2014). Only reads with an alignment score superior to 10 were used. The count was performed using paired-end mode and the same GTF file as for the previous steps. The FPKM (Fragment Per Kilobase per Million mapped reads) values were calculated using the *rpkm()* function from the edgeR package (version 3.34.0) (M. D. Robinson et al., 2009). Proper clustering of the replicates was examined by principal component analysis using the *plotPCA()* function from the DESeq2 package (version 1.32.0) (Love et al., 2014). The principal component 1 accounted for 52% of the variance and separated cold-treated samples from the naïve controls. The principal component 2 accounted for 30% of the remaining variance and separated samples based on the biological replicate they belonged to. After this control, the differential expression analysis was performed using the DESeq2 package (Love et al., 2014). First, the normalization factors were computed using the median of ratios method and subsequently used to calculate normalized counts. The design was set as `~ Replicate + Condition` and pairwise comparisons were performed (N vs Ph and N vs Pd). Fold changes were shrunken using the *lfcShrink()* function and the “ashr” method (Stephens, 2017). A gene was considered as significantly differentially expressed if the Benjamini-Hochberg adjusted p-value was inferior to 0.05. A high-confidence list of cold-regulated genes was established by keeping only the genes showing an absolute log₂ fold change (log₂FC) of at least 1.

2.6.2 ChIP-seq analysis

Quality assessment:

The quality of the reads was assessed using FastQC (version 0.11.7, Andrews S., 2010 <http://www.bioinformatics.babraham.ac.uk/projects/fastqc/>) and the results were aggregated using MultiQC (version 1.9) (Ewels et al., 2016).

Mapping:

The reads were then mapped to the reference genome of *Arabidopsis thaliana* (TAIR10) using Bowtie2 (version 2.3.5.1) (Langmead & Salzberg, 2012) (Suppl. Table 6). The mapping was performed in *--local* mode to allow trimming and in mixed mode (performing unpaired alignments of each mate if a paired alignment cannot be found). The two alignment files produced for each Ph-H3K4me3 sample were then merged using *samtools merge* (version 1.9) (Heng Li et al., 2009). All alignment files were filtered to remove non-mapping (*-F 4*) and multimapping (*-q 1*) reads using *samtools view* and the PCR duplicates were removed using *samtools rmdup*.

Peak calling:

The peak calling was performed using MACS2 (version 2.2.5) (Gaspar, 2018) on the filtered reads. The format was set to *BAMPE* so that only properly paired fragments will be used and the *--broad* option was used since histone marks are being analysed. The *--keep-dup* option was set to 1 so that duplicate reads would not be considered and the p-value threshold was set to 0.01. The effective genome size was set to 119481543. Lists of reproducible peaks for each condition and mark were established by running an irreproducible discovery rate (IDR) analysis (Q. Li et al., 2011) on the broadPeak files, using the p-value to rank the peaks. A peak was considered reproducible if it had an IDR ≤ 0.05 .

Differential methylation analysis:

Prior to the analysis, the bam alignment files were transformed to bed files containing the coordinates of the midpoints of the fragments. The differential methylation analysis was then performed using diffReps (version 1.55.6) (Shen et al., 2013). The DNA input files were used so that fold enrichments could be computed for the differentially methylated sites. As replicates were available, the negative binomial test was used for statistical testing. The fragment size was set to 0 as the midpoints of fragments were used for the analysis. The window size and step size were set to 200 and 20 respectively for H3K27me3 and to 50 and 5 for H3K4me3. For H3, two window sizes (200 and 500) were used and the results were combined. The *--nsd* parameter was set to *broad* for H3K27me3 and H3 and *sharp* for H3K4me3. A region was considered differentially methylated if it satisfied all four following criteria: (i) an enrichment above 1 in at least one condition (ii) a read count of at least 100 in at least one condition (iii) an absolute log₂FC of at least 0.322, corresponding to a change of at least 25% and (iv) an adjusted p-value inferior to 0.001. The assignment of differentially methylated regions to genes was done using ChIPseeker (Yu et al., 2015), keeping only the regions assigned to promoters, 5' or 3' UTR, exons or introns.

Global fold changes (over the whole gene body) were obtained using featureCounts (Liao et al., 2014) and a SAF file generated from the TxDb PlantSmart 28 annotation (Suppl. Table 6). Only reads with an alignment score superior to 10 were used and the count was performed using paired-end mode. The fold changes were then computed using DESeq2 (Love et al., 2014) in the same fashion as described for the RNA-seq analysis (section 2.6.1) but no filter was applied on the adjusted p-value in order to obtain a fold change for each gene.

Data visualization:

The signal tracks were generated on replicates pooled using *samtools merge*. Bigwig tracks were generated using DeepTools *bamCoverage* (version 3.3.1) (Ramírez et al., 2016), normalized as RPKM (Reads Per Kilobase per Million mapped reads). The bin size was set to 10 bp and non-covered regions were skipped. The tracks were then visualized in the IGV

genome browser (J. T. Robinson et al., 2011). The metagene plots were produced using deepTools *computeMatrix* (Ramírez et al., 2016) on the merged RPKM bigwig files, scaling all genes to 2000 bp using the *scale-regions* option and examining a window going from 500 bp upstream of the TSS (Transcription Start Site) to 500 bp downstream of the TES (Transcription End Side). The plots were generated using deepStats *dsCompareCurves* (Richard, 2020) with 1000 bootstraps. The annotation of peaks and differentially methylated regions was performed using the ChIPseeker R package (version 1.28.3) (Yu et al., 2015).

2.6.3 Gene ontology analysis

Gene ontology term enrichment analyses were performed using the topGO package (version 2.44.0) (Alexa & Rahnenfuhrer, 2021). The TAIR10 annotation (Suppl. Table 6) was used as a background list and the gene – GO term relationships were provided by the org.At.tair.db package (version 3.13.0) (Carlson, 2019). The enrichment analysis was done using the *weight01* algorithm and statistical testing was performed using the Fisher exact test.

2.6.4 Chromatin state analysis

This analysis was based on the chromatin topology established by Sequeira-Mendes et al. (2014). The list of genes in each chromatin state was established by overlapping the genomic coordinates of all the genes of *Arabidopsis thaliana* and the genomic intervals provided by Sequeira-Mendes et al. (2014) using the GenomicRanges package in R (version 1.44.0) (Lawrence et al., 2013). The TxDb file was generated using *makeTxDbFromGFF()* from the GenomicFeatures package (version 1.44.0) (Lawrence et al., 2013), based on the Araport11 (June 2016 release) GFF3 annotation file (Suppl. Table 6) (C. Y. Cheng et al., 2017). For the TAIR10 annotation, the gene coordinates were obtained from BioMart, Plantsmart28 (Suppl. Table 6) (Durinck et al., 2005). A gene was considered as being in a certain state if at least 150 bp (approximate length of DNA wrapped around a single nucleosome) of its gene body or promoter region overlapped with said state. A gene can therefore present several states along its coding sequence.

2.6.4.1 Chromatin state analysis at the gene level

Cold-regulated genes were extracted from the RNA-seq data generated by Calixto et al. (2018). A gene was considered up- (respectively down-) regulated at a certain time point if it was significantly up (resp. down-) regulated at said time point and if it showed no up- or down-regulation at any of the previous time points. For the “late” up- (resp. down-) regulated genes, only genes that (i) showed significantly up- (resp. down-) regulation in at least four of the nine time points of the fourth day of cold stress, (ii) showed no significant opposite regulation at the other “late” time points and (iii) showed no significant up- or down-regulation during the first day of cold exposure were retained. This filtering aimed at removing “artificially” up- (resp. down-) regulated genes that might appear so simply because of the dampening of the circadian clock upon long-term cold exposure. For heat stress, the lists of differentially expressed genes after different lengths of 32°C treatment were obtained from the RNA-seq data generated by Garcia-Molina et al. (2020). For drought stress, the list of up- and down-regulated genes after 2 h of air-drying were extracted from Ding et al. (2013). The lists of genes differentially

regulated 24 h after a flagellin treatment or 6 or 24 h after a *Pseudomonas syringae* infection were obtained from the RNA-seq data kindly provided by Arsheed Sheikh (personal communication, 2020). For the EBS and SHL study, the lists of genes targeted by those proteins were extracted from the ChIP-seq data published in Qian et al. (2018) and Yang et al. (2018). The DEK2 target genes were kindly provided by Rayapuram et al. (2020, personal communication) and the DEK3 target genes were extracted from the ChIP-seq data provided in Waidmann et al. (2014).

The different list of genes of interest were then overlapped with the list of genes in each state. For each chromatin state, the proportion of genes of interest in that state was compared to the proportion of genes in said state in the complete genome. The significance between the two proportions was examined using the Marascuilo procedure, with a confidence level of 0.95. The Marascuilo procedure was performed using R code adapted from the NIST/SEMATECH tutorial (*NIST/SEMATECH e-Handbook of Statistical Methods*, Section 7.4.7.4, accessed on June 2019 at <http://www.itl.nist.gov/div898/handbook/>).

2.6.4.2 Chromatin state analysis at the binding site level (DEK2 and hDEK)

The coordinates of the DEK2 binding sites were kindly provided by Rayapuram et al. (2020, personal communication). A DEK2 binding site was considered bivalent if it overlapped with a S2 domain for at least 150 bp. This was tested using the GenomicRanges package (version 1.44.0) (Lawrence et al., 2013). The controls were generated by shifting the coordinates of the DEK2 binding site up- or downstream by the indicated number of base pairs and the significance of the difference was tested by a permutation test (see section 2.6.8 for details).

For the human DEK study, the coordinates of the hDEK peaks were obtained from the ChIP-seq data available at ENCODE (GSE91587) (The ENCODE Project Consortium, 2012). As the DEK ChIP-seq was performed in human HeLa-S3 cells, the coordinates of H3K4me3 and H3K27me3 domains in the same cell line were also downloaded from ENCODE (GSM733682 and GSM733696 respectively). A bivalent region was defined as a domain of at least 150 bp where both histone methylation marks were present. The overlapping with hDEK binding sites, the controls and significance investigations were performed as described for DEK2.

2.6.5 Chromatin accessibility

The coordinates of accessible domains, as well as the coordinates of the loci opening and closing upon cold exposure were obtained from Raxwal et al. (2020). A bivalent region (resp. H3K4me3 or H3K27me3 monovalent region) was considered as accessible (resp. opening or closing upon cold exposure) if at least 150 bp of it overlapped an accessible locus (resp. opening or closing locus), which was tested using the GenomicRanges package (version 1.44.0) (Lawrence et al., 2013). The controls were generated by shifting the coordinates of the bivalent or monovalent regions up- or downstream by the indicated number of base pairs and the significance was tested by a permutation test (see section 2.6.8 for details).

2.6.6 ChromDB

The analysis was performed as described in Vyse et al. (2020).

2.6.7 Multiple sequence alignment

The protein sequences of all H3 variants were obtained from TAIR (www.arabidopsis.org, accessed on July 30th, 2021). The amino acid sequences were then aligned using ClustalW with standard parameters (Thompson et al., 1994).

2.6.8 Statistics and data visualization

Unless stated otherwise, statistical analyses and plots were generated using R or GraphPad Prism version 7.0 (GraphPad Software). Normal distribution was tested using the Shapiro-Wilk's method. For normally distributed data, ANOVA tests and any post-hoc tests were performed using the agricolae package (version 1.3-5) (Felipe de Mendiburu & Muhammad Yaseen, 2020). Non-parametric tests were performed using the adequate R function. Permutation tests were performed using the *peakPermTest()* function from the CHIPpeakAnno package (version 3.26.0) (L. J. Zhu et al., 2010) with 1000 permutations. Venn diagrams were plotted using the ggvenn package (version 0.1.9) and the significance of overlaps was calculated using a Fisher exact test.

3 RESULTS

3.1 BIVALENCY POISES STRESS INDUCIBLE GENES FOR TRANSCRIPTIONAL CHANGES

In order to prevent a constitutive stress response, stress-inducible genes need to be tightly repressed in the absence of any adverse environmental condition. While the exact mechanisms by which cold-induced genes are repressed are still unclear, previous work from our lab showed an enrichment of H3K27me3 targets among early cold-induced genes (Vyse et al., 2020), suggesting that this methylation mark might be involved in their repression. However, the chromatin landscape is infinitively more complex than the absence or presence of a single histone PTM and a more comprehensive and unbiased approach was necessary in order to decipher the role of chromatin topography in the repression of cold-induced genes.

3.1.1 Cold-regulated genes are enriched in bivalent targets

In order to identify additional chromatin marks involved in the repression of cold-induced genes prior to any cold exposure, their chromatin topography was examined using an unbiased approach based on the classification established by Sequeira-Mendes et al. (2014). By examining the distribution of 11 histone modifications and three histone variants as well as other epigenetic features, the authors classified the chromatin of *Arabidopsis thaliana* into nine states. A list of cold-inducible genes was obtained using the RNA-seq data from Calixto et al. (2018), and they were split into seven sets based on the time point where their induction was first detected. For each gene set and chromatin state, the percentage of genes containing a domain of said state in their gene body (TSS to TES) was computed and compared to the percentage observed for all genes in the genome, which served as a control (Figure 5A). As previous work from our lab showed an enrichment of H3K27me3 targets among cold-induced genes, the states characterized by the presence of this mark were of particular interest (Vyse et al., 2020). This included State 4 and 5, containing high levels of H3K27me3 but little of other histone modifications, State 8, containing H3K27me3 as well as other repressive marks such as H3K9me2 and H3K27me1 and State 2 which is characterized by the co-existence of the repressive H3K27me3 and the activating mark H3K4me3 (Sequeira-Mendes et al., 2014). State 4 and 5 were not particularly enriched among cold-inducible genes, while State 8 was underrepresented: while around 8% of all genes carried a S8 domain, this was the case for less than 3% of the cold-inducible genes (Figure 5A). This was not unexpected, as State 8 is mostly found on repetitive elements or intergenic regions (Sequeira-Mendes et al., 2014). On the other hand, State 2 was strongly enriched in genes induced at any time point in the cold, except for the last one, and particularly for genes expressed very early during cold exposure: 60% of genes induced after 3 h at 4°C carried a S2 domain on their gene body (compared to 22% of all genes). As the State 2 is predominantly found on promoters (Sequeira-Mendes et al., 2014), the analysis was repeated considering an artificial promoter of 500 bp or 1 kb directly 5' upstream from the transcription start site, to ensure that no biases were introduced by only considering the gene body in the initial strategy (Suppl. Figure 1A and B). When including an artificial promoter, the proportion of genes containing a S2 domain increased for each gene list: around 40% of all genes and more than 70% of the early cold-inducible genes possessed

a S2 domain. Overall, the pattern observed when considering only the coding region was conserved as the enrichment compared to the genome was still visible for all cold-induced gene sets. As the intergenic regions can be very small in *Arabidopsis thaliana*, subsequent analyses were performed using the gene body-only strategy in order to avoid miss-assigning a domain from a neighbouring gene. Altogether, this analysis indicates that many of the cold-induced genes in general, and the early ones in particular, are not only marked by H3K27me3 as previously thought (Vyse et al., 2020) but also carry the activating mark H3K4me3: they are bivalent. However, as this approach relies on *in silico* predictions of the chromatin states and simply suggests bivalency without proving it, the genes carrying a S2 domain will be designated as “S2 genes” and not bivalent genes, until the bivalency can be verified *in vivo*.

As bivalency is thought to allow both positive and negative changes of transcriptional activity (Bernstein et al., 2006; Voigt et al., 2013), it was interesting to examine whether it could also be marking genes which are repressed during cold exposure. The chromatin state analysis was therefore repeated for cold-repressed genes, but this time only focusing on State 2 (Figure 5B). An enrichment of S2 genes was observed for all down-regulated genes, irrelevant of the time point at which they are first detected to be down-regulated: between 45 and 49% of all cold-repressed genes carried a S2 domain. This suggests a more general role of the H3K4me3-H3K27me3 double mark in the transcriptional response to cold: S2 is found both on inactive genes that should be induced during cold exposure as well as genes which are transcribed in naïve conditions but should be repressed during a stress episode.

Chromatin states are more likely to be inherited through DNA replication and mitosis if they occur on a broader locus (Escobar et al., 2021; Stewart-Morgan et al., 2020). Since the early cold-inducible genes were more likely to have S2 domain than non-cold-regulated or late up-regulated ones, the size of S2 domains for those different categories of genes was compared, in order to determine whether this higher enrichment was associated with an increased inheritance likelihood (Figure 5C). While non cold-regulated S2 genes showed a median bivalent domain size of about 400 bp, almost all cold-regulated genes lists displayed broader S2 domains. The early up-regulated and late down-regulated genes showed the largest average size, with a median around 1000 bp. Albeit slightly higher, the late up-regulated genes S2 domain size was not found to be significantly different to the one of non-cold-regulated genes. Overall, the S2 domain size distribution resembled the S2 enrichment: all the cold-down-regulated S2 genes showed larger S2 domains than non-cold-induced ones, while only the early cold-up-regulated S2 genes presented this characteristic. To eliminate the possibility that the larger S2 domains on cold-regulated genes were simply due to longer gene bodies, the S2 domain size was plotted as a percentage of the gene body length (Suppl. Figure 1C). This analysis was consistent with the domain size examination: down-regulated genes had a higher fraction of their gene body in a S2 state than non-cold-regulated S2 genes (between 25 and 45% versus 20% for non-cold-regulated genes). For the cold-induced genes, only the early ones had a higher S2 fraction, which reached an average of 50% of the gene body for genes induced after 3 h of cold treatment. Altogether, this showed that cold-regulated genes are not only enriched in S2 genes, but they also carry larger domains than their non-cold-regulated counterparts, independently of gene length. As this last part implies that the S2 state is more likely to be maintained in daughter cells during cell division, this suggests that S2 plays a critical role in the regulation of cold-responsive genes.

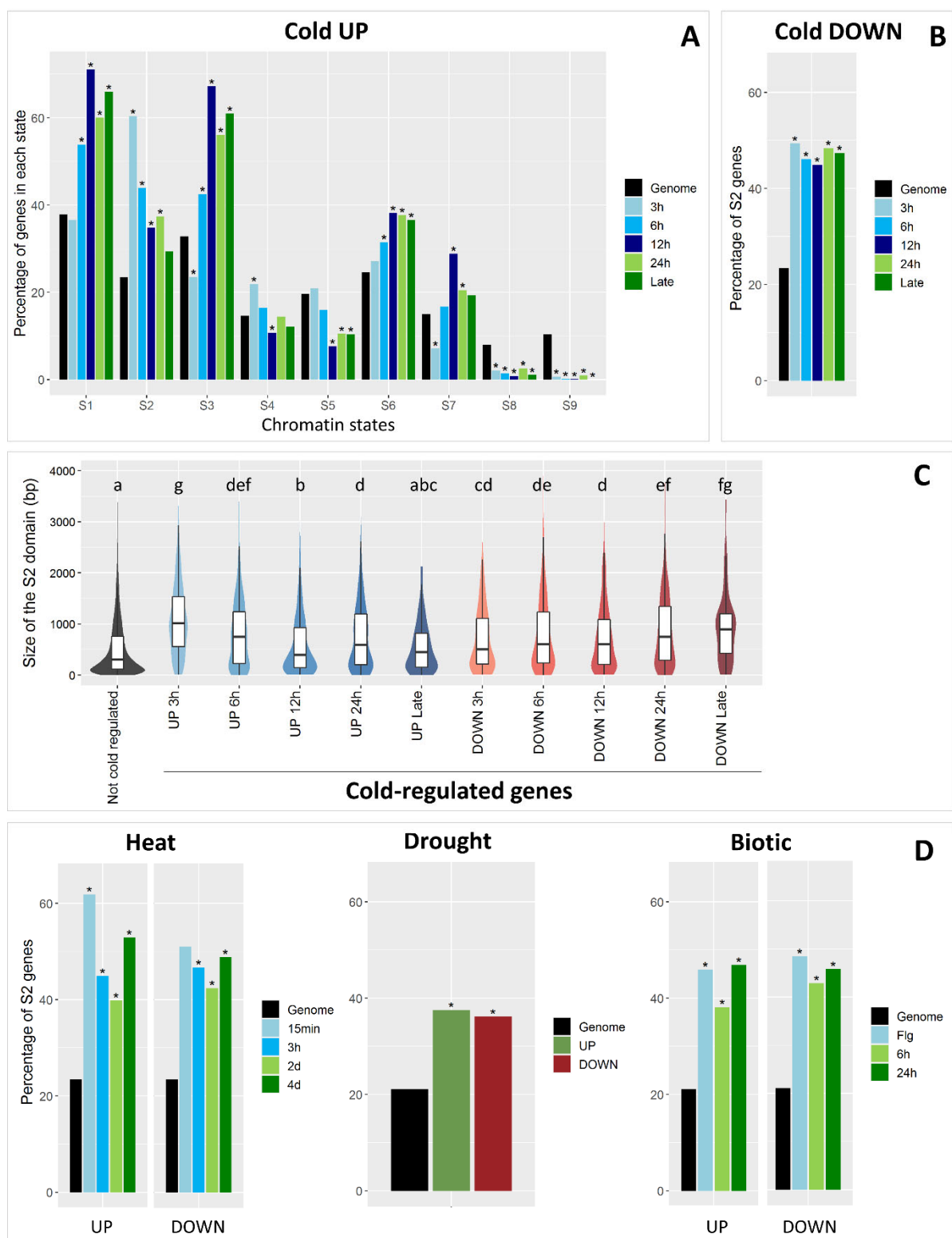


Figure 5: Bivalency is a common characteristic of stress inducible genes. The chromatin states coordinates were obtained from Sequeira-Mendes et al. (2014) and the cold-regulated genes were obtained from Calixto et al. (2018). * indicates significance compared to the genome, tested by Marascuilo procedure ($\alpha=0.05$). (A) Chromatin state analysis of genes induced at different time points during cold exposure, compared to the genome (B) Enrichment of S2 genes among genes repressed at different time points during cold exposure compared to the genome. (C) Size of the S2 domain in S2 genes induced (UP) or repressed (DOWN) at various time points during cold exposure. The “Not cold regulated list” contains S2 genes whose expression is not affected by cold. Significance was tested by Kruskal-Wallis test followed by a Dunn’s test with Benjamini Hochberg procedure ($\alpha=0.05$). Identical

letters indicate no significant difference. **(D)** Enrichment of S2 genes among genes induced (UP) or repressed (DOWN) by various stresses, compared to the genome. The heat-responsive gene sets were obtained from Garcia-Molina et al. (2020) and contain differentially expressed genes after the indicated time at 32°C. The drought-responsive genes were obtained from Ding et al. (2013) and are differentially expressed after 2 h of air-drying. The biotic-responsive genes were obtained by personal communication from Sheikh et al. (2020) and are differentially expressed 24 h after flagellin treatment (Flg) or 6h or 24 h after *Pseudomonas syringae* infection.

3.1.2 Bivalency is a common feature of stress-regulated genes

As cold-regulated genes are enriched in putative bivalent genes, the chromatin state analysis was widened to other types of stresses in order to determine whether bivalency is a specific feature of cold-responsive genes or common to all stress-regulated genes (Figure 5D). First, heat-regulated genes were examined using published RNA-seq data (Garcia-Molina et al., 2020). Heat up- or down-regulated genes were divided into four lists each depending on the time point at which they were first detected as differentially expressed. Similarly to cold-responsive genes, a strong enrichment of S2 genes was observed for all differentially expressed genes compared to non-heat-regulated genes: at least 40% of heat-regulated genes carry a S2 domain. The enrichment for early down-regulated genes is not significant but this is probably due to the very small number of genes in this list compared to other time points (51 vs several hundreds in the other lists). Interestingly, the up-regulated genes show a similar pattern to that of the cold up-regulated genes: the earlier the time point, the stronger the enrichment in S2 genes, with about 60% of early induced genes carrying a S2 domain. As heat and cold responses share many common regulators such as CBFs or certain Ethylen Responsive Factors (ERFs) (Garcia-Molina et al., 2020), the lists of early up-regulated genes for each stress were compared to verify whether these similar enrichments were simply due to the presence of the same genes in both lists. Only 30 genes were present in both sets, representing around 10% of each list (data not shown). This indicated that most of the S2 genes identified for each stress are specific to said stress and not simply common stress regulators.

As described in the introduction, temperature stresses might cause dehydration. Since bivalency was shown to be a common feature of temperature-regulated genes, it was also examined in relation to drought-responsive genes. This analysis was based on the RNA-seq data published by Ding et al. (2013) (Figure 5D). Here again, an enrichment of S2 genes was observed for both up- and down-regulated genes, albeit to a reduced extent compared to temperature-regulated genes, as less than 40% of drought-regulated genes carried a S2 domain. Finally, since bivalency seems to mark genes induced by a variety of abiotic stress, its role in the biotic stress response was examined by investigating genes induced or repressed 24 h after flagellin treatment (Flg) or 6 h or 24 h after infection by *Pseudomonas syringae*, based on a RNA-seq performed by Sheikh et al. (2020, personal communication) (Figure 5D). For all treatments, an enrichment of State 2 was observed among the differentially expressed genes: between 40 and 50% of all the genes whose expression was affected by the tested biotic stresses had a S2 domain. Altogether, this broader chromatin state analysis showed that bivalency is a common feature of many stress-regulated genes, in particular of genes up-regulated early during a temperature stress.

These results were validated by a complementary approach: a list of all genes containing a S2 domain was generated based on the genomic coordinates provided by Sequeira-Mendes et

al. (2014) and was then used in a gene ontology (GO) analysis. The GO biological process term enrichment analysis was performed using the weight01 algorithm from topGO and returned a list of 82 enriched terms. The 20 terms with the lowest p-value, representing the top enriched GO terms, are presented in Figure 6A. Most of the enriched terms identified through this analysis are stress-related, either biotic (response to nematode, fungus, bacterium) or abiotic (response to hypoxia, desiccation, light stimulus). Interestingly, the term “response to cold” was identified among the 82 enriched terms. Several terms related to phytohormones involved in stress responses were also identified (response to abscisic acid, jasmonic acid and salicylic acid). Altogether, this indicates that the S2 state is indeed preferentially located on genes that are required for a proper stress response. The term enrichment analysis was also performed for molecular function, which led to the identification of GO terms related to DNA binding, transcription factor activity and protein kinase activity, in particular serine/threonine kinase activity (Figure 6B). All of these are key signalling processes responsible for triggering a proper stress response and are induced early during the cold response, further proving that bivalency is a feature of the early responders to stress (Byun et al., 2014; Calixto et al., 2018).

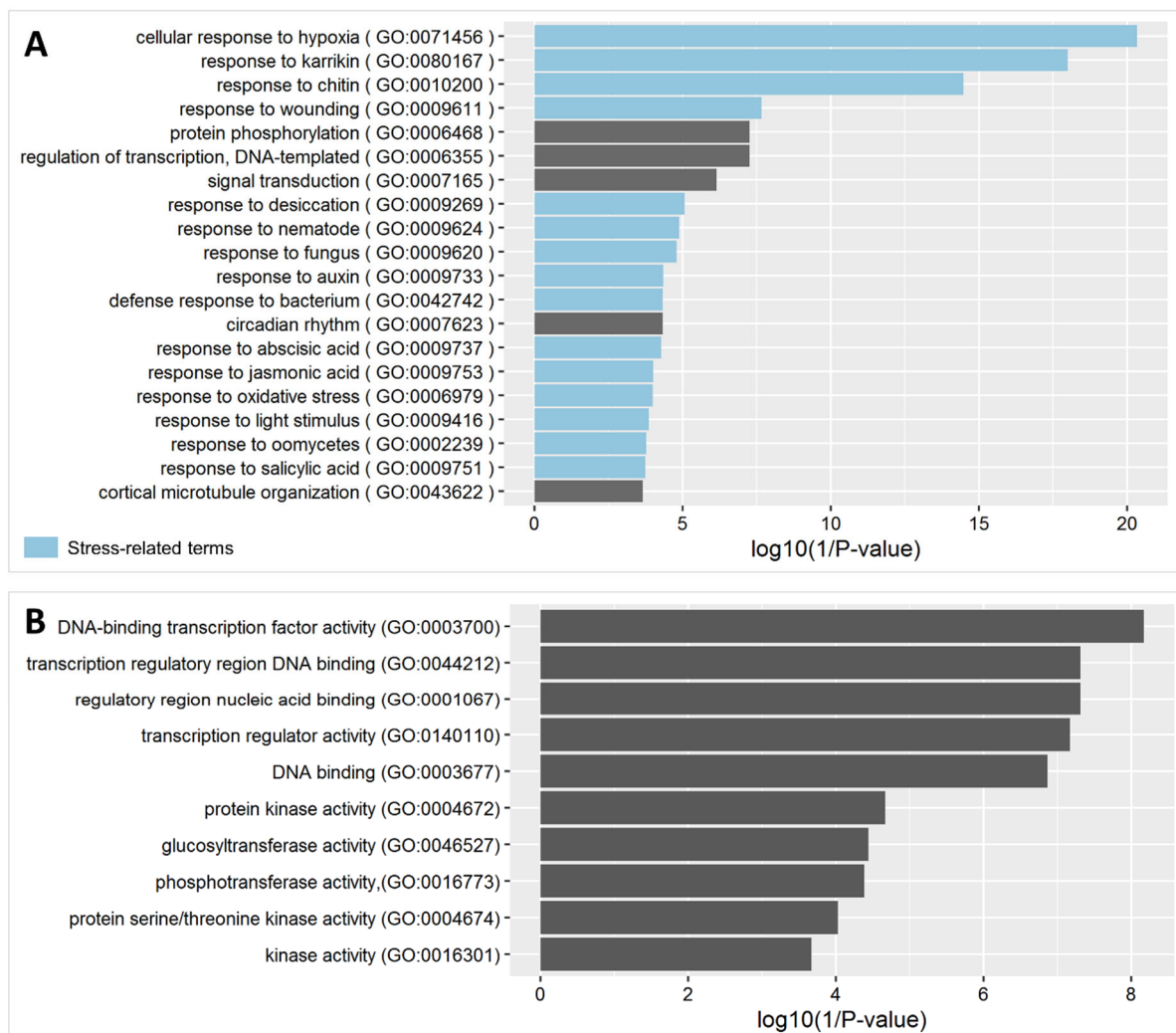


Figure 6: GO term enrichment analysis of S2 genes. Genes containing at least one S2 domain were compared to all TAIR10 genes. The enrichment analysis was performed by topGO using the weight01 algorithm, significance was tested using Fisher’s exact test and the 20 terms with the lowest p-values are displayed here. Blue bars highlight stress-related terms. The GO term enrichment analysis was performed for biological process (A) and molecular function (B).

3.1.3 H3K4me3 and H3K27me3 co-occur on S2 genes

Since the *in silico* analysis showed that many cold-responsive genes carry S2 domains, it was important to validate whether H3K4me3 and H3K27me3 co-occur at those genes *in planta*. Indeed, the data used to establish the chromatin topology and therefore to identify S2 domains came from numerous studies that used plants grown in widely different conditions (3 week-old plants grown in continuous light for H3K4me3 (X. Zhang et al., 2009), 10 day-old seedlings grown in long days for H3K27me3 (X. Zhang et al., 2007) for example). As the localization of these histone methylation marks on the genome is highly dynamic and changes during development but also the day-night cycle (Baerenfaller et al., 2016; Nishio et al., 2020), it was necessary to verify whether they actually co-occur at the same time on stress-responsive genes predicted to be bivalent. To that end, the genome-wide distributions of both methylation marks were investigated by ChIP-seq to detect loci carrying both of them in naïve conditions, i.e. in plants that did not experience any stress. Chromatin was extracted from 21 day-old plants and immunoprecipitated using antibodies raised against H3K4me3 or H3K27me3. The purified DNA was then sequenced. Finally, the reads were mapped to the TAIR10 genome assembly and peaks were called. A bivalent domain was defined as a window of at least 150 bp where a H3K4me3 peak and a H3K27me3 peak overlapped. 1652 bivalent genes, i.e. genes containing a bivalent domain in their gene body, were identified, 72% of which were predicted to carry one in the *in silico* analysis (Figure 7B). The number of bivalent genes detected through this analysis was much smaller than the 8166 genes predicted to have a S2 domain. This can be explained by two reasons: (i) the criteria used to define bivalency were very stringent and might not detect genes where the bivalent domain is very short or genes that carry both marks but on adjacent domains, (ii) the ChIP-seq experiment was performed on plants of different age and growth conditions than the ones used for the *in silico* topography, so it is possible that some genes do not carry one mark or the other in the conditions investigated here. Still, this approach validated the existence of a bivalent domain on many S2 cold-regulated genes, such as *WRKY48*, *PHENYLALANINE AMMONIA LYASE (PAL1)* or *JACALIN-RELATED LECTIN 34 (JAL34)* (Figure 7A). It also led to the identification of additional bivalent cold-regulated genes such as *LTI30* or *SUGAR TRANSPORT PROTEIN 13 (MSS1)* which were not among the predictions, either where the S2 domain did not overlap exactly with the gene body (*LTI30*) or for which no S2 domain was predicted (*MSS1*) (Figure 7C). Interestingly, a GO biological function term enrichment analysis ran on the 1652 bivalent genes identified 76 enriched terms, which were similar to the ones identified during the analysis of the S2 genes. The GO analysis of bivalent genes showed an enrichment for terms related to biotic and abiotic stress response (response to fungus, light stimulus, hypoxia in the top 20 terms but also freezing, induced systemic resistance in the complete list) (Figure 8). Many terms related to growth and development (positive regulation of development, leaf morphogenesis) were also identified, suggesting that bivalency holds a dual role in plants, acting in development as for mammals but also in the stress response. Both processes require a precise timing of transcriptional induction and repression of key regulators, which could be achieved by the co-existence of H3K4me3 and H3K27me3 on those genes. Altogether, the chromatin immunoprecipitation assays confirmed the predictions made during the *in silico* analysis and led to the identification of many genes where H3K4me3 and H3K27me3 co-occur at the same time point, which can therefore be considered bivalent. Even though they are far less numerous, the rest of this study will focus on those bivalent genes rather than S2 genes, as the former were proven to carry both histone methylation marks in the exact conditions used

for all following experiments. In the following parts, S2 genes will therefore refer to genes identified as carrying a State 2 domain in the *in silico* analysis, while bivalent genes will refer to those proven to carry H3K4me3 and H3K27me3 *in vivo*.

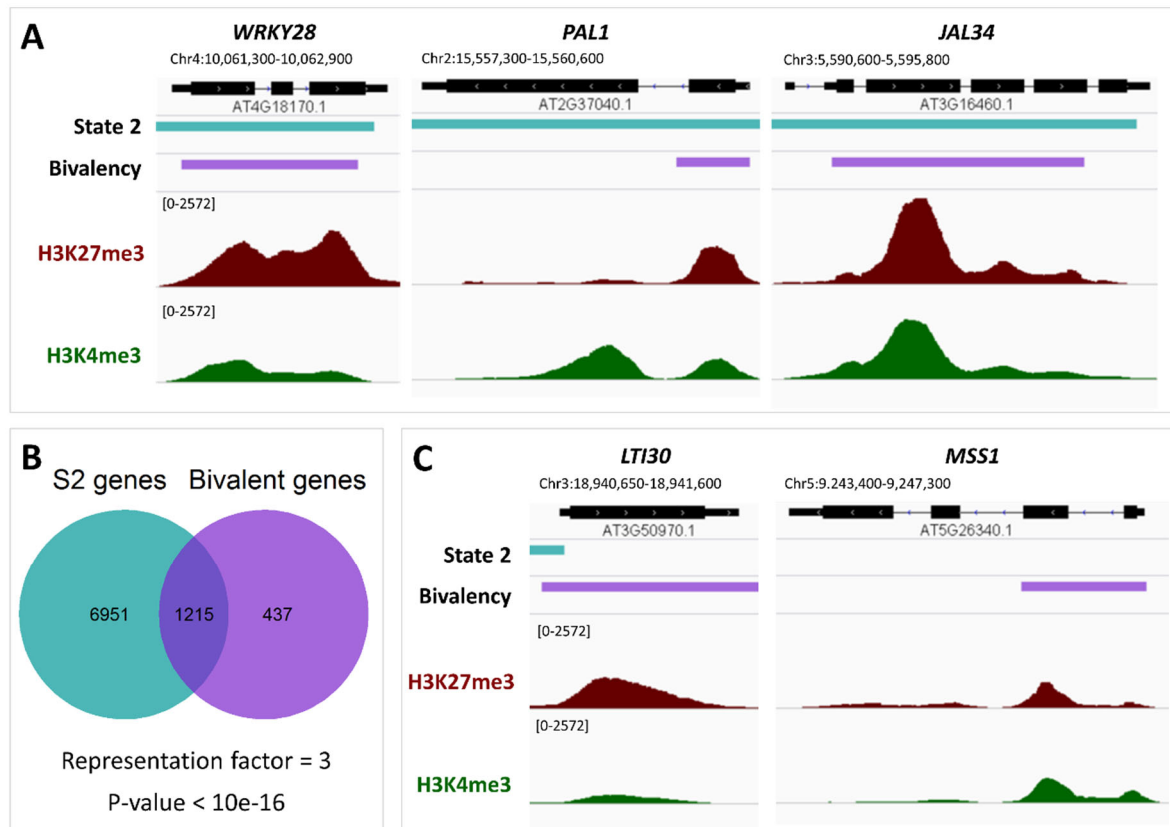


Figure 7: Many S2 genes appear to be bivalent in vivo. Bivalent domains represent windows of at least 150 bp where both H3K4me3 and H3K27me3 peaks were detected. **(A)** Genome browser views of ChIP-seq signals at genes predicted to be bivalent. The ChIP-seq was performed on 21 day-old seedlings grown at 20°C. State 2 coordinates were obtained from Sequeira-Mendes et al. (2014) and are shown by blue bars. Bivalency domains represent windows of at least 150 bp where both H3K4me3 and H3K27me3 peaks were detected and are shown with purple bars. The tracks were obtained by merging two biological replicates and the numbers in brackets at the top of each track denote the scale of that track in Reads Per Kilobase per Million mapped reads (RPKM). **(B)** Venn diagram showing the overlap of genes containing a S2 domain or a bivalent domain. Significance was assessed by Fisher's exact test. **(C)** Genome browser views of ChIP-seq signals (as RPKM) at newly identified bivalent genes.

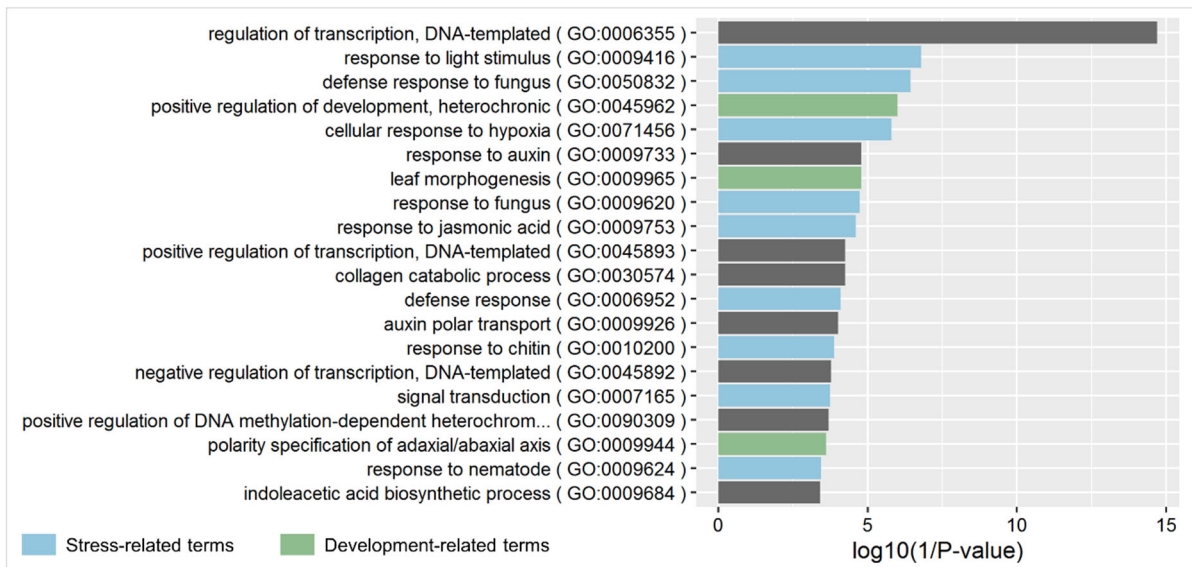


Figure 8: GO biological process term enrichment analysis of bivalent genes. Genes containing at least one bivalent domain were compared to all *TAIR10* genes. A bivalent domain is a locus of at least 150 bp where both H3K4me3 and H3K27me3 peaks are present. The enrichment analysis was performed by topGO using the weight01 algorithm, significance was tested using Fisher's exact test and the 20 terms with the lowest p-values are displayed here. Blue bars highlight stress-related terms while green bars denote development-related terms.

3.1.4 Towards the identification of bivalent domains *in planta*

Investigating the co-occurrence of H3K4me3 and H3K27me3 peaks led to the identification of numerous genes carrying both methylation marks at a given time point but it remains unclear whether both marks are present on the same chromatin fibre or even the same nucleosome and therefore whether the genes are truly bivalent. To investigate this possibility, a sequential ChIP (Re-ChIP) was performed: cross-linked chromatin was immunoprecipitated first using an anti-H3K4me3 antibody and a second time using an anti-H3K27me3 antibody (Figure 9). This technique leads to the purification of DNA fragments that were bound to nucleosomes carrying both methylation marks only (Desvoyes et al., 2018). The reverse order of antibodies (H3K27me3-H3K4me3) was also attempted but led to very low yields already after the first immunoprecipitation step and therefore almost no DNA could be detected in the second immunoprecipitation during qPCR. *KANADI 2* (*KAN2*) and *P1R1* were used as positive controls as they were previously shown to be bivalent by Sequeira-Mendes et al. (2014), while *PROLINE-RICH EXTENSIN-LIKE RECEPTOR KINASE 10* (*PERK10*) does not carry H3K4me3 nor H3K27me3 and was therefore used as a negative control (Figure 9A). Both the positive controls and the cold-inducible S2 genes *ULT1* and *WRKY48* showed a strong enrichment in the H3K4me3-H3K27me3 sample compared to *PERK10*, suggesting that the nucleosomes at those loci carry both methylation marks and are therefore bivalent. Furthermore, no enrichment was detected when the second immunoprecipitation was performed without an antibody, proving that it was not due to carry-over from the first antibody. These results suggested that the cold-inducible S2 genes identified in the *in silico* analysis are indeed bivalent at the nucleosomal level.

However, the suitability of *PERK10* as a negative control is questionable, although it was used as such by Sequeira-Mendes et al. (2014). Indeed, it does not even carry H3K4me3 and is

therefore already absent from the samples after the first immunoprecipitation step. A more valid negative control would be a gene carrying H3K4me3 but no H3K27me3, as such a locus should be purified in the first immunoprecipitation step but not in the second. *EUKARYOTIC INITIATION FACTOR 4A-III (EIF4A-III)* and *TIP41* were therefore examined as additional negative controls as individual H3K4me3 and H3K27me3 ChIP-qPCR proved that they satisfied those criteria (data not shown). In the Re-ChIP however, both genes showed an enrichment in the H3K4me3-H3K27me3 sample that was similar to the one observed for the S2 and bivalent genes investigated previously (Figure 9B). As *EIF4A-III* and *TIP41* are not carrying H3K27me3 and are therefore not bivalent, this suggests that the enrichment observed in the H3K4me3-H3K27me3 samples is unspecific. The %input values observed were rather low (< 0.5% for all genes tested) and coupled with the low yield of the first immunoprecipitation when using the anti-H3K27me3 antibody (data not shown), it is possible that this particular antibody does not perform properly in combination with the Re-ChIP-IT kit (Active Motif) used here. Therefore, the bivalency of the four S2 genes presented here could not yet be confirmed. Further optimization of the Re-ChIP method is required in order to determine whether the co-occurrence of H3K4me3 and H3K27me3 observed on some cold-responsive genes is due to bivalent (di-methylated) nucleosomes. Instead, the bivalency could stem from the marks being present on different but neighbouring nucleosomes, or even occurring on different chromatin strands.

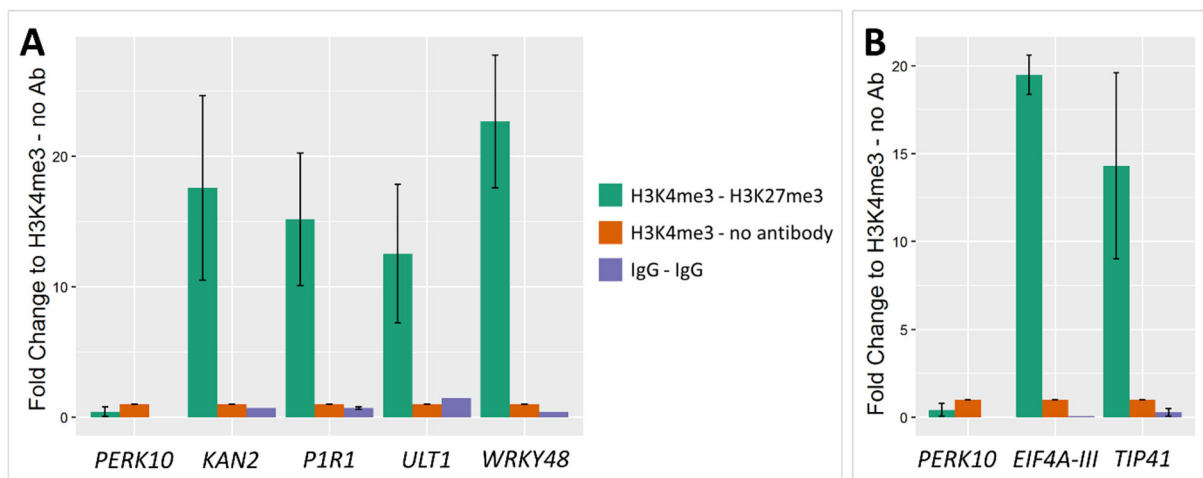


Figure 9: Validation of the in silico bivalency using Re-ChIP. The Re-ChIP was performed on 21 day-old seedlings grown at 20°C, using an anti-H3K4me3 antibody in the first IP and an anti-H3K27me3 antibody in the second (H3K4me3-H3K27me3). The specificity of the Re-ChIP and of the second IP were verified using anti-IgG antibodies (IgG-IgG) and no antibody in the second IP (H3K4me3-no antibody) respectively. The data is shown as %input, normalized to the %input obtained for the H3K4me3-no antibody sample. The error bars represent the sem of two biological replicates. **(A)** Validation of the bivalency on cold-inducible genes. PERK10 is a gene carrying neither H3K4me3 nor H3K27me3. KAN2 and P1R1 are genes known to be bivalent. ULT1 and WRKY48 are cold-induced genes predicted to be bivalent from the in silico analysis. **(B)** ReChIP on H3K4me3-monovalent genes. EIF4A-III and TIP41 were not predicted to be bivalent, as they carry H3K4me3 but no H3K27me3.

3.1.5 Bivalency prepares genes for changes in expression upon stress exposure

Previous studies showed that bivalency leads to the repression but poising of its target genes in the context of cell differentiation, allowing them to undergo rapid adjustments of their transcriptional activity (Bernstein et al., 2006; Voigt et al., 2013). The possibility that bivalency acts in a similar fashion in the regulation of cold-responsive genes was therefore explored through the characterization of *Arabidopsis thaliana* bivalent genes.

First, the distribution of each methylation mark was compared for bivalent and monovalent genes using metagene plots (Figure 10A). As it is known that bivalent nucleosomes are mostly asymmetrically modified, i.e. each modification is present on only one H3 tail, the comparison of the levels of each mark on bivalent vs monovalent genes could provide important information on the “true bivalent” nature of those loci (Voigt et al., 2012). H3K4me3 profiles varied widely between bivalent and monovalent genes (Figure 10A left). The signal peaked just downstream from the transcription start site on both categories of genes but the peak of monovalent genes reached around 900 RPKM compared to 400 for bivalent genes, fitting with the hypothesis that only half of the H3 tails could be methylated. The distribution itself was also different: monovalent genes showed a sharp peak just downstream from the transcription start site while bivalent genes had a wider H3K4me3 domain spanning almost the entire gene body. This broader domain suggests that H3K4me3 is more mitotically stable on bivalent loci than on the monovalent ones. In contrast, for H3K27me3 (Figure 10A right), no clear difference was observed between bivalent and monovalent genes: in both cases, H3K27me3 covered the entire gene body and its levels appeared only slightly lower on bivalent genes (around 50 RPKM less, i.e. less than a 10% reduction), suggesting that the presence of H3K4me3 on bivalent genes did not prevent the deposition of H3K27me3.

Since H3K4me3 levels are commonly considered to correlate with gene expression, the different levels of this mark on monovalent and bivalent genes suggest that they might have different transcriptional activities. To examine this hypothesis, a RNA-seq was performed in plants grown side by side with the ones used for the ChIP-seq. The average FPKM (Fragment Per Kilobase per Million mapped reads) of bivalent genes was compared to the one of H3K4me3 or H3K27me3 monovalent genes, as well as non-methylated genes (Figure 10B). While H3K4me3 monovalent and bivalent genes were both actively transcribed, bivalent genes were less expressed than their counterparts (the median for bivalent genes is around 3 FPKM, compared to 10 for H3K4me3 monovalent genes). This proves that the difference in H3K4me3 levels observed on the metagene plots (Figure 10A left) correlated with a different transcriptional activity: higher H3K4me3 levels are associated with an increased transcription. Interestingly, although the levels of H3K27me3 were sensibly the same on monovalent and bivalent genes, they showed a striking difference in expression. H3K27me3 monovalent genes were mostly repressed with a median FPKM of 0, while bivalent genes were expressed at an intermediate level. This indicates that the presence of H3K27me3 on a gene does not automatically lead to its repression. This also highlights that the levels of H3K27me3 alone cannot be used to determine the transcriptional activity of a gene, but the entire chromatin environment, such as the presence or absence of other marks, should also be considered.

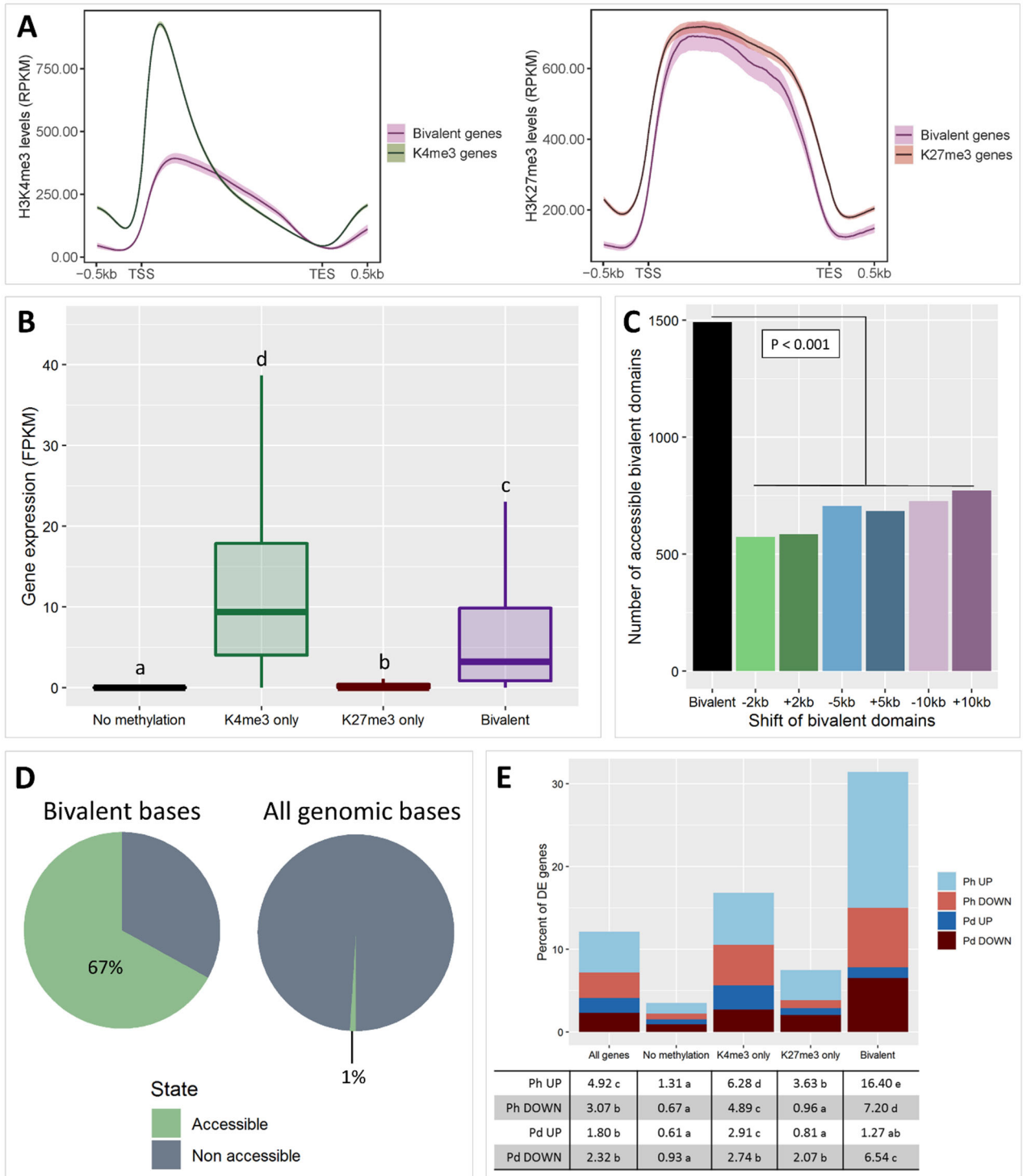


Figure 10: Characterization of bivalent genes. Bivalent genes contain a domain on their gene body of at least 150 bp where both H3K4me3 and H3K27me3 peaks are detected (A) Metagene plots showing the profiles of H3K4me3 (left) and H3K27me3 (right) on bivalent genes (purple) and genes carrying only H3K4me3 (green) or H3K27me3 (red), as RPKM. The ribbons represent the 95% confidence interval of the mean computed using 1000 bootstraps. (B) Gene expression level of non-methylated genes, H3K4me3 or H3K27me3 monovalent genes and bivalent genes. The RNA-seq reads were normalized as FPKM (Fragment Per Kilobase per Million mapped reads). Significance was tested by Kruskal-Wallis test followed by a Dunn's test with Benjamini Hochberg procedure ($\alpha = 0.05$). Identical letters indicate no significant difference. (C) Number of bivalent domains overlapping with accessible regions. The accessible regions were obtained from Raxwal et al. (2020) The ± 2 kb, ± 5 kb and ± 10 kb are control sets where the coordinates of the bivalent domains were shifted up- (+) or downstream (-) by the indicated number of bases. Significance was tested by permutation test. (D) Pie charts showing the

percentage of bivalent bases (left) and genomic bases (right) identified as accessible in the data from Raxwal et al. (2020) (E) Percentage of differentially expressed (DE) genes after 3 h (Ph) or 3 d (Pd) at 4°C in the same genes sets as described in (B). Identical letters next to the percentages indicate no significant difference, calculated by Marascuilo procedure ($\alpha = 0.05$).

A strong factor determining the transcriptional activity of a gene is the accessibility of the chromatin at that locus. Indeed, the looser the chromatin, the easier it is for the transcriptional machinery to assemble there. It was therefore of interest to examine the accessibility of bivalent loci. To that end, the coordinates of bivalent domains were compared to the coordinates of the accessible loci identified by FAIRE-seq (Formaldehyde-Assisted Isolation of Regulatory Elements) or DNase-seq by Raxwal et al. (2020) (Figure 10C). The plants used in the study from Raxwal et al. (2020) were 10 day-old seedlings grown in long days and on medium containing sugar, meaning the data is not directly comparable to the 21 day-old seedlings grown in short days and sugar-free medium used in the present study. While the analysis provides interesting insights, the results should therefore be considered with caution. Out of the 1684 bivalent domains, almost 1500 overlapped with accessible loci. This was twice as high as any of the controls created by shifting the bivalent domain coordinates and shown to be highly significant by a permutation test, proving that bivalent domains coincide with a more opened chromatin. Notably, about 67% of the total length of bivalent domains were described as accessible, while only 1% of the whole chromatin was identified as such (Figure 10D), confirming the strong correlation between bivalency and accessibility. It is worth noting that H3K27me3 monovalent domains did not show an enrichment of accessible regions compared to the control regions (Suppl. Figure 2B). Loci carrying only H3K4me3 overlapped with accessible regions with a higher frequency than the control sets: around 11500 out of the 15000 H3K4me3 peaks were at least partially accessible (Suppl. Figure 2B). However, only about 45% of the total length of H3K4me3 domains were identified as accessible, which is less than what was observed for the bivalent domains (Suppl. Figure 2C). Collectively, these results indicate that bivalent loci present a more opened chromatin and that this correlation is not due to the presence of one of the marks in particular but to their co-existence, as it is stronger on bivalent domains than for H3K4me3 or H3K27me3 monovalent loci.

The *in silico* study suggested that bivalency marks genes whose expression needs to be adjusted quickly upon stress exposure and might potentiate those transcriptional changes. To verify this, plants were exposed to 4°C for 3 h (Ph) or three days (Pd) and the transcriptional changes were monitored using RNA-seq. As this study focuses on histone methylation, only nuclear genes were considered and a total of 4034 genes showed differential expression upon cold exposure. Those differentially expressed genes were classified into four categories, depending on whether they were up- or down-regulated and the time point at which they were first detected to be differentially expressed. Then, the percentages of bivalent, H3K4me3 monovalent or H3K27me3 monovalent genes belonging to those four categories were calculated (Figure 10E). Both H3K4me3 and H3K27me3 monovalent genes were more likely to be differentially regulated than genes carrying none of those marks, with H3K4me3 monovalent genes showing a higher proportion (17%) of differentially regulated genes than the H3K27me3 monovalent set (8%). On the other hand, more than 30% of bivalent genes underwent a change in transcriptional activity upon cold exposure. This was not only higher than for any other category but also greater than the percentage computed for all genes irrelevant of their methylation status (12%). This indicates that bivalent genes are more likely to be differentially regulated upon cold stress than non-bivalent genes. Interestingly, this

increased likelihood of differential regulation was particularly strong for early up-regulated genes (Ph UP), less pronounced but still significant for down-regulated genes (Ph DOWN and Pd DOWN) but not detected for late up-regulated genes (Pd UP). This coincides perfectly with the *in silico* analysis that showed an enrichment of S2 genes among cold down-regulated and early up-regulated genes but not for late up-regulated genes (Figure 5A and B).

In conclusion, the presence of H3K4me3 on bivalent genes is sufficient to overcome the transcriptional repression that is normally associated with the presence of H3K27me3. The lower levels of H3K4me3 on bivalent genes compared to their monovalent counterparts correlate with a lower transcriptional activity that can however be quickly adjusted upon cold exposure. Bivalency spreads over the whole coding regions of its target genes, implying that it is stable through mitosis. Additionally, bivalent regions are more accessible than monovalent ones, suggesting that the co-occurrence of the methylation marks has a role in maintaining an open chromatin conformation. This could happen either through *cis* effects, i.e. inherent physical properties of bivalent histones or through *trans* mechanisms such as the reading of bivalency by protein effectors.

3.1.6 Identification of potential bivalency readers

Post-translational histone modifications are recognized by various readers, which can hinder or facilitate gene transcription, as well as modulate the chromatin structure around their binding sites. It would therefore be of great interest to identify readers able to recognize H3K4me3-H3K27me3 bivalency, as it would provide insight into the role of bivalency in the cold response. While many readers were already identified for each individual histone mark, bivalency readers remain largely undiscovered. Previous work suggested that EBS and SHL could achieve this function: indeed, both proteins contain a PHD and a BAH domain that can bind H3K4me3 and H3K27me3 respectively (Z. Li et al., 2018; Qian et al., 2018; Z. Yang et al., 2018). Therefore, the potential role of these two proteins as bivalency readers was first investigated *in silico* by examining the enrichment of S2 genes among their targets (Figure 11A). The EBS targets were obtained from Yang et al. (2018) while the SHL targets were obtained from Qian et al. (2018). The targets common to both proteins were identified by overlapping the list of genes bound by EBS and SHL. The specific targets from EBS or SHL showed a similar enrichment for S2 genes: about 50% of the targets carried a S2 domain. Furthermore, 67% of the genes targeted by both EBS and SHL carried a S2 domain. All of these percentages were significantly higher than the one observed for the set containing all the nuclear genes (20%), which confirms the potential of EBS and SHL to act as bivalency readers.

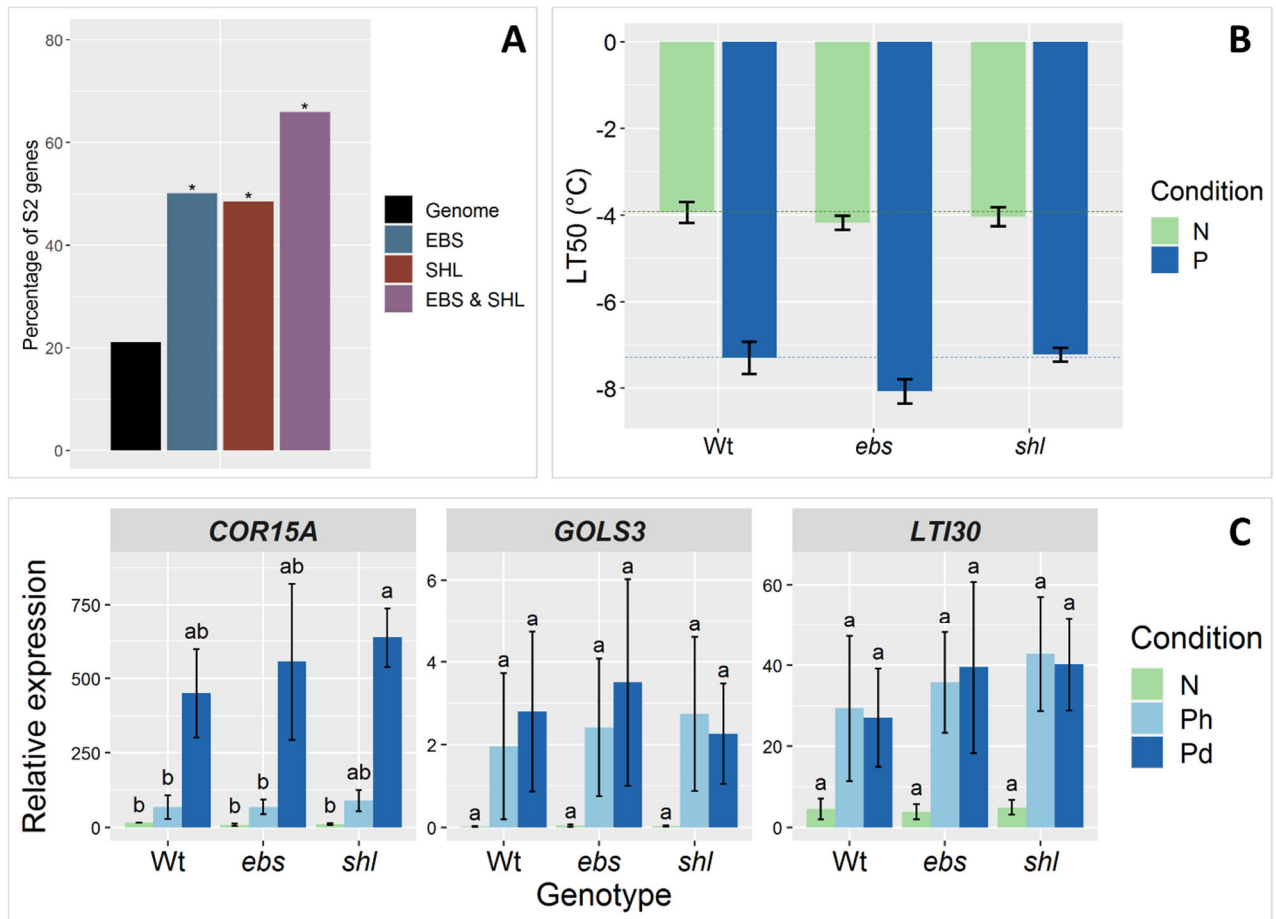


Figure 11: Role of the putative bivalency readers SHL and EBS in the cold response. (A) Enrichment of S2 genes among EBS and SHL targets, based on the chromatin state coordinates from Sequeira-Mendes et al. (2014). The EBS targets were obtained from Yang et al. (2018) while the SHL targets were obtained from Qian et al. (2018). The EBS & SHL list contain genes that are targeted by both proteins. * indicates significance compared to the genome, tested by Marascuilo procedure ($\alpha = 0.05$). **(B)** Freezing tolerance of *ebs* and *shl* mutants, before or after cold acclimation, measured by electrolyte leakage assay. Plants were grown for 21 days at 20°C (N) and then exposed to 4°C for three days (P). Error bars represent the sem of four biological replicates. Statistical significance was assessed by 2-way ANOVA followed by a Dunnett post hoc test to compare each mutant to the wild type for each condition but no significant difference was found. **(C)** Gene expression changes of the cold marker genes COR15A, GOLS3 and LTI30 in *ebs* and *shl* mutant plants exposed to cold. RNA was isolated from 21 day-old seedlings grown at ambient temperature (N) and exposed to 4°C for 3 h (Ph) or three days (Pd). Transcript levels were measured by reverse transcription and qPCR. TIP41 was used as an internal control. Error bars represent the sem of four biological replicates. Significance was tested by 2-way ANOVA followed by a Tukey test ($\alpha = 0.05$). Identical letters indicate no significant difference.

To verify whether those putative bivalency readers actually play a role in the cold response, the freezing tolerance of *ebs* and *shl* mutants was measured thanks to an electrolyte leakage assay, before and after a 3 d treatment at 4°C, also called cold acclimation (Figure 11B). Both *ebs* and *shl* mutants showed a similar basal freezing tolerance (without acclimation) to the wild type. After three days at 4°C, the freezing tolerance of both mutants increased compared to the one from naïve mutant plants, indicating that they were able to cold acclimate. In every individual replicate (n=4), *ebs* mutant plants showed a slightly higher freezing tolerance than the wild type after cold acclimation but this did not prove to be significant when the results were pooled. Overall, neither EBS nor SHL seemed to play a considerable role in the physiological response to cold. However, the slight increase in freezing tolerance after cold acclimation observed for the *ebs* mutant suggested that their impact on cold tolerance might be too limited

to be detected in the electrolyte leakage assay, indicating the need for a method that could reliably identify smaller changes in the cold response. As it was hypothesized that the reading of bivalency would impact the transcriptional activity of the bivalent genes, this parameter was investigated in *ebs* and *shl* mutants. 21 day-old plants (N) were placed at 4°C for 3 h (Ph) or three days (Pd), and the expression levels of several *COR* genes were measured using RT-qPCR (Figure 11C). *LTI30* and *GOLS3* were selected as they were found to be bivalent, while *COR15A* is not (Figure 7C and Suppl. Figure 4). No difference was detected in any of the mutants compared to the wild type for the tested genes, whether before or during the cold exposure and whether or not the genes were bivalent. Taken together, the *in vivo* results do not indicate that either protein is involved in the cold response or the regulation of the transcriptional activity of bivalent *COR* genes.

In parallel to the work on EBS and SHL, another family of putative bivalency reader was identified: the DEK-domain containing proteins. DEK2 was shown to bind to bivalent peptides *in vitro* and both DEK3 and DEK2 were described to be involved in the regulation of stress tolerance (Waidmann et al., 2014 and Rayapuram et al., 2020, personal communication). Additionally, DEK2 and DEK3 were shown to bind to H3 and H2A.Z, a variant often associated to bivalency (Sequeira-Mendes et al., 2014; Waidmann et al., 2014). Altogether, these observations suggested that these two DEK proteins might act as bivalency readers. To test this hypothesis, a chromatin state enrichment analysis was performed on the DEK2 and DEK3 target genes, using the same strategy as described previously and the list of target genes established by Waidmann et al. (2014) for DEK3 and Rayapuram et al. (2020, personal communication) for DEK2 (Suppl. Figure 3A). Contrary to the expectations, the DEK3 target genes did not present an enrichment of the State 2 as they showed a similar proportion of S2 genes compared to the genome set. They were however enriched in the States 1, 3, 6 and 7, characteristic of actively transcribed genes: 60% of DEK3 genes had an S1 or S3 domain (compared to 40% of all TAIR10 genes) and around 45% had an S6 or S7 domain (compared to around 20% of all genes). This refuted the hypothesis of DEK3 acting as a bivalency reader. However, the DEK2 target genes showed an enrichment of S2 genes compared to the proportion observed for the whole genome: 30% of DEK2 targets have a S2 domain on their gene body compared to 20% of all the TAIR10 genes. This enrichment was even more striking when taking into account an artificial promoter of 1 kb upstream from the TSS: 60% of DEK2 targets vs 40% (data not shown). However, while this approach revealed an enrichment of S2 genes among DEK2 targets, it did not show whether DEK2 binds directly on the bivalent regions. To verify this, the overlap of DEK2 binding peaks and S2 domains was examined (Figure 12A). A DEK2 peak was considered to be in a bivalent state if the overlap was of at least 150 bp. From the 22 680 DEK2 peaks identified by Rayapuram et al. (2020, personal communication), 9000 were found to overlap a S2 domain, which represents about 40% of the peaks (Figure 12A). The significance of this finding was verified by shifting the coordinates of the DEK2 peaks to generate controls sets: less than 5000 of the control peaks of any given set overlapped with a S2 domain, which was shown to be a significant reduction using a permutation test. This analysis was performed for all the chromatin states and a significant enrichment was observed only for the States 1 and 2 (Suppl. Figure 3B). As State 1 is characterized by high levels of H3K4me3, this analysis suggested a preferential binding of DEK2 on regions carrying H3K4me3 or H3K4me3-H3K27me3.

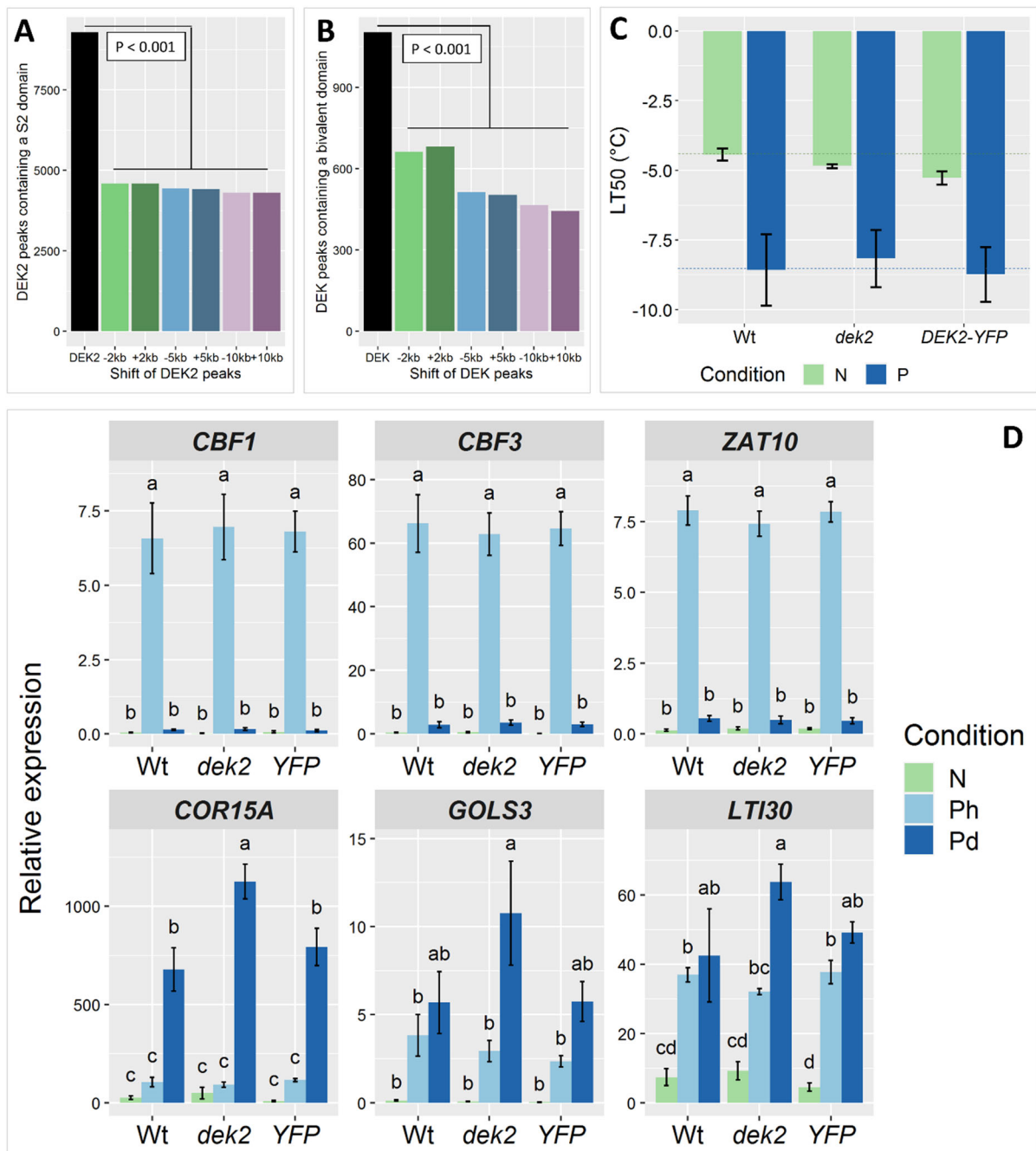


Figure 12: Role of the putative bivalency reader DEK2 in the cold response. (A) Number of DEK2 peaks containing a S2 domain. The S2 coordinates were obtained from Sequeira-Mendes et al. (2014) and the coordinates of DEK2 peaks were provided by Rayapuram et al. (2020, personal communication). The ± 2 kb, ± 5 kb and ± 10 kb are control sets where the coordinates of the DEK2 peaks were shifted up- (+) or downstream (-) by the indicated number of bases. Significance was tested by permutation test. **(B)** Number of hDEK peaks containing a bivalent domain in human HeLa-S3 cells. The coordinates of hDEK peaks were obtained from ENCODE (GSE91587) and the bivalent domains were determined as loci of at least 150 bp where both H3K4me3 and H3K27me3 were present. The histone methylation datasets were obtained from ENCODE (GSM733682 and GSM733696). The ± 2 kb, ± 5 kb and ± 10 kb are control sets where the coordinates of the hDEK peaks were shifted up- (+) or downstream (-) by the indicated number of bases. Significance was tested by permutation test. **(C)** Freezing tolerance of *dek2* mutant and its complementation line DEK2::DEK2-YFP, before or after cold acclimation, measured by electrolyte leakage assay. Plants were grown for 21 days at 20°C (N) and then exposed to 4°C for three days (P). Error bars represent the sem of two biological replicates. Statistical significance was assessed by 2-way ANOVA followed by a Dunnett post hoc test to compare each mutant to the wild type for each condition but no significant difference was found. **(D)** Gene expression changes of the cold marker genes CBF1, CBF3, ZAT10, COR15A, GOLS3 and LTI30 in

dek2 mutant plants and its complementation line *DEK2::DEK2-YFP* exposed to cold. RNA was isolated from 21 day-old seedlings grown at ambient temperature (N) and exposed to 4°C for 3 h (Ph) or three days (Pd). Transcript levels were measured by reverse transcription and qPCR. TIP41 was used as an internal control. Error bars represent the sem of four biological replicates. Significance was tested by 2-way ANOVA followed by a Tukey test ($\alpha = 0.05$). Identical letters indicate no significant difference.

As the *in silico* analysis confirmed the role of DEK2 as a bivalency reader suggested by the *in vitro* assay of Rayapuram et al. (2020, personal communication), its potential role in cold tolerance was investigated, first at the physiological level using electrolyte leakage assays. The freezing tolerance of *dek2* and *DEK2::DEK2-YFP* plants was measured before (N) and after a cold exposure of three days at 4°C (P). While none of these trends were significant, it seemed that the *dek2* mutant was slightly more freezing tolerant than wild type plants prior to cold acclimation but performed slightly worse after acclimation (Figure 12C). However, these changes were minute and not always reverted in the complementation line. Indeed, the *DEK2::DEK2-YFP* plants showed an even higher freezing tolerance than the *dek2* mutant before cold acclimation. As this assay was only conducted twice and the replicates did not always revealed similar behaviours for the mutant lines (Suppl. Figure 3C), the results displayed here should be considered with caution until more repetitions are performed. As the DEK family comprises four members in *Arabidopsis thaliana*, it is also likely that they are functionally redundant and that the absence of DEK2 alone only has a minor impact on the freezing tolerance of the plant. In an effort to detect more minute changes in the cold response, the transcriptional activity of several cold-induced genes was investigated using RT-qPCR, either in naïve plants (N) or in plants exposed to 4°C for 3 h (Ph) or 3 d (Pd). All genes tested showed a strong induction upon cold exposure in all lines, confirming that the absence of DEK2 did not have a major impact on the cold response (Figure 12D). However, *COR15A* showed a significantly higher induction in *dek2* after three days in the cold compared to the wild type (around 50% higher), while this gene was induced to wild-type levels in the complementation line. Although not significant, a similar trend was observed for *LT130* (50% higher induction in *dek2*) and *GOLS3* (almost two-fold higher induction in *dek2*). As it was unexpected that DEK2 would impact the transcription of *COR15A* since it was not identified as a bivalent gene, the expression of *CBF1*, *CBF3* and *ZAT10* was also examined to verify whether all cold-responsive genes were over-induced. None of these genes showed a higher induction in *dek2* plants compared to wild type ones, which indicates that this over-induction is not a general phenomenon on all cold-responsive genes nor an overall over-induction of the CBF-dependant pathway but a gene specific event. Interestingly, the genes that do not show an over-induction in the *dek2* mutants (*CBF1*, *CBF3*, *ZAT10* and *CBF2* (data not shown for *CBF2*)) carry H3K4me3 but no H3K27me3 prior to cold, while *GOLS3* and *LT130* are bivalent (Figure 7C and Suppl. Figure 4). *COR15A* was not found to be bivalent but carries high levels of H3K27me3 and low levels of H3K4me3. These results suggest that, thanks to its ability to bind to bivalent histones, DEK2 functions as a repressor of cold-responsive genes carrying H3K27me3 and limit the range of their induction.

Many eukaryotes possess DEK proteins, including flies and mammals, and their function as histone chaperones appears to be conserved across multiple species (Sawatsubashi et al., 2010; Waidmann et al., 2014). To investigate whether bivalency reading might also be a shared aptitude of DEK proteins, the potential conservation of this ability for human DEK (hDEK) was examined *in silico*. To that end, the genomic coordinates of the hDEK peaks in HeLa S3 cells, as well as the ones of the H3K4me3 and H3K27me3 domains in the same cell line, were

obtained from ENCODE. Bivalent regions were defined as regions of at least 150 bp carrying H3K4me3 and H3K27me3. The overlapping of hDEK peaks and bivalent domains was then examined using the same strategy as previously described for DEK2. Out of the 9760 hDEK peaks identified in HeLa S3 cells, 1100 overlapped with a bivalent domain (Figure 12B). While the proportion of hDEK peaks overlapping with a bivalent state was lower than the one of DEK2 (10% vs 40%), it was significantly higher than the ones observed in the control sets (around 5%). This suggests that the role of DEK2 as a potential bivalency reader might be shared with its human homologue hDEK.

3.2 COLD EXPOSURE TRIGGERS CHANGES IN HISTONE METHYLATION

Many cold-inducible genes are marked by H3K4me3-H3K27me3 bivalency prior to any cold exposure, which is thought to poise them for activation. As the activation of bivalent genes in mammals is proposed to happen due to the resolution of bivalency into monovalency (Voigt et al., 2013), it would be insightful to examine whether H3K4me3 and H3K27me3 are subjected to changes when the plant is facing adverse temperatures and whether these potential histone methylation dynamics have an impact on the transcriptional activation of cold-inducible genes.

3.2.1 Cold-triggered changes in methylation

3.2.1.1 Global changes of methylation upon cold exposure

The impact of cold exposure on H3K4me3 and H3K27me3 was first investigated at the genome-wide level, in order to estimate the magnitude of the potential changes. A histone extraction was performed on samples isolated from 21 day-old naïve plants (N) and plants that were exposed to 4°C for 3 h (Ph) or 3 d (Pd) and the levels of both methylation marks were then measured by Western Blot (Figure 13). The fluorescent signals of the marks were normalized to the levels of H3, which was measured using an antibody that binds to this histone regardless of the presence of any potential post-translational mark. Cold exposure, whether short or long, did not lead to any considerable change in the levels of H3K4me3 (Figure 13A). On the other hand, it triggered a loss of H3K27me3 already after 3 h of cold treatment that persisted after three days (Figure 13B). In both cold treated samples, the levels of H3K27me3 were reduced by around 50% compared to the non-treated sample, proving that chilling stress had a tremendous impact on the genome wide levels of this repressive mark. However, as the Western Blot method can only detect substantial changes at the genome-wide level, the apparent absence of variation for H3K4me3 does not mean that this methylation mark was not affected by cold on a local scale. Based on these observations, it appeared necessary to perform a ChIP-seq for both methylations marks, to examine whether the levels of H3K4me3 really remain unchanged at the gene level and to identify which regions are affected by the loss of H3K27me3.

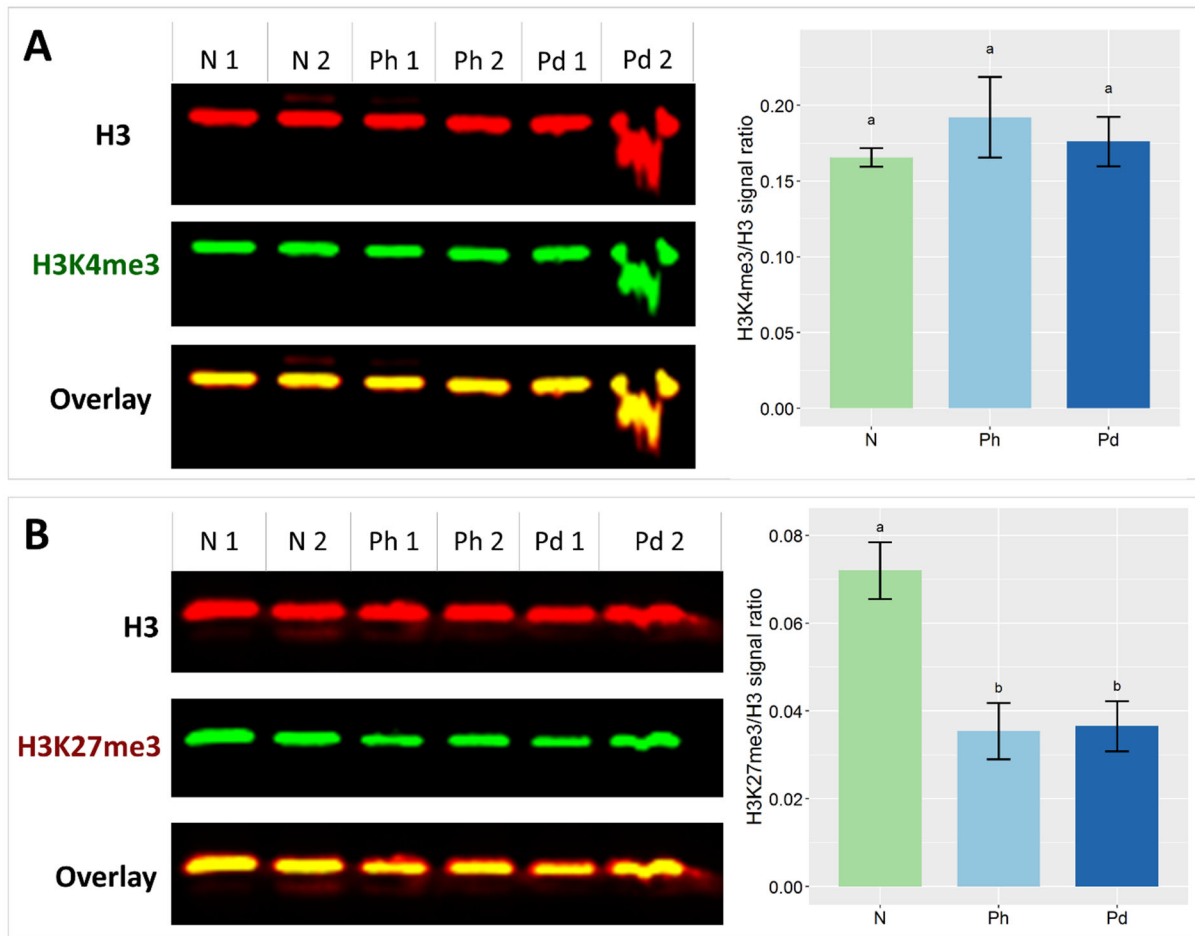


Figure 13: Impact of cold treatment on the global levels of H3K4me3 and H3K27me3. Plants were grown for 21 days at 20°C (N) and then exposed to 4°C for 3 h (Ph) or 3 d (Pd). Global levels of H3K4me3 (A) and H3K27me3 (B) after cold exposure were measured by Western Blot. The membrane images show the signal of H3 in red, H3K4me3 or H3K27me3 in green and the overlay of H3 and the respective methylation signal. As the H3 antibody recognizes H3 independently of the potential post-translational marks, it serves as a loading control. Each membrane shows two biological replicates per condition. Additional pseudo-replicates were generated by performing a second histone extraction on the biological replicates shown here and the Western Blots were performed a second time, displaying similar results as those displayed here. The right panels display the ratio of each methylation mark signal divided by the signal from H3, for each of the four pseudo-replicates. Significance was tested by one-way ANOVA followed by a Tukey post-hoc test ($\alpha = 0.05$). Identical letters indicate no significant difference.

To that end, a chromatin extraction and immunoprecipitation was performed on 21 day-old seedlings that did not experience cold (N) or were placed at 4°C for 3 h (Ph) or three days (Pd), using antibodies against H3K4me3, H3K27me3 and H3. This was performed on two independent biological replicates and the purified DNA samples recovered from the immunoprecipitations were then sequenced. This experiment was performed on plants grown and treated at the same time as the ones used for the RNA-seq previously described (section 3.1.5) so that the changes in histone methylation could be correlated to the transcriptional ones. After the sequencing, reads were mapped to the TAIR10 genome and an irreproducible discovery analysis was ran on the peaks called from each replicate in order to obtain a robust list of reproducible peaks for each condition, i.e. regions that were consistently identified as carrying H3K4me3 (resp. H3K27me3) in each of the two biological replicates. First, the number of peaks in each condition was examined, in order to determine whether cold exposure led to the deposition of the methylation marks on new regions or their removal from previously

methylated regions (Figure 14A and B). As it was described that drought stress leads to the fragmentation of H3K27me3 regions into smaller islands, it was of interest to examine if cold might have a similar effect on any of the marks investigated here (Sani et al., 2013). To that end, the size distribution of the peaks was compared for the different conditions (Figure 14C and D). For H3K4me3, about 14 000 peaks were identified in each condition and cold treated samples had a few hundreds more peaks than the non-treated ones (about 300 for Ph and 500 for Pd) (Figure 14A). As the size distribution of those peaks did not change drastically, this excluded the hypothesis that H3K4me3 peaks got fragmented during cold exposure and suggested that those additional peaks originated from H3K4me3 being deposited at new loci (Figure 14C). Around 6000 H3K27me3 reproducible peaks were identified in each condition (Figure 14B). The Ph samples showed a similar number of peaks to the naïve ones while the Pd samples had around 150 additional peaks. The size distribution of the Pd peaks was shifted slightly to the left in comparison to the naïve peaks, indicating that Pd peaks were on average slightly smaller than naïve peaks (Figure 14D). This suggested that the additional Pd peaks might come from the fragmentation of a fraction of pre-existing H3K27me3 peaks.

However, the variations observed were minute and not sufficient to explain the changes observed in the Western Blot experiment. Indeed, this approach only examined the absence or presence of the methylation marks but gave no indication on their levels. Therefore, histone methylation was investigated in a quantitative manner, by examining the average signal of each mark on all genes using metagene plots (Figure 14E and F). The average H3K4me3 signal increased very slightly around the transcription start site of all genes already after 3 h of cold treatment and this gain was maintained and even increased in magnitude after three days (Figure 14E). Conversely, H3K27me3 levels showed a minor decrease on the whole gene body after 3 h of cold exposure and were even further reduced after three days (Figure 14F). While these results were consistent with what was observed on the Western Blot for H3K27me3 and indicated the existence of genome wide changes in the levels of those methylation marks, they only show the average signal on all genes. To get a more precise picture and examine whether these changes are happening on all genes or only a subset of them, a differential methylation analysis was performed.

The diffReps algorithm was therefore used to identify regions that were significantly differentially methylated upon cold exposure. The algorithm identifies these regions by sliding a window across the whole genome, and the optimal window size was determined for each mark individually. For H3K27me3, a window of 200 bp was used as it corresponds to the approximate length of DNA wrapped around one nucleosome, while it was reduced to 50 bp for H3K4me3, whose domains are narrower. Only the regions showing a significant signal change of at least 25% and with a read count of at least 100 in at least one condition were retained. The extend of the cold-triggered changes was investigated through the examination of the number, size and fold change of the differentially methylated regions (Figure 15A to C). As a different window size was used for each histone mark, the data had to be analysed separately. Finally, the differentially methylated regions were annotated using the ChIPseeker package to identify whether certain genetic features were more likely to be affected (Figure 15D) (Yu et al., 2015).

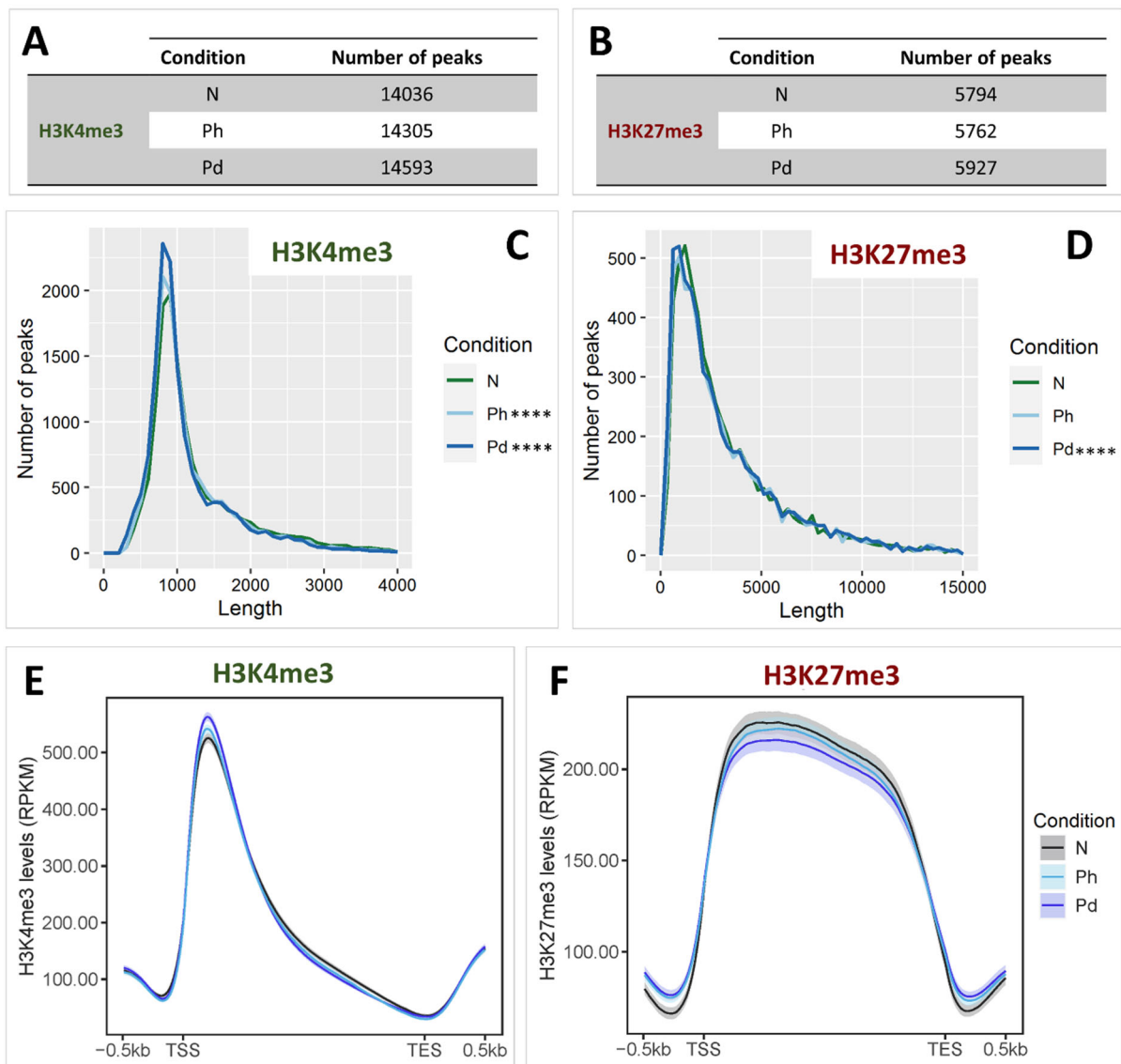


Figure 14: Global changes of H3K27me3 and H3K4me3 upon cold exposure. Plants were grown for 21 days at 20°C (N) and then exposed to 4°C for three hours (Ph) or three days (Pd) (A) and (B) Total number of reproducible H3K4me3 (A) and H3K27me3 (B) peaks detected in the CHIP-seq. Reproducible peaks were identified by peak calling by MACS2 followed by IDR analysis. (C) and (D) Length distribution of H3K4me3 and H3K27me3 peaks respectively. Significant difference in the distributions of the length of cold treated peaks vs naïve peaks was evaluated by two-sided two-sample Kolmogorov-Smirnov test. **** indicates p -value < 0.0001 (E) and (F) Metagene plots showing the levels of H3K4me3 and H3K27me3 respectively on all TAIR10 nuclear genes. Signal is shown as RPKM. The ribbons represent the 95% confidence interval of the mean computed using 1000 bootstraps.

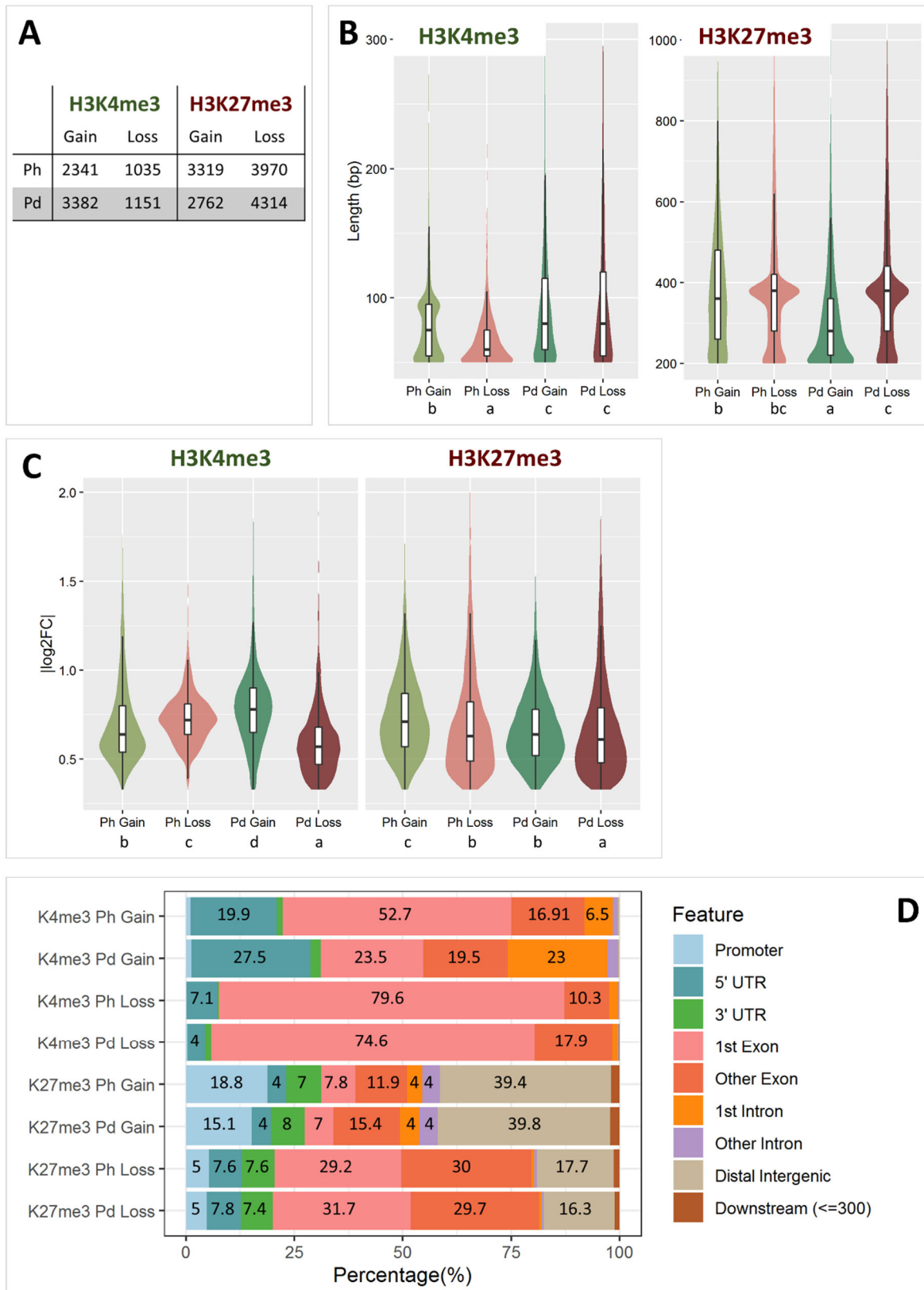


Figure 15: Characterization of differentially methylated regions. Differential methylation analysis of H3K4me3 and H3K27me3 levels after 3 h (Ph) or 3 d (Pd) at 4°C, measured by ChIP-seq and analysed using diffReps. **(A)** Number of regions gaining or losing methylation upon cold exposure. **(B)** Size of the regions gaining or losing H3K4me3 (left) or H3K27me3 (right) upon cold exposure. Significance was tested by Kruskal-Wallis test followed by a Dunn's test with Benjamini Hochberg procedure ($\alpha=0.05$). Identical letters indicate no significant difference. **(C)** Absolute log₂FC of the regions gaining or losing H3K4me3 (left) or H3K27me3 (right) upon cold exposure. Significance was tested by Kruskal-Wallis

test followed by a Dunn's test with Benjamini Hochberg procedure ($\alpha = 0.05$). Identical letters indicate no significant difference. **(D)** Genomic feature distribution of the differentially methylated regions. The attribution was performed by ChIPseeker. The numbers show the percentages of regions attributed to each genomic feature.

For H3K4me3, between 3000 and 4000 differentially methylated regions were identified in each condition and about 2/3 of those showed a gain of methylation (Figure 15A). The number of regions losing H3K4me3 was stable between Ph and Pd whereas 1000 more regions gaining H3K4me3 were identified at Pd compared to Ph. While the H3K4me3 peaks had a median size of around 1000 bp, the majority of the regions showing differential methylation were shorter than 200 bp, indicating that the gain (resp. loss) of H3K4me3 occurred at a precise locus and did not affect the entire peak. Interestingly, the regions showing differential H3K4me3 methylation after three days of cold exposure were larger than the ones detected at 3 h, with the regions losing H3K4me3 at 3 h being the shortest (Figure 15B left). These differences in size distribution did not directly correlate with variation in fold change, as the regions gaining H3K4me3 after three days in the cold showed the highest fold change, followed closely by the regions losing H3K4me3 at the 3 h time point (Figure 15C left). As described previously, H3K4me3 is located predominantly around the transcription starting site, covering sections of both the 5' UTR and first exon (Figure 10A, Suppl. Figure 2A). It was therefore not surprising that most regions showing a differential methylation of this mark were located in those genetic features (Figure 15D). Interestingly, the loss of H3K4me3 happened preferentially on the first exon, suggesting that the levels remained stable on the 5' UTR, confirming the previous observation that the loss of H3K4me3 happened on a specific part of the peaks instead of the whole. H3K4me3 gain was localized both on 5' UTR and first exon, closely matching the general distribution of this mark. Altogether, the examination of the number, size and fold changes of H3K4me3 differentially methylated regions supported the previous observation based on the metagene plot that the stronger changes happen after three days of cold exposure and consist of a gain of this methylation mark around the TSS of the underlying genes (Figure 14E).

The analysis of H3K27me3 identified more differentially methylated regions than for H3K4me3: around 7000 regions in each condition (Figure 15A). These were equally distributed between gain and loss after 3 h of cold, while after three days of treatment, more regions losing the mark were detected. Similarly to H3K4me3, the differentially methylated regions were shorter than the average length of H3K27me3 peaks, again suggesting that cold had specific and localized effects on H3K27me3 levels. Interestingly, while at the Ph time point differentially methylated regions were approximately of the same length regardless of the direction of the change, at the Pd time point, the regions losing H3K27me3 were much larger than the ones gaining it, with medians around 400 bp and 250 bp respectively (Figure 15B right). This difference in size was associated with slightly lower fold changes for regions losing H3K27me3 upon cold exposure at both time points (Figure 15C right). H3K27me3 loss occurred predominantly on exons, especially the first one. As shown previously (Figure 10B and Suppl. Figure 2A), this mark spans a large portion of the gene body and 5' UTR, which indicates that the loss did not happen indiscriminately on every methylated nucleosome but appears to be specific to those located on exons. On the contrary, H3K27me3 gain was mainly localized in intergenic regions or more unfrequently in the promoter but scarcely ever within the gene body. This discrepancy in features annotation between regions gaining or losing H3K27me3 was identical for both examined time points. The different localization of the changes coupled to

the higher number and larger size of the regions losing methylation support the global reduction in H3K27me3 levels on gene bodies observed on the metagene plot after three days in the cold and on the Western Blot (Figure 13B and Figure 14F).

Altogether, these analyses confirmed that cold exposure alters the levels of both H3K4me3 and H3K27me3. While H3K4me3 levels remain constant at the genome wide-level, moderate and spatially restricted increases (resp. decreases) of this activating mark could be detected around TSSs. On the other hand, cold triggers a substantial loss of H3K27me3, mostly affecting the exons of coding genes, while modest gains of this repressive mark were found in intergenic regions.

3.2.1.2 H3K4me3 and H3K27me3 differential methylations target separate sets of genes

Cold stress triggered changes in the levels of both H3K4me3 and H3K27me3 at specific loci mostly located within gene bodies but it remains unclear how many and which genes are affected. Since previous analyses showed that both of these methylation marks can co-occur on certain genes prior to the occurrence of cold, it is especially intriguing to examine whether the same gene can undergo both H3K27me3 and H3K4me3 differential methylation. In order to elucidate these questions, the differentially methylated genes were identified, based on the annotations provided by ChIPseeker (Figure 15D). Every differentially methylated region belonging to a promoter, intron, exon or 5' or 3' UTR was assigned to its respective gene (Figure 16A). It is important to note here the distinction between differentially methylated regions (a portion of the genome where the methylation levels were significantly different before and after cold exposure, usually smaller than a gene) and differentially methylated genes (genes that contained at least one differentially methylated region). As a gene could contain several regions showing differential methylation (e.g. a gain of methylation on each exon), the numbers of differentially methylated genes are smaller than the ones of differentially methylated regions. These smaller numbers are also due to the fact that some differentially methylated regions are located in intergenic regions and were therefore not assigned to any gene.

Around 2000 genes gained H3K4me3 at each time point during cold exposure, while less than 1000 showed a decrease in the levels of this mark (Figure 16A). Interestingly, the ratio between genes gaining or losing H3K4me3 was similar to the one observed at the region level. For H3K27me3, around 4000 genes were identified as containing at least one differentially methylated domain at each time point (Figure 16A). At both time points, around 2/3 of the identified genes showed a loss of H3K27me3, a higher discrepancy than the one observed when examining the number of differentially methylated regions (Figure 15A). This is likely due to the fact that almost half of the domains losing H3K27me3 were located in intergenic regions and therefore could not be assigned to any gene (Figure 15D). Interestingly, proportionally less genes were identified from the differentially methylated regions for H3K27me3 than for H3K4me3. This can be partially justified by the discrepancy in localization between the two marks: as H3K27me3 covers a larger span of the gene body, it provides more potential domains that can be differentially methylated compared to H3K4me3 which is mostly located on a narrower region around the TSS. It is therefore more likely for a gene to have multiple domain showing a gain or loss of H3K27me3 than of H3K4me3. Furthermore, as described

previously, a non-negligible fraction of H3K27me3 differentially methylated regions were located in intergenic regions while almost all H3K4me3 differentially methylated regions were located within the gene body or the promoter (Figure 15D), which also contributed to the proportionally reduced number of genes identified for H3K27me3. Altogether, the examination of the number of genes affected by the differential methylation was consistent with the conclusions from the region-level analysis (Figure 15): cold exposure mainly caused a gain in H3K4me3 and a loss in H3K27me3 as those were the categories with the highest number of genes.

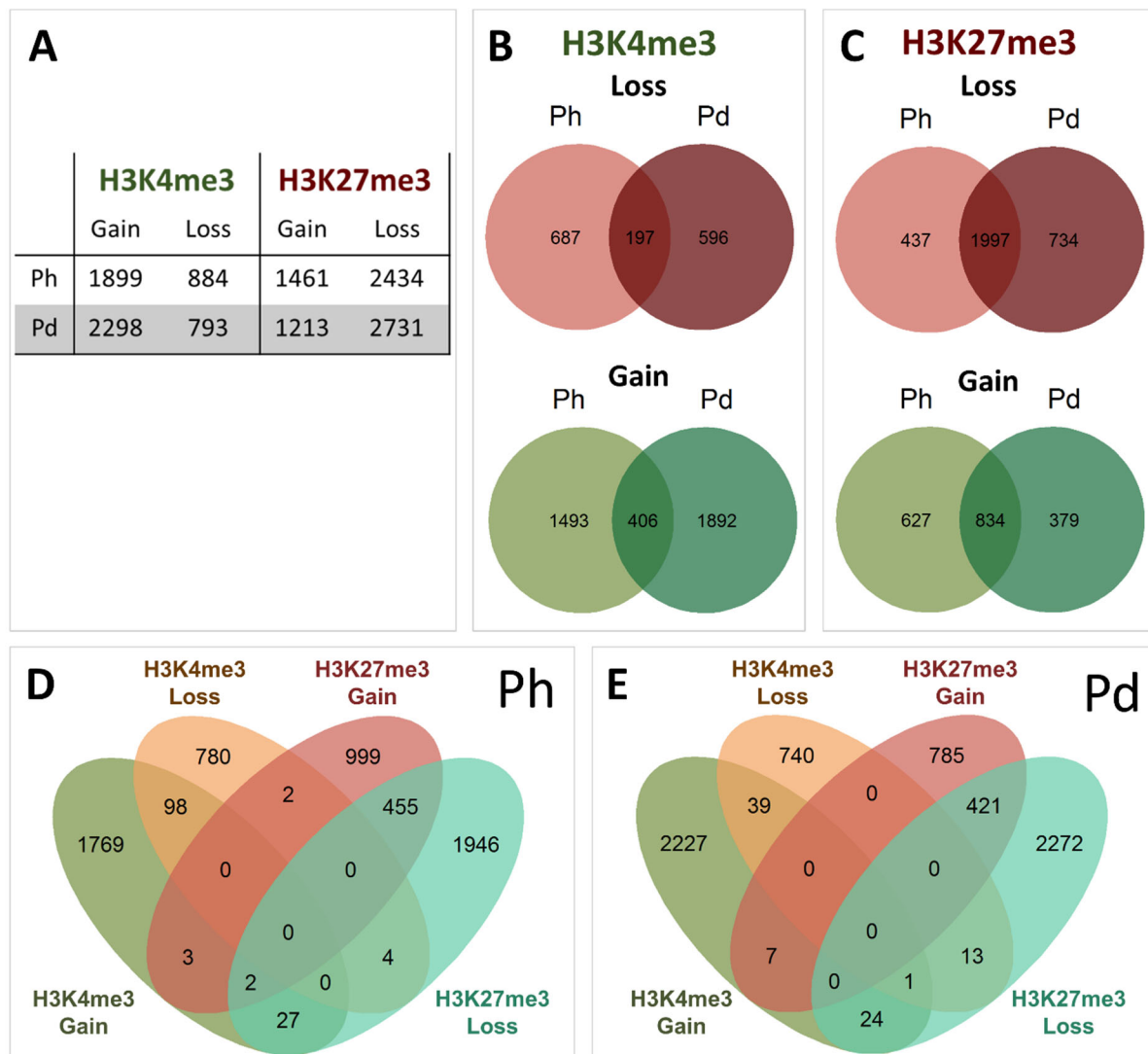


Figure 16: Characterization of differentially methylated genes. A gene was considered differentially methylated if it presented at least one differentially methylated region in its promoter or coding sequence, based on the analysis of H3K4me3 and H3K27me3 levels after 3 h (Ph) or 3 d (Pd) at 4°C presented in Figure 15. (A) Number of genes gaining or losing methylation upon cold exposure. (B) and (C) Persistence of the loss and gain of H3K4me3 (B) or H3K27me3 (C) during cold exposure, analysed by overlapping the genes showing the same differential methylation at Ph and Pd. (D) and (E) Overlap of genes gaining or losing H3K4me3 and H3K27me3 at Ph (D) or Pd (E).

To determine whether cold-triggered differential methylation is stable over time or is rather dynamic during the stress episode, the persistence of the changes was examined by identifying genes that showed the same differential methylation at both analysed time points. For H3K4me3, only about 20% of the genes showing a gain or loss of the mark after 3 h in the cold

still presented this variation after three days (Figure 16B). On the other hand, the majority of H3K27me3 changes that occurred after 3 h were still detected after three days, with about 80% of the genes that lost H3K27me3 at Ph still displaying this loss at Pd (Figure 16C). This suggested that H3K4me3 levels are dynamic and regularly re-adjusted, while H3K27me3 changes are more stable and persist for longer spans of time.

Next, the possibility for a gene to show both H3K4me3 and H3K27me3 differential methylation was examined by overlapping the lists of genes gaining or losing each mark, for each time point separately (Figure 16D and E). This approach revealed an unexpected phenomenon: a non-negligible number of genes showed bi-directional changes for the same methylation mark, i.e. they both gained and lost the same methylation mark at different loci. For H3K4me3, this was a rare occurrence, only about 3% at Ph and even fewer at Pd. Examination in the genome browser revealed that for many of them, a small region of “loss” was associated to a larger or even multiple windows of “gain” (data not shown). Therefore, “true” bi-directional changes of H3K4me3 levels were rare occurrences. However, for H3K27me3, around 13% of the differentially methylated genes showed bi-directional changes. Interestingly, many of these genes were common to both time points. Examination in the genome browser showed that the gains of H3K27me3 were localized mainly on exons while the losses happened in the introns, suggesting a potential re-localization of the methylated nucleosomes from exons to intron (data not shown). A GO term enrichment analysis performed on the genes showing bi-directional differential H3K27me3 methylation identified several terms related to cell wall as well as terpenoid, sesquiterpene and other secondary metabolites biosynthesis and catalysis (Suppl. Figure 5). Surprisingly, very few genes showed differential methylation for both marks, around 40 for each time point (Figure 16D and E). The biggest overlap was found between genes gaining H3K4me3 and losing H3K27me3, which are both associated with transcriptional activation. The two histone marks could also have different kinetics, meaning that the levels of one are changing early in the cold response while the other is affected later. However, the overlaps at Pd were not more important than at Ph, infirming this hypothesis. This was confirmed by looking at the overlap of genes showing differential H3K4me3 methylation at Ph and differential H3K27me3 methylation at Pd and vice versa, which did not show larger overlaps than the time-point specific ones (data not shown). Additionally, the representation factors of the pair-wise overlaps (genes gaining or losing H3K4me3 vs genes gaining or losing H3K27me3) were extremely low (0.1), indicating that they contained less genes than expected by chance. This confirmed that H3K4me3 and H3K27me3 differential methylations occur on separate sets of genes. Together with the observation that H3K4me3 changes are very dynamic while H3K27me3 variations are persistent (Figure 16B and C), this suggests that the changes in H3K27me3 and H3K4me3 might have different purposes and therefore target different types of genes.

To examine this hypothesis, a GO biological process term enrichment analysis was performed on the genes showing differential methylation for each mark and time point (Figure 17 and Figure 18). The genes showing both gain and loss of the same mark were excluded from this analysis to avoid biases due to counting the same gene in two different categories. As certain categories showed a significant enrichment for a multitude of terms, only the 20 terms with the lowest p-value are displayed here. Genes gaining H3K4me3 after 3 h of cold treatment showed an enrichment for terms related to stress responses (hypoxia, high light intensity, salt stress) and the second most enriched term was “response to cold” (Figure 17A). Many terms

related to photosynthesis were also identified, such as “photosystem II assembly” or “light harvesting in photosystem I”. After three days of cold exposure, again numerous stress-related terms were identified, many of which were already found to be enriched at the earlier time point (response to salt stress, hypoxia) (Figure 17B). The term “response to cold” was once more listed among the highest ranked terms and this time “cold acclimation” was also identified as well as “response to freezing” (not in the top 20 terms but present in the full list), indicating that at this stage of the cold exposure, the deposition of H3K4me3 occurred not only on genes that are necessary for the immediate response to chilling stress but also on genes required for the preparation of a potential freezing episode. Many enriched terms at this time point were related to the circadian clock (circadian rhythm, entrainment of circadian clock, circadian regulation of gene expression). Interestingly, many of the enriched terms identified at Ph or Pd were also identified in the GO term enrichment analysis of genes up-regulated at the same time point (Suppl. Figure 6A and C), which suggests a correlation between H3K4me3 deposition and transcriptional induction. On the other hand, the genes losing H3K4me3 after 3 h of cold exposure displayed an enrichment for heat response, development-related terms (“embryo development”, “vegetative to reproductive transition of the meristem”) and protein folding (Figure 17C). Surprisingly, these terms were not identified in the GO term enrichment analysis of the genes showing a down-regulation at this time point (Suppl. Figure 6B). After three days of chilling temperature, genes losing H3K4me3 displayed again an enrichment for development-related terms (Figure 17D). The analysis also identified terms related to photosynthesis (“light harvesting in photosystem I and II”) but also chromatin regulation (“nucleosome positioning”, “chromosome condensation”). Only the terms related to photosynthesis and light stimulus response were identified in the GO term enrichment analysis of late down-regulated genes (Suppl. Figure 6D). This indicates that the loss of H3K4me3 might not be directly correlated to gene repression.

Contrary to the diverse sets of terms obtained at the two time points for H3K4me3 differentially methylated genes, the GO term enrichment analysis for genes gaining or losing H3K27me3 identified similar terms at both time points (Figure 18). This was consistent with the fact that many of the changes that occurred after 3 h persisted after three days (Figure 16C). Genes gaining H3K27me3 showed an enrichment for development-related terms (xylem, cotyledon and petal development, shoot formation) consistent with a slowdown of plant growth during cold exposure (Figure 18A and B). Many of those development-related terms referred to flowering (“maintenance of floral or inflorescence meristem identity”, “transition from vegetative to reproductive growth”), suggesting that cold might prevent this developmental transition. The analysis also uncovered an enrichment of terms related to transcription regulation. Genes losing H3K27me3 showed an enrichment for terms related to stress response (light, herbivore, induced systemic resistance) (Figure 18C and D). Another difference to the H3K4me3 analyses was that there was virtually no overlap between the terms identified as enriched for the differentially H3K27me3 methylated genes and differentially expressed genes (Suppl. Figure 6). It is also interesting to note that, while both genes gaining H3K4me3 and losing H3K27me3 showed an enrichment for stress response related terms, the terms identified for H3K4me3 gain were of stresses closely related to cold, such as water deprivation or salt stress. On the contrary, genes losing H3K27me3 displayed a wider range of stress types, including terms that could be related to stress memory such as systemic acquired resistance.

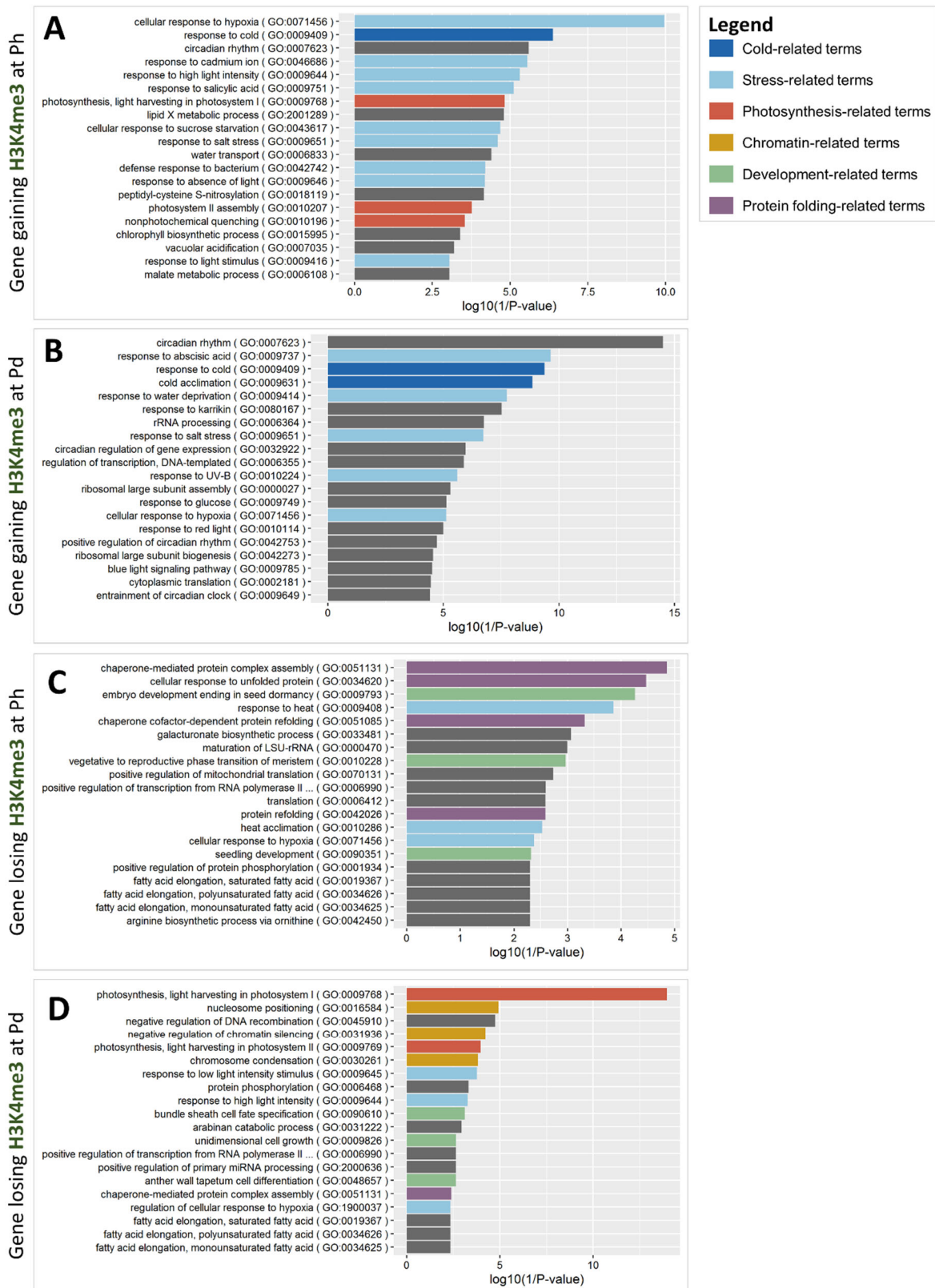


Figure 17: GO biological process term enrichment analysis of genes showing differential H3K4me3 methylation. The enrichment analysis was performed by topGO using the weight01 algorithm and significance was tested using Fisher's exact test comparing the list to all TAIR10 annotated genes. The 20 terms with the lowest p-values are displayed. (A) GO enrichment analysis of genes gaining H3K4me3 after 3 h of cold exposure. (B) GO enrichment analysis of genes gaining H3K4me3 after three days of cold exposure. (C) GO enrichment analysis of genes losing H3K4me3 after 3 h of cold exposure. (D) GO enrichment analysis of genes losing H3K4me3 after three days of cold exposure.

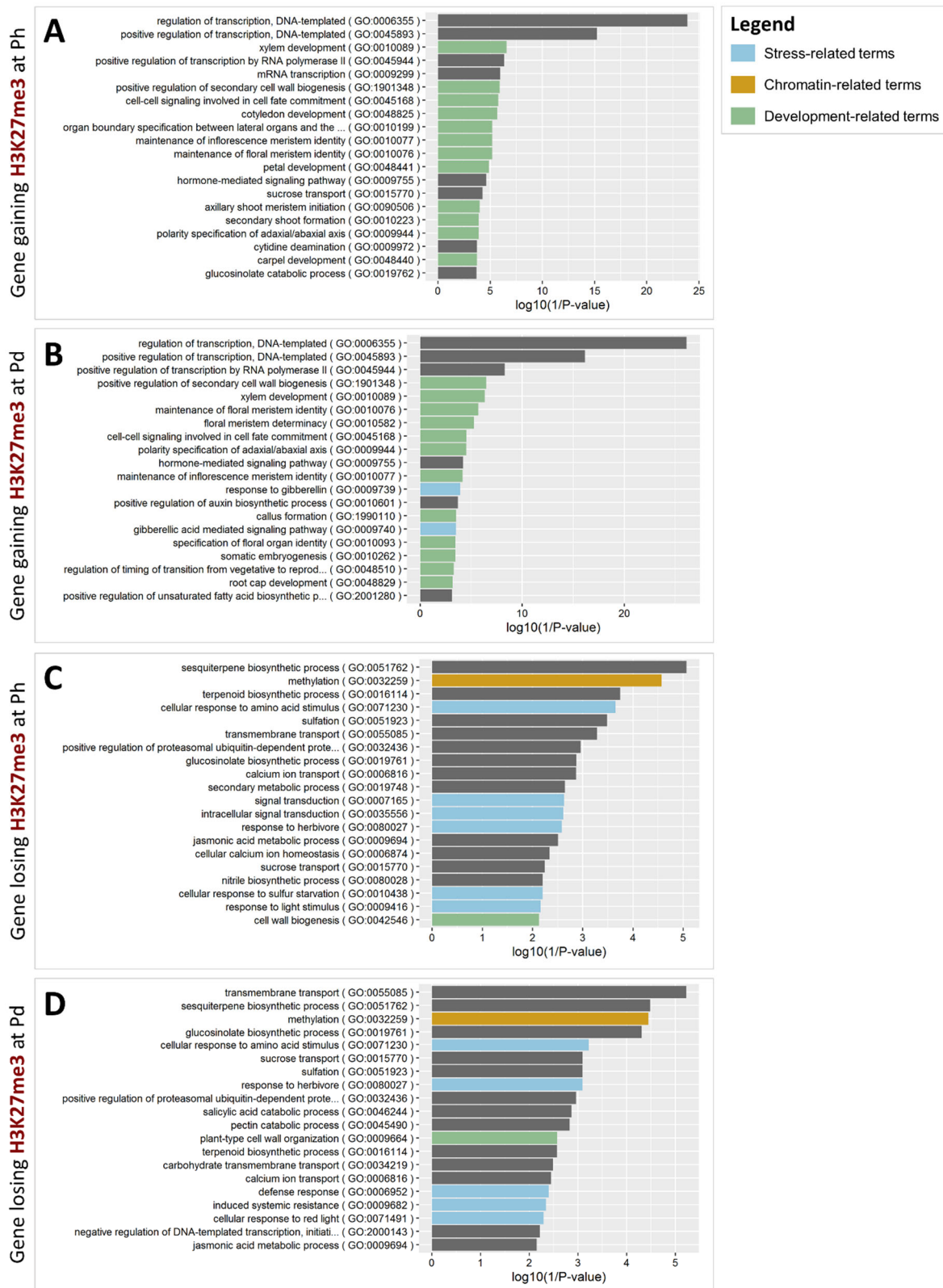


Figure 18: GO biological process term enrichment analysis of genes showing differential H3K27me3 methylation. The enrichment analysis was performed by topGO using the weight01 algorithm and significance was tested using Fisher's exact test comparing the list to all TAIR10 annotated genes. The 20 terms with the lowest p-values are displayed. (A) GO enrichment analysis of genes gaining H3K27me3 after 3 h of cold exposure. (B) GO enrichment analysis of genes gaining H3K27me3 after three days of cold exposure. (C) GO enrichment analysis of genes losing H3K27me3 after 3 h of cold exposure. (D) GO enrichment analysis of genes losing H3K27me3 after three days of cold exposure.

Altogether, the identification of differentially methylated genes revealed that cold affects the levels of H3K4me3 and H3K27me3 on thousands of genes. Although numerous genes carry both methylation marks prior to the cold exposure, very few underwent differential methylation of both H3K4me3 and H3K27me3. The GO term enrichment analysis confirmed that differential methylation affects different sets of genes depending on the considered mark. Coupled to the drastic difference of persistence of the cold-induced changes, this further strengthened the hypothesis that H3K27me3 and H3K4me3 differential methylation might serve different purposes during the cold response.

3.2.1.3 Bivalency is not resolved to monovalency upon cold exposure

As described previously in section 3.1, many cold-induced genes are bivalent prior to any cold exposure. During cell differentiation, most of the bivalent domains in embryonic stem cells are resolved into H3K27me3 or H3K4me3 monovalent loci (Bernstein et al., 2006; Voigt et al., 2013). Considering that both methylation marks composing the bivalency are undergoing dynamic changes in their levels during cold exposure (see section 3.2.1.1), it was hypothesized that bivalent genes might also be undergoing differential methylation leading to the resolution of bivalency into monovalency during chilling stress in *Arabidopsis thaliana*. To examine this possibility, the number and size of bivalent regions was examined after different lengths of cold exposure (Figure 19A). To increase resolution, a bivalent region was here defined as a domain of at least 1 bp where a H3K4me3 peak and a H3K27me3 peak overlapped. The number of bivalent domains decreased slightly after 3 h of cold exposure and even further after 3 d: around 200 less bivalent regions were detected for plants exposed to 4°C for three days compared to naïve plants (Figure 19A). The size distribution of the bivalent domains was similar in all conditions but showed a reduced number of bivalent domains whose size was around 500 bp. This indicates that the smaller number of bivalent regions detected after cold treatment was due to a complete loss of certain medium-sized bivalent domains and not to an extension of some of them leading to the fusion of neighbouring bivalent regions.

In order to obtain more insight into the cold-triggered changes in bivalency, the genes affected by those changes were identified and divided into genes gaining and losing bivalency at each examined time (Figure 19B). Consistent with the observed decrease in the total number of bivalent regions, about twice more genes were found to be losing bivalency in the cold than gaining it. Interestingly, about two thirds of the genes losing bivalency after 3 h in the cold remained non-bivalent at the 3 d time point, while only 40% of the genes gaining bivalency after 3 h were still bivalent after three days of cold. This indicates that the gain of bivalency is a transient phenomenon, while the loss is a more persistent one. A GO biological term enrichment analysis revealed that the genes gaining bivalency upon cold exposure are enriched for terms related to stress responses (response to toxic substance, to nematode, drought recovery) (Suppl. Figure 7A and B). The genes losing bivalency showed an enrichment for genes related to the response to phytohormones (salicylic acid, jasmonic acid) and also genes involved in the development (regulation of organ growth, hydrotropism) (Suppl. Figure 7C and D).

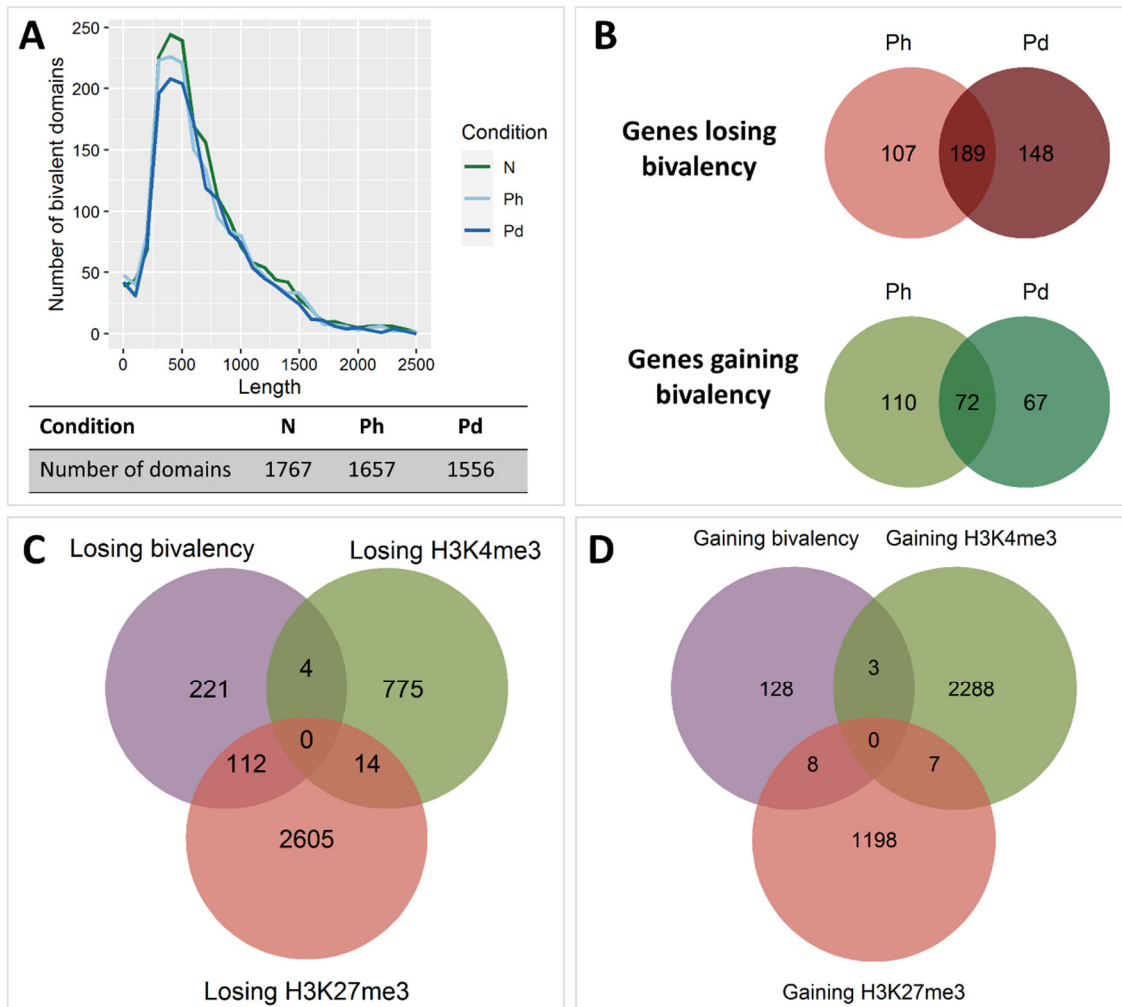


Figure 19: Cold-triggered changes in bivalency. (A) Length distribution of bivalent regions upon 3 h (Ph) or three days (Pd) of cold exposure. Bivalent regions were here defined as regions of at least 1 bp that carry both H3K4me3 and H3K27me3. No significant difference in distribution of the length of cold-treated domain vs naïve domain was detected by two-sided two-sample Kolmogorov-Smirnov test. (B) Venn diagrams showing the genes losing (upper panel) or gaining (lower panel) bivalency upon cold exposure. A gene was considered bivalent if at least 150 bp of its gene body carried both H3K4me3 and H3K27me3. (C) Venn diagram showing the overlap between genes losing bivalency after 3 d at 4°C and genes losing H3K4me3 or H3K27me3 at the same time point. (D) Venn diagram showing the overlap between genes gaining bivalency after 3 d at 4°C and genes gaining H3K4me3 or H3K27me3 at the same time point.

As a gain (resp. loss) of bivalency could be due to the gain (resp. loss) of H3K4me3 or H3K27me3, it was relevant to examine whether a particular mark was the major contributor to the change. To that end, the genes losing bivalency after three days in the cold were overlapped with the genes losing H3K4me3 and/or H3K27me3 at the same time point. About 30% of the genes losing bivalency showed a reduction in H3K27me3, while only 1% of them lost H3K4me3 (Figure 19C). Similar proportions were observed for the 3 h time point (data not shown), which suggested that the loss of bivalency is mostly driven by a loss of H3K27me3. This is consistent with the persistence of the loss of bivalency over time, as it was previously shown that the vast majority of the changes in H3K27me3 occurring after 3 h of cold exposure persisted after three days (Figure 16C). On the other hand, very few of the genes gaining bivalency in the cold showed differential methylation and the proportions were similar for H3K4me3 and H3K27me3 (Figure 19D). However, a visual inspection of the H3K4me3 and

H3K27me3 levels on some of those genes using a genome browser revealed that several of them (such as *VIN3*, *NPF5.2*, *ZAT11*, *WRKY36*) showed a slight gain of H3K4me3 that was probably too small to be detected or considered significant in the differential methylation analysis (data not shown). While these observations should be considered with caution as not all of the genes gaining bivalency were examined, they suggest that the gain of bivalency was due to a gain of H3K4me3. This is consistent with the observed temporary nature of the gain of bivalency as changes in H3K4me3 levels were shown to mostly be transient (Figure 16B). All in all, cold did not lead to a drastic resolution of bivalency into monovalency as only a small percentage of bivalent genes lost this characteristic, contrary to what is observed during cell differentiation (Bernstein et al., 2006). This suggests that bivalency might hold a different role in the plant stress response. The loss of bivalency was mostly associated with a stable decrease in H3K27me3 while some genes transiently gained bivalency by accumulating H3K4me3.

3.2.1.4 Bivalent genes are not more likely to undergo differential methylation

Bivalent genes are generally proposed to be loci of highly dynamic methylation, where the levels of H3K4me3 and H3K27me3 are rapidly adjusted to allow gene induction upon perception of differentiation signals (Voigt et al., 2013). To determine whether this property is conserved in the context of plant stress responses, it was necessary to examine whether bivalent genes were more likely to be differentially methylated than non-bivalent genes upon cold exposure. While about 15% of all genes and 32% of the H3K4me3 monovalent genes underwent H3K4me3 differential methylation upon cold exposure, less than 11% of bivalent genes showed a similar fate (Figure 20A). They were particularly less likely to gain H3K4me3, which might be due to the fact that bivalent genes already displayed larger H3K4me3 domains than monovalent genes prior to any cold exposure (Figure 10A), potentially reducing the need for H3K4me3 accumulation during a stress episode. For H3K27me3, the percentages of genes undergoing differential methylation were similar for bivalent and monovalent genes and bivalent genes were slightly less likely to gain H3K27me3, especially after 3 h at 4°C (Figure 20B). Overall, the bivalent genes were not more likely to undergo differential methylation than H3K4me3 or H3K27me3 monovalent genes, contrary to what was expected. This suggests that bivalency is a stable feature, participating in the induction or repression of a gene by processes other than rapid adjustments of the levels of each methylation mark.

Bivalency could for example take part in the control of gene expression by regulating chromatin accessibility. Indeed, previous results showed that bivalent regions are associated with a more accessible chromatin prior to any stress exposure (Figure 10C) and it is known from investigations of *Solanum tuberosum* tubers that bivalent loci get even more accessible upon cold exposure (Zeng et al., 2019). Since the chromatin of *Arabidopsis thaliana* also undergoes variations in accessibility during a chilling treatment (Raxwal et al., 2020), the changes in accessibility of bivalent regions was examined in order to determine whether they also tend to open upon cold exposure. To that end, the regions identified as opening or closing by Raxwal et al. (2020) were overlapped with the domains identified as bivalent in naïve conditions. Out of the 1684 bivalent regions, 600 were overlapping with a domain closing upon cold exposure, which was significantly higher than what was observed for the control sets (Figure 20C). On the other hand, the overlap between bivalent and opening regions was significantly lower than the controls, with only 267 bivalent regions getting more accessible. Altogether, this analysis

indicates that bivalent regions become less accessible upon cold exposure and that bivalency might be involved in the control of chromatin accessibility.

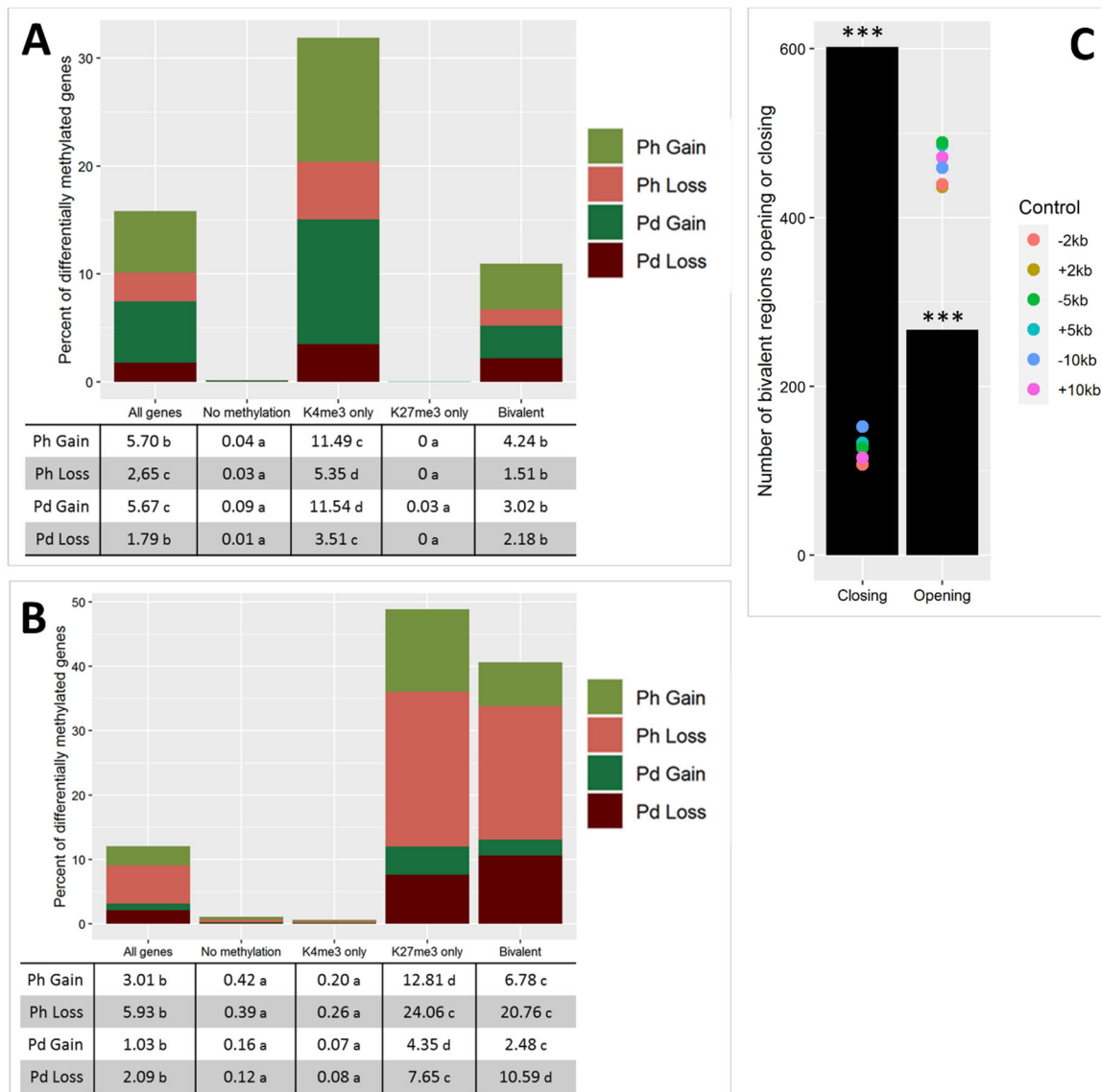


Figure 20: Fate of bivalent genes during cold exposure. (A) and (B) Percentage of genes showing H3K4me3 (A) or H3K27me3 (B) differential methylation after 3 h (Ph) or 3 d (Pd) at 4°C in all nuclear genes, non methylated genes, H3K4me3 or H3K27me3 monovalent genes and bivalent genes. Identical letters next to the percentages indicate no significant difference, calculated by Marascuilo procedure ($\alpha = 0.05$). (C) Number of bivalent domains overlapping with regions getting more (opening) or less (closing) accessible upon cold exposure. The coordinates of opening and closing regions were obtained from Raxwal et al. (2020). The ± 2 kb, ± 5 kb and ± 10 kb are control sets where the coordinates of the bivalent domains were shifted up- (+) or downstream (-) by the indicated number of bases. Significance was tested by permutation test, *** indicate p-value ≤ 0.001 .

3.2.1.5 Differential methylation partially correlates with changes in expression

Cold exposure led to differential methylation of H3K4me3 and H3K27me3 on numerous genes. As these marks are described as activating and silencing respectively, this differential methylation might participate in the transcriptional regulation of differentially expressed genes. To test this possibility, the relationships and potential correlations between transcriptional activity and differential methylation were examined.

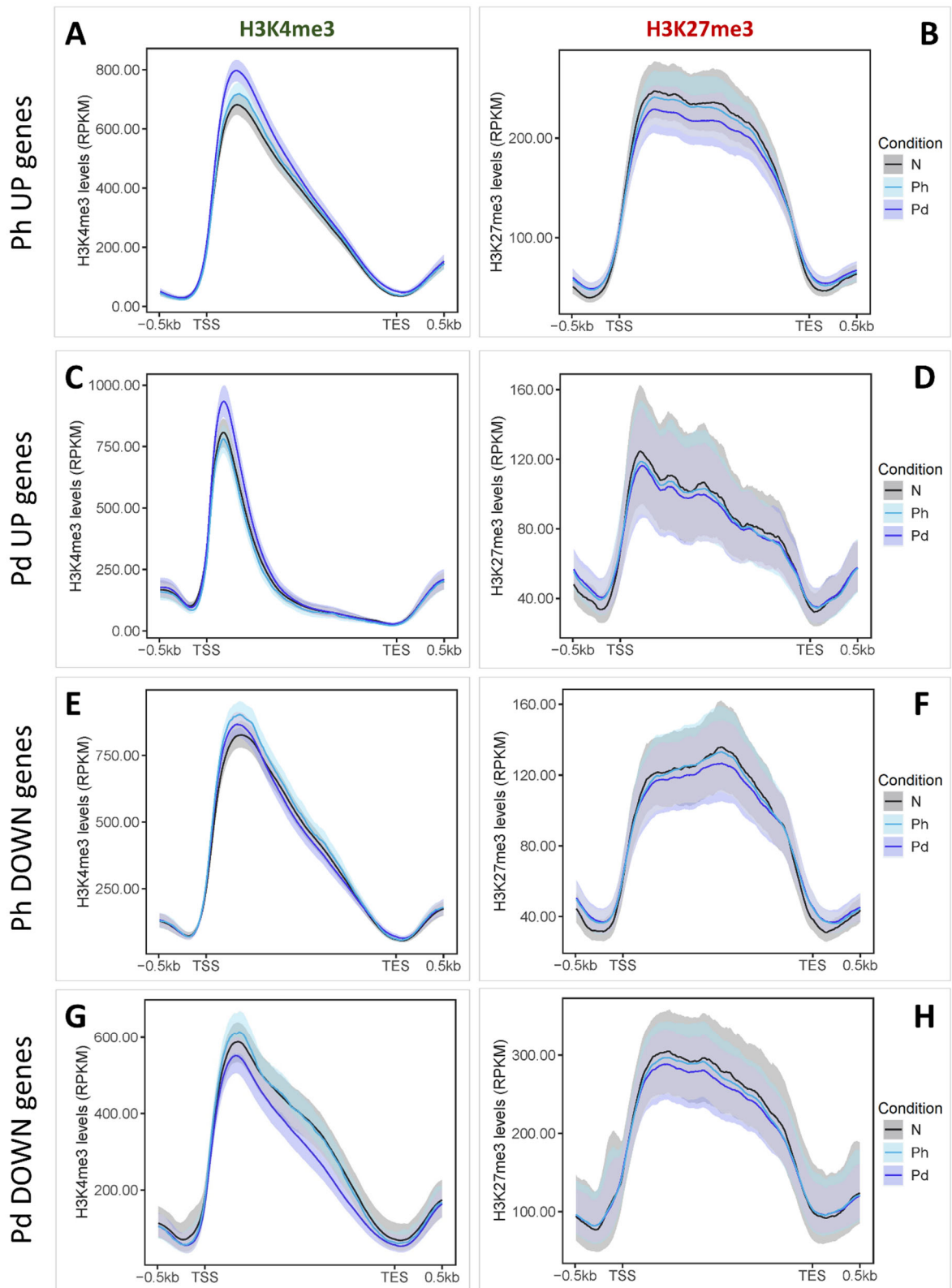


Figure 21: Changes of methylation levels on differentially expressed genes. Metagenes plots showing the levels of H3K4me3 (A), (C), (E) and (G) and H3K27me3 (B), (D), (F) and (H) on cold-differentially expressed genes. Cold DE genes were identified from the RNA-seq described in 3.1.5 and divided into genes induced after 3 h (Ph UP, (A) and (B)), induced first after three days (Pd UP, (C) and (D)), repressed after 3 h (Ph DOWN, (E) and (F)) and repressed first after three days (Pd DOWN, (G) and (H)). Signal is shown as RPKM. The ribbons represent the 95% confidence interval of the mean computed using 1000 bootstraps.

First, the changes in the levels of H3K4me3 and H3K27me3 on cold-regulated genes were investigated using metagene plots (Figure 21). The genes that were found to be differentially expressed upon cold exposure using the RNA-seq described previously (3.1.5) were divided into four different lists depending on the direction of the transcriptional change (up- or down-regulated) and the time point at which their expression was first described to change. Genes whose expression was induced early during cold exposure showed a slight gain of H3K4me3 around the TSS, which was amplified after three days (Figure 21A). Similarly, late cold-induced genes (genes whose induction was first detected after three days) showed a strong gain of H3K4me3 around the TSS at the same time point, but this gain was not already present at 3 h (Figure 21C). Conversely, the H3K4me3 levels were slightly reduced on genes repressed after three days of cold exposure, not just around the TSS but over the whole the gene body, but this trend was not visible after just 3 h (Figure 21E and G). This suggests that the change in transcriptional activity of a gene is positively correlated with H3K4me3 levels at that locus at the later time point of cold exposure but not automatically at the earlier one. On the other hand, the levels of H3K27me3 were reduced on all cold-differentially expressed genes after three days but not after 3 h of cold exposure only (Figure 21B, D, F and H). This is consistent with the global reduction in H3K27me3 signal observed with the Western Blot and suggests that transcriptional changes do not require differential H3K27me3 methylation. However, this approach is very global and does not take into account the magnitude of the transcriptional change nor the fact that some of the differentially expressed genes might not be targets of the investigated histone marks.

To better assess a potential correlation between differential methylation and differential expression, the cold-induced changes in expression were plotted as a function of the variations in the levels of H3K4me3 and H3K27me3 (Figure 22). Only genes that were found to be significantly differentially regulated upon cold exposure ($p\text{-adj} < 0.05$) and possessed at least one significantly H3K4me3 (resp. H3K27me3) differentially methylated region were examined. As a single gene might have different domains gaining or losing a certain mark, a global fold change was computed using featureCounts, a similar strategy as the one used in the RNA-seq analysis. After 3 h of cold exposure, no correlation was found between the changes in expression and the variation in the levels of any of the investigated methylation marks (Figure 22A and B). After three days however, a positive correlation was uncovered for H3K4me3: genes gaining H3K4me3 were more likely to show an increase in expression while genes losing the same mark were usually repressed (Figure 22C). The opposite effect was observed for H3K27me3, where expression changes and methylation changes were negatively correlated: genes losing H3K27me3 were more likely to be induced by cold while genes gaining the mark showed a lower expression in the cold (Figure 22D). These results matched the proposed hypothesis that induction of cold-responsive genes is associated with an increase in the activating mark H3K4me3 and a reduction of the repressive mark H3K27me3 and vice-versa for repressed genes. However, as this was observed only for the late time point, this suggests that the two phenomena do not occur at the same pace. Indeed, after three days, the plants are already fully accustomed to the cold and the stress response is stably established, meaning that the chromatin state and the expression levels correlate. On the other hand, after only three hours of cold exposure, the plants are still at the beginning of their response to the stress and not all processes might be fully accomplished yet. To try and decipher which one might happen first, a similar approach was used, this time correlating the methylation changes at the early time point with the expression changes at the latest and vice versa (data not

shown). While the H3K4me3 changes at Ph did not correlate with the expression changes at Pd, a significant positive correlation (0.296, p-value < 0.0001) was observed between the late H3K4me3 changes and the early changes in expression (data not shown). This suggests that the transcriptional activity of a gene changes prior to its H3K4me3 methylation status.

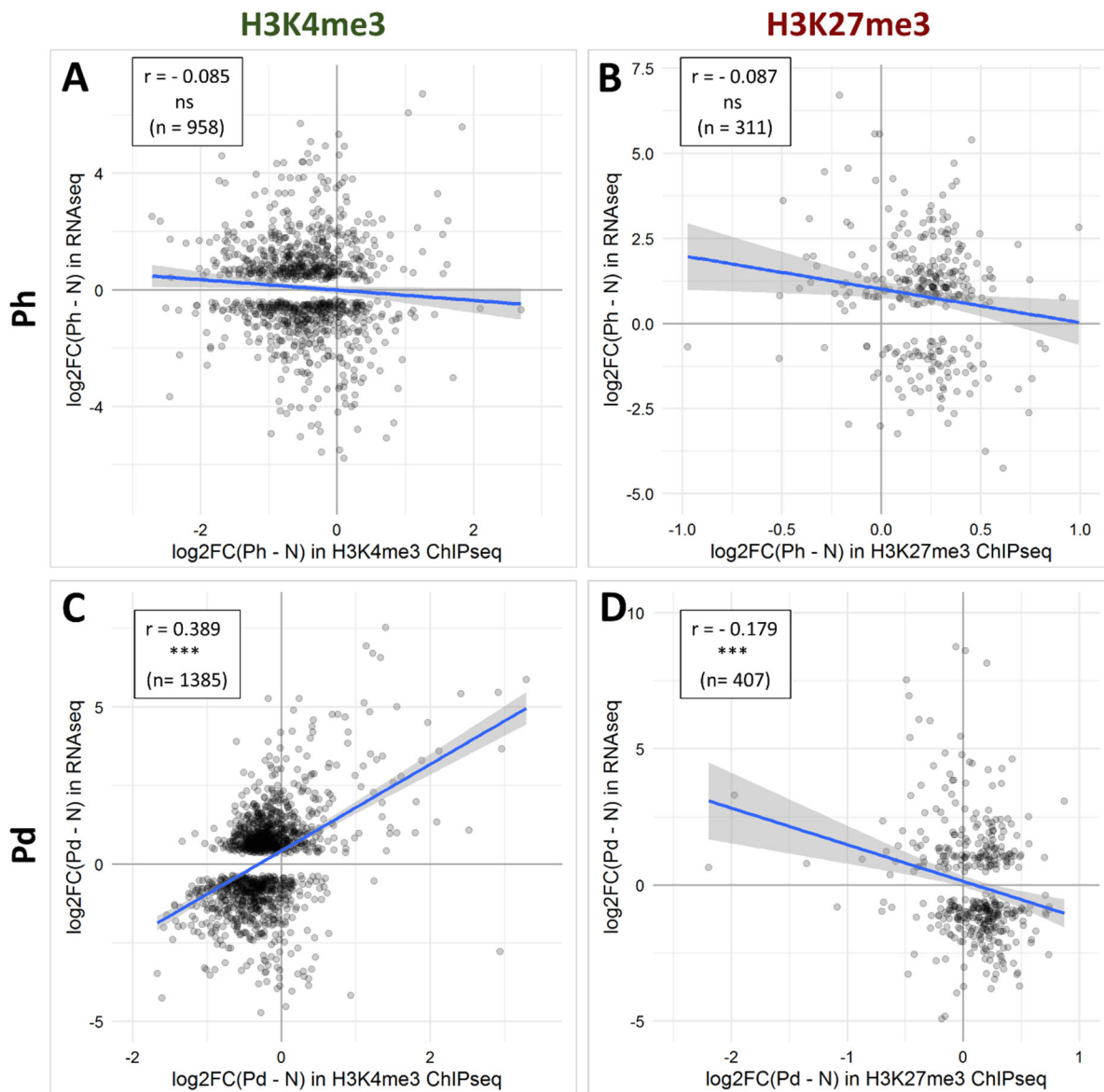


Figure 22: Correlation between the changes in methylation and the changes in expression. The differential expression data was obtained from the RNA-seq described in 3.1.5. (A) and (C) show the correlation between H3K4me3 methylation changes and expression changes while (B) and (D) show the correlation between H3K27me3 methylation changes and expression changes. (A) and (B) depict the correlation at the 3 h time point while (C) and (D) depict the one at the 3 d time point. In all graphs, the X axis denotes the log2 fold change in methylation signal over the whole gene (TSS to TES) at the respective time point compared to non-cold-treated plants and the Y axis shows the log2 fold change in expression for the same comparison. Only genes showing both a significant difference in expression and the respective methylation at the indicated time point are shown on the scatterplots, their number is indicated as n. The correlation analyses were performed using the Spearman method, the correlation coefficient is indicated as r. ns indicates a non-significant correlation and *** denotes a p-value < 0.001.

For H3K27me3, none of the correlations across time point was significant, so no conclusion can be reached (data not shown). It is also worth noting that the correlation observed for H3K27me3 and expression changes after three days of cold exposure was lower than the one seen for H3K4me3, and that the number of genes showing both H3K27me3 and expression changes was smaller than for the activating mark. Therefore, it seems that the link between H3K27me3 and transcriptional activity is weaker than the one of H3K4me3, which is consistent with the observations from the metagene plots (Figure 21).

As changes in expression are positively correlated with differential H3K4me3 methylation and negatively correlated with differential H3K27me3 methylation, one can hypothesize that differential methylation participates in transcriptional regulation or vice versa. To examine this possibility, it was necessary to first identify genes that were significantly differentially expressed and showed a matching significant change in methylation status that could be examined in further experiments. This was achieved using Venn diagrams, by overlapping the list of up-regulated genes with the lists of genes gaining H3K4me3 and losing H3K27me3 and overlapping the list of down-regulated genes with the lists of genes losing H3K4me3 and gaining H3K27me3, for each time point (Figure 23). As this approach aims at establishing a list of reliable candidate genes that could be used in further ChIP-qPCR and RT-qPCR experiments, for example to study mutants, only genes showing an absolute expression log₂FC of at least 1 were kept, explaining the potential discrepancy in numbers compared to the correlation analyses (Figure 22). Interestingly, the overlap between significantly differentially methylated and significantly differentially expressed genes were very small (Figure 23). Only about 10% of up- or down-regulated genes showed a change in H3K4me3 levels, with the biggest overlap happening for the late up-regulated genes. This coincides with the stronger correlation between methylation and expression observed at this time point (Figure 22C and Figure 21C). This suggests that changes in transcriptional activity can happen even in the absence of significant variations in H3K4me3 methylation and that differential H3K4me3 methylation does not always impact the expression levels. Similar conclusions can be reached for H3K27me3: the overlaps between differentially methylated and differentially expressed genes were even smaller for this mark (Figure 23). As the correlation between H3K27me3 and expression changes was weaker than for H3K4me3 (Figure 22D), it was not unexpected. While it appears that differential methylation is not always associated with differential expression, the Venn diagrams provided list of genes whose methylation status and expression were affected by cold. Those are promising reporters that could be used to investigate the role of differential histone methylation in the induction of the *COR* genes.

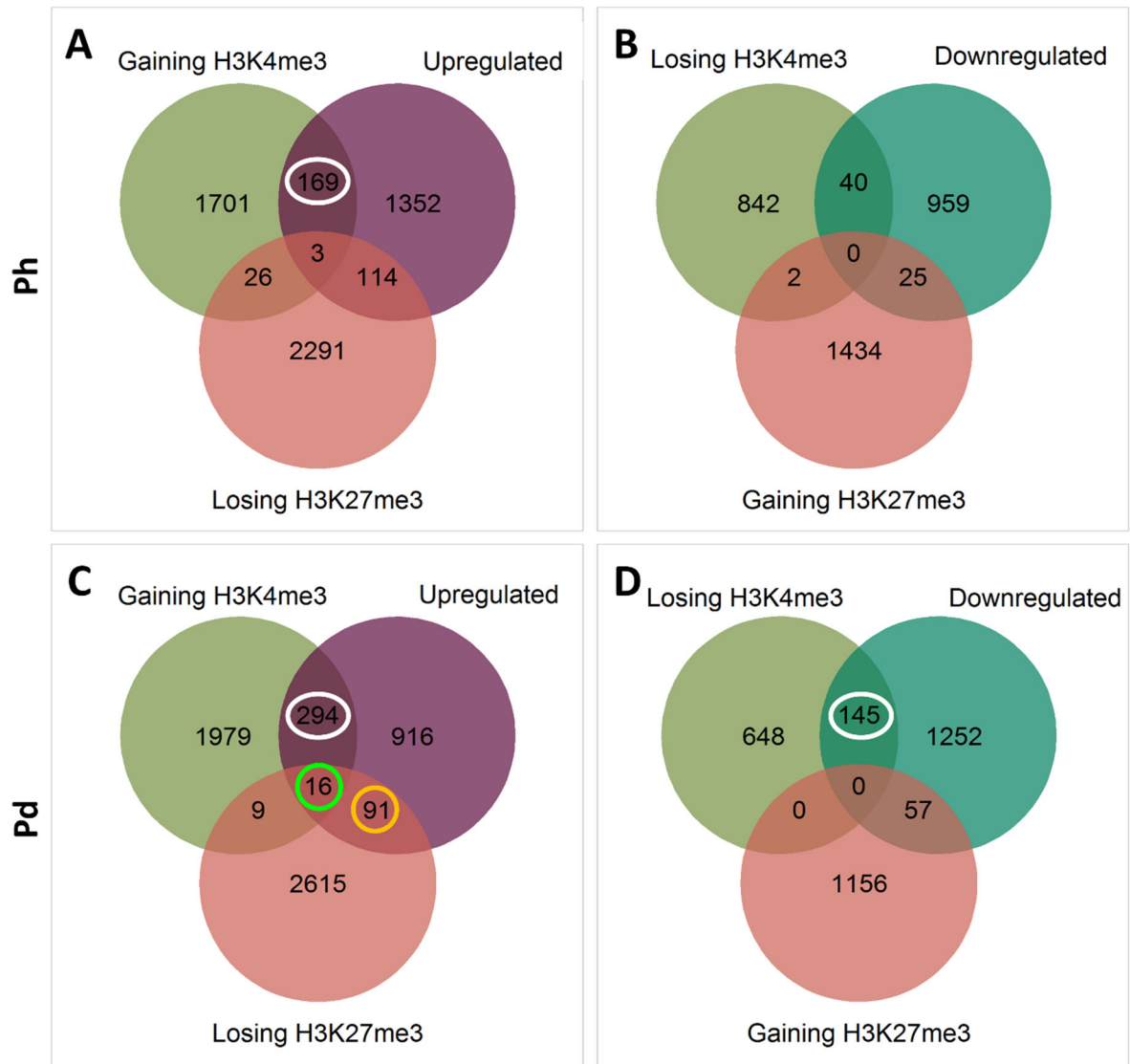


Figure 23: Identification of differentially methylated and differentially expressed genes. (A) and (C) Overlap of genes gaining H3K4me3, losing H3K27me3 and up-regulated by cold at Ph (A) or Pd (C). **(B) and (D)** Overlap of genes losing H3K4me3, gaining H3K27me3 and down-regulated by cold at Ph (B) or Pd (D). The white circles indicate the genes that showed differential expression and differential methylation of H3K4me3 only. The green circle indicates the genes that were up-regulated, gained H3K4me3 and lost H3K27me3. The yellow circle indicates the genes that were up-regulated and lost H3K27me3 only.

The methylation status of some of those genes is displayed in Figure 24. *COR15A* and *LT130* were found among the 16 genes that are induced by cold and lose H3K27me3 and gain H3K4me3 after three days at 4°C (green circle in Figure 23C and Figure 24). Other genes displaying a similar behaviour are, among others, *GOLS3*, *PAL1* and *COR15B* (green circle in Figure 23C, data not shown). Certain cold-induced genes only showed differential methylation for one of the two investigated histone marks: *CIPK25* lost H3K27me3 (yellow circle in Figure 23C and Figure 24) while *CBF3* and *TCF1* gained H3K4me3 (white circle in Figure 23A and C respectively, Figure 24). Interestingly, all *CBF* genes showed a similar differential methylation pattern: the gain of H3K4me3 triggered by a 3 h cold exposure was maintained after three days, even though their expression returned to naïve levels at the later time point (white circle in Figure 23A, Figure 12D and Figure 24). Finally, no cold-repressed gene showed differential methylation for both marks (Figure 23B and D). However, many down-regulated genes showed

a loss of H3K4me3, such as *PIN-FORMED 7 (PIN7)* (white circle in Figure 23D, Figure 24). Importantly, the differential methylation analysis also allowed the identification of genes whose methylation levels are not affected by cold exposure: *FUSCA 3 (FUS3)* showed constant high levels of H3K27me3 while *ACTIN7* displayed constant high levels of H3K4me3 (Suppl. Figure 8). These genes can therefore be used to normalize the %input in ChIP-qPCR experiments, in order to account for variability in the efficiency of the immunoprecipitation.

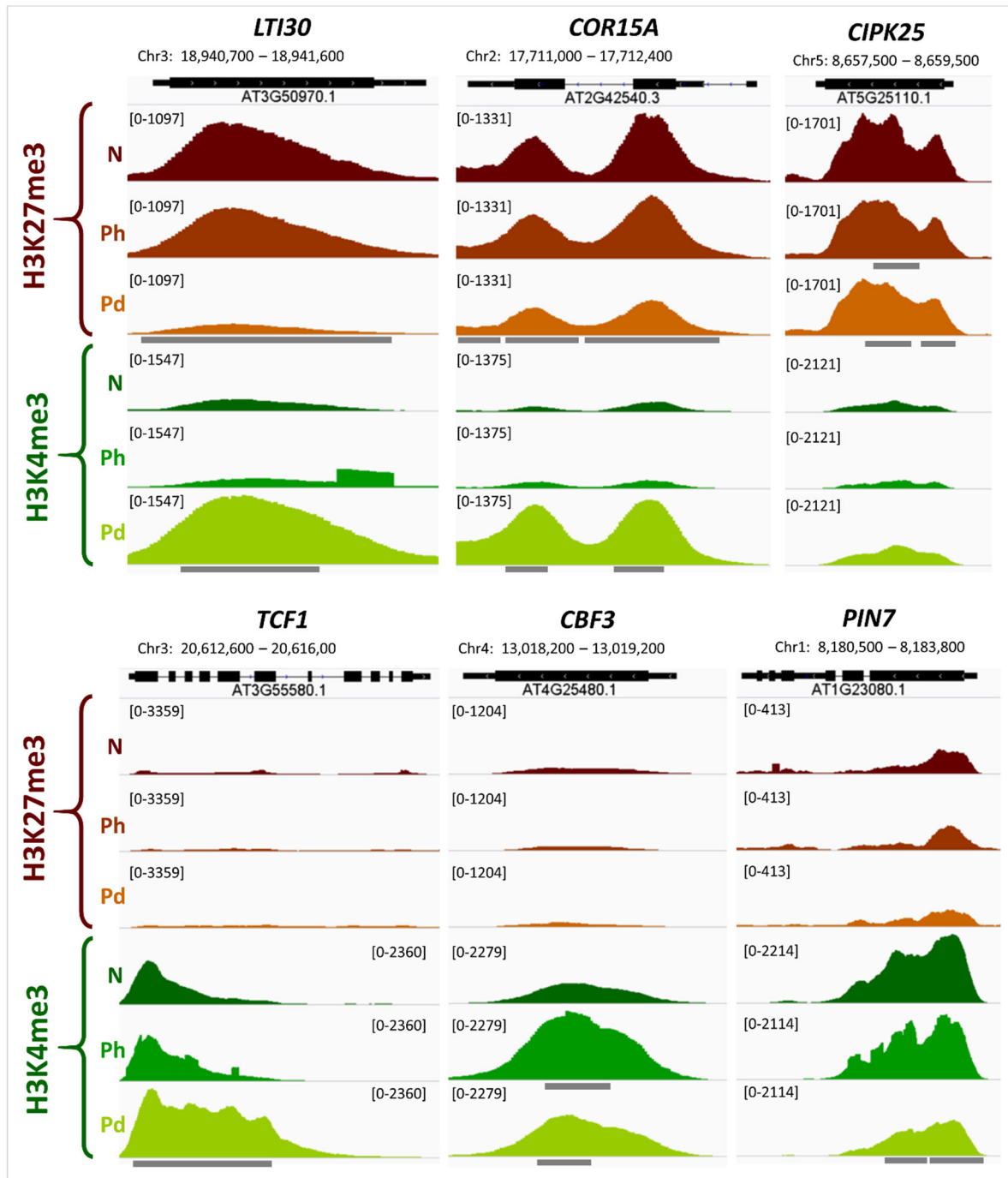


Figure 24: Genome browser views at differentially methylated genes H3K27me3 and H3K4me3 ChIP-seq signals in naive plants (N) and plants exposed to cold for 3 h (Ph) or 3 d (Pd), from two merged biological replicates. The numbers in brackets at the top of each track denote the scale of that track in RPKM and the gray bars indicate regions of significant differential methylation identified by diffReps (Figure 15). *LTI30* and *COR15A* are induced by cold, lose H3K27me3 and gain H3K4me3. *CIPK25* is induced by cold and loses H3K27me3. *TCF1* and *CBF3* are induced by cold and gain H3K4me3. *PIN7* is repressed by cold and loses H3K4me3.

Finally, the findings from the ChIP-seq were validated by performing ChIP-qPCR on a few genes identified in the differential methylation analysis. Consistent with the ChIP-seq, *COR15A*, *LT130* and *TCF1* showed a significant gain of H3K4me3 upon cold exposure (Suppl. Figure 9A) and *COR15A* and *LT130* additionally showed a significant loss of H3K27me3 (Suppl. Figure 9B). These genes are therefore ideal candidates to investigate which actors might be involved in differential methylation upon cold exposure and to determine whether this process is necessary for a proper regulation of gene expression during a stress episode.

3.2.1.6 Differential methylation is not caused by a change in nucleosome density

While the differential methylation analysis of the ChIP-seq data allowed the identification of numerous genes gaining or losing H3K4me3 or H3K27me3 during cold exposure, it appeared necessary to verify that these differences were caused by real variations in the levels of the methylation marks and not simply by a change in nucleosome density. As previously mentioned, the ChIP-seq was also performed for H3, using an antibody capable of binding to this histone regardless of the post-translational modifications it might carry on its N-terminal tail. Therefore, the levels of H3 on differentially methylated regions was investigated using metagene plots (Figure 25A to D). To simplify the study, a master set containing the differentially methylated regions of both time points was created for each modification and direction of the change (loss or gain). Interestingly, the regions undergoing methylation changes associated with an activation of the transcription did not show substantial variations in H3 levels. Indeed, regions losing H3K27me3 upon cold exposure did not show any significant difference in H3 signal after treatment (Figure 25B) while regions gaining H3K4me3 displayed a slight gain of H3 after 3 d in the cold, but the magnitude of the variation was much smaller than that of the H3K4me3 gain at the same loci (Figure 25C, data not shown). On the other hand, regions undergoing methylation changes associated with a repression of the transcription presented more considerable variations in H3 signal (Figure 25A and D). Domains losing H3K4me3 had lower H3 level at Pd, but higher at Ph (Figure 25A). Regions gaining H3K27me3 upon cold exposure showed an increase of H3 signal after 3 d at 4°C, but not at 3 h (Figure 25D). Altogether, this suggested that the gain of H3K4me3 and loss of H3K27me3 were likely not caused by changes in nucleosome density. For regions losing H3K4me3 or gaining H3K27me3, a potential contribution of nucleosome density to the differential methylation could not be excluded. As the variations in H3 levels observed on the metagene plots were small, it was difficult to determine whether they were significant and whether they were occurring at all differentially methylated loci or were driven by only a few of them.

To discriminate between these two possibilities, a differential binding analysis was conducted for H3, in a manner similar to the one adopted for the differential methylation analysis. Domains presenting a change in H3 signal upon cold exposure were identified using the diffReps algorithm and only the regions with an adjusted p-value inferior to 0.001 and a change of at least 25% were kept. Between 600 and 900 regions were detected as gaining or losing H3 at the two time points considered, which was five times less than the number of differentially methylated domains (Figure 25E). To determine whether these two phenomenon (differential methylation and change in H3 level) actually co-occurred on the same locus, the regions with increased H3 level were overlapped with the regions gaining H3K4me3 or H3K27me3. Almost no region gaining H3K27me3 showed a significant increase in H3 signal, while only a handful of loci showed both an increase in H3K4me3 methylation and in H3 (Figure 25F). These loci

represented less than 2% of the total number of regions gaining H3K4me3 upon cold exposure. The regions showing both a loss of H3 and H3K4me3 or H3K27me3 were not more numerous and represented again less than 2% of the regions losing methylation upon cold exposure. This second strategy confirmed that the changes in methylation levels are for the most part not caused by a difference in nucleosome density, as the vast majority of the regions gaining (resp. losing) the investigated marks did not show a significant gain (resp. loss) of H3 upon cold exposure. As this study is focusing on the role of histone methylation in the induction of *COR* genes, these observations were further validated by examining the H3 levels by ChIP-qPCR on the cold-induced genes gaining H3K4me3 or losing H3K27me3 identified previously (Figure 23 and Figure 24). No significant variation in H3 levels was detected on any of the investigated genes (Suppl. Figure 9C), confirming that changes in nucleosome density are not major contributors to differential methylation.

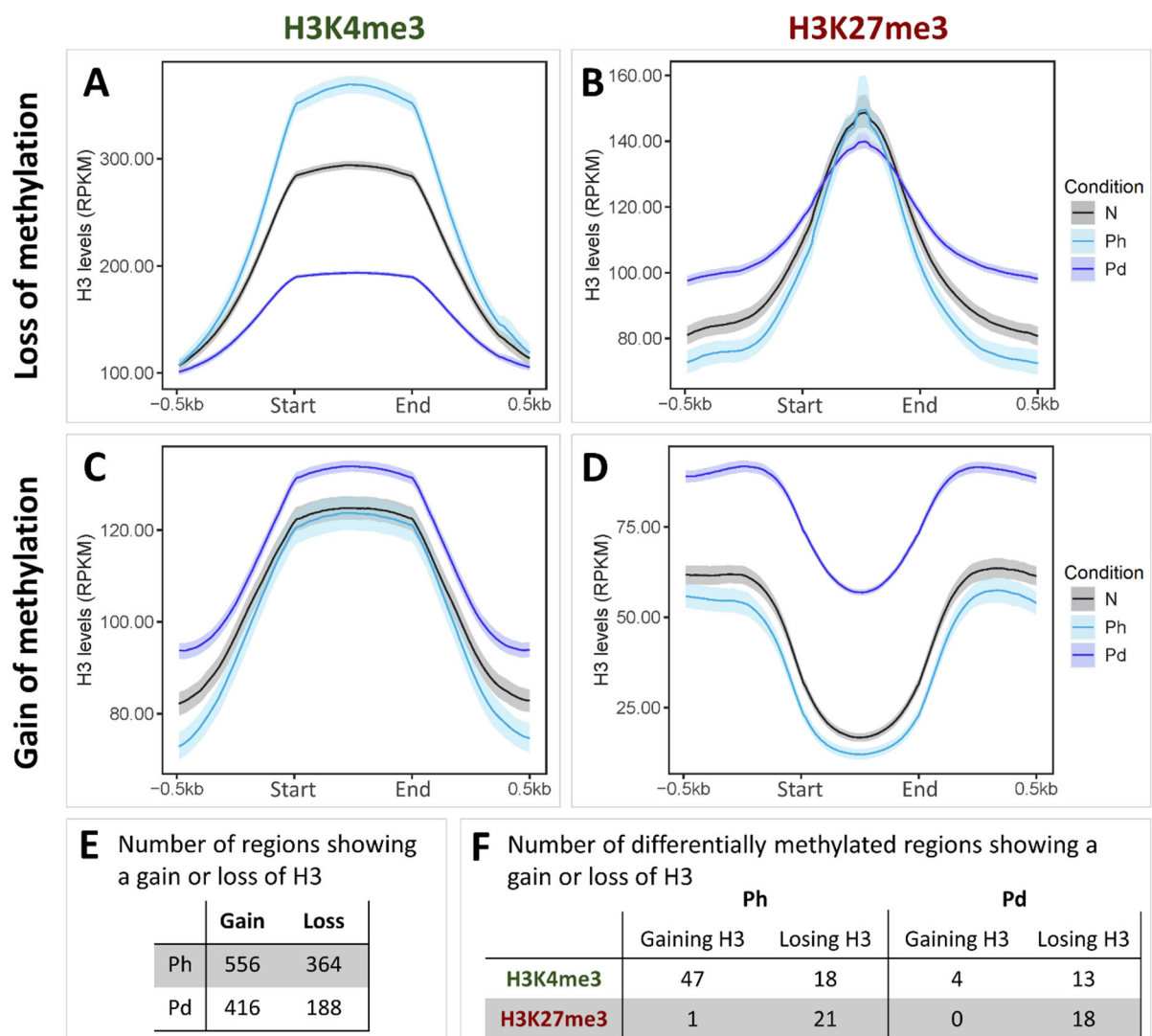


Figure 25: Changes of H3 levels upon cold exposure. Plants were grown for 21 days at 20°C (N) and then exposed to 4°C for 3 h (Ph) or 3 d (Pd) (A), (B), (C) and (D) Metagene plots showing the levels of H3 on regions previously identified as differentially methylated by diffReps (Figure 15): regions losing H3K4me3 (A), losing H3K27me3 (B), gaining H3K4me3 (C) or gaining H3K27me3 (D). The differentially methylated regions for each mark and direction of change were pooled for both time points and scaled to 500 bp. The H3 signal is shown as RPKM. The ribbons represent the 95% confidence interval of the mean computed using 1000 bootstraps. (E) Number of regions showing a significant gain or loss of H3 upon cold exposure, according to the diffRep algorithm. (F) Number of regions showing a gain or loss of H3 during cold exposure that also displayed H3K4me3 or H3K27me3 differential methylation.

Altogether, the genome-wide investigations of H3K4me3 and H3K27me3 distributions revealed that both marks underwent active differential methylation during cold exposure but they had different dynamics and affected distinct sets of genes. H3K4me3 (resp. H3K27me3) differential methylation, albeit not always associated with changes in expression, globally displayed a positive (resp. negative) correlation with transcriptional variations of the underlying genes. In particular, the induction of numerous *COR* genes was associated with a gain of H3K4me3 and/or a loss of H3K27me3, raising the possibility that differential methylation might participate in their transcriptional regulation.

3.2.2 Identifying the actors involved in cold-triggered histone methylation dynamics

As described in the previous section, cold exposure affects the levels of H3K4me3 and H3K27me3 on numerous genes, but the mechanisms leading to these changes remain undiscovered. As deciphering them would also allow to determine whether the alteration of the chromatin status contributes to the induction of *COR* genes, efforts were then directed towards the identification of the actors involved in this process.

3.2.2.1 Cold affects the transcription and splicing of many chromatin regulators

To shed a light on the actors potentially implicated in cold-triggered chromatin changes, an *in silico* approach was used, based on the hypothesis that a protein involved in the process will likely be regulated by cold (Figure 26A and B). Therefore, a list containing most of the chromatin-related proteins of *Arabidopsis thaliana* was extracted from the ChromDB database (Gendler et al., 2008) and overlapped with genes which are either differentially spliced (DAS) or differentially expressed (DE) during cold exposure, taken from the same published dataset described previously (Calixto et al., 2018) (Figure 26A). While the chromatin regulators did not show a particular enrichment in cold-DE genes, they displayed a highly significant enrichment for cold-DAS genes, with a representation factor of 1.78 (Figure 26B). 14 chromatin genes were both differentially expressed and spliced during the cold. As the present study focuses on H3K4me3 and H3K27me3, a more careful look was given to genes involved in the setting and removal of those two marks. H3K4me3 is set by members of the Trithorax family (TrxG) and some of its members are cold-regulated: *ATX1*, *ATX4*, *ATRX6*, *ULT1* and *ULT2* were found to be differentially expressed during cold exposure, while *ATX2* was differentially spliced. H3K27me3 is deposited by proteins from the Polycomb family (PcG). While *CLF1*, *MSI1-5* and *VRN1* were identified as cold DE, *EMF2*, *SWN*, *VEL1*, *VRN2* and *VRN5* were found to be cold-DAS. Finally, both marks are removed by demethylases from the Jumonji family (JMJ): six of them were found to be cold-DE, two cold-DAS and *JMJ30* was both differentially expressed and spliced upon cold exposure. Altogether, numerous writers and erasers of H3K4me3 and H3K27me3 appeared to be cold-regulated at the transcriptional and post-transcriptional level, which could have an impact on their activity and therefore explain the variations observed for those marks upon cold exposure.

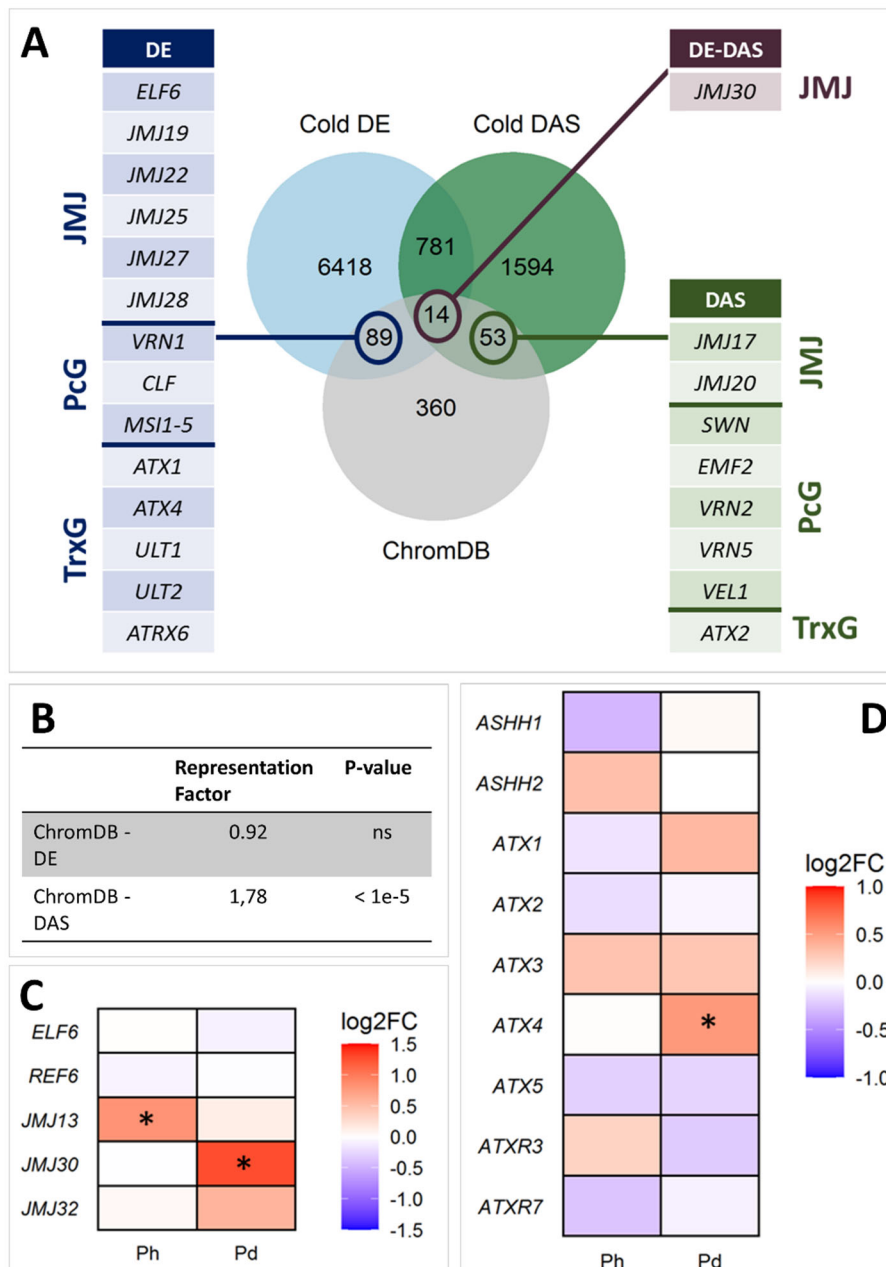


Figure 26: Cold regulation of the expression and splicing of chromatin actors. (A) Venn diagram showing the overlap of cold-regulated genes with chromatin regulatory genes. The chromatin regulatory genes were extracted from the Chromatin Database (ChromDB) while the differentially expressed (Cold DE) and differentially alternatively spliced (Cold AS) genes were extracted from Calixto et al. (2018). A gene was considered DE or DAS if it was differentially expressed or spliced in at least one of the measured time points. The members of the Jumonji (JMJ), Polycomb (PcG) and Trithorax (TrxG) families present in each overlap are listed in the adjacent tables. (B) Representation factor and significance of the pairwise overlaps. Significance was assessed by Fisher's exact test. (A) and (B) were previously published in Vyse et al. (2020). (C) and (D) Expression changes of genes encoding H3K27me3 demethylases (C) or H3K4me3 methyltransferases (D) according to the previously described RNA-seq (see 3.1.5). Plants were exposed to cold for either 3 h (Ph) or 3 d (Pd). The color indicates the log2 fold change compared to non-cold treated conditions. Stars show the adjusted p-value given by featureCounts, * indicates p-adj < 0.05.

Efforts were then narrowed onto the mechanisms potentially involved in the induction of COR genes. As shown previously (3.2.1.5), many of them underwent a loss of H3K27me3 and/or a gain of H3K4me3 during cold exposure. Therefore, the *in silico* approach was confirmed by examining the results from the RNA-seq experiment described earlier (3.1.5), with a particular

focus on H3K27me3 demethylases and H3K4me3 methyltransferases in order to identify interesting candidates for loss of function experiments (Figure 26C and D). Of the five known H3K27me3 demethylases that are present in *A. thaliana* (ELF6, REF6, JMJ13, 30 and 32), three showed a slight induction during cold exposure: *JMJ13* after 3 h and *JMJ32* (not significant) and *JMJ30* after three days (Figure 26C). However, *ELF6* did not appear to be DE even though it was identified as such in the *in silico* approach, likely because this RNA-seq did not examine as many time points as the one from Calixto et al. (2018). Nine *A. thaliana* proteins are described as potential H3K4me3 methyltransferases: ATX1-5, ATRX3 and 7, ASHH1 and 2 (K. Cheng et al., 2020). Only one of them, *ATX4*, was found to be up-regulated by cold (Figure 26D). *ATX1*, which was also identified as cold DE in the *in silico* approach showed a slight up-regulation after three days which was not significant.

As four of the five H3K27me3 demethylases showed a transcriptional or post-transcriptional cold regulation in at least one of the approaches, all of them were deemed promising candidates for the loss of function studies. For H3K4me3 methyltransferases, *ATX1* and *ATX4* both showed a slight induction in our RNA-seq data. However, previous studies showed a much stronger induction for *ATX1* than for *ATX4* after 24 h which was maintained during deacclimation (Vyse et al., 2020) and other work underlined the role of *ATX1* as a positive regulator of stress tolerance while *ATX4* acts as a negative regulator (Yong Ding, Fromm, et al., 2012; Yutong Liu et al., 2018; L. Yuan et al., 2013). Therefore, *ATX1* was selected as a candidate for the loss of function experiments.

3.2.2.2 Role of H3K4me3 methyltransferases and H3K27me3 demethylases in the cold response

In order to identify the enzymes responsible for the cold-triggered loss of H3K27me3 and the gain of H3K4me3, knock-out lines for the candidates selected in the previous section (3.2.2.1) were collected. A freezing tolerance screening was conducted in order to identify the most promising lines (Figure 27). The hypothesis behind this strategy was that if H3K27me3 could not be removed (resp. H3K4me3 could not be set), this would impact the cold response abilities of the plant and lead to a lower freezing tolerance. Therefore, plants grown for 21 d in short days were exposed to 4°C for three days and their freezing tolerance before (N) and after cold acclimation (P) was measured by electrolyte leakage assay.

For the H3K27me3 demethylases, *elf6*, *jmj13* and *jmj32* did not show any difference of freezing tolerance before or after acclimation compared to the wild type (Figure 27A and B). *ref6* displayed a slightly lower freezing tolerance, especially after acclimation, but this was not significant. *jmj30* and the *jmj30-jmj32* double mutant showed a slightly higher freezing tolerance after cold acclimation, but yet again the difference was not significant. As the proteins are close homologs, they might be redundant in functions. Therefore, a quadruple mutant for *elf6-ref6-jmj30-jmj32* (thereafter noted *qm*) was obtained from a collaborator (Yamaguchi et al., 2020). The quadruple mutant also did not display any significant difference of freezing tolerance compared to the wild type, neither before nor after cold acclimation (Figure 27C). The *atx1* mutant also showed the same freezing tolerance as the wild type in both tested conditions (Figure 27D).

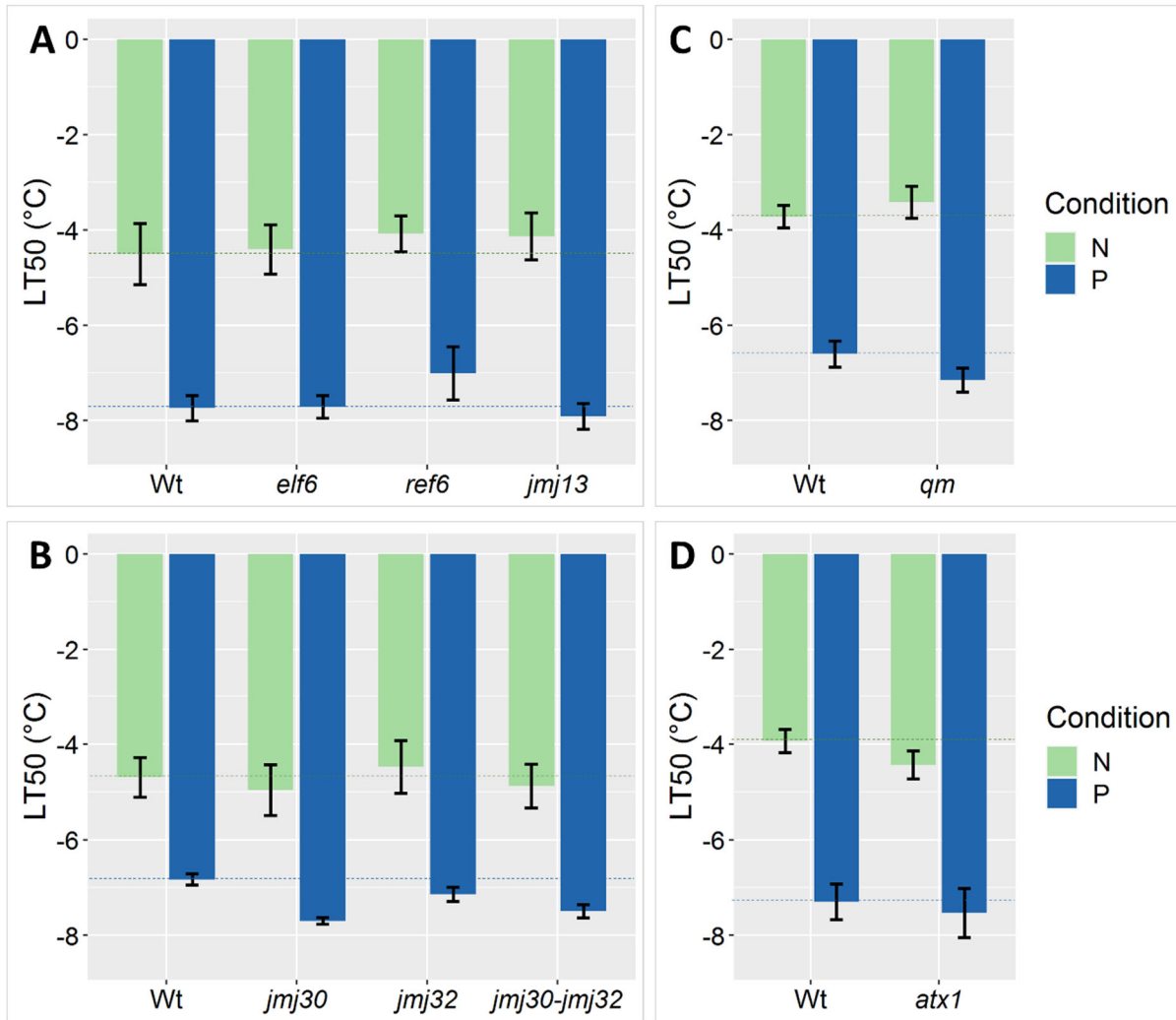


Figure 27: Freezing tolerance of histone modifier mutants. Plants were grown for 21 d (N) and exposed to 4°C for three days (P). The freezing tolerance was assessed by an electrolyte leakage assay. (A), (B) and (C) Freezing tolerance of H3K27me3 demethylase mutants. qm denotes the *elf6-ref6-jmj30-jmj32* quadruple mutant. (D) Freezing tolerance of an H3K4me3 methyltransferase mutant. Error bars represent the sem at least three biological replicates. Statistical significance was assessed by 2-way ANOVA followed by a Dunnett post hoc test ($\alpha = 0.05$) to compare each mutant to the wild type for each condition. No significant difference was found.

As none of the tested mutants showed a significantly lowered cold tolerance, the screening failed to reduce the list of potential candidates involved in cold-triggered differential methylation. It is possible that differential methylation is actually not required for cold acclimation or that the proteins investigated here are not responsible for the differential methylation. To settle this question, a ChIP-qPCR was performed in the *atx1* mutant as well as the quadruple H3K27me3 demethylases mutant in order to examine the cold-triggered changes of H3K4me3 and H3K27me3 (Figure 28). Plants were grown and stressed following the same scheme as the one described for the electrolyte leakage assay. The levels of H3K4me3 and H3K27me3 on *COR15A* and *LT130* were examined as these genes were identified as gaining H3K4me3 and losing H3K27me3 upon cold exposure in the ChIP-seq experiment (Figure 23 and Figure 24). Firstly, while not significant, a clear gain of H3K4me3 and loss of H3K27me3 could be observed in the wild-type plants after three days in the cold (Pd) (Figure 28A and B). However, the *atx1* mutant also showed a similar gain of H3K4me3 after cold exposure (Figure 28A), indicating that it is not responsible for H3K4me3 deposition,

or that other proteins can compensate its absence. Similarly, the cold-triggered loss of H3K27me3 could also be observed in the *qm* mutant (Figure 28B), suggesting a role of the fifth H3K27me3 demethylase JMJ13 in H3K27me3 removal or that the demethylation occurred through a passive mechanism.

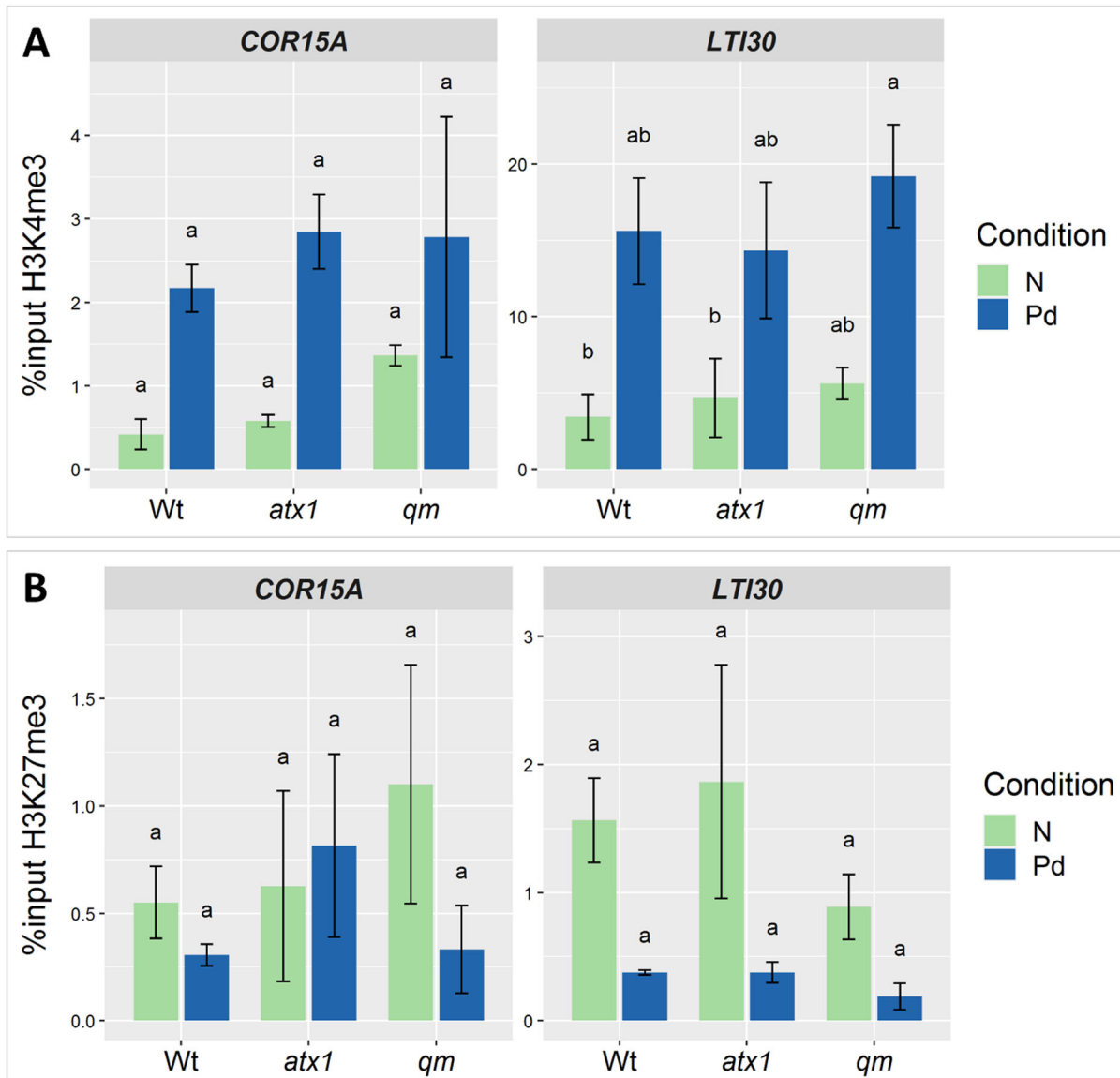


Figure 28: H3K4me3 and H3K27me3 levels in histone modifier mutants on two cold-induced genes. Plants were grown for 21 d (N) and exposed to 4°C for three days (P). The levels of H3K4me3 (A) and H3K27me3 (B) on COR15A and LTI30 were measured by ChIP-qPCR. After cross-linking, the chromatin was extracted and immunoprecipitated using anti-H3K4me3 or anti-H3K27me3 antibodies. The purified DNA was amplified by qPCR and the results are presented as %input. *qm* denotes the *elf6-ref6-jmj30-jmj32* quadruple mutant. Error bars represent the sem of three biological replicates. Significance was tested by 2-way ANOVA followed by a Tukey test ($\alpha = 0.05$). Identical letters indicate no significant difference.

While the *in silico* analyses revealed that numerous chromatin regulators are induced upon cold exposure, none of the tested mutant seemed to be involved in cold-triggered differential methylation, preventing the examination of the role of this process on the induction of *COR* genes.

3.3 PERSISTING H3K27ME3 LOSSES MIGHT BE RESPONSIBLE FOR COLD STRESS MEMORY

The results presented in the previous parts of this study showed that cold triggers changes in the histone methylation status of *COR* genes, which correlate with their transcriptional activation. Yet, as the changes in gene expression seem to precede the variations of the methylation status (Figure 22), one might wonder whether those chromatin responses actually play a role in the induction of *COR* genes and the cold response. Unfortunately, the investigations of mutant lines did not provide a definitive answer so far. However, as exposed previously (section 1.1.3), when exposed to a chilling episode, plants do not only adapt to it, they also store the information for improved survival in case this stress ever reoccurs (Byun et al., 2014; Zuther et al., 2019). Work on other types of abiotic stresses indicated that histone methylation plays a crucial part in the storage of the stress history of the plant (Yong Ding, Fromm, et al., 2012; Friedrich et al., 2018; Sani et al., 2013; Yamaguchi et al., 2021). It was therefore hypothesized that the changes in histone methylation might be important for cold stress memory and the re-induction of *COR* genes rather than for the direct response to cold stress.

3.3.1 Plants can remember cold stress

Previous work from Zuther et al. (2019) already showed that *Arabidopsis thaliana* can remember previous cold exposures, leading to a higher acquired freezing tolerance in plants that already experienced a chilling episode. Efforts were therefore first directed towards the establishment of a priming and triggering regime leading to cold memory, in order to verify whether the observations from Zuther et al. (2019) could be reproduced and then to investigate the potential involvement of chromatin regulation in this process. Two schemes with varying length of priming and triggering stresses were tested (Figure 29). The short priming scheme was very similar to the one used by Zuther et al. (2019): 21 day-old plants were exposed to 4°C for three days, placed back at 20°C for seven days (PL) before being triggered (i.e. exposed to a second cold episode) at 4°C for three days (PLT). Their freezing tolerance was compared to the one of 28 day-old plants that experienced only the triggering stress (T) (Figure 29A). As observed by Zuther et al. (2019), plants that experienced a priming cold episode showed a higher freezing tolerance after the triggering stress than the plants that were not primed. While this difference was significant in each biological replicate individually (data not shown), this significance was lost when pooling the three replicates together, mostly due to the higher variability of the freezing tolerance of the T plants. This seemed to correlate with slight variations in growth development between the different assays (data not shown). It is also worth noting that, as the freezing tolerance of primed plants after the lag phase (PL) was not significantly different to the one of the naïve plants (N), the higher freezing tolerance of PLT plants was likely not simply due to residual cold acclimation from the priming but to an actual memory of the priming episode.

In parallel, a scheme with a longer priming stress of seven days was investigated. In this second scheme, the length of the triggering stress was reduced to two days (Figure 29B). Here again, one could observe that plants which experienced cold prior to the triggering stress (PLT) showed a higher freezing tolerance than the non-primed plants (T). While each biological replicate showed a significant difference between PLT and T plants, this was not the case

when pooling the biological replicates together. However, the trends were clear and both of the tested priming schemes allowed the establishment of a cold memory lasting at least seven days, leading to an improved freezing tolerance upon triggering.

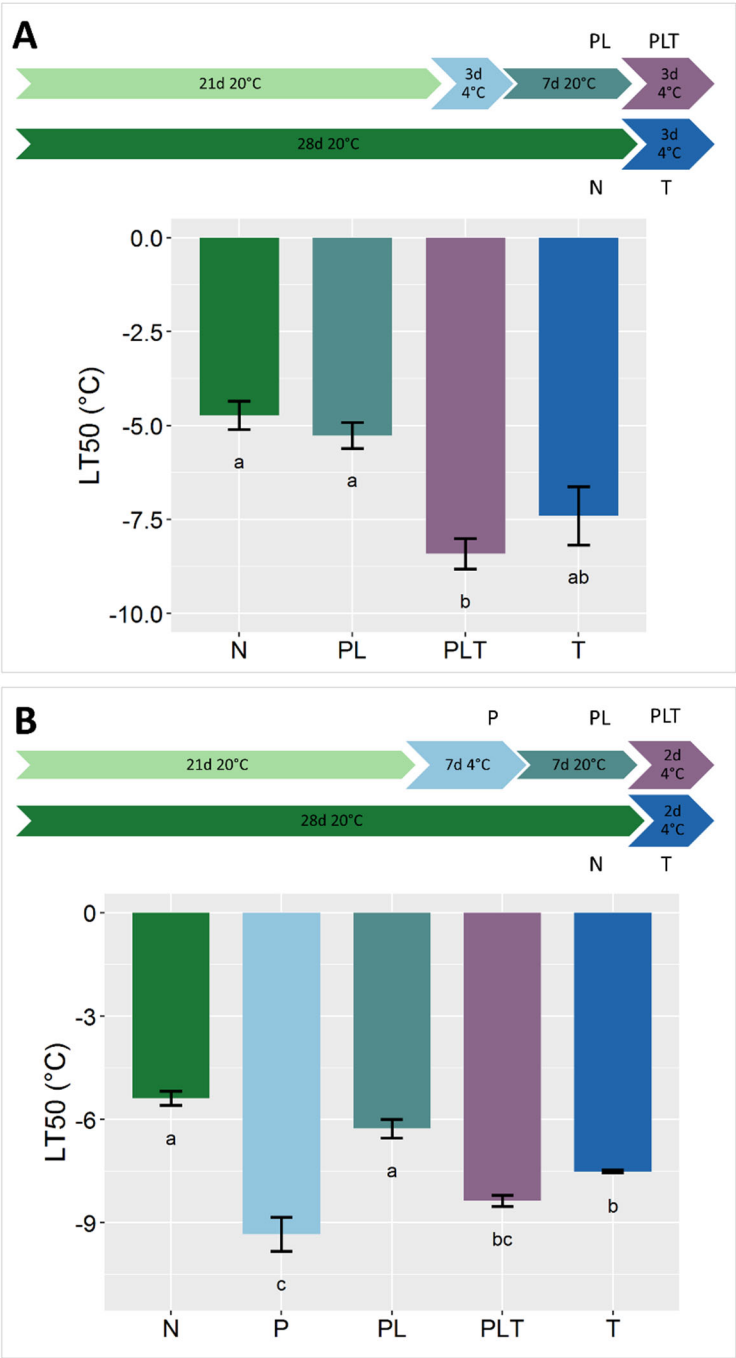


Figure 29: Different priming schemes can lead to cold memory. (A) Short priming scheme: plants were grown for 21 d at 20°C and then primed for 3 d at 4°C. They were then placed back at 20°C for seven days (PL) before being triggered at 4°C for three days (PLT). The control plants were grown 28 d at 20°C (N) and triggered at 4°C for three days (T). **(B)** Long priming scheme: plants were grown for 21 d at 20°C and then primed for 7 d at 4°C (P). They were then placed back at 20°C for seven days (PL) before being triggered at 4°C for two days (PLT). The control plants were grown 28 d at 20°C (N) and triggered at 4°C for two days (T). The freezing tolerance in the different conditions was assessed by an electrolyte leakage assay. Error bars represent the sem of at least three biological replicates. Statistical significance was assessed by one-way ANOVA followed by a Tukey post hoc test ($\alpha = 0.05$). Identical letters indicate no significant difference.

3.3.2 ELF6 is necessary for cold stress memory

The memory of heat and drought stress was shown to be at least partly encoded at the chromatin level (Yong Ding, Fromm, et al., 2012; Friedrich et al., 2018). Since many chromatin regulators are regulated at the transcriptional and/or post-transcriptional levels not only during cold acclimation as previously described (Figure 26) but also during deacclimation (Vyse et al., 2020), it was hypothesized that chromatin regulation might also be involved in cold stress memory. To test this hypothesis and identify potential actors, a screening assay examining the cold memory abilities of chromatin modifier mutants was conducted. The candidates used in the screening assay were selected based on their transcriptional activity during cold acclimation and deacclimation (Vyse et al., 2020), as well as preliminary results obtained in a survival screening assay (Bachelor thesis, Josephin Laskowski, 2017). The *elf6*, *jmj30*, *jmj32*, *repressor of silencing 1 (ros1)* and *vin3* mutants were identified as having a potentially reduced cold memory in the survival assay. Furthermore, *JMJ30* and *JMJ32* were found to be up-regulated after three days in the cold (Figure 26C) and this up-regulation was maintained for at least 24 h upon return to ambient temperatures (Vyse et al., 2020). *ELF6* showed a similar expression profile as its cold-induction was maintained for 12 h during deacclimation. *VIN3* is induced by cold, and while its up-regulation was apparently quickly reversed upon deacclimation (Vyse et al., 2020), its involvement in vernalization coupled to the survival assay results still suggested it to be a potential actor of cold stress memory (De Lucia et al., 2008, Bachelor thesis, Josephin Laskowski, 2017).

Mutant lines for each of these candidates were therefore subjected to a P7L7T2 priming and triggering scheme after which their freezing tolerance was assessed using an electrolyte leakage assay (Figure 30A). To maximise the number of mutants that could be investigated in one assay, the freezing tolerance was measured only for the PLT and T plants, as the benefit of priming is visible when comparing these two conditions (Figure 29). *ros1* and *vin3* mutants showed an improved freezing tolerance in primed and triggered plants compared to triggered-only plant that was similar to what was observed in the wild-type (Figure 30B and Suppl. Figure 10A). However, in *elf6.3* plants, the benefit of priming seemed reduced, as the difference between PLT and T plant was smaller than in the wild type. A second screening conducted on *jmj30*, *jmj32* and *jmj30-jmj32* double mutants did not reveal any difference in memory ability of the mutants compared to the wild-type (Suppl. Figure 10A). Efforts were thereafter focused on validating the findings concerning the priming abilities of the *elf6.3* mutant. While the reduced benefit of priming of *elf6.3* mutants compared to wild type was visible in all performed replicates, the trend was not significant when the data was pooled (Figure 30C). This was probably due to slight variation in plant growth from one assay to the next, which affected the freezing tolerance of the seedlings. However, since the difference in LT_{50} between PLT and T plants was always of the same magnitude, the ΔLT_{50} ($\Delta LT_{50} = LT_{50, T} - LT_{50, PLT}$) was used as a measurement for the priming abilities of the plants (Figure 30D). While the wild type plants showed a ΔLT_{50} of about 1.25°C, it was only of 0.5°C in the *elf6.3* mutants, which corresponds to a reduction of about 60% of the priming benefit. Similar results were observed when the plants were subjected to the P3L7T3 priming scheme: while the primed and triggered wild-type plants showed a significantly higher freezing tolerance than the triggered-only plants, the *elf6.3* seedlings showed a similar freezing tolerance independent of the stress history (Suppl. Figure 10B). It is important to note that the *elf6.3* mutants displayed a similar freezing tolerance to wild type plants in T conditions, indicating that ELF6 does not play a role in the initial cold

response but that its absence negatively impacts the establishment or maintenance of cold memory, independently of the length of the priming stress. As one could still observe a slight priming benefit in the *elf6.3* mutant, this suggests that it is not the only actor involved and the other H3K27me3 demethylases might act redundantly.

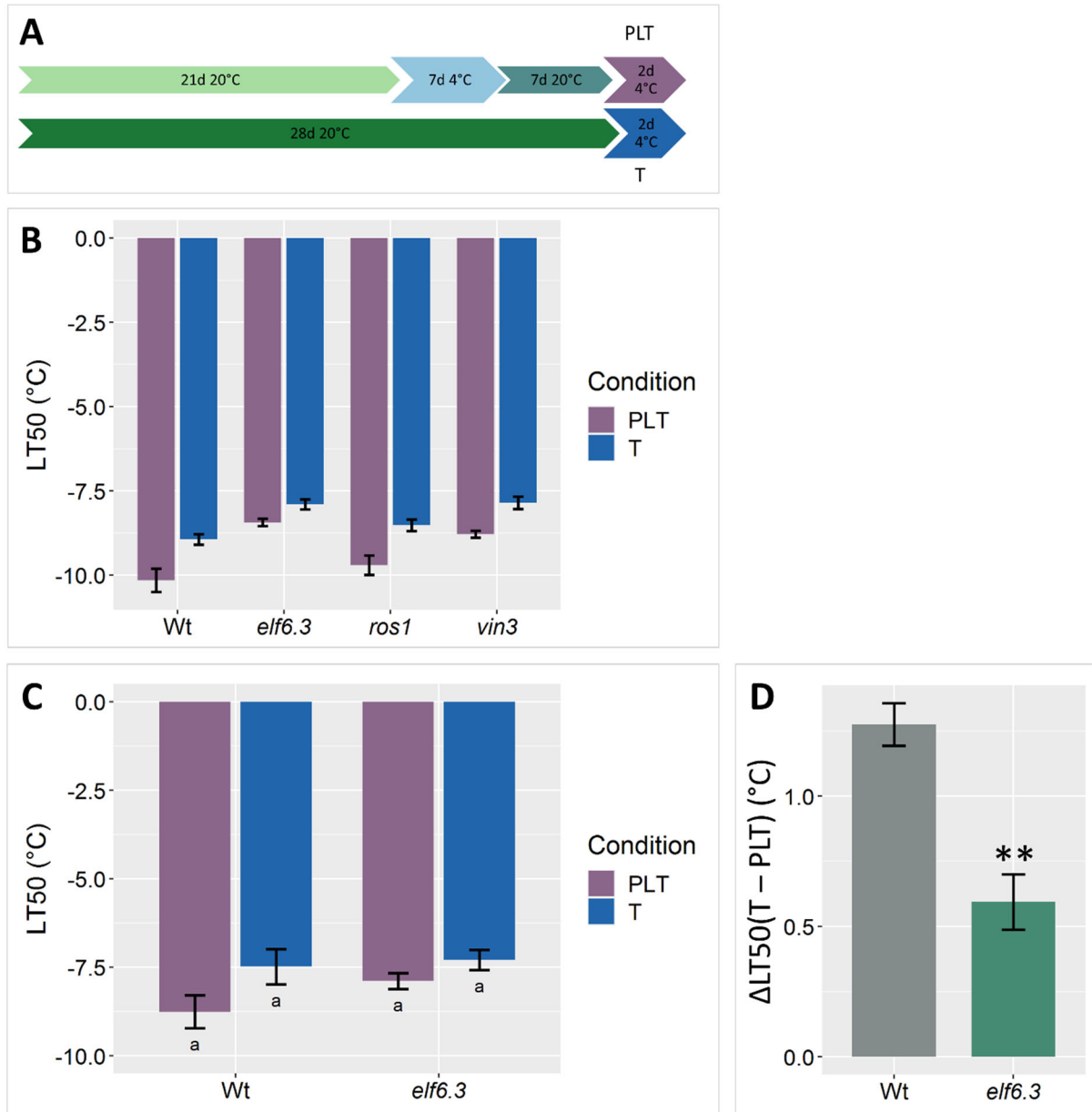


Figure 30: ELF6 is required for cold memory. (A) Priming scheme used for the screening. Plants were grown for 21 d at 20°C and then primed for 7 d at 4°C (P). They were then placed back at 20°C for seven days (PL) before being triggered at 4°C for two days (PLT). The control plants were grown 28 d at 20°C (N) and triggered at 4°C for two days (T). The freezing tolerance of the different mutants was assessed in the PLT and T conditions by an electrolyte leakage assay. (B) Example of a screening assay on *elf6.3*, *ros1* and *vin3* mutants. Error bars represent the sem of four technical replicates. (C) Freezing tolerance of the *elf6.3* mutants in primed and triggered (PLT) and triggered-only (T) conditions. Error bars represent the sem of three biological replicates. Statistical significance was assessed by two-way ANOVA followed by a Tukey post hoc test ($\alpha = 0.05$). Identical letters indicate no significant difference. (D) Benefit of priming on the freezing tolerance in Wt and *elf6.3* plants, displayed as the difference in LT₅₀ between T and PLT plants in the assays shown in (C). Error bars represent the sem of three biological replicates. Significance was assessed by unpaired t-test, ** shows p-value < 0.01.

3.3.3 Cold-induced differential methylation persistence and transcriptional memory

Results from the previous section indicated that ELF6 is involved in cold memory. As ELF6 is described as an H3K27me3 demethylase and the investigation of H3K27me3 dynamics revealed that many genes lose H3K27me3 during cold exposure, one can hypothesise that the cold memory is, at least partly, encoded by a sustained loss of H3K27me3 on certain genes. The persistence of the cold-triggered changes in H3K4me3 and H3K27me3 levels was therefore examined by performing ChIP-qPCR on plants exposed to 4°C for three days and then placed back at 20°C for seven days (Figure 31A and B). As the number of genes that can be investigated by ChIP-qPCR is limited by the small amount of DNA recovered after the immunoprecipitation step and as it is possible that not all cold-triggered histone methylation changes are maintained during the lag phase, candidate genes had to be carefully selected. It was shown previously that plants can remember drought stress and that this memory is associated with a higher induction of certain stress-responsive genes (called trainable) during the second drought episode (Yong Ding et al., 2013; Yong Ding, Fromm, et al., 2012). As the higher induction was associated with the maintenance of the drought-triggered H3K4me3 deposition on those genes, it was hypothesized that a similar mechanism regulates cold stress memory. Efforts were therefore directed first towards the identification of potential cold-trainable genes. This work was performed in collaboration with a bachelor student and was previously published (Reyhan Divarci, BSc thesis, 2018). Briefly, a list of potential cold trainable genes was established by identifying genes fitting the three following criteria: (i) is drought-trainable (ii) is induced or repressed by cold and (iii) is an H3K27me3 target. The eventual trainable behaviour of these genes was then tested using RT-qPCR. While the result were not definitive, they suggested that some of those candidates might be cold trainable. As several of these genes were subsequently shown as undergoing differential methylation during cold exposure (Figure 23 and Figure 24), they were selected for investigation with ChIP-qPCR. This included *LTI30* (H3K4me3 gain and H3K27me3 loss), as well as *TCF1* and *VIN3* (H3K4me3 gain). *COR15A*, which was shown to both gain H3K4me3 and lose H3K27me3 during cold exposure, was not identified as potentially trainable and was therefore used as a control.

The cold-induced gain of H3K4me3 on *COR15A*, *LTI30* and *TCF1* was lost after seven days at 20°C: no difference could be observed between plants that experienced the first cold stress (PL7) and plants that did not (N28) (Figure 31A). On *VIN3* however, the levels of H3K4me3 in PL7 plants were at an intermediate level between the naïve plants N28 and the cold-treated plants Pd. Although the difference of H3K4me3 levels between N28 and PL7 plant was not significant, this trend suggests that the cold-triggered gain of H3K4me3 on *VIN3* was maintained even after the return to favourable temperatures while on other genes it was quickly reversed. As the levels of H3 did not significantly differ in the tested conditions, one can conclude, as already shown previously, that the higher levels of H3K4me3 were not due to an increased nucleosome density (Figure 31C).

COR15A and *LTI30* were both shown to undergo H3K27me3 loss during cold exposure (Figure 24, Suppl. Figure 9B). After seven days at 20°C, the loss of H3K27me3 appeared mostly reversed on *COR15A* (Figure 31B). On *LTI30* however, the level of H3K27me3 at PL7 was slightly higher than the one observed after cold stress (Pd) but lower than in plants that did not

experience cold (N28). Similar to *VIN3*, these differences were not significant but the trend suggested that the cold-triggered loss of H3K27me3 was not totally reversed on that gene. It is also worth noting that the H3 levels were also stable on *LT130* in all tested conditions, proving that the lower levels of H3K27me3 were not simply due to a lower nucleosome density (Figure 31C).

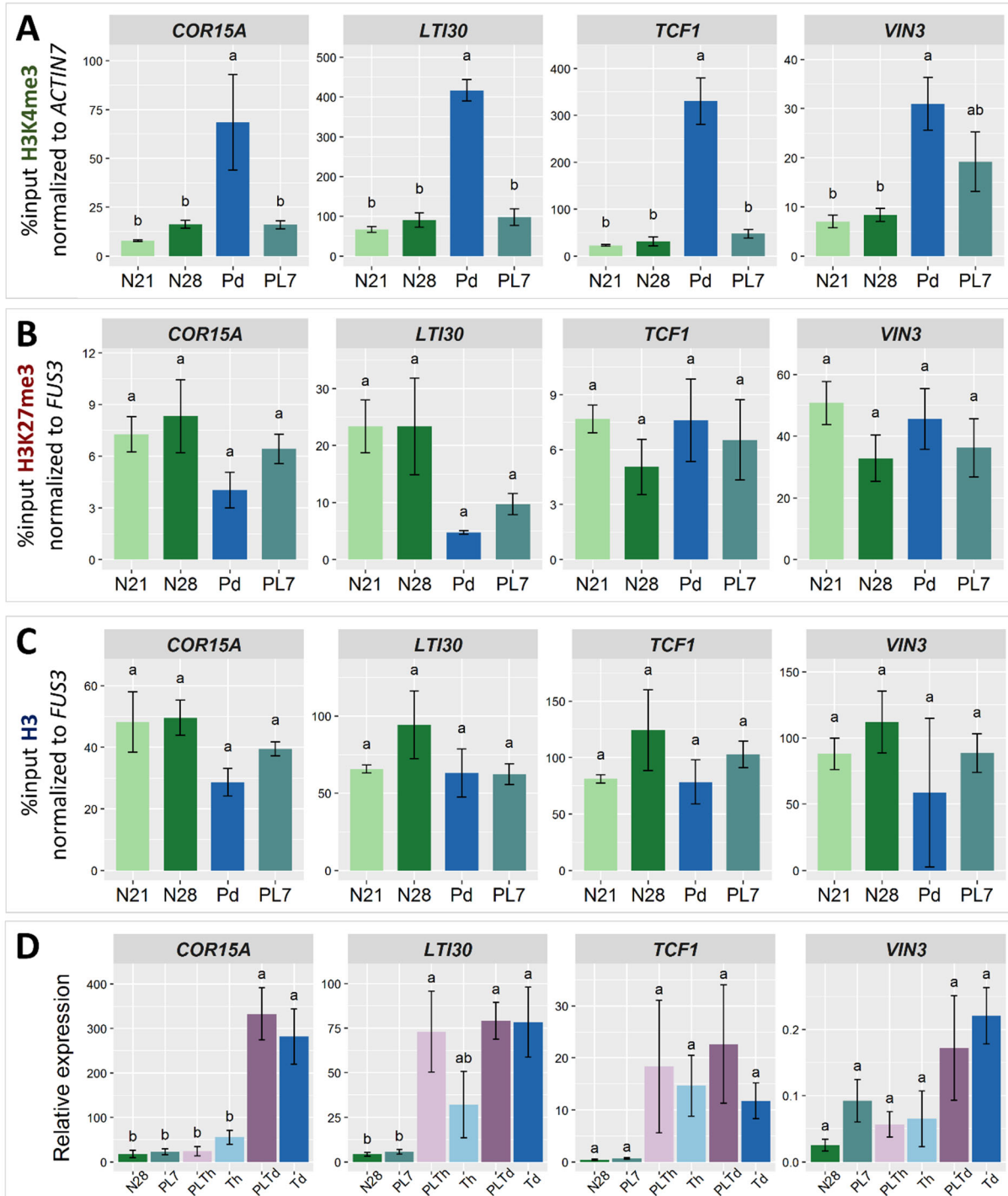


Figure 31: Some cold-triggered methylation changes persist after return to ambient temperature. (A) H3K4me3 levels after cold treatment and recovery, as %input normalized to ACTIN7. (B) H3K27me3 levels after cold treatment and recovery, as %input normalized to FUS3. (C) H3 levels after cold treatment and recovery, as %input normalized to FUS3. For all panels, plants were grown for 21 d (N21) and exposed to 4°C for three days (Pd). After this cold treatment, plants were returned at 20°C for 7 d (PL7) and compared to plants grown 28 d at 20°C without experiencing a cold episode (N28). After

cross-linking, the chromatin was extracted and immunoprecipitated using anti-H3K4me3, anti-H3K27me3 or anti-H3 antibodies. The purified DNA was amplified by qPCR. Error bars represent the sem of three to five biological replicates. Statistical significance was tested by one-way ANOVA followed by a Tukey post-hoc test ($\alpha = 0.05$). Identical letters indicate no significant difference. **(D)** Relative expression of four cold-inducible genes during a priming and triggering scheme. 21 d old plants were primed at 4°C for 3 d and then placed back at 20°C for 7 d (PL7). They were then cold-treated again for 3 h (PLTh) or 3 d (PLTd). The control plants (non primed) were grown for 28 d (N28) and placed at 4°C for 3 h (Th) or 3 d (Td). Transcript levels were measured by reverse transcription and qPCR. TIP41 was used as an internal control. Error bars represent the sem of 3-6 biological replicates. Significance was tested by one-way ANOVA followed by a Tukey test ($\alpha = 0.05$). Identical letters indicate no significant difference.

Altogether, this showed that some of the cold-triggered changes in H3K4me3 and H3K27me3 levels persisted even upon a return to ambient temperature. To determine whether this impacts the transcriptional activity of the affected genes during the stress-free period or their induction during a second cold episode, the expression of the same four genes was measured using RT-qPCR in plants that were primed for three days at 4°C, then placed back at 20°C for a week (PL7) and then exposed to cold again for 3 h (PLTh) or 3 d (PLTd) (Figure 31D). They were compared to non-primed plants (N28, Th and Td). *COR15A* and *TCF1*, which returned to a “naïve” chromatin status after the lag phase, showed similar expression in N28 and PL7 plants (Figure 31D). Both genes were induced by cold and this induction was of the same magnitude in PLT and T plants. As expected, the stress history of the plants therefore did not affect the transcriptional behaviour of those two genes. On the other hand, *VIN3*, on which the H3K4me3 gain persisted in the lag phase, showed a slightly higher expression in PL7 plants compared to N28 plants, consistent with the observed elevated H3K4me3 levels. However, this did not affect the induction triggered by cold, as it was of the same magnitude in PLT and T plants. It appeared that the persistence of H3K4me3 gain on *VIN3* is associated with a sustained induction even when the cold stress had passed. *LT130* displayed opposite results to *VIN3*: the expression was similar in PL7 and N28 plants. After 3 h of cold exposure however, the primed plants (PLTh) showed a higher relative *LT130* expression than their non-primed counterparts (Th). No difference was observed anymore after three days at 4°C, indicating that *LT130* was induced faster in primed plants compared to plants that did not experience cold before. This suggests that the persisting reduction in H3K27me3 levels does not lead to a sustained induction of the gene but might facilitate its re-induction when the plant experiences cold again.

Once again, this highlights that the two histone methylation marks seem to play different roles in the regulation of transcription. Indeed, the persistence of higher levels of H3K4me3 correlated to a sustained induction of *VIN3* in the absence of cold, while H3K27me3 loss had no impact on the transcription of *LT130* until the plant experienced cold again. On the other hand, genes whose chromatin reverted back to its initial status after cold exposure did not show any difference in expression between primed and non-primed plants, suggesting that the persistence of cold-triggered changes might be used as a predictor of gene trainability.

4 DISCUSSION

The response of plants to cold stress relies on the rapid and coordinated induction of numerous *COR* genes that are required for the establishment of defences. As the constant expression of those genes would be noxious for the plant, it is crucial that their transcription is tightly regulated depending on the environmental conditions experienced by the plant. Chromatin modifications represent an important level of transcriptional control as they determine the accessibility of the DNA to the transcriptional machinery through *cis* and *trans* effects. This study expands on the sparse knowledge that certain histone PTMs are involved in the induction of *COR* genes during the cold response through the examination of the role of the antagonistic marks H3K27me3 and H3K4me3 in the repression and activation of those genes, as well as in transcriptional cold memory.

4.1 BIVALENCY POISES COLD-INDUCIBLE GENES

4.1.1 Bivalency is involved in plant stress response

Former work from our lab suggested that the repressive histone methylation mark H3K27me3 might be involved in the silencing of stress-responsive genes in optimal environmental conditions: cold-induced genes in particular were found to be enriched in H3K27me3 targets (Kleinmanns & Schubert, 2014; Vyse et al., 2020). However, when an *in silico* approach was used in this study to examine the chromatin status of cold-inducible genes prior to cold exposure, no enrichment was found for pure Polycomb states (Figure 5A). Rather, cold-inducible genes, especially the early induced ones, were enriched in State 2, which is characterized by the co-occurrence of the repressive mark H3K27me3 and the activating mark H3K4me3, forming an atypical chromatin state called bivalency. Widening the approach to genes that are induced by other types of stresses such as heat, drought or even bacterial infection proved that bivalency is a common characteristic of stress regulated genes (Figure 5D). The GO term enrichment analysis of the S2 genes supported this conclusion as it identified terms related to various biotic and abiotic stress responses (Figure 6A). This is consistent with the findings of Dong et al. (2021): while the authors used a different strategy to identify S2 genes (each gene was assigned to a single state depending on which one was present at its TSS), they also discovered an enrichment of stress-response related terms for S2 targets. However, both approaches relied on the *in silico* model from Sequeira-Mendes et al. (2014), which is based on data from independent studies using plants of different ages and grown in various conditions. To ensure that the S2 genes actually carry both methylation marks at the same locus at the same time point in the conditions used in this study, individual ChIP-seq for each histone methylation mark were performed and any gene where the peaks of the individual modifications co-localized for at least 150 bp was considered bivalent. While this approach identified far fewer genes than the *in silico* strategy, possibly due to the harsher criteria used, it confirmed that, in the growth conditions and growth stage used in this study, many cold-induced genes carry both H3K27me3 and H3K4me3 prior to the occurrence of cold (Figure 7). It is however worth noting that this approach does not demonstrate that those loci are truly bivalent. Indeed, the observed co-occurrence of the methylation marks on a gene could stem from the co-existence of distinct cell populations, one where the gene carries

H3K4me3 and another where it is decorated with H3K27me3. This point will be discussed in more details in section 4.1.5.

Interestingly, the *in silico* analyses revealed that S2 is particularly enriched among the genes that are expressed early during the cold exposure and this phenomenon was also observed for heat-responsive genes (Figure 5A and D). On the contrary, genes whose induction occurs later (after more than 24 h of low temperatures) were not enriched in S2 (Figure 5A). This was confirmed *in vivo*, as bivalent genes were more likely to already be up-regulated at the 3 h time point than after three days (Figure 10E). This observation strengthens the idea that bivalency is marking genes induced early in the cold response. Moreover, the S2 genes are enriched in transcription factors, kinases (in particular Ser/Thr kinases) and other functions related to DNA binding and transcriptional regulation, which can be considered the “first responders” to stress (Figure 6B). Indeed, once the cold is perceived, the calcium signalling and MAPK cascades converge to activate both transcriptions factors and splicing factors (such as the Ser/Thr kinases) in order to initiate the transcriptome reprogramming (Figure 1) (Byun et al., 2014; Calixto et al., 2018). Xi et al. (2020) monitored H3K4me3 and H3K27me3 levels in the context of vernalization and were also able to identify loci carrying both marks prior to the cold exposure. These bivalent genes were enriched in transcription factors, confirming the observations from this study. Altogether, this suggests that bivalency is necessary for the poising of stress “first responders”, allowing their quick induction once the plant faces adverse conditions. Conversely, the activation of late cold-inducible genes does not need to be rapid and can therefore be regulated by slower mechanisms. As they do not require poising, bivalency is not as essential for them as for the “first responders”, offering an explanation for the discrepancy in S2 enrichment between those gene sets.

H3K4me3-H3K27me3 bivalency was initially identified in mammalian embryonic stem cells, as a poising mechanism for genes involved in cell differentiation, allowing them to quickly change between a silenced and a transcriptionally active state (Bernstein et al., 2006). In *Arabidopsis*, the earliest reports on bivalency also linked it to the regulation of developmental processes, especially flowering: the flowering inductor *FT* and the flower homeotic gene *AG* were both identified as bivalent (Jeong et al., 2009; Saleh et al., 2007). Furthermore, many transcription factors that are vernalization-regulated are bivalent (Xi et al., 2020). However, recent studies alluded to its role in the plant stress response: additionally to the *in silico* approach from Dong et al. (2021) mentioned above, bivalency was found to be located on cold-responsive genes in *Solanum tuberosum*, maintaining them in an accessible state favourable to the binding of transcription factors upon cold exposure (Zeng et al., 2019). While those previous investigations of bivalency in *Arabidopsis thaliana* focused on a unique stressor (cold, bacterial infection), the *in silico* approach presented here was used to examine a variety of adverse conditions (cold, heat, drought, bacterial infection) and time points, demonstrating that this chromatin state is a universal feature of early stress-responsive genes (Figure 5). Contrary to earlier studies such as the one from Dong et al. (2021) that solely relied on *in silico* data, these observations were then confirmed by examining the *in vivo* distribution of H3K4me3 and H3K27me3 (Figure 7). Finally, this study consolidates the emerging idea that bivalency plays a dual role both in development regulation and stress response in plants: a GO term enrichment analysis of the genes found to be bivalent with the *in vivo* strategy identified GO terms related to both processes (Figure 8). As both development and stress responses require

to maintain certain genes in a rapidly reversible silenced state, it is not surprising that bivalency contributes to poising in both contexts.

4.1.2 The H3K4me3 profile of bivalent genes suggests its mitotic stability

In order to understand how bivalency poises genes for induction, bivalent and monovalent genes were compared, revealing striking differences. First of all, bivalent genes were expressed to a higher level than their silenced H3K27me3 monovalent counterparts in naïve conditions, even though both types of genes carried similar levels of the repressive mark, suggesting that the presence of H3K4me3 on bivalent genes is enough to overcome the silencing imposed by H3K27me3 (Figure 10A and B). On the contrary, the levels of H3K4me3 correlated with transcriptional activity: bivalent genes carried around 50% less of this activating mark than monovalent genes and while they were transcribed, their expression was lower than that of monovalent genes. This was not unexpected, as it is known that H3K4me3 favours the recruitment of transcription factors and of the transcriptional machinery (B. Li et al., 2007). Since the H3K4me3 monovalent genes are genes whose expression is required in naïve conditions, they need to carry high levels of H3K4me3 around their TSS to help their transcription. On the other hand, the transcription of bivalent stress-responsive genes is not required before the occurrence of a stress: as they are not currently transcribed, they do not require as high H3K4me3 levels as active genes. It is also possible that the presence of H3K27me3 blocks the methylation of K4 on the same tail, leading to lower levels of this mark at bivalent loci compared to monovalent ones where both H3 of a nucleosome might be trimethylated at K4. While this was not examined in plants yet, studies on mammalian cells indeed showed that bivalent nucleosomes are asymmetrically modified, meaning that the two methylation marks do not occur on the same H3 tail and therefore that a bivalent nucleosome only carry H3K4me3 on one tail (Voigt et al., 2012). However, the situation might be different in plants. Indeed, while Schmitges et al. (2011) proved that the activity of the PRC2 complex of mammals and *Drosophila* is inhibited by the presence of H3K4me3 in *cis* (i.e. on the same H3 tail), preventing the existence of doubly-methylated tails, this observation could not be extended to plant PRC2 as the activity of PRC2 was inhibited by H3K4me3 if it contained the EMF2 subunit, but not if it contained VRN2 (Schmitges et al., 2011). Plant bivalent histones could therefore be symmetrically modified, explaining why the levels of H3K27me3 were almost identical on bivalent and monovalent genes. This underlines the importance of determining the exact nature (i.e. symmetric or asymmetric) of bivalent nucleosomes in plants.

The levels of H3K4me3 were not the only difference between H3K4me3 monovalent and bivalent genes: this methylation mark spanned a broader domain on bivalent genes, suggesting that bivalency is more stable and inheritable than H3K4me3 monovalency. Indeed, during DNA replication, the parental histones which are evicted ahead of the replication fork are reincorporated randomly in the leading and lagging DNA strands, ensuring that the local chromatin state is inherited in both daughter cells (Escobar et al., 2021; Stewart-Morgan et al., 2020). However, since the newly synthesized histones are not methylated prior to their deposition, they have to be appropriately modified after their incorporation, to avoid the loss of information through dilution over successive cell divisions (Escobar et al., 2021). Since the histones H3-H4 are deposited as tetramers, the information to be copied has to be extracted from nearby parental histones rather than simply from the other H3 of the same nucleosome. This implies that a chromatin state is more likely to be stably inherited over successive mitosis

if it spreads over several nucleosomes (Escobar et al., 2021; Stewart-Morgan et al., 2020; Yamasu & Senshn, 1990). For H3K27me3 for example, the PRC2 complex can bind to methylated parental histones directly after the replication fork and then proceeds to methylate the new nucleosomes (Hansen et al., 2008). This explains why, in *lhp1* plants where the spreading of H3K27me3 after vernalization is impaired and the mark therefore only covers the nucleation region, the silencing of *FLC* is lost much quicker than in wild type plants where H3K27me3 spread over the entire *FLC* locus (H. Yang et al., 2017). As H3K27me3 spans the whole gene body both on monovalent and bivalent genes (Figure 10A right), the length of the H3K4me3 domain would be the most critical determinant of the mitotic stability of bivalency. Therefore, the broader H3K4me3 domains on bivalent genes might be necessary to ensure that this chromatin state is transmitted to daughter cells during mitosis. This way, stress-inducible genes remain bivalent even in newly formed cells, thus making bivalency a true epigenetic mark. It is especially crucial for H3K4me3 to be maintained on bivalent genes, as its loss was suggested to lead to their irreversible silencing (D. Kumar et al., 2021). Broad H3K4me3 domains might not be so important for active monovalent genes: indeed, active loci do not show local recycling of parental H3-H4 tetramers and the chromatin state is instead re-established during transcription (Escobar et al., 2019; Stewart-Morgan et al., 2019). In particular, H3K4me3 re-accumulation after DNA replication is faster on highly expressed genes and several H3K4me3 methyltransferases are known to interact with Ser5pho RNA polymerase II, suggesting that H3K4me3 is also re-established during transcription (B. Li et al., 2007; Reverón-Gómez et al., 2018; Voigt et al., 2013). As H3K4me3 monovalent genes are transcriptionally active, the maintenance of the mark over cell divisions might be achieved by co-transcriptional processes while the silenced bivalent genes purely rely on co-replication copy mechanisms and therefore require broader domains (Figure 10B). The same reasoning might explain why early inducible genes carry larger S2 domains than late inducible genes: if bivalency is more crucial to their activation, broader domains ensure that it will be maintained through cell divisions (Figure 5C). Interestingly, bivalency spans broader domains in plants than in mammalian cells, as already described in *Solanum tuberosum* by Zeng et al. (2019): one might hypothesize that this is due to the dual role of bivalency in plants. Since it is not only involved in development but also in stress responses, bivalency needs to be maintained over the whole life-span of the plant, whereas in animals it was described as being mostly resolved to an active or silenced state after cell differentiation, suggesting that bivalency might have to persist through fewer cell cycles than in plants (Bernstein et al., 2006; Voigt et al., 2013).

4.1.3 Bivalency might poise genes through enhanced accessibility

The commonly accepted model for the action of bivalency is its quick resolution into an active or silenced state through the loss of one of the methylation marks (Bernstein et al., 2006). However upon cold exposure, only a few hundred of bivalent genes lost bivalency, mainly due to H3K27me3 removal, but most retained their initial chromatin state (Figure 19B). Investigating specific cold-induced bivalent genes such as *LT130* revealed that H3K27me3 levels were reduced but not completely erased upon cold exposure (Figure 24 and Suppl. Figure 9B). This suggests that, during cold stress exposure in plants, bivalency is not resolved into monovalency but that the balance between repressive and active marks is adjusted. While unexpected, this might be explained by the different role of bivalent genes in both systems. Indeed, in the context of cell differentiation, bivalent genes are definitively changing their

status: they will then remain active or silenced through the rest of the life span of the organism. However, the changes in expression of stress-responsive genes are only transient and should be reversed once the stress episode subsides. Therefore, instead of drastic changes, a certain plasticity needs to be conserved to allow a return to a silenced state after the cold exposure, which might explain why bivalency is not completely disappearing at most loci. Since bivalency appears to be involved in developmental processes as well as stress responses in *Arabidopsis thaliana*, it would be particularly interesting to compare the fate of this state during gene activation in both contexts to validate this hypothesis. Still, the idea that bivalency poises genes for activation by allowing a rapid adjustment of their methylation status implies that bivalent genes are loci of particularly dynamic histone methylation. However, they were not more likely to undergo differential methylation than their monovalent counterparts upon cold exposure (Figure 20A and B). It is therefore possible that changes in histone methylation are actually not essential for the induction of bivalent genes. Bivalency could instead poise genes for induction through different mechanisms such as regulating chromatin accessibility or providing an anchoring point for histone readers.

Indeed, when compared to the chromatin accessibility data provided by Raxwal et al. (2020), the bivalent loci identified in this study were shown to be in a more open chromatin state, with more than 65% of the bivalent bases identified as accessible (vs 1% of all bases of the genome) (Figure 10C and D). H3K27me3 monovalent domains were not more open than the rest of the genome (Suppl. Figure 2B). While H3K4me3 monovalent loci were more accessible, this was less than what was observed for bivalent loci, even though the levels of H3K4me3 were lower on bivalent domains (Figure 10A, Suppl. Figure 2B and C). This suggests that the co-occurrence of both methylation marks confers a greater chromatin accessibility to the underlying locus than each mark separately. It is also worth noting that a higher expression is not linked to a higher accessibility: H3K4me3 monovalent genes were transcribed at higher levels than bivalent ones but were less accessible, confirming that the increased accessibility is likely due to the chromatin state and not simply deriving from the transcriptional activity (Figure 10B). While these observations have to be considered with caution since the accessibility data were obtained from plants grown in different conditions than for the ChIP-seq presented here and might therefore not be exactly comparable, this study is not the first suggesting a link between bivalency and open chromatin. In mouse embryonic stem cells, the presence of H3K4me3 at bivalent genes was proven to be essential to maintain chromatin accessibility and basal transcription (Mas et al., 2018). In *Solanum tuberosum*, bivalent regions are more accessible than non-bivalent ones and become even more accessible upon cold exposure (Zeng et al., 2019). This is contrary to the results presented earlier in this study, which showed that bivalent regions tended to lose accessibility upon cold exposure (Figure 20C). However, this loss of accessibility might be explained by the binding of transcription factors and RNA polymerase on those genes during their transcriptional activation, as the methods used by Raxwal et al. (2020) (FAIRE-seq and DNase-seq) identify both nucleosome-bound and transcription factor-bound loci as closed (Tsompana & Buck, 2014). It would therefore be particularly interesting to use a complementary approach such as MNase-seq or ATAC-seq (Assay for Transposase-Accessible Chromatin followed by sequencing) to investigate nucleosome occupancy and therefore determine the exact nature of closing loci, i.e. whether they consist of condensed or transcription factor-bound chromatin. Still, the results presented here suggest that bivalency could potentiate silenced genes for rapid induction by maintaining them in an open chromatin state allowing transcription factors and the

transcriptional machinery to bind, while the chromatin of non-bivalent genes would first need to undergo remodelling to become accessible, slowing down their activation.

4.1.4 EBS, SHL and DEK2 are putative bivalency readers

While a link was established in the literature between bivalency and chromatin accessibility, it remains unclear whether this relies on *cis* effects of the methylation marks or on their reading by effectors. These potential bivalency readers could also contribute to gene poising through accessibility-independent mechanisms. Until now, no bivalency reader was described in *Arabidopsis thaliana* but the experiments performed in this study identified several potential candidates. EBS and SHL are commonly described as bivalency readers in the literature since they both possess a PHD and a BAH domain, recognizing H3K4me3 and H3K27me3 respectively (Z. Li et al., 2018; Qian et al., 2018; Z. Yang et al., 2018). This description is however debatable as these proteins do not have a higher affinity for double methylated peptides than for mono-methylated ones and the BAH and PHD domains of both EBS and SHL are too close to one another for the same protein to bind two methylated lysines (Qian et al., 2018; Voigt et al., 2012; Z. Yang et al., 2018). However, bivalency is thought to occur through the asymmetric methylation of the nucleosomes rather than the double methylation of a single histone tail and EBS and SHL could bind to those asymmetrically methylated nucleosomes by forming homo- or heterodimers. Therefore, an *in silico* analysis was conducted to test whether EBS and SHL preferentially bind to bivalent loci. The targets of these two proteins were found to be enriched in S2 genes, suggesting that EBS and SHL might indeed act as bivalency readers (Figure 11A). Further work is still required to validate these findings, such as investigating the binding of EBS and SHL to bivalent nucleosomes rather than the short di-methylated peptides used in the studies from Qian et al. (2018) and Yang et al. (2018). EBS and SHL targets are enriched in genes related to the cold response according to a GO biological function term analysis (data not shown) and they were found to bind to numerous cold-inducible genes such as *CORs*, *CBFs*, *KINs*, *RDs* and *GOLSs* (Z. Li et al., 2018; Qian et al., 2018; Z. Yang et al., 2018). Together with their suspected role as bivalency readers, this suggested that these two proteins could be involved in the cold response by regulating the expression of bivalent *COR* genes. Thus, the induction of those genes was examined in *ebs* and *shl* mutants, as well as their freezing tolerance (Figure 11B and C). These mutants did not reveal any significant difference to wild type plants, implying that neither of these proteins is involved in the cold response nor in the transcriptional regulation of bivalent cold-induced genes. It is however possible that EBS and SHL are redundantly contributing to the cold response: they share many targets (including bivalent cold-inducible ones) and a functional redundancy of EBS and SHL was previously observed in the control of the flowering time (Z. Li et al., 2018). It would therefore be necessary to investigate the cold response of the *ebs-shl* double mutant. However, the double mutants have a strong phenotype, including poor germination rate, dwarfism and extremely early flowering (Z. Li et al., 2018). This renders the analysis of the cold response in those plants extremely difficult, as it would be impossible to determine whether potential differences are directly due to the absence of EBS and SHL or simply consequences of the developmental phenotype. This issue could be overcome by the creation of an inducible knock-out mutant line, where the expression of *EBS* and *SHL* could be inhibited only shortly before the cold treatment, allowing the investigation of their potential role in the cold response in plants that do not have a developmental phenotype.

Contrary to EBS and SHL, DEK2 was shown to preferentially bind H3K4me3-H3K27me3 doubly methylated peptides but does not recognize peptides carrying only one of these methylation marks (Rayapuram et al., 2020, personal communication). However, as described earlier, these *in vitro* analyses with peptides might not reflect the *in vivo* situation where nucleosomes are most likely asymmetrically modified (Voigt et al., 2012). The potential binding of DEK2 to bivalent loci was therefore investigated with an *in silico* approach, which revealed that DEK2 is preferentially found on S1 and S2 domains, suggesting that, additionally to bivalency, DEK2 can also recognize H3K4me3 monovalent nucleosomes *in vivo* (Figure 12A and Suppl. Figure 3B). This was unexpected as the *in vitro* analyses did not show an association of DEK2 with H3K4me3 peptides and highlights the limitations of using peptides to determine the binding specificity of histone modification readers. DEK2 targets are enriched in genes related to the cold response, including bivalent cold-inducible genes such as *LT130* (Rayapuram et al., 2020, personal communication). This prompted the analysis of a potential role of DEK2 on the transcriptional regulation of *COR* genes (Figure 12D). The *dek2* mutants showed an over-induction of some *COR* genes during cold exposure, which was reversed in the *DEK2::DEK2-YFP* complementation line. This is consistent with the observations from Rayapuram et al. (2020, personal communication) that suggested DEK2 to act as a negative regulator of expression. However, this over-induction could not be generalized to all cold-inducible genes, as the *CBFs* and *ZAT10* were induced to wild-type levels, meaning that DEK2 act in a CBF-independent manner (Figure 12D). Interestingly, all genes that were over-induced in the *dek2* mutants are bivalent prior to the cold exposure or become bivalent during the stress episode, consolidating the hypothesis that DEK2 can read bivalency (Figure 7C and Figure 24 and Suppl. Figure 4). Genome-wide transcriptomic analyses are however required to firmly confirm this idea. Since no difference in expression of bivalent genes was observed in the absence of cold, DEK2 does not appear to act as a repressor but rather limits the range of expression of bivalent loci. A similar mechanism was observed on dehydration memory genes, where the presence of H3K27me3 did not prevent their induction upon stress exposure but its absence led to their over-induction without affecting their basal expression levels in non-stress conditions (N. Liu et al., 2014). The authors therefore suggested that H3K27me3 does not act as a repressive mark per se on those genes but rather defines their maximum potential for expression. Since these dehydration memory genes also carried H3K4me3, one can hypothesize that DEK2 might be also be involved in regulating their range of expression. It would be especially interesting to examine whether the over-induction of bivalent genes in the *dek2* mutant is simply due to the fact that bivalency is no longer read or to a potential reduction of H3K27me3 levels that would lift the upper limit of expression of those genes.

Even though some *COR* genes were induced to higher levels in the *dek2* mutant, this did not have a significant impact on the basal and acquired freezing tolerance of the plants (Figure 12C). However, *Arabidopsis thaliana* possesses four DEK proteins and some of them were already shown to act redundantly, such as DEK3 and DEK4 in the control of flowering time (Pendle et al., 2005; Zong et al., 2021). Furthermore, DEKs were implicated in the regulation of flowering and development, as well as the response to heat and salt stress, which are all processes in which bivalent genes were identified (Brestovitsky et al., 2019; Saleh et al., 2007; Waidmann et al., 2014; Zong et al., 2021). It is therefore possible that several DEK proteins are involved in the transcriptional regulation of bivalent *COR* genes and that higher order mutants would be required to observe physiological effects on the cold tolerance. DEK3 in particular was already shown to be a negative regulator of cold, heat and salt stress tolerance

(Brestovitsky et al., 2019; Waidmann et al., 2014). It represses its target genes by promoting nucleosome condensation and H2A.Z (a variant associated to bivalency) removal. Altogether, these results suggested DEK3 as an interesting candidate for bivalency reading. This was contradicted by the *in silico* analysis presented in this study, which did not reveal an enrichment of S2 genes among the DEK3 targets (Suppl. Figure 3A). However, environmental conditions are known to affect the phosphorylation status of DEK3 and therefore its interaction to numerous proteins, raising the possibility that DEK3 might recognize different marks and therefore bind to different loci in different conditions (Waidmann et al., 2021). Consequently, identifying the targets of DEK3 in cold-treated plants would be required to reach a more definite conclusion. More generally, it would be relevant to investigate the binding of all *Arabidopsis* DEK proteins to bivalent loci before and during cold exposure and their potential interaction with bivalent nucleosomes *in vitro*, in order to determine whether DEK2 is the only bivalency reader among them. Interestingly, my *in silico* approach demonstrated that human DEK genomic binding sites are preferentially bivalent loci, suggesting that the bivalency reader function might be a characteristic of DEK proteins that is conserved across species (Figure 12B).

While it was not investigated in this study, FORGETTER1 (FGT1) appears as another potential bivalency reader as it preferentially binds to S2 loci (Brzezinka et al., 2016). This chromatin-remodeller interactor binds to H3 and while it did not show a particular affinity for modified peptides, the authors did not use H3K27me3 nor H3K4me3-H3K27me3 peptides. FGT1 could be involved in the correlation between bivalency and chromatin accessibility that was observed in this study (Figure 10C and D). Indeed, FGT1 is essential to the maintenance of a low nucleosome density around the TSS of heat stress memory genes and one can hypothesize that, if it indeed binds to bivalent loci, it could assume a similar function there. Recently, mouse bivalency readers were identified by nucleosome pull-down assays using asymmetrically methylated nucleosomes (Bryan et al., 2021). This approach is particularly elegant as it mirrors the *in vivo* bivalency more exactly than the commonly used modified peptides or histones. While some of the proteins identified could also recognize monovalent nucleosomes, others such as the histone acetyltransferase KAT6B and the histone chaperone SRCAP only bound asymmetrically modified nucleosomes: they are specific bivalency readers. Some of those proteins have homologs in *Arabidopsis thaliana*, expanding the list of potential plant bivalency readers. For example, PIE1 is a homolog of SRCAP which, similarly to its mammalian counterpart, mediates the incorporation of H2A.Z into the chromatin (Deal et al., 2007; Gómez-Zambrano et al., 2018; Luo et al., 2020). As the presence of H2A.Z in the gene body was associated with environmental responsiveness, PIE1 and its interactors could provide a link between bivalency and transcriptional poising (Brestovitsky et al., 2019). These additional candidates suggest that the reading of bivalency could contribute to the regulation of gene expression through a multitude of mechanisms, including limiting the induction range (DEK2), modulating accessibility (FGT1) or incorporating additional chromatin features (PIE1) and highlights the importance of identifying those readers in order to complete our understanding of bivalency and transcriptional poising.

4.1.5 Bivalency or bistability?

In this study, bivalent domains (and by extension, genes) were defined as loci where H3K4me3 and H3K27me3 co-occur at the same point in time. While similar criteria were used in most of

the studies investigating bivalency in *Arabidopsis thaliana* (Jeong et al., 2009; Saleh et al., 2007; Xi et al., 2020), this does not actually prove that the underlying chromatin is bivalent as this co-occurrence could also be observed if a gene was marked by H3K4me3 in certain cells and H3K27me3 in others. The “true” bivalent nature of the cold-responsive genes was examined using Re-ChIP as this method allows to discriminate between the two possibilities. While at first glance it appeared that the nucleosomes at those loci carried both H3K4me3 and H3K27me3, the examination of additional controls casted doubts on these results as a similar enrichment was observed on bivalent and H3K4me3 monovalent genes (Figure 9). This suggested either that the anti-H3K27me3 antibody used in this experiment was unspecific and able to also recognize H3K4me3 or that it was not able to immunoprecipitate the chromatin efficiently. As performing the Re-ChIP in the reverse order (immunoprecipitating the H3K27me3-bound chromatin first) led to low yields already after the first immunoprecipitation, it is likely that the binding efficiency of the anti-H3K27me3 antibody is reduced when used in combination with the Re-ChIP kit. Additionally, the same antibody was also used in the ChIP-qPCR and ChIP-seq experiments and no enrichment of H3K4me3 targets was observed in those samples, rejecting the hypothesis of unspecific binding. The Re-ChIP protocol is therefore under further optimization in order to determine whether the cold-inducible genes are truly bivalent. In the meantime, several hints however indicate that the co-occurrence of H3K4me3 and H3K27me3 observed on certain cold-inducible genes could be due to true bivalency. First of all, the levels of H3K27me3 were similar on monovalent and bivalent genes, which is contrary to what one would expect if only a subpart of the cells were carrying H3K27me3 at “bivalent” loci. Furthermore, H3K4me3 was distributed more broadly over bivalent genes compared to monovalent ones, implying the existence of two sub-types of H3K4me3-marked genes where the methylation serves different purposes. Finally, Sequeira-Mendes et al. (2014) proved the existence of bivalency in *Arabidopsis thaliana* at selected S2 genes by performing Re-ChIP in both directions (H3K4me3-H3K27me3 and H3K27me3-H3K4me3), which suggests that the S2 cold-inducible genes identified here might also be bivalent. These results should however be considered with caution as the authors only tested a handful of loci and used a non-methylated gene as a negative control rather than monovalent loci, which might be critical to detect issues with the Re-ChIP, as described above (Figure 9) (Sequeira-Mendes et al., 2014).

Nonetheless, it is still possible that the co-occurrence of H3K4me3 and H3K27me3 on cold-inducible genes stems from different cells possessing either the repressive or the activating mark rather than from true bivalency. Indeed, modelling studies suggested that bivalency is actually rare and occurs only as a transitional state between active (H3K4me3-marked) and repressed (H3K27me3-marked) chromatin (Sneppen & Ringrose, 2019). Poised loci are predicted to be bistable rather than bivalent, i.e. to carry not both but only one mark at a given time and to easily and frequently switch between the two states. While the molecular mechanisms differ from the ones involved in bivalency, bistability also provides a strategy for fast changes in expression of the underlying genes. If the cold-inducible genes constantly oscillate between a silenced and active state, they are always transcribed in a fraction of the cells at each point in time. Upon cold exposure, this active state simply has to be stabilized once it occurs instead of inducing the complete transition from silenced to active state. This is reminiscent of the ON/OFF switch observed at *FLC* during vernalization: throughout the cold period, the transcript levels of *FLC* progressively diminish at the whole plant scale (Angel et al., 2011, 2015; H. Yang et al., 2017). Rather than a similar decrease in each cell, this is due

to the complete silencing of the *FLC* locus in more and more cells as the cold episode drags on. Cold-inducible transcripts could be accumulated in a similar fashion, as the active state of these loci is stabilized in incrementally more cells over the stress period. Identifying the true nature (bivalent or bistable) of cold-inducible genes is therefore essential to the elucidation of their poising mechanisms and the establishment of the Re-ChIP method or single cell ChIP will provide the required answer.

4.2 COLD-INDUCED DYNAMICS OF HISTONE METHYLATION

The *in silico* and *in vivo* analyses described previously showed that many cold-inducible genes carry H3K27me3 and H3K4me3 prior to the cold exposure. As the chromatin state of a gene influences its transcription, investigating the potential dynamics of those methylation marks upon cold exposure might provide insights onto how these genes are activated. While Kwon et al. (2009) showed that certain cold-inducible genes lose H3K27me3 upon cold exposure, previous work from our lab demonstrated that this could not be generalized to all H3K27me3-carrying *COR* genes, highlighting the need for genome-wide analyses (Vyse et al., 2020). Furthermore, the cold-induced dynamics of H3K4me3 were not investigated so far. To the best of our knowledge, this study is therefore the first to fill this knowledge gap by exploring the short-term consequences of cold stress on H3K4me3 and H3K27me3 on a genome wide scale. Indeed, only one other study examined the epigenome of cold-treated *Arabidopsis thaliana* using ChIP-seq but the authors focused on cold as a developmental cue and therefore investigated plants that were exposed to 4°C for 40 days (Xi et al., 2020). The data presented here therefore provide interesting insights on the role of histone methylation in the cold stress response.

4.2.1 Cold triggers changes in H3K4me3 and H3K27me3

To investigate the impact of low temperatures on H3K27me3 and H3K4me3, their levels were monitored during a cold treatment using ChIP-seq. Low temperatures did not lead to a striking gain or loss of the methylation marks, as the number and size of the detected peaks remained constant (Figure 14). However, a differential methylation analysis revealed that several thousand genes underwent significant H3K27me3 or H3K4me3 changes upon cold exposure (Figure 16A). Around 5000 genes showed a significant change in H3K27me3 levels and two thirds of them had lost the repressive mark. Approximately 3000 genes displayed differential H3K4me3 methylation upon cold exposure, with around three quarters of them gaining the activating mark. The differential methylation analyses were confirmed on some selected *COR* genes using ChIP-qPCR (Suppl. Figure 9). Furthermore, the examination of the levels of H3 at those loci proved that the methylation dynamics were due to active deposition and removal of the marks rather than changes in nucleosome density (Figure 25). In the case of H3K27me3, the observed loss could also have been due to the deposition of additional marks around the lysine 27 that could prevent binding of the antibody. Indeed, it has already been described that the PcG-mediated silencing of H3K27me3-carrying genes can be lifted through the phosphorylation of the neighbouring serine 28 residue (Nga Ieng Lau & Cheung, 2011). However, the anti-H3K27me3 antibody used in this study (Table 8) was shown to recognize and bind to H3K27me3-S28pho doubly modified peptides, rejecting this possibility and confirming that the loss observed here is truly due to an active removal of the methylation

mark. Additionally, the H3K27me3 differential methylation analysis was consistent with previous studies as it confirmed that cold induces a loss of H3K27me3 on *COR15A* and *GOLS3* as observed by Kwon et al. (2009) but no significant difference was observed for *ULT1*, *WRKY48* or *PRR1*, similarly to earlier results from our lab presented in Vyse et al. (2020). Altogether, this study confirmed that cold leads to an active demethylation of H3K27me3 at some but not all genes carrying this modification and revealed that the levels of this repressive mark increase at other loci. Furthermore, it demonstrated that H3K27me3 is not the only histone PTM affected by low temperatures, as the distribution of H3K4me3 was also altered, mainly due to genes gaining this activating mark. These results are diametrically opposed to the histone methylation changes induced by 40 days of cold treatment, which consist predominantly of a loss of H3K4me3 and a gain of H3K27me3 (Xi et al., 2020). While these contrasting observations could also be partially attributed to the different plant ages used in both studies, they demonstrate that the effects of cold on the chromatin status vary greatly depending on the length of the stress episode. This might reflect different responses of the plant to low temperatures, from immediate defence against the stress to the adjustment of its development. Examining those differences in more details might help dissect the dual role of cold as a stressor and as a developmental cue.

Differential methylation analyses are commonly performed by comparing read numbers over the whole peaks or gene bodies (Xi et al., 2020; Yamaguchi et al., 2021; W. Yan et al., 2018). Here however, the levels of H3K27me3 and H3K4me3 in the different conditions were compared using a sliding window strategy (diffReps), which provides a more detailed report of the changes and their localization. This approach revealed that, rather than being homogeneous over complete methylation peaks or gene bodies, the cold-triggered changes occur on small and localized regions (Figure 15). H3K4me3 loss for instance happened mainly on first exons while the mark usually spans the TSS and 5' UTR, implying that it was not removed from the whole peak but only on specific domains (Figure 14E and Figure 15D). Similarly, while H3K27me3 covers the whole gene body, the losses were mostly detected on exons (Figure 14F and Figure 15D). However, closer inspection using a genome browser revealed that H3K27me3 is accumulated to higher levels on exons than introns (Figure 24 and Suppl. Figure 4), it is therefore possible that levels were reduced over the whole gene body but only detected as significant by diffReps on regions of higher methylation, i.e. the exons. Interestingly, consistent with previous knowledge, exons presented higher levels of H3 (data not shown), indicating that the increased H3K27me3 signal on those genomic features might not stem from preferential methylation of exon-bound histones but simply from the higher nucleosome density at these loci (Chodavarapu et al., 2010).

The differential methylation analysis revealed that cold also triggers a gain of H3K27me3, mostly localized in intergenic regions (Figure 15D). As this study focuses on the role of histone modifications in the transcriptional regulation of *COR* genes, this particular observation was not further investigated but represents a compelling opening for a follow-up study. Indeed, intergenic regions contain enhancers that participate in the transcriptional regulation of neighbouring genes (B. Zhu et al., 2015). Similarly to promoters, those enhancers can be active or silenced and are associated with the presence of H3K27ac and H3K27me3 respectively. The intergenic regions gaining H3K27me3 might therefore be enhancers that become inactive during cold exposure. As enhancers are particularly underinvestigated in plants genomes (Weber et al., 2016), it would be extremely interesting to confirm whether

H3K27me3 is indeed accumulated at the intergenic regions identified in the differential methylation analysis and whether this gain has consequences on the chromatin structure or the expression of nearby genes.

Few studies investigated the genome-wide consequences of a stress episode on the distribution of the two antagonistic marks H3K4me3 and H3K27me3. Sani et al. (2013) conducted a similar study on plants exposed to osmotic stress for 24 h and observed, as here, that the stress induced changes in the levels of both marks, consisting mainly of a loss of H3K27me3 and a gain of H3K4me3. However, the localization of those changes revealed a striking difference: after an osmotic stress, H3K27me3 was preferentially removed from the edges of the peaks in a process coined “etching” by the authors, which is thought to reverse the spreading of the repressive mark. In this study however, the loss of H3K27me3 was mostly seen at highly methylated regions, i.e. in the middle of the peaks. As the methodologies used for the differential methylation analyses differ (diffReps on two biological replicates here and CHIPDIFF on a single replicate in Sani et al. (2013)), this discrepancy might stem from inherent biases of those algorithms. However, independently of the differential methylation analysis, Sani et al. (2013) observed a fragmentation of pre-existing H3K27me3 peaks into smaller ones during osmotic stress, which was not occurring (at least not in comparable magnitudes) upon cold exposure (Figure 14B and D). This suggests that, although both stresses have similar consequences on the levels of H3K27me3, the demethylation might be achieved by different mechanisms.

While the results of the differential methylation analysis could be confirmed using ChIP-qPCR on selected targets, it is worth noting that they were not entirely consistent with the changes observed on the Western Blots (Figure 13 and Suppl. Figure 9). Indeed, the genome wide levels of H3K4me3 appeared unaffected by cold on the blots while the ChIP-seq revealed intense redistribution of the mark (Figure 13A and Figure 15). As cold led to both gain and loss of this active mark depending on the gene considered (Figure 16A), it is likely that its global levels, as measured by the Western-Blot, remained constant, highlighting the need to examine histone methylation changes at the gene-specific level before stating that a certain mark is unaffected by cold or any other treatment. The discrepancy between the two techniques is more challenging to explain in the case of the repressive mark. Indeed, the Western Blot showed that cold led to a rapid and significant loss of H3K27me3 of around 50% (Figure 13B). This decrease was not observed in the ChIP-seq, as the global levels of H3K27me3 appeared to remain constant during a cold exposure (Figure 14). While the differential methylation analysis revealed that most of the cold-induced H3K27me3 variations consisted of a loss of the repressive mark, those variations did not account for the significant loss of the mark observed on the Western-Blot (Figure 16 and Suppl. Figure 9). As the Western Blot was only performed on two biological replicates, these results should be confirmed before drawing definitive conclusions, but this might reveal an issue in the normalization strategy used during the ChIP-seq analysis. Indeed, the standard ChIP-seq analysis strategies are only semi-quantitative as they cannot distinguish the technical and biological contributions to the variations in library size. They are therefore adapted for cases where the global levels of the histone mark or protein of interest remain constant across conditions. If the levels of the mark vary by a factor as significant as the one observed here in the Western Blot however, the analysis might underestimate the fold changes at the loci detected as differentially methylated and/or fail to detect some of the changes, as they will be erased during the library size

normalization step. This might explain the low fold changes observed in this study (Figure 15C). It might therefore be necessary to use a spike-in strategy instead. This technique relies on the addition of a specific amount of chromatin from another organism (usually *Drosophila melanogaster*) to each sample to estimate the technical variation in library size and the normalization is performed using this factor rather than the total library size (Egan et al., 2016). This allows a robust quantitative analysis and might give a more accurate depiction of the genome wide dynamics of H3K27me3 during a cold stress as it would not underestimate the magnitude of the changes.

4.2.2 Differential methylation partially correlates with differential expression.

H3K4me3 is predominantly found on active genes while H3K27me3 is present on silent loci, leading to their characterization as an active and repressive mark respectively. As cold led to changes in the levels of both of these histone PTMs, it was hypothesized that they might correlate with variations in transcriptional activity of the associated genes. Interestingly, at the earlier time point (3 h of cold exposure), no correlation could be seen between changes in expression and changes in any of the marks (Figure 22A and B). After three days however, a positive (resp. negative) correlation was found between transcriptional changes and H3K4me3 (resp. H3K27me3) (Figure 22C and D). These observations were consistent with the hypotheses that H3K4me3 and H3K27me3 act respectively as positive and negative transcriptional regulators. Furthermore, the correlation was stronger for H3K4me3 than for H3K27me3, which is consistent with a previous report on flower morphogenesis that revealed that H3K4me3 is a stronger predictor of transcriptional changes than H3K27me3 (Engelhorn et al., 2017). Since the correlations were only identified after a longer cold exposure, differential methylation and differential expression likely occur at distinct paces. To decipher the order, the correlations studies were repeated, this time comparing early transcriptomic changes to the late epigenomic variations and vice versa (data not shown). While no conclusion could be reached for H3K27me3, this approach suggested that the changes in expression preceded the adjustments of H3K4me3 levels as the positive correlation was only observed when comparing early transcriptional changes to late H3K4me3 methylation variations. A more detailed time-course experiment could confirm this conclusion. Coupled to the previously mentioned interactions between certain H3K4me3 methyltransferases and the transcriptional machinery, one can hypothesize that the variations in the levels of this active mark are a direct consequence of the differential expression of the underlying genes (B. Li et al., 2007; Reverón-Gómez et al., 2018; Voigt et al., 2013). This does however not exclude the possibility that H3K4me3 levels could impact transcriptional activity through a positive feedback loop.

It is important to note that, despite the correlations observed, only a fraction of the cold DE genes underwent methylation changes and vice versa, indicating that differential expression is neither the only cause nor a direct consequence of the differential methylation (Figure 23). This is not unique to cold, as Sani et al. (2013) also observed an absence of correlation between H3K4me3 or H3K27me3 differential methylation and gene expression. Furthermore, Yamaguchi et al. (2020) and Lämke et al. (2016) showed that not all genes induced by a heat stress gained H3K4me3. The ChIP-seq presented here also confirms previous work from our lab, where it was shown that the cold-triggered loss of H3K27me3 on *COR15A* and *GOLS3* observed by Kwon et al. (2009) could not be generalized to all H3K27me3-carrying *COR* genes

(Vyse et al., 2020). The genome-wide differential methylation analysis support this conclusion, as many cold-induced genes did not undergo a loss of H3K27me3 (Figure 23). This corroborates the idea that H3K27me3 itself does not prevent transcription and that its removal is therefore not necessary for induction, as previously observed for drought-inducible genes (N. Liu et al., 2014). Instead, this repressive mark might serve to limit the expression range of its target genes, as proposed by Liu et al. (2014) or to ensure the proper timing of their induction, as observed by Zhao et al. (2021). Altogether, the relationship between H3K4me3, H3K27me3 and transcriptional activity appears more complicated than the straightforward and commonly described activating and silencing roles of the methylation marks.

4.2.3 Differential methylation affects stress responsive and developmental genes

In order to decipher the potential role of H3K4me3 and H3K27me3 differential methylation, GO biological function term enrichment analyses were performed on the DM genes. The terms enriched for H3K4me3-gaining genes were closely related to the physiological changes that plants are undergoing during cold exposure (Figure 17A and B). After three hours for example, the GO analysis identified terms related to lipid metabolism, photosynthesis and non-photochemical quenching, which are reminiscent of the energy adjustments and membrane modifications triggered by cold (Ruelland et al., 2009). After three days however, terms such as cold acclimation and freezing tolerance were identified, suggesting that the dynamics of H3K4me3 reflect a shift from the immediate response to cold towards the preparation for future harsher conditions (Ruelland et al., 2009; Thomashow, 1999). Terms related to phytohormone signalling were also found (salicylic and abscisic acid), indicating that the changes of H3K4me3 occur at different levels of the cold signalling pathway, affecting not only the final actors of cold defence but also the secondary messengers. It is also worth noting that many terms linked to the circadian rhythm were identified. Cold leads to the dampening of the circadian clock, as the amplitude of expression of genes showing a diurnal variation is greatly reduced in plants exposed to low temperatures (Bieniawska et al., 2008). Genes with a diurnal cycle of expression possess a specific H3K9ac-H3K27ac-H3S28pho chromatin signature and gain H3K4me3 as an additional activating mark when the plant experiences a water deficit (Baerenfaller et al., 2016). The analysis presented here suggests that H3K4me3 acts as a supplementary activating mark for those genes also during a cold episode, expanding on the conclusions from Baerenfaller et al. (2016). On the other hand, the loss of H3K4me3 happened preferentially on genes related to development or photosynthesis, consistent with the slowed down growth, lower energy demands and lower photosynthetic activities at chilling temperatures (Figure 17C and D) (Ruelland et al., 2009; Scott et al., 2004; Shibasaki et al., 2009). Additionally, several terms linked to chromatin regulation (nucleosome positioning, chromosome condensation) were identified at the late time point, suggesting that the chromatin might be actively reorganized during a prolonged cold episode.

As most H3K27me3 changes occurred early during the cold response and persisted over the following days, similar GO terms were identified for both time points. Genes gaining H3K27me3 were mostly linked to development, similarly to what was observed for genes losing H3K4me3 (Figure 18A and B). As both types of changes are correlating with gene repression and as cold leads to growth arrest, this was not unexpected. However, the GO term analysis specifically identified flowering-related terms (transition from vegetative to reproductive phase,

maintenance of the floral meristem) stemming from the observed gain of H3K27me3 on positive regulators of the floral transition such as *AGAMOUS-LIKE* transcription factors. The cold-induced gain of H3K27me3 on floral regulators was already described previously by Xi et al. (2020) but after 40 days of low temperatures. The results presented here show that the accumulation of the repressive mark starts early during cold exposure, with some floral regulator already showing a significant gain 3 h after the onset of the stress, and that it also occurs in plants that do not require vernalization to flower. However, Xi et al. (2020) described this increase of H3K27me3 as promoting the switch to reproductive growth while the genes identified as gaining the repressive mark in this study were positive regulators of this transition. As higher levels of H3K27me3 correlate with a lower expression, this would rather suggest that the accumulation of this methylation mark participates in delaying the transition until the conditions are more favourable. Genes losing H3K27me3 showed an enrichment for terms related to the stress response (Figure 18C and D), reminiscent of what was observed for genes gaining H3K4me3, which is consistent with the fact that both types of changes correlated to transcriptional induction. However, the sets of terms were distinct for both marks. Indeed, the gain of H3K4me3 occurred on genes involved in the response to cold and other closely related abiotic stresses (water deprivation, salt stress) while the GO analysis of genes losing H3K27me3 identified more general terms related to defence and stress signalling (signal transduction, induced systemic resistance, defence response). Interestingly, the terms identified for H3K4me3 gain coincided with the ones found in the GO analysis of up-regulated genes at the same time point (Suppl. Figure 6), while this similarity was not observed for genes losing H3K27me3, confirming that H3K4me3 levels are more correlated to transcriptional activity than H3K27me3.

Altogether, H3K4me3 gain occurs on genes immediately necessary and specific to the cold stress response, while H3K27me3 loss targets genes involved in more general stress responses and memory. Histone methylation changes associated with transcriptional silencing (H3K4me3 loss and H3K27me3 gain) happen on genes related to development and might contribute to delaying the transition to reproductive development.

4.2.4 Mechanisms of the differential methylation

Many *COR* genes are undergoing H3K4me3 gain and/or H3K27me3 loss during their induction upon cold exposure. In order to determine whether these chromatin status changes contribute to their induction or are rather a consequence from it, efforts were directed towards the identification of the actors responsible for the differential methylation. Indeed, investigating the induction of the *COR* genes in knock-out mutants of these actors would allow to determine the potential influence of chromatin changes on their transcriptional activation. An *in silico* approach was used to narrow down the list of potential candidates (Figure 26). Based on the RNA-seq generated in this study, the dataset from Calixto et al. (2018) and the RT-qPCR screening of chromatin modifiers published previously in collaboration with Prof. Dr. Hinch (Vyse et al., 2020), ATX1 and the five H3K27me3 Jumonji demethylases were identified as being potentially involved in the cold-triggered differential methylation. Indeed, those six proteins were induced by cold and they were already shown to be involved in stress-induced chromatin changes (Figure 26) (Yong Ding et al., 2011; Song et al., 2021; Yamaguchi et al., 2021).

During a dehydration stress, ATX1 mediates the accumulation of H3K4me3 at key stress-responsive genes, including cold-inducible genes such as *COR15A* and *RD* genes, thereby allowing their transcriptional activation (Yong Ding et al., 2011). ATX1 also participates in moderate heat stress tolerance through similar mechanisms, making it a prime candidate as a regulator of *COR* genes induction during cold exposure (Song et al., 2021). However, *COR15A* and *LT130* still accumulated H3K4me3 upon cold exposure in the *atx1* knock-out plants, implying that ATX1 is not responsible for the cold-induced gain of this activating mark (Figure 28A). At least seven other H3K4me3 methyltransferases are encoded in the genome of *Arabidopsis thaliana* and some of them were already proven to act redundantly (K. Cheng et al., 2020). For example, *atx3-atx4-atx5* triple mutants have a growth retardation and anther development phenotype that is not observed in the single or double mutants, proving that those three methyltransferases act redundantly in the context of development and reproduction (Chen et al., 2017). Furthermore, both ATX4 and ATX5 were shown to be involved in the drought response and the phenotype was exacerbated in the double mutant, proving that the methyltransferases also act redundantly in the stress response (Yutong Liu et al., 2018). It is therefore likely that ATX1 is involved in the trimethylation of H3K4 at *COR* genes during cold exposure but that its absence is compensated by one or more other H3K4me3 methyltransferases. Another possibility would be that each methyltransferase acts on a specific set of genes and that neither *COR15A* nor *LT130* are targeted by ATX1. However, as ATX1 trimethylates H3K4 on the *COR15A* locus during ABA treatment and drought stress, this is unlikely (Yong Ding et al., 2011). The H3K4me3 methyltransferases could also act in a stress-specific manner, explaining why ATX1 is not required for cold stress response. To determine whether they act redundantly or in a stress-specific fashion, more H3K4me3 methyltransferase mutants should be investigated, including higher order mutants. ATRX7/SDG25 appears to be a prime candidate as it acts redundantly with ATX1 in heat stress tolerance (Song et al., 2021). On the other hand, ATX4 was shown in the *in silico* analysis to be induced by cold (Figure 26D) but its function as a repressor of the drought response rather suggests it as a negative regulator of cold tolerance (Chen et al., 2017).

Four out of the five H3K27me3 Jumonji demethylases (ELF6, REF6, JMJ30 and JMJ32) are implicated in the removal of H3K27me3 during heat stress, which is necessary for heat stress memory (Yamaguchi et al., 2021). As *JMJ13* was found to be induced by cold in the RNA-seq presented in this study, all five demethylases were considered to be interesting candidates and therefore screened. As none of the single mutants displayed a difference in basal nor acquired freezing tolerance and JMJ demethylases are known to act redundantly, the ChIP experiments were performed on the *elf6-ref6-jmj30-jmj30* quadruple mutant generated by Yamaguchi et al. (2021) (Figure 27) (W. Yan et al., 2018). Upon cold exposure, a loss of H3K27me3 on *COR15A* and *LT130* of the same magnitude as the one observed in wild type plants could be detected in the quadruple mutant, suggesting that none of these demethylases are involved in the cold-triggered demethylation (Figure 28B). As ELF6, REF6 and JMJ13 are known to act redundantly and *JMJ13* is induced by cold, it is possible that JMJ13 is able to compensate the absence of the other demethylases (W. Yan et al., 2018). To test this hypothesis, it would be necessary to investigate a higher order mutant where *JMJ13* is also knocked-out. Unfortunately, the *elf6-ref6-jmj13* presents a strong dwarf phenotype, rendering the analysis of cold tolerance impossible due to the strong differences to wild-type plants already prior to any stress exposure (W. Yan et al., 2018). It would therefore be necessary to generate an inducible mutant line, where the expression of the H3K27me3 demethylases could be inhibited shortly prior to the

stress episode, allowing the investigation of their role in the cold response in plants that developed normally. It is however possible that the cold-triggered loss of H3K27me3 is not due to an active demethylation. Indeed, the Western Blot experiment revealed that around half of H3K27me3 is lost genome-wide after only 3 h of cold exposure, which appears too substantial and rapid to be due to the action of the demethylases (Figure 13B). As the levels of H3 remained constant at the loci where a loss of H3K27me3 was detected, this loss was not stemming from a reduced nucleosomal density (Figure 25 and Suppl. Figure 9C). If the nucleosomal density remains constant, the lowered methylation levels can only be caused by an active demethylation or by the replacement of methylated histones by non-methylated ones. Histone replacement was already shown to occur during certain abiotic stresses. For example, H2A.Z is evicted from temperature-responsive genes during a moderate heat treatment and from drought-responsive genes during a drought stress and this eviction is proposed to favour the transcription of the affected genes (S. V. Kumar & Wigge, 2010; Sura et al., 2017). On the contrary, the H1.3 variant is induced during drought stress and its incorporation in the chromatin is necessary for a proper stress response (Rutowicz et al., 2015). To test whether histone replacement might cause the observed loss of H3K27me3, the expression levels of all H3 variants during cold exposure were examined using the RNA-seq generated in this study (Suppl. Figure 11B). This revealed that the atypical variant *HTR11* was strongly induced by cold. Interestingly, HTR11 is one of two H3 variants which do not have a lysine at the position 27 and can therefore not carry H3K27me3 (Suppl. Figure 11C). The loss of H3K27me3 induced by cold could therefore stem from the replacement of H3 histones methylated at the lysine 27 by HTR11 which cannot carry this modification. This hypothesis is supported by the previous identification of a similar mechanism in the response to wounding: upon wounding, the *HTR15* variant is induced and incorporated in the chromatin (A. Yan et al., 2020). As HTR15 does not have a lysine at the position 27, this leads to the loss of the repressive mark H3K27me3 at specific loci, allowing the transcriptional activation of underlying genes, such as *WOX11*, which are necessary for cell proliferation. HTR11 could undertake a similar role in the de-repression of *COR* genes carrying H3K27me3, opening an avenue for new investigations in the role of atypical histone variants in the cold stress response. It would be crucial to first confirm the incorporation of HTR11 in the chromatin upon cold exposure through the examination of plants expressing a tagged-version of this variant or using HTR11-specific antibodies.

In conclusion, the actors involved in the deposition of H3K4me3 and the removal of H3K27me3 at *COR* genes remain undiscovered, preventing the investigation of the role that their chromatin methylation status plays in their transcriptional induction. Further avenues of research include the examination of mutants of the atypical H3 variant HTR11 and of higher order H3K4me3 methyltransferases mutants.

4.3 COLD STRESS MEMORY IS ENCODED AT THE CHROMATIN LEVEL

4.3.1 Persisting chromatin changes correlate with transcriptional memory

Cold exposure led to changes in the levels of H3K4me3 and H3K27me3 at numerous genes (Figure 16). As it has been shown that stress-induced chromatin changes can be maintained for several days after the stress subsided, for instance in the case of drought or heat (Yong Ding, Fromm, et al., 2012; Sani et al., 2013), the persistence of cold-induced changes was

investigated using ChIP-qPCR on selected target genes (Figure 31A and B). For most genes, the changes in H3K4me4 and H3K27me3 levels were fully reversed within seven days, indicating that they are not generally maintained. However, both the dehydrin *LT130* and the vernalization actor *VIN3* did not return to their naïve chromatin status. *VIN3* gained H3K4me3 during cold exposure and this accumulation, albeit reduced, was still visible after seven days of lag phase (Figure 31A). Low temperatures led to both a gain of H3K4me3 and a loss of H3K27me3 on *LT130* but only the H3K27me3 variations persisted during the lag phase (Figure 31A and B). Interestingly, in both cases, the methylation marks in PL plants were at an intermediate level between the ones of non-cold treated (N28) and cold-treated (P) plants, suggesting that they are not maintained indefinitely but rather slowly reverse over time and that the cold-induced changes might completely disappear after a longer time at ambient temperature. Both the persistence of H3K4me3 and H3K27me3 cold-induced changes were associated with transcriptional memory but the type differed depending on the methylation mark.

VIN3 showed a sustained induction as it was expressed at a higher levels in PL plants than in the non-primed control (Figure 31C). The sustained induction and the maintained H3K4me3 gain did not impact its re-activation: *VIN3* was induced at the same level and speed in primed and non-primed plants during the triggering stress. While there is a clear correlation between H3K4me3 levels and expression, the causality relationship between both parameters remains unclear: is the sustained induction caused by the persistence of higher levels of H3K4me3 or is H3K4me3 is retained because *VIN3* still expressed even after the stress subsides? A third possibility is that gene expression and H3K4me3 act together in a positive feedback loop favouring transcriptional memory. Indeed, H3K4me3 participates in the recruitment of the transcriptional machinery and facilitates transcriptional elongation while the mark itself can be deposited in a transcriptional-dependant manner (Yong Ding, Ndamukong, et al., 2012; B. Li et al., 2007; Reverón-Gómez et al., 2018; Voigt et al., 2013). While the results presented in this study cannot provide a definitive answer, the literature offers additional insights, as the association of persisting H3K4me3 accumulation and sustained transcriptional induction has also been observed during heat stress memory. A first heat exposure triggers the transcriptional induction of *HEAT SHOCK PROTEIN (HSP) 18, 21 and 22* and *ASCORBATE PEROXIDASE 2 (APX2)* as well as a gain of H3K4me3 at those loci, which both persist even after the stress subsides (Lämke et al., 2016). The methyltransferases ATX1 and ATRX7 are responsible for the deposition of H3K4me3 on heat-responsive genes upon heat exposure, and their presence is also required for their induction and sustained expression during deacclimation, proving that the deposition of H3K4me3 dictates the heat transcriptional memory (Song et al., 2021). This suggests that the sustained transcription of *VIN3* might stem from the persistence of H3K4me3 at that locus. However, this hypothesis should be considered with caution as ATX1 did not appear to be involved in the cold-induced accumulation of H3K4me3 on *COR* genes, so the mechanisms of heat and cold memory could differ (Figure 28A).

On the other hand, *LT130* was expressed at a similar level in primed and non-primed plants at the end of the lag phase, but was induced faster in primed plants upon cold re-exposure: *LT130* is ++ trainable (Figure 31C). This observation is consistent with the work of Finnegan et al. (2011), which demonstrated that the lower levels of H3K27me3 on *VIN3* in the *clf-swn* or *emf2-vrn2* mutants led to its faster induction during a cold episode, suggesting that the lower levels

of H3K27me3 in primed plants are directly responsible for the trainability of *LT130*. Kwon et al. (2009) already described that the cold-induced loss of H3K27me3 on *COR15A* and *GOLS3* persists for up to three days after return to ambient temperature. In the present study, H3K27me3 returned to naïve levels on those two genes within seven days, suggesting that the cold-triggered loss of H3K27me3 might persist for different period of times depending on the gene. It is worth noting that while the persisting low levels of H3K27me3 on *LT130* were associated to a faster re-induction of the gene upon triggering, this was not observed for *COR15A* and *GOLS3* by Kwon et al. (2009). It is therefore possible that the sustained loss of H3K27me3 is not the only parameter leading to a faster re-induction of *LT130*. However, the persistence of reduced levels of H3K27me3 has already been linked to transcriptional trainability in the context of other abiotic stresses. Osmotic stress for instance leads to the loss of H3K27me3 at many loci which is reversed at different paces depending on the gene, as observed here for cold stress (Sani et al., 2013). The authors also observed that this persisting loss correlates with a ++ trainability of the affected genes. Similarly, Yamaguchi et al. (2021) demonstrated that a heat treatment led to sustained H3K27me3 demethylation on *HSP22* and *HSP17.6C*, which was necessary for the faster induction of those genes upon re-exposure to heat as the re-induction was slower in the *elf6-ref6-jmj30-jmj32* mutant than in wild-type plants. Altogether, this consolidates the idea that, rather than directly controlling transcriptional activity, H3K27me3 modulates the range of expression and speed of induction of its target genes and thereby participates in stress memory (Finnegan et al., 2011; N. Liu et al., 2014).

Interestingly, the two types of transcriptional memory displayed by *VIN3* and *LT130* are consistent with the different roles played by those genes in the cold response. Indeed, *LT130* is a dehydrin that can bind to membranes and lower their lipid phase transition, thereby participating in freezing tolerance (Eriksson et al., 2011; Puhakainen et al., 2004). Dehydrins are thought to protect membranes until their lipid composition can be adjusted to better cope with low temperatures, making them essential for the early response to cold. The transcriptional memory of *LT130* might reflect this function: as the accumulation of *LT130* is essential to limit the damages early in the stress response, the gene is not induced to a higher level during a second cold stress (as no difference was observed after 3 d) but faster, potentially allowing the plant to re-acquire freezing tolerance more rapidly upon triggering (Figure 31C). As *LT130* is not necessary in the absence of cold, it does not need to be sustainably expressed during the lag phase. The gene is therefore silenced again upon return to ambient temperature and the H3K4me3 gained during the cold exposure is lost, while the loss of H3K27me3 is maintained, improving the responsiveness of *LT130* to a subsequent cold stress (Figure 31A and B). On the other hand, *VIN3* is not known to participate in the response to cold stress but it acts as a cold sensor for vernalization (Antoniou-Kourouniotti et al., 2018; Hepworth et al., 2018). Indeed, *VIN3* is gradually induced during cold exposure, thereby measuring the duration of the stress (Bond et al., 2009; Sung & Amasino, 2004). *VIN3* binds to the PRC2 complex and promotes the deposition of H3K27me3 on *FLC*, leading to its cold-triggered silencing and therefore to vernalization (De Lucia et al., 2008; Sung & Amasino, 2004). As it participates to the long-term silencing of *FLC*, it might be beneficial for the plant to sustain the induction of *VIN3* for a while after the cold subsides in case the increase in temperature is only transient, which might explain the maintenance of higher levels of H3K4me3 at that locus (Figure 31A and C). On the other hand, the levels of H3K27me3 on *VIN3* do not vary during cold exposure (Figure 31B). This might stem from its function as a cold duration sensor, which would be compromised by the increased responsiveness that

could emerge should H3K27me3 levels be reduced at that locus. Interestingly, previous studies reported that *VIN3* is rapidly repressed upon return to ambient temperatures (in three to five days), contradicting the results presented in this work where its expression was maintained for at least seven days (De Lucia et al., 2008; Hepworth et al., 2018). However, as these studies focused on vernalization, they used vernalization-responsive plants that were exposed to a long period of cold (several weeks), while the plants used here were not vernalization-responsive and only received short cold treatments, which might explain the discrepancy.

Overall, this study demonstrated that, upon return to ambient temperature, cold-induced changes to the histone methylation status are reversed at a different pace depending on the gene. Some had still not recovered their naïve methylation levels seven days after the cold treatment ended and both for H3K4me3 and H3K27me3, the persistence of cold-induced changes was associated with transcriptional memory. While this study showed a correlation between sustained histone methylation changes and transcriptional memory on *LT130* and *VIN3* which is consistent with the literature, the number of genes investigated here was modest. The conclusions presented here should be considered with caution until more genes are examined, ideally using genome-wide methods, to determine whether they can be generalized to all persisting chromatin changes. In particular, the maintenance of methylation changes was only examined for genes that were induced by cold as this study focuses on *COR* genes transcriptional regulation but it would be interesting to widen this study to other differentially methylated genes. Indeed, as described previously (section 4.2.2), many cold-differentially methylated genes were not differentially expressed, raising questions about the purpose of changing their chromatin status. It was hypothesized that this might stem from differential methylation and expression having distinct kinetics. However, the persistence of some chromatin changes upon return to ambient temperature and its correlation with transcriptional memory offers an alternative explanation. The transcriptional activation of those genes might not be necessary for the cold response but rather for deacclimation and stress-recovery, in which case their cold-triggered differential methylation might be a strategy used by the plant to prepare for deacclimation. It would therefore interesting to also investigate non cold-induced genes in futures experiments to examine this theory.

4.3.2 H3K27me3 loss as a support of cold stress memory

Previous studies showed that *Arabidopsis thaliana* is able to remember previous cold stresses for at least seven days, leading to an improved survival during subsequent cold episodes (Byun et al., 2014; Leuendorf et al., 2020; van Buer et al., 2016; Zuther et al., 2019). The work presented here confirmed these conclusions, as both a short (3 d) and a long (7 d) priming episode led to a higher freezing tolerance in primed vs non-primed plants upon a triggering stress (Figure 29). However, the benefits from priming were not always consistent as they were sometimes reduced or, in rarer cases, could barely be detected (data not shown). These different outcomes seemed to stem from slight variations in the growth stage and/or growth conditions of the plants, suggesting that cold memory might not be as robust a mechanism as heat or drought memory and might be influenced by other endogenous and exogenous parameters. Still, a majority of the conducted assays revealed that primed plants performed better than non-primed ones upon a second exposure to cold, consistent with previous reports (Byun et al., 2014; Leuendorf et al., 2020; van Buer et al., 2016; Zuther et al., 2019). Despite

cold stress memory being reported in several studies, its molecular support remained undiscovered until now. As chromatin regulation was repeatedly identified as participating to the memory of other abiotic stresses and also to the memory of cold as a developmental cue, its potential role in cold stress memory was examined using an unbiased screening approach. Candidates were identified from an *in silico* strategy (published in Vyse et al. (2020), Figure 26) and tested in an electrolyte leakage assay. This led to the identification of the H3K27me3 demethylase ELF6 as an essential contributor to cold stress memory, as the *elf6* mutants only displayed a slight improvement in freezing tolerance after priming compared to wild-type plants (Figure 30). This is, to the best of our knowledge, the first chromatin modifying protein to be reported as being involved in cold stress memory.

Taken together with the previously described correlation between persisting H3K27me3 demethylation and faster re-induction of *LTI30*, the identification of ELF6 as a required actor for cold priming suggests that the loss of H3K27me3 might be the molecular support of cold stress memory. ELF6 could participate in the maintenance of low levels of H3K27me3 on certain *COR* genes, allowing them to be re-induced faster during a triggering event and ultimately leading to an improved survival of the plant. As H3K27me3 levels were still reduced upon cold exposure on *LTI30* and *COR15A* in the *elf6-ref6-jmj30-jmj32* quadruple mutant (Figure 28B), it is unlikely that this demethylase participates in the cold-induced removal of H3K27me3 but it could prevent the re-deposition of the repressive mark during the lag phase on specific genes. However, crucial confirmation is still lacking for the validation of this model. Indeed, it is still unclear whether ELF6 directly contributes to the maintenance of low levels of H3K27me3 on *LTI30* during the lag phase. The examination of H3K27me3 levels on this gene as well as its induction dynamics in the *elf6* mutant would be essential to the validation of the current hypothesis.

This study is not the first to describe H3K27me3 as a support of memory. During vernalization for instance, the cold episode is “remembered” at the chromatin level through the sustained accumulation of H3K27me3 on *FLC*. This leads to the silencing of *FLC* event after the cold subsides and therefore to the initiation of flowering. H3K27me3 was also linked to abiotic stress memory: the sustained loss of the repressive mark on stress-inducible genes has been shown to be involved in the memory of heat and drought as it leads to the higher induction of those genes upon a second stress, similarly to what was observed here (Sani et al., 2013; Yamaguchi et al., 2021). In particular, our model is consistent with the one presented by Yamaguchi et al. (2021) for heat stress memory. Indeed, the authors showed that ELF6, together with three other H3K27me3 demethylases (REF6, JMJ30 and JMJ32), demethylates heat-inducible genes such as *HSP22* and *HSP17.6C* during an initial heat episode. This demethylation is essential to the ++ trainable behaviour of those genes, as both the demethylation and the trainability were reduced in the *elf6-ref6-jmj30-jmj32* quadruple mutant (*qm*). It is therefore possible that cold stress memory is controlled by a similar mechanism. In particular, a small benefit from priming could still be observed in the *elf6* mutant, suggesting that ELF6 might act redundantly with other H3K27me3 demethylases. There is however a critical difference between the data from Yamaguchi et al. (2021) and the one presented here: the heat-induced removal of H3K27me3 was strongly inhibited in the *qm* mutant. On the contrary, our data showed that H3K27me3 levels were still reduced upon cold exposure on *COR15A* and *LTI30* in the *qm* mutant (Figure 28B), suggesting that none of these proteins are involved in the observed demethylation. Several hypotheses were discussed previously

concerning the mechanisms of cold-induced H3K27me3 removal, leading to the conclusion that methylated histones might be replaced by the HTR11 variant which cannot carry H3K27me3. It is therefore possible that the removal of H3K27me3 and the maintenance of the loss are performed by two separate systems. Upon cold exposure, H3K27me3 could be removed at numerous loci through histone replacement, a process allowing for a rapid and global response. Once the stress subsides, these atypical HTR11 could be progressively replaced by typical H3 that can be targeted by the PRC2 complex for H3K27me3 deposition. At this point, ELF6 and other Jumonji demethylases could counteract the action of PRC2, preventing or slowing down the deposition of H3K27me3 only at specific loci such as *LT130*. However, this model is highly speculative and should be confirmed by (i) examining H3K27me3 dynamics on *COR* genes in *elf6* or *qm* mutant plants and (ii) tracking the potential incorporation of the atypical HTR11 variant in the chromatin upon cold exposure.

4.4 H3K4ME3 AND H3K27ME3 PLAY DISTINCT ROLES IN THE CONTROL OF COR GENES TRANSCRIPTION

Over the course of this study, both H3K4me3 and H3K27me3 were identified as potential contributors to the transcriptional regulation of *COR* genes and both the gain of H3K4me3 and the loss of H3K27me3 were correlated with an increase in gene expression. While the two methylation marks might appear to be redundant in function, their distinct characteristics and dynamics suggest that they actually fulfil separate roles. The first evidence for this argument is that, even though several thousand genes underwent H3K4me3 or H3K27me3 differential methylation upon cold exposure, very few showed variations in the levels of both marks (Figure 16D and E). Their number was 10 times inferior to what would be expected by chance (representation factor of 0.1), confirming that H3K4me3 and H3K27me3 differential methylations occur on separate sets of genes. Furthermore, the GO analyses demonstrated that different biological functions were enriched for the H3K4me3 and H3K27me3 DM genes, supporting the hypothesis that the marks might be involved in the control of distinct parts of the cold response such as the immediate stress defences and the long-term adaptation to lower temperatures (Figure 17 and Figure 18 and section 4.2.3). This point was further corroborated by the examination of the correlation between expression and methylation changes, which confirmed that, while both marks correlate with expression changes (positively for H3K4me3 and negatively for HK27me3), this was stronger for H3K4me3 (Figure 22C and D). The overlaps between DE and DM genes were also greater for the activating mark than for its repressive counterpart (Figure 23). These observations imply that H3K4me3 and H3K27me3 differential methylations might not be two converging mechanisms leading to the activation of the stress response but that they might instead have different functions in the adjustment to adverse environmental conditions.

Additionally, both types of differential methylation presented distinct dynamics: the H3K4me3 methylation changes appeared transient, as the sets of affected genes differed greatly between the 3 h and the 3 d time points (Figure 16B). On the contrary, most of the H3K27me3 variations induced early in the cold exposure persisted and were still detectable after three days (Figure 16C). This was not unexpected, as it is already known from investigations in HeLa cells that H3K4me3 has a rapid turnover and is a highly dynamic mark, while H3K27me3 is more stable (Zheng et al., 2014). Furthermore, in the same cells, the re-establishment of

H3K27me3 on fresh histones after DNA replication is completed later than the one of H3K4me3, confirming the slower dynamics of the repressive mark (Alabert et al., 2015; Reverón-Gómez et al., 2018). This characteristic seems conserved in plants, as it was demonstrated that genes which are differentially expressed during flower morphogenesis first undergo adjustments of their H3K4me3 levels and only subsequently of H3K27me3 (Engelhorn et al., 2017). Similar observations were made for genes undergoing expression changes during seasonal oscillations, confirming that H3K4me3 has faster dynamics than H3K27me3 also in *Arabidopsis thaliana* (Nishio et al., 2020). Mathematical modelling proved that marks with slow dynamics are more robust against rapidly fluctuating environmental conditions, thereby providing the plant with a sort of noise filter and a short-term transcriptional memory (Berry et al., 2017). Indeed, the signal triggering the deposition or removal of a mark has to persist until a new equilibrium of its level is reached. The slower the dynamics, the longer the signal should last in order to affect the levels of the mark, making this particular chromatin feature immune to short-lived environmental perturbations. The different dynamics of H3K4me3 and H3K27me3 could therefore confer them different responsiveness to changes in environmental signals. The *in vivo* examination of their levels during seasonal and diel cycles confirmed this idea, as H3K4me3 shows diel variations and short and long-term seasonal changes while H3K27me3 only displays long-term seasonal changes, suggesting that H3K27me3 is more robust to environmental variations than H3K4me3 (Nishio et al., 2020).

Based on those observations, the following model emerges, where H3K4me3 directly contributes to the immediate transcriptional response to temperature changes while H3K27me3 modulates the long-term responsiveness of cold-regulated genes and acts as a memory component. As it is required for transcriptional regulation, H3K4me3 needs to be quickly deposited on *COR* genes upon cold exposure if it was not already present in naïve conditions, through bivalency for instance (Yong Ding, Ndamukong, et al., 2012). This high responsiveness to temperature variations is facilitated by the rapid turn-over of H3K4me3. The direct implication of this mark in transcription explains the strong correlation of H3K4me3 differential methylation with differential gene expression, the enrichment of terms related to the immediate defence against cold among the H3K4me3 DM genes and the short persistence of H3K4me3 changes between the two time points investigated here. On the other hand, while being consistently described in the literature as a silencing mark, H3K27me3 per se is not an obstacle to gene expression. Indeed, not all H3K27me3-carrying *COR* genes lost the mark during their induction. Furthermore, in many cases such as flower morphogenesis, transcriptional activation precedes H3K27me3 removal (Engelhorn et al., 2017; Müller-Xing et al., 2022). As H3K27me3 does not need to be rapidly removed upon cold exposure, its dynamics can be slower, allowing the mark to be more robust against temperature fluctuations (Berry et al., 2017). Hence, H3K27me3 levels will only be modified in case of a prolonged stress, which might explain why differential H3K27me3 methylation targets genes which are required for the long-term stress response such as growth reprogramming (Figure 18). However, once those changes occurred, they are stable for the remainder of the cold episode (Figure 16C). They might also persist longer upon deacclimation, even once the transcriptional activity of the underlying genes returned to naïve levels, providing the plant with a form of stress memory. The loss of H3K27me3 was indeed maintained during the seven days of lag phase on *LT130* even though the gene was not expressed anymore (Figure 31). While the lower levels of H3K27me3 on *LT130* in primed plants did not impact its basal transcriptional level, they correlated with a faster induction upon re-exposure to cold, strengthening the idea

that H3K27me3 modulates gene expression rather than directly controlling it. On the contrary, the rapid turn-over of H3K4me3 might hinder its maintenance on genes once the cold subsides. Indeed, H3K4me3 returned to naïve levels on most genes during deacclimation, correlating with the reversal of their cold-induction (Figure 31A and C). The cold-triggered gain of H3K4me3 was only maintained on the sustainably expressed *VIN3*, possibly due to a positive feedback loop between transcription and H3K4me3 deposition (B. Li et al., 2007). The association between persisting H3K4me3 and sustained transcription of *VIN3* reinforces the idea that this mark directly contributes to gene expression.

4.5 ON THE IMPORTANCE OF CONSIDERING THE WHOLE CHROMATIN STATUS

This study used a comprehensive *in silico* approach to uncover chromatin features potentially involved in the transcriptional regulation of *COR* genes (Figure 5), which led to the identification of bivalency as a marker of early-responder to cold stress. Bivalent genes presented distinct chromatin accessibility, basal expression levels and cold-responsiveness compared to their monovalent counterparts (Figure 10), highlighting the importance of examining the chromatin status as a whole rather than focusing on a single mark or feature. The work presented here is a step in the right direction as it focused on the interplay between H3K4me3 and H3K27me3, but further investigations could benefit from considering other chromatin features. For instance, the State 2 identified as enriched among cold-regulated genes is also characterized by the presence of H2A.Z (Sequeira-Mendes et al., 2014). This histone variant is known to co-localize with H3K4me3 and H3K27me3 in embryonic stem cells too and has been proposed to participate in transcriptional poising both in mammals and plants (Coleman-Derr & Zilberman, 2012; Ku et al., 2012; B. Li et al., 2005). In *Arabidopsis thaliana* for instance, H2A.Z is evicted from the chromatin during the heat response, rendering it more accessible to the transcriptional machinery and leading to the expression of the underlying genes (Cortijo et al., 2017; S. V. Kumar & Wigge, 2010). Similarly, H2A.Z is evicted from up-regulated genes during drought stress and the pre-stress levels of H2A.Z positively correlate with the responsiveness to drought of the underlying genes, i.e. the higher the H2A.Z levels prior to the stress, the stronger the induction upon drought stress (Sura et al., 2017). As H2A.Z and bivalency have both been implicated in poising and they can be found at the same loci, they might act in concert. This hypothesis is substantiated by the recent identification of SRCAP as a mouse bivalency reader (Bryan et al., 2021). This histone chaperone incorporates H2A.Z into the chromatin, suggesting that bivalency acts as a placeholder for H2A.Z deposition (Wong et al., 2007). Interestingly, the potential plant bivalency reader DEK2 identified in this study has been shown to interact with H2A.Z, as well as its homologs DEK3 and DEK4 (Figure 12) (Brestovitsky et al., 2019, Rayapuram et al., personal communication, 2020). Additionally, DEK3 influences the distribution of H2A.Z, suggesting that the DEK proteins of *Arabidopsis* might hold a similar function to SRCAP and contribute to the co-localization of bivalency and H2A.Z. So far, H2A.Z has not been investigated in the context of cold, but its association with bivalency and its role in gene responsiveness to environmental stresses suggest that it might participate in the poising of bivalent cold-responsive genes. Examining the interplay between bivalency and H2A.Z might therefore shed light on the mechanisms allowing the quick activation of bivalent genes upon cold exposure.

While the chromatin topology established by Sequeira-Mendes et al. (2014) proved itself to be a precious source of data as it led to the identification of H3K4me3-H3K27me3 bivalency as a

regulator of cold-responsive genes, it also restricted the identification of candidates to the chromatin features used to build up the classification. This implies that other histone PTMs might play a key role in the transcriptional regulation of *COR* genes but were not uncovered in this *in silico* study due to the limitations set by the topology used. The *in silico* analyses performed here demonstrated that many chromatin modifiers are regulated by cold, whether at the transcriptional or post-transcriptional level (Figure 26 and Suppl. Figure 11) (Vyse et al., 2020). Many categories of regulators were represented: members of the Trithorax and Polycomb group, Jumonji demethylases but also writers and erasers of other histone PTMS, histone variants, actors of the DNA methylation pathway and chromatin remodellers, suggesting that numerous chromatin features could potentially contribute to the regulation of *COR* genes. For instance, histone acetylation does not appear in the chromatin states from Sequeira et al. (2014) but this modification is known to be affected by cold exposure (Yong Hu et al., 2011; Lim et al., 2020; Pavangadkar et al., 2010). Investigating histone acetylation might be especially crucial in the light of the recent report from Zhao et al. (2021) which revealed the existence of a new form of bivalency: H3K27me3-H3K18ac. This chromatin signature is found on camalexin biosynthetic genes and ensures their timely induction during a pathogen infection. Not only does this new bivalency highlight the potential of histone acetylation as regulator of transcription, it also demonstrates that activating marks other than H3K4me3 could counterbalance the silencing effects of H3K27me3. As sequencing costs decrease, more and more ChIP-seq datasets for various histone PTMs and variants are released and should be capitalized on to identify other chromatin features decorating *COR* genes which could therefore be involved in their transcriptional regulation.

4.6 CONCLUSION AND PERSPECTIVES

The present study used an *in silico* approach to identify chromatin features involved in the transcriptional regulation of cold-inducible genes and revealed the central role of the antagonistic histone PTMs H3K4me3 and H3K27me3. Those marks were found to co-localize on early-cold-inducible genes, forming a specific chromatin signature called bivalency. Bivalency might poise stress-responsive genes for a rapid induction upon cold exposure by maintaining them in an accessible chromatin state, allowing the binding of the transcriptional machinery. Furthermore, EBS, SHL and DEK2 were identified as putative plant bivalency readers using an *in silico* approach, indicating that bivalency could also regulate transcriptional activity in *trans*. Indeed, DEK2 was shown to be crucial to the proper induction of bivalent genes during a cold episode as its absence led to their over-induction. The fate of bivalency during a cold exposure was examined using individual H3K4me3 and H3K27me3 ChIP-seq, revealing that, contrary to the resolution of bivalency into monovalent domains observed in differentiating embryonic stem cells, most of the bivalent domains remained as such.

Cold stress triggered a dynamic redistribution of H3K4me3 and H3K37me3 as several thousands of genes underwent differential methylation for one mark and/or the other. These variations were not equally distributed, as the majority of H3K4me3 DM genes showed an accumulation of the mark, while around 50% of H3K27me3 was lost upon cold exposure. Differential methylation correlated with changes in gene expression: H3K4me3 gain and H3K27me3 loss were associated with transcriptional activation. However, both marks appeared as fulfilling different functions: H3K4me3 differential methylation primarily targeted genes involved in the immediate response and defence toward cold stress while H3K27me3

DM genes were related to long-term adaptation. Interestingly, not all DM genes were differentially expressed, suggesting that the chromatin status might be also be adjusted in preparation of deacclimation and stress recovery. The examination of H3K4me3 methyltransferase and H3K27me3 demethylase mutants did not yet lead to the identification of the actors involved in the changes of the chromatin status. However, transcriptomic analyses suggested that the loss of H3K27me3 might be mediated by the incorporation of the atypical H3 variant HTR11.

The potential persistence of cold-induced changes in histone methylation upon return to ambient temperature was examined by performing ChIP-qPCR seven days after the cold episode ended. The changes were reversed at a different pace depending on the gene considered and some were still maintained after a full week at 20°C. The persistence of cold-induced variations was associated with transcriptional memory, the nature of which differed depending on the mark. The persistence of higher levels of H3K4me3 on *VIN3* correlated with a sustained induction while the lower levels of H3K27me3 on *LT130* led to a faster re-induction of the gene during a second cold episode, again underlining the distinct roles played by both marks on the transcriptional activity of their targets.

Finally, the existence of cold stress memory in *Arabidopsis thaliana* was confirmed, as plants that experienced a priming stress showed an improved freezing tolerance upon re-exposure to cold compared to non-primed plants. A screening of chromatin modifier mutants revealed the essential role of the H3K27me3 demethylase ELF6 in cold stress memory, as almost no priming benefit was observed in the *elf6* mutants. Taken together with the transcriptional memory displayed by *LT130*, this suggests that cold could be memorized by plants through H3K27me3: upon cold exposure, H3K27me3 is removed from specific genes and ELF6 prevents its re-deposition on specific genes upon return to ambient temperature. The maintenance of lower levels of the repressive mark allows a faster re-induction of those genes should the stress re-occur, thereby leading to an improved freezing tolerance.

Based on all these observations, the following model emerged to describe the role of the chromatin status in the regulation of the transcriptional activity of COR genes (Figure 32). Prior to the cold exposure, cold-inducible genes are repressed but poised for induction through bivalency. The induction of the genes is associated with a gain of the active mark H3K4me3 and/or a loss of the repressive mark H3K27me3 but it remains unclear whether these changes of the chromatin status are necessary for the transcriptional activation. The gain of H3K4me3 might be mediated by ATX methyltransferases while the loss of H3K27me3 might stem from active demethylation by the Jumonji demethylase or by the replacement of methylated H3 with the atypical HTR11 variant. The bivalency reader DEK2 ensures that the bivalent genes are not over-induced. After the cold stress subsides, the changes to the chromatin status are reversed at a different pace depending on the gene considered. Genes whose chromatin status fully reverses to the naïve one do not present transcriptional memory. On the other hand, a maintenance of higher H3K4me3 levels might cause a sustained induction while the persistence of lower levels of H3K27me3 might allow a faster re-induction of the gene during a subsequent cold episode. ELF6 might prevent the re-deposition of H3K27me3 on those genes, thereby participating to the improved freezing tolerance of primed plants.

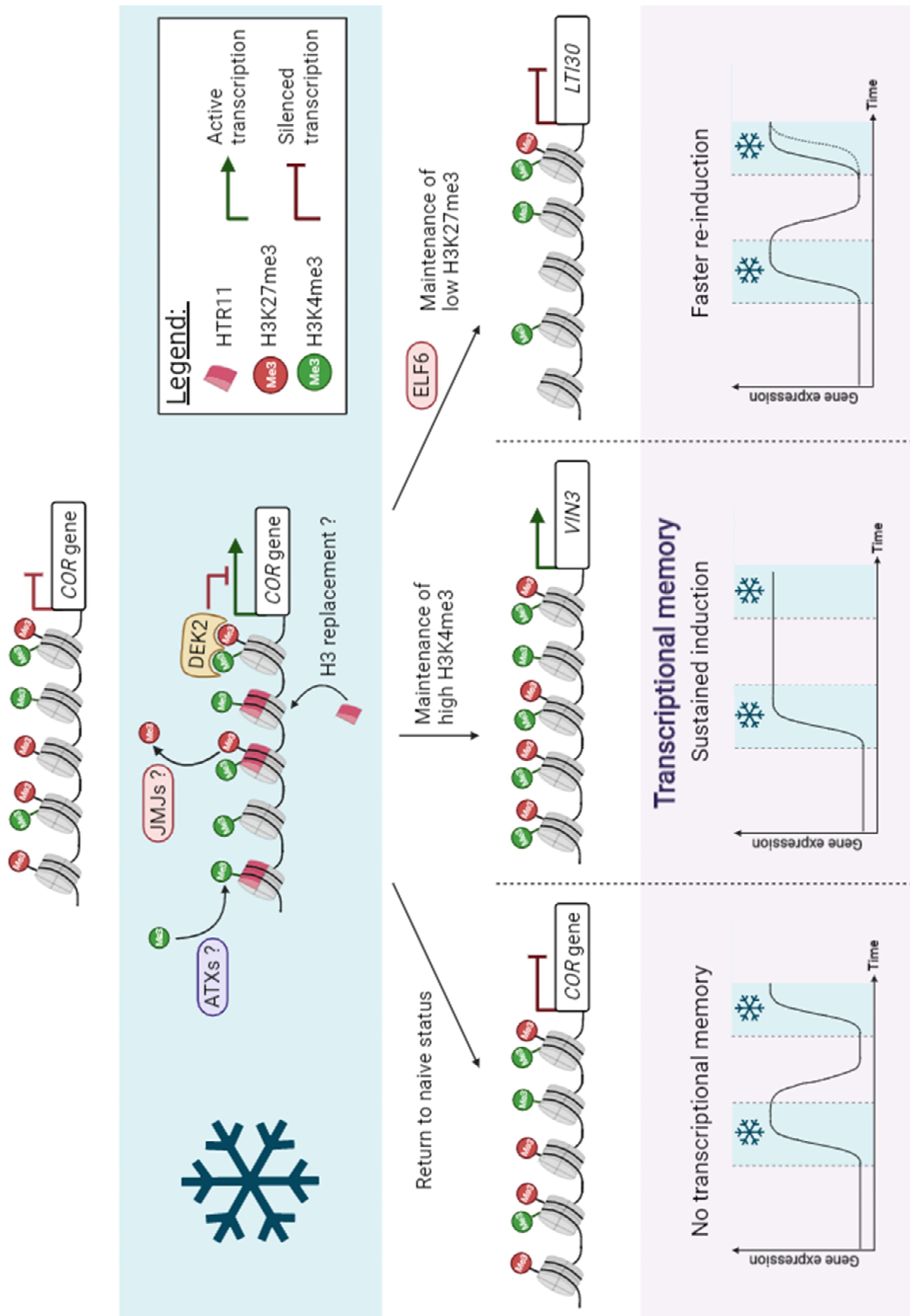


Figure 32: Influence of the chromatin methylation status on the transcriptional activity of COR genes. In naïve conditions, many COR genes are bivalent: they carry both H3K4me3 and H3K27me3. They are silenced but maintained in an accessible poised state. Upon cold exposure, the genes are induced. This transcriptional activation correlates with a gain of H3K4me3, potentially mediated by the

ATXs methyltransferases, and a loss of H3K27me3, mediated either by the Jumonji demethylases or by replacement of the canonical H3 with the atypical variant HTR11. DEK2 limits the induction range of the genes by reading bivalency. After the cold subsides, the chromatin might be returned to its pre-cold status, in which case no transcriptional memory can be observed. In specific cases, cold-induced changes can be maintained: the maintenance of higher levels of H3K4me3 are associated with a sustained induction while the maintenance of lower levels of H3K27me3 by ELF6 leads to a faster re-induction upon a subsequent cold stress.

This study provides a comprehensive overview of the dynamics of H3K4me3 and H3K27me3 prior, during and after a cold stress episode and of their potential role in the transcriptional regulation of *COR* genes. In particular, it demonstrated that both marks co-occur on numerous early cold-inducible genes, reminiscent of the bivalency decorating genes involved in cell differentiation in embryonic stem cells. However, it is still unclear whether this co-occurrence stems from true bivalency, i.e. nucleosomes carrying both methylation marks at once, or rather from bistability, i.e. the rapid switching from an active to a silenced state. This question should be addressed by sequential ChIP or single-cell approaches in future work. Furthermore, while both marks undergo differential methylation upon cold exposure that correlates with changes in expression, it is still unclear if and how differential methylation contribute to the transcriptional activation of the underlying genes. To address this particular point, it would be necessary to identify the actors involved in cold-triggered differential methylation. Unfortunately, so far none of the tested candidates seemed to be implicated in this process. Several avenues should be examined in the future, such as higher order mutants of the ATX methyltransferases or the potential role of the atypical HTR11 variant. However, while the majority of studies examining the role of chromatin marks on gene expression were performed in mutant lines where the writer or the eraser of the mark of interest were knocked-out, this approach is not ideal. Indeed, these mutants usually present strong phenotypes and as the enzymes target several hundreds of loci, direct and indirect effects are difficult to differentiate. The advent of CRISPR technologies offers a unique possibility to edit the epigenome at specific locations and time points, allowing us to study the impact of chromatin modifications on the gene transcription in a locus-specific manner and in an otherwise wild-type organism (Nakamura et al., 2021). In particular, Fukushima et al. (2019) demonstrated the possibility of using CRISPR to trigger the deposition of H3K7me3 at genes of interest *in vivo* in *Oryzias latipes* embryos. While reports of CRISPR epigenome editing in plants are still scarce, this method was already used by the Jacobsen lab (Papikian et al., 2019) to induce DNA methylation in *Arabidopsis thaliana*, demonstrating that this strategy could also be used in plants. This method therefore emerges as a powerful tool that could allow us to continue uncovering the interactions between chromatin status and transcriptional regulation during the cold stress response.

5 REFERENCES

- Achard, P., Gong, F., Cheminant, S., Alioua, M., Hedden, P., & Genschika, P. (2008). The cold-inducible CBF1 factor-dependent signaling pathway modulates the accumulation of the growth-repressing DELLA proteins via its effect on gibberellin metabolism. *Plant Cell*, *20*(8), 2117–2129. <https://doi.org/10.1105/tpc.108.058941>
- Agarwal, M., Hao, Y., Kapoor, A., Dong, C. H., Fujii, H., Zheng, X., & Zhu, J. K. (2006). A R2R3 type MYB transcription factor is involved in the cold regulation of CBF genes and in acquired freezing tolerance. *Journal of Biological Chemistry*, *281*(49), 37636–37645. <https://doi.org/10.1074/jbc.M605895200>
- Agrawal, A. A., & Karban, R. (1999). Why Induced Defenses May Be Favored Over Constitutive Strategies in Plants. In *The Ecology and Evolution of Inducible Defenses* (pp. 45–61). <https://doi.org/10.2307/j.ctv1ddd1cn.8>
- Alabert, C., Barth, T. K., Reverón-Gómez, N., Sidoli, S., Schmidt, A., Jensen, O., Imhof, A., & Groth, A. (2015). Two distinct modes for propagation of histone PTMs across the cell cycle. *Genes and Development*, *29*(6), 585–590. <https://doi.org/10.1101/gad.256354.114>
- Alexa, A., & Rahnenfuhrer, J. (2021). *topGO: Enrichment Analysis for Gene Ontology*.
- Alexandre, C., Möller-Steinbach, Y., Schönrock, N., Gruissem, W., & Hennig, L. (2009). Arabidopsis MSI1 Is Required for Negative Regulation of the Response to Drought Stress. *Molecular Plant*, *2*(4), 675–687. <https://doi.org/10.1093/mp/ssp012>
- Allen, D. J., & Ort, D. R. (2001). *Impacts of chilling temperatures on photosynthesis in warm-climate plants*. *6*(1), 36–42.
- Angel, A., Song, J., Dean, C., & Howard, M. (2011). A Polycomb-based switch underlying quantitative epigenetic memory. *Nature*, *476*(7358), 105–109. <https://doi.org/10.1038/nature10241>
- Angel, A., Song, J., Yang, H., Questa, J. I., Dean, C., & Howard, M. (2015). Vernalizing cold is registered digitally at FLC. *Proceedings of the National Academy of Sciences of the United States of America*, *112*(13), 4146–4151. <https://doi.org/10.1073/pnas.1503100112>
- Antoniou-Kourounioti, R. L., Hepworth, J., Heckmann, A., Duncan, S., Qüesta, J., Rosa, S., Säll, T., Holm, S., Dean, C., & Howard, M. (2018). Temperature Sensing Is Distributed throughout the Regulatory Network that Controls FLC Epigenetic Silencing in Vernalization. *Cell Systems*, *7*(6), 643–655.e9. <https://doi.org/10.1016/j.cels.2018.10.011>
- Ascenzi, R., & Gantt, J. S. (1997). A drought-stress-inducible histone gene in *Arabidopsis thaliana* is a member of a distinct class of plant linker histone variants. *Plant Molecular Biology*, *34*(4), 629–641. <https://doi.org/10.1023/A:1005886011722>
- Asensi-Fabado, M. A., Amtmann, A., & Perrella, G. (2017). Plant responses to abiotic stress: The chromatin context of transcriptional regulation. In *Biochimica et Biophysica Acta - Gene Regulatory Mechanisms* (Vol. 1860, Issue 1, pp. 106–122). Elsevier B.V. <https://doi.org/10.1016/j.bbagr.2016.07.015>
- Baerenfaller, K., Shu, H., Hirsch-Hoffmann, M., Fütterer, J., Opitz, L., Rehrauer, H., Hennig, L., & Gruissem, W. (2016). Diurnal changes in the histone H3 signature H3K9ac|H3K27ac|H3S28p are associated with diurnal gene expression in *Arabidopsis*. *Plant Cell and Environment*, *39*(11), 2557–2569. <https://doi.org/10.1111/pce.12811>
- Banerjee, A., Wani, S. H., & Roychoudhury, A. (2017). Epigenetic Control of Plant Cold Responses. *Frontiers in Plant Science*, *8*(September), 1–5. <https://doi.org/10.3389/fpls.2017.01643>
- Bastow, R., Mylne, J. S., Lister, C., Lippman, Z., Martienssen, R. A., & Dean, C. (2004). Vernalization requires epigenetic silencing of FLC by histone methylation. *Nature*, *427*(6970), 164–167. <https://doi.org/10.1038/nature02269>
- Bednar, J., Horowitz, R. A., Grigoryev, S. A., Carruthers, L. M., Hansen, J. C., Koster, A. J., & Woodcock, C. L. (1998). Nucleosomes, linker DNA, and linker histone form a unique structural motif that directs the higher-order folding and compaction of chromatin. *Proceedings of the National*

- Academy of Sciences of the United States of America, 95(24), 14173–14178. <https://doi.org/10.1073/pnas.95.24.14173>
- Bennet, L., Melchers, B., & Proppe, B. (2020). *Curta: A General-purpose High-Performance Computer at ZEDAT, Freie Universität Berlin*. <https://doi.org/10.17169/refubium-26754>
- Bernatavichute, Y. V., Zhang, X., Cokus, S., Pellegrini, M., & Jacobsen, S. E. (2008). Genome-wide association of histone H3 lysine nine methylation with CHG DNA methylation in *Arabidopsis thaliana*. *PLoS ONE*, 3(9). <https://doi.org/10.1371/journal.pone.0003156>
- Bernstein, B. E., Mikkelsen, T. S., Xie, X., Kamal, M., Huebert, D. J., Cuff, J., Fry, B., Meissner, A., Wernig, M., Plath, K., Jaenisch, R., Wagschal, A., Feil, R., Schreiber, S. L., & Lander, E. S. (2006). A Bivalent Chromatin Structure Marks Key Developmental Genes in Embryonic Stem Cells. *Cell*, 125(2), 315–326. <https://doi.org/10.1016/j.cell.2006.02.041>
- Berry, S., Dean, C., & Howard, M. (2017). Slow Chromatin Dynamics Allow Polycomb Target Genes to Filter Fluctuations in Transcription Factor Activity. *Cell Systems*, 4(4), 445–457.e8. <https://doi.org/10.1016/j.cels.2017.02.013>
- Bieniawska, Z., Espinoza, C., Schlereth, A., Sulpice, R., Hinch, D. K., & Hannah, M. A. (2008). Disruption of the *Arabidopsis* circadian clock is responsible for extensive variation in the cold-responsive transcriptome. *Plant Physiology*, 147(1), 263–279. <https://doi.org/10.1104/pp.108.118059>
- Blakey, C. A., & Litt, M. D. (2015). Histone modifications—models and mechanisms. *Epigenetic Gene Expression and Regulation*, 21–42. <https://doi.org/10.1016/B978-0-12-799958-6.00002-0>
- Bond, D. M., Dennis, E. S., & Finnegan, E. J. (2011). The low temperature response pathways for cold acclimation and vernalization are independent. *Plant, Cell and Environment*, 34(10), 1737–1748. <https://doi.org/10.1111/j.1365-3040.2011.02370.x>
- Bond, D. M., Dennis, E. S., Pogson, B. J., & Finnegan, E. J. (2009). Histone acetylation, vernalization insensitive 3, flowering locus C, and the vernalization response. *Molecular Plant*, 2(4), 724–737. <https://doi.org/10.1093/mp/ssp021>
- Brehove, M., Wang, T., North, J., Luo, Y., Dreher, S. J., Shimko, J. C., Ottesen, J. J., Luger, K., & Poirier, M. G. (2015). Histone core phosphorylation regulates DNA accessibility. *The Journal of Biological Chemistry*, 290(37), 22612–22621. <https://doi.org/10.1074/jbc.M115.661363>
- Brestovitsky, A., Ezer, D., Waidmann, S., Maslen, S. L., Balcerowicz, M., Cortijo, S., Charoensawan, V., Martinho, C., Rhodes, D., Jonak, C., & Wigge, P. A. (2019). DEK influences the trade-off between growth and arrest via H2A.Z-nucleosomes in *Arabidopsis*. *BioRxiv*. <https://doi.org/10.1101/829226>
- Bryan, E., Warburton, M., Webb, K. M., McLaughlin, K. A., Spanos, C., Ambrosi, C., Major, V., Baubec, T., Rappsilber, J., & Voigt, P. (2021). Nucleosomal Asymmetry Shapes Histone Mark Binding and Promotes Poising at Bivalent Domains. *BioRxiv*, 2021.02.08.430127. <https://doi.org/10.1101/2021.02.08.430127>
- Brzezinka, K., Altmann, S., Czesnick, H., Nicolas, P., Gorka, M., Benke, E., Kabelitz, T., Jähne, F., Graf, A., Kappel, C., & Bäurle, I. (2016). *Arabidopsis* FORGETTER1 mediates stress-induced chromatin memory through nucleosome remodeling. *ELife*, 5(September), 1–23. <https://doi.org/10.7554/eLife.17061.001>
- Buszewicz, D., Archacki, R., Palusiński, A., Kotliński, M., Fogtman, A., Iwanicka-Nowicka, R., Sosnowska, K., Kuciński, J., Pupel, P., Ołędzki, J., Dadlez, M., Misicka, A., Jerzmanowski, A., & Koblowska, M. K. (2016). HD2C histone deacetylase and a SWI/SNF chromatin remodelling complex interact and both are involved in mediating the heat stress response in *Arabidopsis*. *Plant Cell and Environment*, 39(10), 2108–2122. <https://doi.org/10.1111/pce.12756>
- Byun, Y. J., Koo, M. Y., Joo, H. J., Ha-Lee, Y. M., & Lee, D. H. (2014). Comparative analysis of gene expression under cold acclimation, deacclimation and reacclimation in *Arabidopsis*. *Physiologia Plantarum*, 152(2), 256–274. <https://doi.org/10.1111/ppl.12163>
- Calixto, C. P. G., Guo, W., James, A. B., Tzioutziou, N. A., Entizne, J. C., Panter, P. E., Knight, H., Nimmo, H., Zhang, R., & Brown, J. W. S. (2018). Rapid and dynamic alternative splicing impacts the *Arabidopsis* cold response transcriptome. *The Plant Cell*, 30(July), tpc.00177.2018.

<https://doi.org/10.1105/tpc.18.00177>

- Cao, R., Tsukada, Y. I., & Zhang, Y. (2005). Role of Bmi-1 and Ring1A in H2A ubiquitylation and hox gene silencing. *Molecular Cell*, 20(6), 845–854. <https://doi.org/10.1016/j.molcel.2005.12.002>
- Carlson, M. (2019). *org.At.tair.db: Genome wide annotation for Arabidopsis*.
- Chan, Z., Wang, Y., Cao, M., Gong, Y., Mu, Z., Wang, H., Hu, Y., Deng, X., He, X. J., & Zhu, J. K. (2016). RDM4 modulates cold stress resistance in Arabidopsis partially through the CBF-mediated pathway. *New Phytologist*, 209(4), 1527–1539. <https://doi.org/10.1111/nph.13727>
- Chanvivatana, Y., Bishopp, A., Schubert, D., Stock, C., Moon, Y. H., Sung, Z. R., & Goodrich, J. (2004). Interaction of Polycomb-group proteins controlling flowering in Arabidopsis. *Development*, 131(21), 5263–5276. <https://doi.org/10.1242/dev.01400>
- Charron, J. B. F., He, H., Elling, A. A., & Denga, X. W. (2009). Dynamic landscapes of four histone modifications during deetiolation in arabidopsis. *Plant Cell*, 21(12), 3732–3748. <https://doi.org/10.1105/tpc.109.066845>
- Chen, L. Q., Luo, J. H., Cui, Z. H., Xue, M., Wang, L., Zhang, X. Y., Pawlowski, W. P., & He, Y. (2017). ATX3, ATX4, and ATX5 encode putative H3K4 methyltransferases and are critical for plant development. *Plant Physiology*, 174(3), 1795–1806. <https://doi.org/10.1104/pp.16.01944>
- Cheng, C. Y., Krishnakumar, V., Chan, A. P., Thibaud-Nissen, F., Schobel, S., & Town, C. D. (2017). Araport11: a complete reannotation of the Arabidopsis thaliana reference genome. *Plant Journal*, 89(4), 789–804. <https://doi.org/10.1111/tpj.13415>
- Cheng, H., Sun, M., & Guo, D. (2020). The identification of A ROS responsive motif that is regulated by snoRNP in Arabidopsis. *BioRxiv*, 28–31. <https://doi.org/10.1101/2020.06.08.141143>
- Cheng, K., Xu, Y., Yang, C., Ouellette, L., Niu, L., Zhou, X., Chu, L., Zhuang, F., Liu, J., Wu, H., Charron, J., & Luo, M. (2020). *Histone tales : lysine methylation , a protagonist in Arabidopsis development*. 71(3), 793–807. <https://doi.org/10.1093/jxb/erz435>
- Chinnusamy, V., Ohta, M., Kanrar, S., Lee, B. ha, Hong, X., Agarwal, M., & Zhu, J. K. (2003). ICE1: A regulator of cold-induced transcriptome and freezing tolerance in arabidopsis. *Genes and Development*, 17(8), 1043–1054. <https://doi.org/10.1101/gad.1077503>
- Cho, J. N., Ryu, J. Y., Jeong, Y. M., Park, J., Song, J. J., Amasino, R. M., Noh, B., & Noh, Y. S. (2012). Control of Seed Germination by Light-Induced Histone Arginine Demethylation Activity. *Developmental Cell*, 22(4), 736–748. <https://doi.org/10.1016/j.devcel.2012.01.024>
- Chodavarapu, R. K., Feng, S., Bernatavichute, Y. V., Chen, P. Y., Stroud, H., Yu, Y., Hetzel, J. A., Kuo, F., Kim, J., Cokus, S. J., Casero, D., Bernal, M., Huijser, P., Clark, A. T., Krämer, U., Merchant, S. S., Zhang, X., Jacobsen, S. E., & Pellegrini, M. (2010). Relationship between nucleosome positioning and DNA methylation. *Nature*, 466(7304), 388–392. <https://doi.org/10.1038/nature09147>
- Chouard, P. (1960). Vernalization and its Relations to Dormancy. *Annual Review of Plant Physiology*, 11(1), 191–238. <https://doi.org/10.1146/annurev.pp.11.060160.001203>
- Chu, M., Li, J., Zhang, J., Shen, S., Li, C., Gao, Y., & Zhang, S. (2018). AtCaM4 interacts with a Sec14-like protein, PATL1, to regulate freezing tolerance in Arabidopsis in a CBF-independent manner. *Journal of Experimental Botany*, 69(21), 5241–5253. <https://doi.org/10.1093/jxb/ery278>
- Chung, B. Y. W., Balcerowicz, M., Di Antonio, M., Jaeger, K. E., Geng, F., Franaszek, K., Marriott, P., Brierley, I., Firth, A. E., & Wigge, P. A. (2020). An RNA thermoswitch regulates daytime growth in Arabidopsis. *Nature Plants*, 6(5), 522–532. <https://doi.org/10.1038/s41477-020-0633-3>
- Cipollini, D., Purrington, C. B., & Bergelson, J. (2003). Costs of induced responses in plants. *Basic and Applied Ecology*, 4(1), 79–89. <https://doi.org/10.1078/1439-1791-00134>
- Cipollini, D., Walters, D., & Voelckel, C. (2017). Costs of Resistance in Plants: From Theory to Evidence. In *Annual Plant Reviews online* (Vol. 47, pp. 263–307). <https://doi.org/10.1002/9781119312994.apr0512>
- Clapier, C. R., & Cairns, B. R. (2009). The biology of chromatin remodeling complexes. *Annual Review*

- of *Biochemistry*, 78, 273–304. <https://doi.org/10.1146/annurev.biochem.77.062706.153223>
- Clapier, C. R., Iwasa, J., Cairns, B. R., & Peterson, C. L. (2017). Mechanisms of action and regulation of ATP-dependent chromatin-remodelling complexes. *Nature Reviews Molecular Cell Biology*, 18(7), 407–422. <https://doi.org/10.1038/nrm.2017.26>
- Coleman-Derr, D., & Zilberman, D. (2012). Deposition of Histone Variant H2A.Z within Gene Bodies Regulates Responsive Genes. *PLoS Genetics*, 8(10). <https://doi.org/10.1371/journal.pgen.1002988>
- Cortijo, S., Charoensawan, V., Brestovitsky, A., Buning, R., Ravarani, C., Rhodes, D., van Noort, J., Jaeger, K. E., & Wigge, P. A. (2017). Transcriptional Regulation of the Ambient Temperature Response by H2A.Z Nucleosomes and HSF1 Transcription Factors in Arabidopsis. *Molecular Plant*, 10(10), 1258–1273. <https://doi.org/10.1016/j.molp.2017.08.014>
- Côté, J., & Richard, S. (2005). Tudor domains bind symmetrical dimethylated arginines. *Journal of Biological Chemistry*, 280(31), 28476–28483. <https://doi.org/10.1074/jbc.M414328200>
- Crevillén, P., Yang, H., Cui, X., Greeff, C., Trick, M., Qiu, Q., Cao, X., & Dean, C. (2014). Epigenetic reprogramming that prevents transgenerational inheritance of the vernalized state. *Nature*, 515(7528), 587–590. <https://doi.org/10.1038/nature13722>
- Cvetkovska, M., Rampitsch, C., Bykova, N., & Xing, T. (2005). Genomic analysis of MAP kinase cascades in Arabidopsis defense responses. *Plant Molecular Biology Reporter*, 23(4), 331–343. <https://doi.org/10.1007/bf02788882>
- De Lucia, F., Crevillén, P., Jones, A. M. E., Greb, T., & Dean, C. (2008). A PHD-polycomb repressive complex 2 triggers the epigenetic silencing of FLC during vernalization. *Proceedings of the National Academy of Sciences of the United States of America*, 105(44), 16831–16836. <https://doi.org/10.1073/pnas.0808687105>
- Deal, R. B., Topp, C. N., McKinney, E. C., & Meagher, R. B. (2007). Repression of flowering in Arabidopsis requires activation of FLOWERING LOCUS C expression by the histone variant H2A.Z. *Plant Cell*, 19(1), 74–83. <https://doi.org/10.1105/tpc.106.048447>
- Derkacheva, M., & Hennig, L. (2014). Variations on a theme: Polycomb group proteins in plants. *Journal of Experimental Botany*, 65(10), 2769–2784. <https://doi.org/10.1093/jxb/ert410>
- Desvoyes, B., Sequeira-Mendes, J., Vergara, Z., Madeira, S., & Gutierrez, C. (2018). Sequential ChIP protocol for profiling bivalent epigenetic modifications (ReChIP). In *Plant Chromatin Dynamics* (pp. 83–97). Springer.
- Ding, Yanglin, Li, H., Zhang, X., Xie, Q., Gong, Z., & Yang, S. (2015). OST1 kinase modulates freezing tolerance by enhancing ICE1 stability in arabidopsis. *Developmental Cell*, 32(3), 278–289. <https://doi.org/10.1016/j.devcel.2014.12.023>
- Ding, Yanglin, Shi, Y., & Yang, S. (2019). Advances and challenges in uncovering cold tolerance regulatory mechanisms in plants. *New Phytologist*, 222(4), 1690–1704. <https://doi.org/10.1111/nph.15696>
- Ding, Yong, Avramova, Z., & Fromm, M. (2011). The Arabidopsis trithorax-like factor ATX1 functions in dehydration stress responses via ABA-dependent and ABA-independent pathways. *Plant Journal*, 66(5), 735–744. <https://doi.org/10.1111/j.1365-313X.2011.04534.x>
- Ding, Yong, Fromm, M., & Avramova, Z. (2012). Multiple exposures to drought “train” transcriptional responses in Arabidopsis. *Nat. Commun.*, 3, 740. <https://doi.org/10.1038/ncomms1732>
- Ding, Yong, Liu, N., Virilouvet, L., Riethoven, J.-J., Fromm, M., & Avramova, Z. (2013). Four distinct types of dehydration stress memory genes in Arabidopsis thaliana. *BMC Plant Biology*, 13(1), 229. <https://doi.org/10.1186/1471-2229-13-229>
- Ding, Yong, Ndamukong, I., Xu, Z., Lapko, H., Fromm, M., & Avramova, Z. (2012). ATX1-Generated H3K4me3 Is Required for Efficient Elongation of Transcription, Not Initiation, at ATX1-Regulated Genes. *PLoS Genetics*, 8(12). <https://doi.org/10.1371/journal.pgen.1003111>
- Dobin, A., Davis, C. A., Schlesinger, F., Drenkow, J., Zaleski, C., Jha, S., Batut, P., Chaisson, M., &

- Gingeras, T. R. (2013). STAR: Ultrafast universal RNA-seq aligner. *Bioinformatics*, 29(1), 15–21. <https://doi.org/10.1093/bioinformatics/bts635>
- Doherty, C. J., Van Buskirk, H. A., Myers, S. J., & Thomashow, M. F. (2009). Roles for Arabidopsis CAMTA transcription factors in cold-regulated gene expression and freezing tolerance. *Plant Cell*, 21(3), 972–984. <https://doi.org/10.1105/tpc.108.063958>
- Dong, C. H., Agarwal, M., Zhang, Y., Xie, Q., & Zhu, J. K. (2006). The negative regulator of plant cold responses, HOS1, is a RING E3 ligase that mediates the ubiquitination and degradation of ICE1. *Proceedings of the National Academy of Sciences of the United States of America*, 103(21), 8281–8286. <https://doi.org/10.1073/pnas.0602874103>
- Dong, C., Ma, Y., Zheng, D., Wisniewski, M., & Cheng, Z.-M. (2018). Meta-Analysis of the Effect of Overexpression of Dehydration-Responsive Element Binding Family Genes on Temperature Stress Tolerance and Related Responses. *Frontiers in Plant Science*, 9(May), 1–15. <https://doi.org/10.3389/fpls.2018.00713>
- Dong, Y., Uslu, V. V., Berr, A., Singh, G., Papdi, C., Steffens, V. A., Heitz, T., & Ryabova, L. (2021). TOR represses stress responses through global regulation of H3K27 trimethylation in plants. *BioRxiv*, 2(June). <https://doi.org/10.1101/2021.03.28.437410>
- Dormann, H. L., Boo, S. T., Allis, C. D., Funabiki, H., & Fischle, W. (2006). Dynamic regulation of effector protein binding to histone modifications: The biology of HP1 switching. *Cell Cycle*, 5(24), 2842–2851. <https://doi.org/10.4161/cc.5.24.3540>
- Douma, J. C., Vermeulen, P. J., Poelman, E. H., Dicke, M., & Anten, N. P. R. (2017). When does it pay off to prime for defense? A modeling analysis. *New Phytologist*. <https://doi.org/10.1111/nph.14771>
- Du, J., Zhong, X., Bernatavichute, Y. V., Stroud, H., Feng, S., Caro, E., Vashisht, A. A., Terragni, J., Chin, H. G., Tu, A., Hetzel, J., Wohlschlegel, J. A., Pradhan, S., Patel, D. J., & Jacobsen, S. E. (2012). Dual binding of chromomethylase domains to H3K9me2-containing nucleosomes directs DNA methylation in plants. *Cell*, 151(1), 167–180. <https://doi.org/10.1016/j.cell.2012.07.034>
- Durinck, S., Moreau, Y., Kasprzyk, A., Davis, S., De Moor, B., Brazma, A., & Huber, W. (2005). BioMart and Bioconductor: A powerful link between biological databases and microarray data analysis. *Bioinformatics*, 21(16), 3439–3440. <https://doi.org/10.1093/bioinformatics/bti525>
- Dutta, A., Choudhary, P., Caruana, J., & Raina, R. (2017). JMJ27, an Arabidopsis H3K9 histone demethylase, modulates defense against *Pseudomonas syringae* and flowering time. *Plant Journal*, 91(6), 1015–1028. <https://doi.org/10.1111/tbj.13623>
- Egan, B., Yuan, C. C., Craske, M. L., Labhart, P., Guler, G. D., Arnott, D., Maile, T. M., Busby, J., Henry, C., Kelly, T. K., Tindell, C. A., Jhunjunwala, S., Zhao, F., Hatton, C., Bryant, B. M., Classon, M., & Trojer, P. (2016). An alternative approach to ChIP-Seq normalization enables detection of genome-wide changes in histone H3 lysine 27 trimethylation upon EZH2 inhibition. *PLoS ONE*, 11(11), 1–20. <https://doi.org/10.1371/journal.pone.0166438>
- Engelhorn, J., Blanvillain, R., Kröner, C., Parrinello, H., Rohmer, M., Posé, D., Ott, F., Schmid, M., & Carles, C. (2017). Dynamics of H3K4me3 Chromatin Marks Prevails over H3K27me3 for Gene Regulation during Flower Morphogenesis in *Arabidopsis thaliana*. *Epigenomes*, 1(3), 8. <https://doi.org/10.3390/epigenomes1020008>
- Eremina, M., Unterholzner, S. J., Rathnayake, A. I., Castellanos, M., Khan, M., Kugler, K. G., May, S. T., Mayer, K. F. X., Rozhon, W., & Poppenberger, B. (2016). Brassinosteroids participate in the control of basal and acquired freezing tolerance of plants. *Proceedings of the National Academy of Sciences of the United States of America*, 114(6), E1038–E1089. <https://doi.org/10.1073/pnas.1700593114>
- Eriksson, S. K., Kutzer, M., Procek, J., Gröbner, G., & Harryson, P. (2011). Tunable membrane binding of the intrinsically disordered dehydrin Lti30, a cold-induced plant stress protein. *Plant Cell*, 23(6), 2391–2404. <https://doi.org/10.1105/tpc.111.085183>
- Escobar, T. M., Loyola, A., & Reinberg, D. (2021). Parental nucleosome segregation and the inheritance of cellular identity. *Nature Reviews Genetics*, 22(6), 379–392. <https://doi.org/10.1038/s41576-020-00312-w>

- Escobar, T. M., Oksuz, O., Saldaña-Meyer, R., Descostes, N., Bonasio, R., & Reinberg, D. (2019). Active and Repressed Chromatin Domains Exhibit Distinct Nucleosome Segregation during DNA Replication. *Cell*, *179*(4), 953–963.e11. <https://doi.org/10.1016/j.cell.2019.10.009>
- Ewels, P., Magnusson, M., Lundin, S., & Käller, M. (2016). MultiQC: Summarize analysis results for multiple tools and samples in a single report. *Bioinformatics*, *32*(19), 3047–3048. <https://doi.org/10.1093/bioinformatics/btw354>
- Fan, D., Dai, Y., Wang, X., Wang, Z., He, H., Yang, H., Cao, Y., Deng, X. W., & Ma, L. (2012). IBM1, a JmjC domain-containing histone demethylase, is involved in the regulation of RNA-directed DNA methylation through the epigenetic control of RDR2 and DCL3 expression in Arabidopsis. *Nucleic Acids Research*, *40*(18), 8905–8916. <https://doi.org/10.1093/nar/gks647>
- Fan, J. Y., Rangasamy, D., Luger, K., & Tremethick, D. J. (2004). H2A.Z alters the nucleosome surface to promote HP1 α -mediated chromatin fiber folding. *Molecular Cell*, *16*(4), 655–661. <https://doi.org/10.1016/j.molcel.2004.10.023>
- Felipe de Mendiburu, & Muhammad Yaseen. (2020). *agricolae: Statistical Procedures for Agricultural Research*.
- Feng, X. J., Li, J. R., Qi, S. L., Lin, Q. F., Jin, J. B., & Hua, X. J. (2016). Light affects salt stress-induced transcriptional memory of P5CS1 in Arabidopsis. *Proceedings of the National Academy of Sciences of the United States of America*, *113*(51), E8335–E8343. <https://doi.org/10.1073/pnas.1610670114>
- Finnegan, E. J., Bond, D. M., Buzas, D. M., Goodrich, J., Helliwell, C. A., Tamada, Y., Yun, J. Y., Amasino, R. M., & Dennis, E. S. (2011). Polycomb proteins regulate the quantitative induction of VERNALIZATION INSENSITIVE 3 in response to low temperatures. *Plant Journal*, *65*(3), 382–391. <https://doi.org/10.1111/j.1365-313X.2010.04428.x>
- Friedrich, T., Faivre, L., Bäurle, I., & Schubert, D. (2018). *Chromatin-based mechanisms of temperature memory in plants*. *March*, 1–9. <https://doi.org/10.1111/pce.13373>
- Fukushima, H. S., Takeda, H., & Nakamura, R. (2019). Targeted in vivo epigenome editing of H3K27me3. *Epigenetics and Chromatin*, *12*. <https://doi.org/10.1186/s13072-019-0263-z>
- Fursova, O. V., Pogorelko, G. V., & Tarasov, V. A. (2009). Identification of ICE2, a gene involved in cold acclimation which determines freezing tolerance in Arabidopsis thaliana. *Gene*, *429*(1–2), 98–103. <https://doi.org/10.1016/j.gene.2008.10.016>
- Gan, E.-S., Xu, Y., Wong, J.-Y., Goh, J. G., Sun, B., Wee, W.-Y., Huang, J., & Ito, T. (2014). Jumonji demethylases moderate precocious flowering at elevated temperature via regulation of FLC in Arabidopsis. *Nature Communications*, *5*, 5098. <https://doi.org/10.1038/ncomms6098>
- García-Alcalde, F., Okonechnikov, K., Carbonell, J., Cruz, L. M., Götz, S., Tarazona, S., Dopazo, J., Meyer, T. F., & Conesa, A. (2012). Qualimap: Evaluating next-generation sequencing alignment data. *Bioinformatics*, *28*(20), 2678–2679. <https://doi.org/10.1093/bioinformatics/bts503>
- García-Molina, A., Kleine, T., Schneider, K., Mühlhaus, T., Lehmann, M., & Leister, D. (2020). Translational Components Contribute to Acclimation Responses to High Light, Heat, and Cold in Arabidopsis. *IScience*, *23*(7), 101331. <https://doi.org/10.1016/j.isci.2020.101331>
- Gaspar, J. M. (2018). Improved peak-calling with MACS2. *BioRxiv*, 1–16. <https://doi.org/10.1101/496521>
- Gendler, K., Paulsen, T., & Napoli, C. (2008). ChromDB: The Chromatin Database. *Nucleic Acids Research*, *36*(suppl_1), D298–D302. <https://doi.org/10.1093/nar/gkm768>
- Gilmour, S. J., Fowler, S. G., & Thomashow, M. F. (2004). Arabidopsis Transcriptional Activators CBF1, CBF2 and CBF3 Have Matching Functional Activities. *Plant Molecular Biology*, *54*, 767–781.
- Gilmour, S. J., Hajela, R. K., & Thomashow, M. F. (1988). Cold Acclimation in Arabidopsis thaliana. *Plant Physiology*, *87*(3), 745–750. <https://doi.org/10.1104/pp.87.3.745>
- Gómez-Zambrano, Á., Crevillén, P., Franco-Zorrilla, J. M., López, J. A., Moreno-Romero, J., Roszak, P., Santos-González, J., Jurado, S., Vázquez, J., Köhler, C., Solano, R., Piñeiro, M., & Jarillo, J.

- A. (2018). Arabidopsis SWC4 Binds DNA and Recruits the SWR1 Complex to Modulate Histone H2A.Z Deposition at Key Regulatory Genes. *Molecular Plant*, 11(6), 815–832. <https://doi.org/10.1016/j.molp.2018.03.014>
- Gratkowska-Zmuda, D. M., Kubala, S., Sarnowska, E., Cwiek, P., Oksinska, P., Steciuk, J., Rolicka, A. T., Zaborowska, M., Bucior, E., Maassen, A., Franzen, R., Koncz, C., & Sarnowski, T. J. (2020). The SWI/SNF ATP-dependent chromatin remodeling complex in arabidopsis responds to environmental changes in temperature-dependent manner. *International Journal of Molecular Sciences*, 21(3), 1–19. <https://doi.org/10.3390/ijms21030762>
- Griffith, M., Lumb, C., Wiseman, S. B., Wisniewski, M., Johnson, R. W., & Marangoni, A. G. (2005). Antifreeze proteins modify the freezing process in planta. *Plant Physiology*, 138(1), 330–340. <https://doi.org/10.1104/pp.104.058628>
- Gu, X., Jiang, D., Yang, W., Jacob, Y., Michaels, S. D., & He, Y. (2011). Arabidopsis homologs of retinoblastoma-associated protein 46/48 associate with a histone deacetylase to act redundantly in chromatin silencing. *PLoS Genetics*, 7(11). <https://doi.org/10.1371/journal.pgen.1002366>
- Gupta, A., Marzinek, J. K., Jefferies, D., Bond, P. J., Harryson, P., & Wohland, T. (2019). The disordered plant dehydrin LTI30 protects the membrane during water-related stress by cross-linking lipids. *Journal of Biological Chemistry*, 294(16), 6468–6482. <https://doi.org/10.1074/jbc.RA118.007163>
- Guy, C. L., Niemi, K. J., & Brambl, R. (1985). Altered gene expression during cold acclimation of spinach. *Proceedings of the National Academy of Sciences of the United States of America*, 82(11), 3673–3677. <https://doi.org/10.1073/pnas.82.11.3673>
- Haltenhof, T., Kotte, A., De Bortoli, F., Schiefer, S., Meinke, S., Emmerichs, A. K., Petermann, K. K., Timmermann, B., Imhof, P., Franz, A., Loll, B., Wahl, M. C., Preußner, M., & Heyd, F. (2020). A Conserved Kinase-Based Body-Temperature Sensor Globally Controls Alternative Splicing and Gene Expression. *Molecular Cell*, 78(1), 57-69.e4. <https://doi.org/10.1016/j.molcel.2020.01.028>
- Hansen, K. H., Bracken, A. P., Pasini, D., Dietrich, N., Gehani, S. S., Monrad, A., Rappsilber, J., Lerdrup, M., & Helin, K. (2008). A model for transmission of the H3K27me3 epigenetic mark. *Nature Cell Biology*, 10(11), 1291–1300. <https://doi.org/10.1038/ncb1787>
- Hepworth, J., Antoniou-kourounioti, R. L., Bloomer, R. H., Selga, C., Cox, D., Harris, B. R. C., Irwin, J., Holm, S., Säll, T., Howard, M., & Dean, C. (2018). Absence of warmth permits epigenetic memory of winter in Arabidopsis. *Nature Communications*, 2018, 8–11. <https://doi.org/10.1038/s41467-018-03065-7>
- Hepworth, J., & Dean, C. (2015). Flowering locus C's lessons: Conserved chromatin switches underpinning developmental timing and adaptation. *Plant Physiology*, 168(4), 1237–1245. <https://doi.org/10.1104/pp.15.00496>
- Hilker, M., Schwachtje, J., Baier, M., Balazadeh, S., Bäurle, I., Geiselhardt, S., Hinch, D. K., Kunze, R., Mueller-Roeber, B., Rillig, M. C., Rolff, J., Romeis, T., Schmölling, T., Steppuhn, A., van Dongen, J., Whitcomb, S. J., Wurst, S., Zuther, E., & Kopka, J. (2015). Priming and memory of stress responses in organisms lacking a nervous system. *Biological Reviews*, 49. <https://doi.org/10.1111/brv.12215>
- Hinch, D. K., & Zuther, E. (2014). *Plant Cold Acclimation: Methods and Protocols* (Springer New York 2014 (ed.); Vol. 1). <https://doi.org/10.1007/978-1-4939-2687-9>
- Hong, L., Schroth, G. P., Matthews, H. R., Yau, P., & Bradbury, E. M. (1993). Studies of the DNA binding properties of histone H4 amino terminus. Thermal denaturation studies reveal that acetylation markedly reduces the binding constant of the H4 “tail” to DNA. *Journal of Biological Chemistry*, 268(1), 305–314. [https://doi.org/10.1016/s0021-9258\(18\)54150-8](https://doi.org/10.1016/s0021-9258(18)54150-8)
- Hu, Yanru, Jiang, L., Wang, F., & Yu, D. (2013). Jasmonate regulates the INDUCER OF CBF expression-C-repeat binding factor/dre binding factor1 Cascade and freezing tolerance in Arabidopsis. *Plant Cell*, 25(8), 2907–2924. <https://doi.org/10.1105/tpc.113.112631>
- Hu, Yanru, Jiang, Y., Han, X., Wang, H., Pan, J., & Yu, D. (2017). Jasmonate regulates leaf senescence and tolerance to cold stress: Crosstalk with other phytohormones. *Journal of Experimental Botany*, 68(6), 1361–1369. <https://doi.org/10.1093/jxb/erx004>

- Hu, Yong, Zhang, L., He, S., Huang, M., Tan, J., Zhao, L., Yan, S., Li, H., Zhou, K., Liang, Y., & Li, L. (2012). Cold stress selectively unsilences tandem repeats in heterochromatin associated with accumulation of H3K9ac. *Plant, Cell and Environment*, 35(12), 2130–2142. <https://doi.org/10.1111/j.1365-3040.2012.02541.x>
- Hu, Yong, Zhang, L., Zhao, L., Li, J., He, S., Zhou, K., Yang, F., Huang, M., Jiang, L., & Li, L. (2011). Trichostatin a selectively suppresses the Cold-Induced transcription of the ZmDREB1 gene in maize. *PLoS ONE*, 6(7). <https://doi.org/10.1371/journal.pone.0022132>
- Huang, S., Zhang, A., Jin, J. B., Zhao, B., Wang, T. J., Wu, Y., Wang, S., Liu, Y., Wang, J., Guo, P., Ahmad, R., Liu, B., & Xu, Z. Y. (2019). Arabidopsis histone H3K4 demethylase JMJ17 functions in dehydration stress response. *New Phytologist*, 223(3), 1372–1387. <https://doi.org/10.1111/nph.15874>
- Hung, F. Y., Chen, J. H., Feng, Y. R., Lai, Y. C., Yang, S., & Wu, K. (2020). Arabidopsis JMJ29 is involved in trichome development by regulating the core trichome initiation gene GLABRA3. *Plant Journal*, 103(5), 1735–1743. <https://doi.org/10.1111/tpj.14858>
- Hung, F. Y., Lai, Y. C., Wang, J., Feng, Y. R., Shih, Y. H., Chen, J. H., Sun, H. C., Yang, S., Li, C., & Wu, K. (2021). The arabidopsis histone demethylase JMJ28 regulates CONSTANS by interacting with FBH transcription factors. *Plant Cell*, 33(4), 1197–1211. <https://doi.org/10.1093/plcell/koab014>
- Ingham, P. W. (1983). Differential expression of bithorax complex genes in the absence of the extra sex combs and trithorax genes. *Nature*, 306(5943), 591–593. <https://doi.org/10.1038/306591a0>
- Jackson, J. P., Johnson, L., Jasencakova, Z., Zhang, X., PerezBurgos, L., Singh, P. B., Cheng, X., Schubert, I., Jenuwein, T., & Jacobsen, S. E. (2004). Dimethylation of histone H3 lysine 9 is a critical mark for DNA methylation and gene silencing in Arabidopsis thaliana. *Chromosoma*, 112(6), 308–315. <https://doi.org/10.1007/s00412-004-0275-7>
- Jacob, Y., Feng, S., LeBlanc, C. A., Bernatavichute, Y. V., Stroud, H., Cokus, S., Johnson, L. M., Pellegrini, M., Jacobsen, S. E., & Michaels, S. D. (2009). ATXR5 and ATXR6 are H3K27 monomethyltransferases required for chromatin structure and gene silencing. *Nature Structural and Molecular Biology*, 16(7), 763–768. <https://doi.org/10.1038/nsmb.1611>
- Jan, N., Andrabi, K. I., & others. (2009). Cold resistance in plants: A mystery unresolved. *Electronic Journal of Biotechnology*, 12(3), 14–15.
- Jaskiewicz, M., Conrath, U., & Peterhalsel, C. (2011). Chromatin modification acts as a memory for systemic acquired resistance in the plant stress response. *EMBO Reports*, 12(1), 50–55. <https://doi.org/10.1038/embor.2010.186>
- Jenks, M. A., & Hasegawa, P. M. (2013). *Plant Abiotic Stress, second Edition*. <https://doi.org/10.1002/9781118764374>
- Jenuwein, T., & Allis, C. D. (2001). Translating the histone code. *Science*, 293(5532), 1074–1080. <https://doi.org/10.1126/science.1063127>
- Jeon, J., & Kim, J. (2011). FVE, an Arabidopsis homologue of the retinoblastoma-associated protein that regulates flowering time and cold response, binds to chromatin as a large multiprotein complex. *Molecules and Cells*, 32(3), 227–234. <https://doi.org/10.1007/s10059-011-1022-6>
- Jeong, J. H., Song, H. R., Ko, J. H., Jeong, Y. M., Kwon, Y. E., Seol, J. H., Amasino, R. M., Noh, B., & Noh, Y. S. (2009). Repression of FLOWERING LOCUS T chromatin by functionally redundant histone H3 lysine 4 demethylases in Arabidopsis. *PLoS ONE*, 4(11). <https://doi.org/10.1371/journal.pone.0008033>
- Ji, H., Wang, Y., Cloix, C., Li, K., Jenkins, G. I., Wang, S., Shang, Z., Shi, Y., Yang, S., & Li, X. (2015). The Arabidopsis RCC1 Family Protein TCF1 Regulates Freezing Tolerance and Cold Acclimation through Modulating Lignin Biosynthesis. *PLoS Genetics*, 11(9), 1–25. <https://doi.org/10.1371/journal.pgen.1005471>
- Jia, Y., Ding, Y., Shi, Y., Zhang, X., Gong, Z., & Yang, S. (2016). The cbfs triple mutants reveal the essential functions of CBFs in cold acclimation and allow the definition of CBF regulons in Arabidopsis. *The New Phytologist*, 212(2), 345–353. <https://doi.org/10.1111/nph.14088>

- Jiang, B., Shi, Y., Zhang, X., Xin, X., Qi, L., Guo, H., Li, J., & Yang, S. (2017). PIF3 is a negative regulator of the CBF pathway and freezing tolerance in Arabidopsis. *Proceedings of the National Academy of Sciences of the United States of America*, *114*(32), E6695–E6702. <https://doi.org/10.1073/pnas.1706226114>
- Jiang, D., Yang, W., He, Y., & Amasino, R. M. (2007). Arabidopsis relatives of the human lysine-specific demethylase1 repress the expression of FWA and FLOWERING LOCUS C and thus promote the floral transition. *Plant Cell*, *19*(10), 2975–2987. <https://doi.org/10.1105/tpc.107.052373>
- Johnson, L., Mollah, S., Garcia, B. A., Muratore, T. L., Shabanowitz, J., Hunt, D. F., & Jacobsen, S. E. (2004). Mass spectrometry analysis of Arabidopsis histone H3 reveals distinct combinations of post-translational modifications. *Nucleic Acids Research*, *32*(22), 6511–6518. <https://doi.org/10.1093/nar/gkh992>
- Jung, J. H., Barbosa, A. D., Hutin, S., Kumita, J. R., Gao, M., Derwort, D., Silva, C. S., Lai, X., Pierre, E., Geng, F., Kim, S. B., Baek, S., Zubieta, C., Jaeger, K. E., & Wigge, P. A. (2020). A prion-like domain in ELF3 functions as a thermosensor in Arabidopsis. *Nature*, *585*(7824), 256–260. <https://doi.org/10.1038/s41586-020-2644-7>
- Jung, J. H., Domijan, M., Klose, C., Biswas, S., Ezer, D., Gao, M., Khattak, A. K., Box, M. S., Charoensawan, V., Cortijo, S., Kumar, M., Grant, A., Locke, J. C. W., Schäfer, E., Jaeger, K. E., & Wigge, P. A. (2016). Phytochromes function as thermosensors in Arabidopsis. *Science*, *354*(6314), 886–889. <https://doi.org/10.1126/science.aaf6005>
- Juntawong, P., Sorenson, R., & Bailey-Serres, J. (2013). Cold shock protein 1 chaperones mRNAs during translation in Arabidopsis thaliana. *Plant Journal*, *74*(6), 1016–1028. <https://doi.org/10.1111/tpj.12187>
- Kagale, S., Divi, U. K., Krochko, J. E., Keller, W. A., & Krishna, P. (2007). Brassinosteroid confers tolerance in Arabidopsis thaliana and Brassica napus to a range of abiotic stresses. *Planta*, *225*(2), 353–364. <https://doi.org/10.1007/s00425-006-0361-6>
- Kalberer, S. R., Wisniewski, M., & Arora, R. (2006). Deacclimation and reacclimation of cold-hardy plants: Current understanding and emerging concepts. *Plant Science*, *171*(1), 3–16. <https://doi.org/10.1016/j.plantsci.2006.02.013>
- Kawamura, Y., & Uemura, M. (2013). Plant low-temperature tolerance and its cellular mechanisms. In *Plant Abiotic Stress* (pp. 109–132). John Wiley & Sons, Ltd. <https://doi.org/https://doi.org/10.1002/9781118764374.ch5>
- Kawashima, T., Lorković, Z. J., Nishihama, R., Ishizaki, K., Axelsson, E., Yelagandula, R., Kohchi, T., & Berger, F. (2015). Diversification of histone H2A variants during plant evolution. *Trends in Plant Science*, *20*(7), 419–425. <https://doi.org/10.1016/j.tplants.2015.04.005>
- Kidokoro, S., Maruyama, K., Nakashima, K., Imura, Y., Narusaka, Y., Shinwari, Z. K., Osakabe, Y., Fujita, Y., Mizoi, J., Shinozaki, K., & Yamaguchi-Shinozaki, K. (2009). The phytochrome-interacting factor PIF7 negatively regulates dreb1 expression under circadian control in Arabidopsis. *Plant Physiology*, *151*(4), 2046–2057. <https://doi.org/10.1104/pp.109.147033>
- Kim, H. J., Hyun, Y., Park, J. Y., Park, M. J., Park, M. K., Kim, M. D., Kim, H. J., Lee, M. H., Moon, J., Lee, I., & Kim, J. (2004). A genetic link between cold responses and flowering time through FVE in Arabidopsis thaliana. *Nature Genetics*, *36*(2), 167–171. <https://doi.org/10.1038/ng1298>
- Kim, J.-M., Sasaki, T., Ueda, M., Sako, K., & Seki, M. (2015). Chromatin changes in response to drought, salinity, heat, and cold stresses in plants. *Frontiers in Plant Science*, *6*(March), 114. <https://doi.org/10.3389/fpls.2015.00114>
- Kim, M.-H., Sasaki, K., & Imai, R. (2009). Cold shock domain protein 3 regulates freezing tolerance in Arabidopsis thaliana. *The Journal of Biological Chemistry*, *284*(35), 23454–23460. <https://doi.org/10.1074/jbc.M109.025791>
- Kim, S. Y., Lee, J., Eshed-Williams, L., Zilberman, D., & Sung, Z. R. (2012). EMF1 and PRC2 cooperate to repress key regulators of arabidopsis development. *PLoS Genetics*, *8*(3). <https://doi.org/10.1371/journal.pgen.1002512>
- Kim, S. Y., Zhu, T., & Renee Sung, Z. (2010). Epigenetic regulation of gene programs by EMF1 and

- EMF2 in Arabidopsis. *Plant Physiology*, 152(2), 516–528. <https://doi.org/10.1104/pp.109.143495>
- Kim, Y., Park, S., Gilmour, S. J., & Thomashow, M. F. (2013). Roles of CAMTA transcription factors and salicylic acid in configuring the low-temperature transcriptome and freezing tolerance of Arabidopsis. *Plant Journal*, 75(3), 364–376. <https://doi.org/10.1111/tpj.12205>
- Kleinmanns, J. A., Schatlowski, N., Heckmann, D., & Schubert, D. (2017). BLISTER Regulates Polycomb-Target Genes, Represses Stress-Regulated Genes and Promotes Stress Responses in Arabidopsis thaliana. *Frontiers in Plant Science*. <https://doi.org/10.3389/fpls.2017.01530>
- Kleinmanns, J. A., & Schubert, D. (2014). Polycomb and Trithorax group protein-mediated control of stress responses in plants. *Biological Chemistry*, 395(11), 1291–1300. <https://doi.org/10.1515/hsz-2014-0197>
- Knezetic, J. A., & Luse, D. S. (1986). The presence of nucleosomes on a DNA template prevents initiation by RNA polymerase II in vitro. *Cell*, 45(1), 95–104. [https://doi.org/10.1016/0092-8674\(86\)90541-6](https://doi.org/10.1016/0092-8674(86)90541-6)
- Knight, H., Trewavas, A. J., & Knight, M. R. (1996). Cold calcium signaling in Arabidopsis involves two cellular pools and a change in calcium signature after acclimation. *Plant Cell*, 8(3), 489–503. <https://doi.org/10.1105/tpc.8.3.489>
- Knight, H., Zarka, D. G., Okamoto, H., Thomashow, M. F., & Knight, M. R. (2004). Abscisic acid induces CBF gene transcription and subsequent induction of cold-regulated genes via the CRT promoter element. *Plant Physiology*, 135(3), 1710–1717. <https://doi.org/10.1104/pp.104.043562>
- Knight, M. R., Campbell, A. K., Smith, S. M., & Trewavas, A. J. (1991). Transgenic Plant Aequorin Reports the Effect of Touch and Cold-shock and Elicitors on Cytoplasmic Calcium. *Nature*, 352, 524–526.
- Köhler, C., & Hennig, L. (2010). Regulation of cell identity by plant Polycomb and trithorax group proteins. *Current Opinion in Genetics and Development*, 20(5), 541–547. <https://doi.org/10.1016/j.gde.2010.04.015>
- Kornberg, R. D. (1977). Structure of chromatin. *Annual Review of Biochemistry*, 46, 931–954. <https://doi.org/10.1146/annurev.bi.46.070177.004435>
- Kreps, J. A., Wu, Y., Chang, H., Zhu, T., Wang, X., Harper, J. F., Mesa, T., Row, M., Diego, S., California, J. A. K., Scripps, T., & Pines, N. T. (2002). Transcriptome Changes for Arabidopsis in Response to Salt, Osmotic, and Cold Stress. *Plant Physiology*, 130(December), 2129–2141. <https://doi.org/10.1104/pp.008532.with>
- Ku, M., Jaffe, J. D., Koche, R. P., Rheinbay, E., Endoh, M., Koseki, H., Carr, S. A., & Bernstein, B. E. (2012). H2A.Z landscapes and dual modifications in pluripotent and multipotent stem cells underlie complex genome regulatory functions. *Genome Biology*, 13(10). <https://doi.org/10.1186/gb-2012-13-10-R85>
- Kudla, J., Becker, D., Grill, E., Hedrich, R., Hippler, M., Kummer, U., Parniske, M., Romeis, T., & Schumacher, K. (2018). Advances and current challenges in calcium signaling. *New Phytologist*, 218(2), 414–431. <https://doi.org/10.1111/nph.14966>
- Kumar, D., Cinghu, S., Oldfield, A. J., Yang, P., & Jothi, R. (2021). Decoding the function of bivalent chromatin in development and cancer. *Genome Research*. <https://doi.org/10.1101/gr.275736.121>
- Kumar, S. V., & Wigge, P. A. (2010). H2A.Z-Containing Nucleosomes Mediate the Thermosensory Response in Arabidopsis. *Cell*, 140(1), 136–147. <https://doi.org/10.1016/j.cell.2009.11.006>
- Kurkela, S., & Borg-Franck, M. (1992). Structure and expression of kin2, one of two cold- and ABA-induced genes of Arabidopsis thaliana. *Plant Molecular Biology*, 19, 689–692.
- Kurkela, S., & Franck, M. (1990). Cloning and characterization of a cold- and ABA-inducible Arabidopsis gene. *Plant Molecular Biology*, 15(1), 137–144. <https://doi.org/10.1007/BF00017731>
- Kuroda, M. I., Kang, H., De, S., & Kassis, J. A. (2020). Dynamic Competition of Polycomb and Trithorax in Transcriptional Programming. *Annual Review of Biochemistry*, 89, 235–253. <https://doi.org/10.1146/annurev-biochem-120219-103641>

- Kwon, C. S., Lee, D., Choi, G., & Chung, W. II. (2009). Histone occupancy-dependent and -independent removal of H3K27 trimethylation at cold-responsive genes in Arabidopsis. *Plant Journal*, *60*(1), 112–121. <https://doi.org/10.1111/j.1365-313X.2009.03938.x>
- Lafos, M., Kroll, P., Hohenstatt, M. L., Thorpe, F. L., Clarenz, O., & Schubert, D. (2011). Dynamic regulation of H3K27 trimethylation during arabidopsis differentiation. *PLoS Genetics*, *7*(4). <https://doi.org/10.1371/journal.pgen.1002040>
- Lämke, J., Brzezinka, K., Altmann, S., & Bäurle, I. (2016). A hit-and-run heat shock factor governs sustained histone methylation and transcriptional stress memory. *The EMBO Journal*, *35*(2), 162–175. <https://doi.org/10.15252/embj.201592593>
- Lång, V., Mäntylä, E., Welin, B., Sundberg, B., & Palva, E. T. (1994). Alterations in water status, endogenous abscisic acid content, and expression of rab18 gene during the development of freezing tolerance in Arabidopsis thaliana. *Plant Physiology*, *104*(4), 1341–1349. <https://doi.org/10.1104/pp.104.4.1341>
- Langmead, B., & Salzberg, S. L. (2012). Fast gapped-read alignment with Bowtie 2. *Nature Methods*, *9*(4), 357–359. <https://doi.org/10.1038/nmeth.1923>
- Lawrence, M., Huber, W., Pagès, H., Aboyoun, P., Carlson, M., Gentleman, R., Morgan, M. T., & Carey, V. J. (2013). Software for Computing and Annotating Genomic Ranges. *PLoS Computational Biology*, *9*(8), 1–10. <https://doi.org/10.1371/journal.pcbi.1003118>
- Legris, M., Klose, C., Burgie, E. S., Rojas, C. C., Neme, M., Hiltbrunner, A., Wigge, P. A., Schäfer, E., Vierstra, R. D., & Casal, J. J. (2016). Phytochrome B integrates light and temperature signals in Arabidopsis. *Science*, *354*(6314), 897–900. <https://doi.org/10.1126/science.aaf5656>
- Leuendorf, J. E., Frank, M., & Schmölling, T. (2020). Acclimation, priming and memory in the response of Arabidopsis thaliana seedlings to cold stress. *Scientific Reports*, *10*(1), 1–11. <https://doi.org/10.1038/s41598-019-56797-x>
- Levitt, J. (1980a). Chilling Injury and Resistance. In *Responses of Plants to Environmental Stresses. Chilling, freezing and high temperature stresses* (pp. 23–64). <https://doi.org/10.1016/b978-0-12-445501-6.50008-7>
- Levitt, J. (1980b). Freezing Injury. In *Responses of Plants to Environmental Stresses. Chilling, freezing and high temperature stresses* (pp. 99–115). <https://doi.org/10.1016/b978-0-12-445501-6.50011-7>
- Levitt, J. (1980c). The Freezing Process. In *Responses of Plants to Environmental Stresses. Chilling, freezing and high temperature stresses* (pp. 79–98). <https://doi.org/10.1016/b978-0-12-445501-6.50010-5>
- Li, B., Carey, M., & Workman, J. L. (2007). The Role of Chromatin during Transcription. *Cell*, *128*(4), 707–719. <https://doi.org/10.1016/j.cell.2007.01.015>
- Li, B., Pattenden, S. G., Lee, D., Gutiérrez, J., Chen, J., Seidel, C., Gerton, J., & Workman, J. L. (2005). Preferential occupancy of histone variant H2AZ at inactive promoters influences local histone modifications and chromatin remodeling. *Proceedings of the National Academy of Sciences of the United States of America*, *102*(51), 18385–18390. <https://doi.org/10.1073/pnas.0507975102>
- Li, F., Hu, Q., Chen, F., & Jiang, J. F. (2021). Transcriptome analysis reveals Vernalization is independent of cold acclimation in Arabidopsis. *BMC Genomics*, *22*(1), 1–14. <https://doi.org/10.1186/s12864-021-07763-3>
- Li, Heng, Handsaker, B., Wysoker, A., Fennell, T., Ruan, J., Homer, N., Marth, G., Abecasis, G., & Durbin, R. (2009). The Sequence Alignment/Map format and SAMtools. *Bioinformatics*, *25*(16), 2078–2079. <https://doi.org/10.1093/bioinformatics/btp352>
- Li, Hui, Ding, Y., Shi, Y., Zhang, X., Zhang, S., Gong, Z., & Yang, S. (2017). MPK3- and MPK6-Mediated ICE1 Phosphorylation Negatively Regulates ICE1 Stability and Freezing Tolerance in Arabidopsis. *Developmental Cell*, *43*(5), 630-642.e4. <https://doi.org/10.1016/j.devcel.2017.09.025>
- Li, Hui, Ye, K., Shi, Y., Cheng, J., Zhang, X., & Yang, S. (2017). BZR1 Positively Regulates Freezing Tolerance via CBF-Dependent and CBF-Independent Pathways in Arabidopsis. *Molecular Plant*,

10(4), 545–559. <https://doi.org/10.1016/j.molp.2017.01.004>

- Li, Q., Brown, J. B., Huang, H., & Bickel, P. J. (2011). Measuring reproducibility of high-throughput experiments. *Annals of Applied Statistics*, 5(3), 1752–1779. <https://doi.org/10.1214/11-AOAS466>
- Li, Z., Fu, X., Wang, Y., Liu, R., & He, Y. (2018). Polycomb-mediated gene silencing by the BAH–EMF1 complex in plants. *Nature Genetics*, 50(September). <https://doi.org/10.1038/s41588-018-0190-0>
- Liao, Y., Smyth, G. K., & Shi, W. (2014). FeatureCounts: An efficient general purpose program for assigning sequence reads to genomic features. *Bioinformatics*, 30(7), 923–930. <https://doi.org/10.1093/bioinformatics/btt656>
- Liese, A., & Romeis, T. (2013). Biochemical regulation of in vivo function of plant calcium-dependent protein kinases (CDPK). *Biochimica et Biophysica Acta - Molecular Cell Research*, 1833(7), 1582–1589. <https://doi.org/10.1016/j.bbamcr.2012.10.024>
- Lim, C. J., Park, J., Shen, M., Park, H. J., Cheong, M. S., Park, K. S., Baek, D., Bae, M. J., Ali, A., Jan, M., Lee, S. Y., Lee, B. H., Kim, W. Y., Pardo, J. M., & Yun, D. J. (2020). The Histone-modifying complex PWR/HOS15/HD2C epigenetically regulates cold tolerance1[OPEN]. *Plant Physiology*, 184(2), 1097–1111. <https://doi.org/10.1104/pp.20.00439>
- Lin, J., Xu, Y., & Zhu, Z. (2020). Emerging Plant Thermosensors: From RNA to Protein. *Trends in Plant Science*, 25(12), 1187–1189. <https://doi.org/10.1016/j.tplants.2020.08.007>
- Liu, H., Lämke, J., Lin, S., Hung, M.-J., Liu, K.-M., Charng, Y., & Bäurle, I. (2018). Distinct heat shock factors and chromatin modifications mediate the organ-autonomous transcriptional memory of heat stress. *The Plant Journal*, 0–1. <https://doi.org/10.1111/tpj.13958>
- Liu, N., & Avramova, Z. (2016). Molecular mechanism of the priming by jasmonic acid of specific dehydration stress response genes in Arabidopsis. *Epigenetics and Chromatin*, 9(1), 1–23. <https://doi.org/10.1186/s13072-016-0057-5>
- Liu, N., Fromm, M., & Avramova, Z. (2014). H3K27me3 and H3K4me3 chromatin environment at super-induced dehydration stress memory genes of Arabidopsis thaliana. *Molecular Plant*. <https://doi.org/10.1093/mp/ssu001>
- Liu, P., Zhang, S., Zhou, B., Luo, X., Zhou, X. F., Cai, B., Jin, Y. H., Niu, D., Lin, J., Cao, X., & Jin, J. B. (2019). The histone H3K4 demethylase JM16 represses leaf senescence in arabidopsis. *Plant Cell*, 31(2), 430–443. <https://doi.org/10.1105/tpc.18.00693>
- Liu, Yue, Tian, T., Zhang, K., You, Q., Yan, H., Zhao, N., Yi, X., & Xu, W. (2018). PCSD: a plant chromatin state database. 46(October 2017), 1157–1167. <https://doi.org/10.1093/nar/gkx919>
- Liu, Yutong, Zhang, A., Yin, H., Meng, Q., Yu, X., Huang, S., Wang, J., Ahmad, R., Liu, B., & Xu, Z. Y. (2018). Trithorax-group proteins ARABIDOPSIS TRITHORAX4 (ATX4) and ATX5 function in abscisic acid and dehydration stress responses. *New Phytologist*, 217(4), 1582–1597. <https://doi.org/10.1111/nph.14933>
- Love, M. I., Huber, W., & Anders, S. (2014). Moderated estimation of fold change and dispersion for RNA-seq data with DESeq2. *Genome Biology*, 15(12), 1–21. <https://doi.org/10.1186/s13059-014-0550-8>
- Lu, F., Cui, X., Zhang, S., Jenuwein, T., & Cao, X. (2011). Arabidopsis REF6 is a histone H3 lysine 27 demethylase. *Nature Genetics*, 43(7), 715–719. <https://doi.org/10.1038/ng.854>
- Luger, K., Mäder, A. W., Richmond, R. K., Sargent, D. F., & Richmond, T. J. (1997). Crystal structure of the nucleosome core particle at 2.8 Å resolution. *Nature*, 389(6648), 251–260. <https://doi.org/10.1038/38444>
- Luger, K., & Richmond, T. J. (1998). The histone tails of the nucleosome. *Current Opinion in Genetics and Development*, 8(2), 140–146. [https://doi.org/10.1016/S0959-437X\(98\)80134-2](https://doi.org/10.1016/S0959-437X(98)80134-2)
- Luo, Y., Hou, X., Zhang, C., Tan, L., Shao, C., Lin, R., Su, Y., Cai, X., Li, L., Chen, S., & He, X. (2020). A plant-specific SWR1 chromatin-remodeling complex couples histone H2A.Z deposition with nucleosome sliding. *The EMBO Journal*, 39(7), 1–16. <https://doi.org/10.15252/embj.2019102008>
- Lyons, J. M. (1973). Chilling Injury In Plants. *Annual Review of Plant Physiology*, 24(1), 445–466.

<https://doi.org/10.1146/annurev.pp.24.060173.002305>

- Macdonald, N., Welburn, J. P. I., Noble, M. E. M., Nguyen, A., Yaffe, M. B., Clynes, D., Moggs, J. G., Orphanides, G., Thomson, S., Edmunds, J. W., Clayton, A. L., Endicott, J. A., & Mahadevan, L. C. (2005). Molecular basis for the recognition of phosphorylated and phosphoacetylated histone H3 by 14-3-3. *Molecular Cell*, *20*(2), 199–211. <https://doi.org/10.1016/j.molcel.2005.08.032>
- Mantyla, E., Lang, V., & Palva, E. T. (1995). Role of Abscisic Acid in Drought-Induced Freezing Tolerance, Cold Acclimation, and Accumulation of LT178 and RAB18 Proteins in *Arabidopsis thaliana*. *Plant Physiology*, *107*(1), 141–148. <https://doi.org/10.1104/pp.107.1.141>
- Mas, G., Blanco, E., Ballaré, C., Sansó, M., Spill, Y. G., Hu, D., Aoi, Y., Le Dily, F., Shilatifard, A., Marti-Renom, M. A., & Di Croce, L. (2018). Promoter bivalency favors an open chromatin architecture in embryonic stem cells. *Nature Genetics*, *50*(10), 1452–1462. <https://doi.org/10.1038/s41588-018-0218-5>
- Mathieu, O., Probst, A. V., & Paszkowski, J. (2005). Distinct regulation of histone H3 methylation at lysines 27 and 9 by CpG methylation in *Arabidopsis*. *EMBO Journal*, *24*(15), 2783–2791. <https://doi.org/10.1038/sj.emboj.7600743>
- Maurer-Stroh, S., Dickens, N. J., Hughes-Davies, L., Kouzarides, T., Eisenhaber, F., & Ponting, C. P. (2003). The Tudor domain “Royal Family”: Tudor, plant Agenet, Chromo, PWWP and MBT domains. *TRENDS in Biochemical Sciences*, *28*(28), 69–74. <http://tibs.trends.com>
- McWilliam, J. R. (1983). *Physiological basis for chilling stress and the consequences for crop production* (Vol. 113). Westview Press, Boulder, Colo.
- Medina, J., Bagues, M., Terol, J., Pérez-Alonso, M., & Salinas, J. (1999). The *Arabidopsis* CBF gene family is composed of three genes encoding AP2 domain-containing proteins whose expression is regulated by low temperature but not by abscisic acid or dehydration. *Plant Physiology*, *119*(2), 463–469. <https://doi.org/10.1104/pp.119.2.463>
- Mellor, J. (2006). It Takes a PHD to Read the Histone Code. *Cell*, *126*(1), 22–24. <https://doi.org/10.1016/j.cell.2006.06.028>
- Mittler, R. (2017). ROS Are Good. *Trends in Plant Science*, *22*(1), 11–19. <https://doi.org/10.1016/j.tplants.2016.08.002>
- Miura, K., & Ohta, M. (2010). SIZ1, a small ubiquitin-related modifier ligase, controls cold signaling through regulation of salicylic acid accumulation. *Journal of Plant Physiology*, *167*(7), 555–560. <https://doi.org/10.1016/j.jplph.2009.11.003>
- Mizuguchi, G., Tsukiyama, T., Wisniewski, J., & Wu, C. (1997). Role of nucleosome remodeling factor NURF in transcriptional activation of chromatin. *Molecular Cell*, *1*(1), 141–150. [https://doi.org/10.1016/S1097-2765\(00\)80015-5](https://doi.org/10.1016/S1097-2765(00)80015-5)
- Molitor, A., & Shen, W. H. (2013). The Polycomb Complex PRC1: Composition and Function in Plants. *Journal of Genetics and Genomics*, *40*(5), 231–238. <https://doi.org/10.1016/j.jgg.2012.12.005>
- Monfared, M. M., Carles, C. C., Rossignol, P., Pires, H. R., & Fletcher, J. C. (2013). The ULT1 and ULT2 *trxG* genes play overlapping roles in *Arabidopsis* development and gene regulation. *Molecular Plant*, *6*(5), 1564–1579. <https://doi.org/10.1093/mp/sst041>
- Monroy, A. F., & Dhindsa, R. S. (1995). Low-temperature signal transduction: Induction of cold acclimation-specific genes of alfalfa by calcium at 25°C. *Plant Cell*, *7*(3), 321–331. <https://doi.org/10.2307/3869854>
- Mori, K., Renhu, N., Naito, M., Nakamura, A., Shiba, H., Yamamoto, T., Suzuki, T., Iida, H., & Miura, K. (2018). Ca²⁺-permeable mechanosensitive channels MCA1 and MCA2 mediate cold-induced cytosolic Ca²⁺ increase and cold tolerance in *Arabidopsis*. *Scientific Reports*, *8*(1), 1–10. <https://doi.org/10.1038/s41598-017-17483-y>
- Mozgová, I., Wildhaber, T., Liu, Q., Abou-Mansour, E., L’Haridon, F., Métraux, J. P., Grisse, W., Hofius, D., & Hennig, L. (2015). Chromatin assembly factor CAF-1 represses priming of plant defence response genes. *Nature Plants*, *1*(September), 1–8. <https://doi.org/10.1038/nplants.2015.127>

- Müller-Xing, R., Ardiansyah, R., Xing, Q., Faivre, L., Tian, J., Wang, G., Zheng, Y., Wang, X., Jing, T., de Leau, E., Chen, S., Chen, S., Schubert, D., & Goodrich, J. (2022). Polycomb Proteins Control Floral Determinacy by H3K27me3-mediated Repression of Pluripotency Genes in *Arabidopsis thaliana*. *Journal of Experimental Botany*, *erac013*. <https://doi.org/10.1093/jxb/erac013>
- Müller, J., Hart, C. M., Francis, N. J., Vargas, M. L., Sengupta, A., Wild, B., Miller, E. L., O'Connor, M. B., Kingston, R. E., & Simon, J. A. (2002). Histone methyltransferase activity of a *Drosophila* Polycomb group repressor complex. *Cell*, *111*(2), 197–208. [https://doi.org/10.1016/S0092-8674\(02\)00976-5](https://doi.org/10.1016/S0092-8674(02)00976-5)
- Nagai, S., Davis, R. E., Mattei, P. J., Eagen, K. P., & Kornberg, R. D. (2017). Chromatin potentiates transcription. *Proceedings of the National Academy of Sciences of the United States of America*, *114*(7), 1536–1541. <https://doi.org/10.1073/pnas.1620312114>
- Nakamura, M., Gao, Y., Dominguez, A. A., & Qi, L. S. (2021). CRISPR technologies for precise epigenome editing. *Nature Cell Biology*, *23*(1), 11–22. <https://doi.org/10.1038/s41556-020-00620-7>
- Nakayama, K., Okawa, K., Kakizaki, T., Honma, T., Itoh, H., & Inaba, T. (2007). *Arabidopsis* Cor15am is a chloroplast stromal protein that has cryoprotective activity and forms oligomers. *Plant Physiology*, *144*(1), 513–523. <https://doi.org/10.1104/pp.106.094581>
- Nga leng Lau, P., & Cheung, P. (2011). Histone code pathway involving H3 S28 phosphorylation and K27 acetylation activates transcription and antagonizes polycomb silencing. *Proceedings of the National Academy of Sciences of the United States of America*, *108*(7), 2801–2806. <https://doi.org/10.1073/pnas.1012798108>
- Nguyen, X. C., Kim, S. H., Hussain, S., An, J., Yoo, Y., Han, H. J., Yoo, J. S., Lim, C. O., Yun, D. J., & Chung, W. S. (2016). A positive transcription factor in osmotic stress tolerance, ZAT10, is regulated by MAP kinases in *Arabidopsis*. *Journal of Plant Biology*, *59*(1), 55–61. <https://doi.org/10.1007/s12374-016-0442-4>
- Nishida, I., & Murata, N. (1996). Chilling sensitivity in plants and cyanobacteria: The crucial contribution of membrane lipids. *Annual Review of Plant Physiology and Plant Molecular Biology*, *47*(1), 541–568. <https://doi.org/10.1146/annurev.arplant.47.1.541>
- Nishio, H., Nagano, A. J., Ito, T., Suzuki, Y., & Kudoh, H. (2020). Seasonal plasticity and diel stability of H3K27me3 in natural fluctuating environments. *Nature Plants*, *6*(9), 1091–1097. <https://doi.org/10.1038/s41477-020-00757-1>
- Nishizawa, A., Yabuta, Y., & Shigeoka, S. (2008). Galactinol and raffinose constitute a novel function to protect plants from oxidative damage. *Plant Physiology*, *147*(3), 1251–1263. <https://doi.org/10.1104/pp.108.122465>
- Novillo, F., Alonso, J. M., Ecker, J. R., & Salinas, J. (2004). CBF2/DREB1C is a negative regulator of CBF1/DREB1B and CBF3/DREB1A expression and plays a central role in stress tolerance in *Arabidopsis*. *Proceedings of the National Academy of Sciences of the United States of America*, *101*(11), 3985–3990. <https://doi.org/10.1073/pnas.0303029101>
- Olate, E., Jiménez-Gómez, J. M., Holuigue, L., & Salinas, J. (2018). NPR1 mediates a novel regulatory pathway in cold acclimation by interacting with HSFA1 factors. *Nature Plants*. <https://doi.org/10.1038/s41477-018-0254-2>
- Oono, Y., Seki, M., Satou, M., Iida, K., Akiyama, K., Sakurai, T., Fujita, M., Yamaguchi-Shinozaki, K., & Shinozaki, K. (2006). Monitoring expression profiles of *Arabidopsis* genes during cold acclimation and deacclimation using DNA microarrays. *Functional and Integrative Genomics*, *6*(3), 212–234. <https://doi.org/10.1007/s10142-005-0014-z>
- Örvar, B. L., Sangwan, V., Omann, F., & Dhindsa, R. S. (2000). Early steps in cold sensing by plant cells: The role of actin cytoskeleton and membrane fluidity. *Plant Journal*, *23*(6), 785–794. <https://doi.org/10.1046/j.1365-313X.2000.00845.x>
- Pagter, M., Alpers, J., Erban, A., Kopka, J., Zuther, E., & Hinch, D. K. (2017). Rapid transcriptional and metabolic regulation of the deacclimation process in cold acclimated *Arabidopsis thaliana*. *BMC Genomics*. <https://doi.org/10.1186/s12864-017-4126-3>

- Papikian, A., Liu, W., Gallego-Bartolomé, J., & Jacobsen, S. E. (2019). Site-specific manipulation of Arabidopsis loci using CRISPR-Cas9 SunTag systems. *Nature Communications*, *10*(1), 729. <https://doi.org/10.1038/s41467-019-08736-7>
- Park, J., Jin, C., Shen, M., Jin, H., Cha, J., Iniesto, E., & Rubio, V. (2018). Epigenetic switch from repressive to permissive chromatin in response to cold stress. *Pnas*. <https://doi.org/10.1073/pnas.1721241115>
- Park, S., Lee, C. M., Doherty, C. J., Gilmour, S. J., Kim, Y., & Thomashow, M. F. (2015). Regulation of the Arabidopsis CBF regulon by a complex low-temperature regulatory network. *Plant Journal*, *82*(2), 193–207. <https://doi.org/10.1111/tpj.12796>
- Pavangadkar, K., Thomashow, M. F., & Triezenberg, S. J. (2010). Histone dynamics and roles of histone acetyltransferases during cold-induced gene regulation in Arabidopsis. *Plant Molecular Biology*, *74*(1), 183–200. <https://doi.org/10.1007/s11103-010-9665-9>
- Pendle, A. F., Clark, G. P., Boon, R., Lewandowska, D., Wah Lam, Y., Andersen, J., Mann, M., Lamond, A. I., Brown, J. W. S., & Shaw, P. (2005). Proteomic Analysis of the Arabidopsis Nucleolus Suggests Novel Nucleolar Functions. *Mol Biol Cell*, *16*(Januara). <https://doi.org/10.1091/mbc.E04>
- Petoukhov, V., & Semenov, V. A. (2010). A link between reduced Barents-Kara sea ice and cold winter extremes over northern continents. *Journal of Geophysical Research Atmospheres*, *115*(21), 1–11. <https://doi.org/10.1029/2009JD013568>
- Pfaffl, M. W. (2001). A New Mathematical Model for Relative Quantification in Real-Time RT-PCR. *Nucleic Acids Research*, *29*(9). <https://doi.org/10.1093/nar/29.9.e45>
- Pokorná, J., Schwarzerová, K., Zelenková, S., Petrášek, J., Janotová, I., Čapková, V., & Opatrný, Z. (2004). Sites of actin filament initiation and reorganization in cold-treated tobacco cells. *Plant, Cell and Environment*, *27*(5), 641–653. <https://doi.org/10.1111/j.1365-3040.2004.01186.x>
- Probst, A. V., Desvoyes, B., & Gutierrez, C. (2020). Similar yet critically different: The distribution, dynamics and function of histone variants. *Journal of Experimental Botany*, *71*(17), 5191–5204. <https://doi.org/10.1093/jxb/eraa230>
- Puhakainen, T., Hess, M. W., Mäkelä, P., Svensson, J., Heino, P., & Palva, E. T. (2004). Overexpression of multiple dehydrin genes enhances tolerance to freezing stress in Arabidopsis. *Plant Molecular Biology*, *54*(5), 743–753. <https://doi.org/10.1023/B:PLAN.0000040903.66496.a4>
- Purdy, S. J., Bussell, J. D., Nelson, D. C., Villadsen, D., & Smith, S. M. (2011). A nuclear-localized protein, KOLD SENSITIV-1, affects the expression of cold-responsive genes during prolonged chilling in Arabidopsis. *Journal of Plant Physiology*, *168*(3), 263–269. <https://doi.org/10.1016/j.jplph.2010.07.001>
- Qian, S., Lv, X., Scheid, R. N., Lu, L., Yang, Z., Chen, W., Liu, R., Boersma, M. D., Denu, J. M., Zhong, X., & Du, J. (2018). Dual recognition of H3K4me3 and H3K27me3 by a plant histone reader SHL. *Nature Communications*, *9*(1), 1–11. <https://doi.org/10.1038/s41467-018-04836-y>
- Rajashekar, C. B., & Lafta, A. (1996). Cell-wall changes and cell tension in response to cold acclimation and exogenous abscisic acid in leaves and cell cultures. *Plant Physiology*, *111*(2), 605–612. <https://doi.org/10.1104/pp.111.2.605>
- Ramírez, F., Ryan, D. P., Grüning, B., Bhardwaj, V., Kilpert, F., Richter, A. S., Heyne, S., Dündar, F., & Manke, T. (2016). deepTools2: a next generation web server for deep-sequencing data analysis. *Nucleic Acids Research*, *44*(W1), W160–W165. <https://doi.org/10.1093/nar/gkw257>
- Raxwal, V. K., Ghosh, S., Singh, S., Katiyar-Agarwal, S., Goel, S., Jagannath, A., Kumar, A., Scaria, V., & Agarwal, M. (2020). Abiotic stress-mediated modulation of the chromatin landscape in Arabidopsis thaliana. *Journal of Experimental Botany*, *71*(17), 5280–5293. <https://doi.org/10.1093/jxb/eraa286>
- Reverón-Gómez, N., González-Aguilera, C., Stewart-Morgan, K. R., Petryk, N., Flury, V., Graziano, S., Johansen, J. V., Jakobsen, J. S., Alabert, C., & Groth, A. (2018). Accurate Recycling of Parental Histones Reproduces the Histone Modification Landscape during DNA Replication. *Molecular Cell*, *72*(2), 239–249.e5. <https://doi.org/10.1016/j.molcel.2018.08.010>

- Reyes-Díaz, M., Ulloa, N., Zúñiga-Feest, A., Gutiérrez, A., Gidekel, M., Alberdi, M., Corcuera, L. J., & Bravo, L. A. (2006). *Arabidopsis thaliana* avoids freezing by supercooling. *Journal of Experimental Botany*, *57*(14), 3687–3696. <https://doi.org/10.1093/jxb/erl125>
- Richard, G. (2020). *gtrichard/deepStats: New tools and much needed fixes*. Zenodo. <https://doi.org/10.5281/zenodo.3668336>
- Ringrose, L., & Paro, R. (2004). Epigenetic regulation of cellular memory by the polycomb and trithorax group proteins. *Annual Review of Genetics*, *38*, 413–443. <https://doi.org/10.1146/annurev.genet.38.072902.091907>
- Roberts, S. M., & Winston, F. (1997). Essential functional interactions of SAGA, a *Saccharomyces cerevisiae* complex of spt, ada, and gcn5 proteins, with the snf/swi and srb/mediator complexes. *Genetics*, *147*(2), 451–465. <https://doi.org/10.1093/genetics/147.2.451>
- Robinson, J. T., Thorvaldsdóttir, H., Winckler, W., Guttman, M., Lander, E. S., Getz, G., & Mesirov, J. P. (2011). Integrative genomics viewer. *Nature Biotechnology*, *29*(1), 24–26. <https://doi.org/10.1038/nbt.1754>
- Robinson, M. D., McCarthy, D. J., & Smyth, G. K. (2009). edgeR: A Bioconductor package for differential expression analysis of digital gene expression data. *Bioinformatics*, *26*(1), 139–140. <https://doi.org/10.1093/bioinformatics/btp616>
- Rossel, J. B., Wilson, P. B., Hussain, D., Woo, N. S., Gordon, M. J., Mewett, O. P., Howell, K. A., Whelan, J., Kazan, K., & Pogson, B. J. (2007). Systemic and intracellular responses to photooxidative stress in *Arabidopsis*. *Plant Cell*, *19*(12), 4091–4110. <https://doi.org/10.1105/tpc.106.045898>
- Roudier, F., Ahmed, I., Bérard, C., Sarazin, A., Mary-Huard, T., Cortijo, S., Bouyer, D., Caillieux, E., Duvernois-Berthet, E., Al-Shikhley, L., Giraut, L., Després, B., Drevensek, S., Barneche, F., Dérozier, S., Brunaud, V., Aubourg, S., Schnittger, A., Bowler, C., ... Colot, V. (2011). Integrative epigenomic mapping defines four main chromatin states in *Arabidopsis*. *EMBO Journal*, *30*(10), 1928–1938. <https://doi.org/10.1038/emboj.2011.103>
- Roy, D., Paul, A., Roy, A., Ghosh, R., Ganguly, P., & Chaudhuri, S. (2014). Differential acetylation of histone H3 at the regulatory region of OsDREB1b promoter facilitates chromatin remodelling and transcription activation during cold stress. *PLoS ONE*, *9*(6). <https://doi.org/10.1371/journal.pone.0100343>
- Roychoudhury, A., Paul, S., & Basu, S. (2013). Cross-talk between abscisic acid-dependent and abscisic acid-independent pathways during abiotic stress. *Plant Cell Reports*, *32*(7), 985–1006. <https://doi.org/10.1007/s00299-013-1414-5>
- Ruelland, E., Vaultier, M. N., Zachowski, A., & Hurry, V. (2009). Cold Signalling and Cold Acclimation in Plants. In *Advances in Botanical Research* (1st ed., Vol. 49, Issue C, pp. 35–150). Elsevier Ltd. [https://doi.org/10.1016/S0065-2296\(08\)00602-2](https://doi.org/10.1016/S0065-2296(08)00602-2)
- Ruthenburg, A. J., Li, H., Milne, T. A., Dewell, S., McGinty, R. K., Yuen, M., Ueberheide, B., Dou, Y., Muir, T. W., Patel, D. J., & Allis, C. D. (2011). Recognition of a mononucleosomal histone modification pattern by BPTF via multivalent interactions. *Cell*, *145*(5), 692–706. <https://doi.org/10.1016/j.cell.2011.03.053>
- Rutowicz, K., Puzio, M., Halibart-Puzio, J., Lirski, M., Kotliński, M., Kroteń, M. A., Knizewski, L., Lange, B., Muszewska, A., Śniegowska-Świerk, K., Kościelniak, J., Iwanicka-Nowicka, R., Buza, K., Janowiak, F., Żmuda, K., Jöesaar, I., Laskowska-Kaszub, K., Fogtman, A., Kollist, H., ... Jerzmanowski, A. (2015). A specialized histone H1 variant is required for adaptive responses to complex abiotic stress and related DNA methylation in *Arabidopsis*. *Plant Physiology*, *169*(3), 2080–2101. <https://doi.org/10.1104/pp.15.00493>
- Saijo, Y., Hata, S., Kyojuka, J., Shimamoto, K., & Izui, K. (2000). Over-expression of a single Ca²⁺-dependent protein kinase confers both cold and salt/drought tolerance on rice plants. *Plant Journal*, *23*(3), 319–327. <https://doi.org/10.1046/j.1365-313X.2000.00787.x>
- Saleh, A., Al-Abdallat, A., Ndamukong, I., Alvarez-Venegas, R., & Avramova, Z. (2007). The *Arabidopsis* homologs of trithorax (ATX1) and enhancer of zeste (CLF) establish “bivalent chromatin marks” at the silent AGAMOUS locus. *Nucleic Acids Research*, *35*(18), 6290–6296.

<https://doi.org/10.1093/nar/gkm464>

- Sane, P. V., Ivanov, A. G., Hurry, V., Huner, N. P. A., & Öquist, G. (2003). Changes in the redox potential of primary and secondary electron-accepting quinones in photosystem II confer increased resistance to photoinhibition in low-temperature-acclimated arabidopsis. *Plant Physiology*, *132*(4), 2144–2151. <https://doi.org/10.1104/pp.103.022939>
- Sangwan, V., Foulds, I., Singh, J., & Dhindsa, R. S. (2001). Cold-activation of Brassica napus BN115 promoter is mediated by structural changes in membranes and cytoskeleton, and requires Ca²⁺ influx. *Plant Journal*, *27*(1), 1–12. <https://doi.org/10.1046/j.1365-313X.2001.01052.x>
- Sani, E., Herzyk, P., Perrella, G., Colot, V., & Amtmann, A. (2013). Hyperosmotic priming of Arabidopsis seedlings establishes a long-term somatic memory accompanied by specific changes of the epigenome. *Genome Biology*, *14*(6), R59. <https://doi.org/10.1186/gb-2013-14-6-r59>
- Sasaki, K., Kim, M. H., & Imai, R. (2013). Arabidopsis COLD SHOCK DOMAIN PROTEIN 2 is a negative regulator of cold acclimation. *New Phytologist*, *198*(1), 95–102. <https://doi.org/10.1111/nph.12118>
- Sawatsubashi, S., Murata, T., Lim, J., Fujiki, R., Ito, S., Suzuki, E., Tanabe, M., Zhao, Y., Kimura, S., Fujiyama, S., Ueda, T., Umetsu, D., Ito, T., Takeyama, K. I., & Kato, S. (2010). A histone chaperone, DEK, transcriptionally coactivates a nuclear receptor. *Genes and Development*, *24*(2), 159–170. <https://doi.org/10.1101/gad.1857410>
- Schmitges, F. W., Prusty, A. B., Faty, M., Stützer, A., Lingaraju, G. M., Aiwezian, J., Sack, R., Hess, D., Li, L., Zhou, S., Bunker, R. D., Wirth, U., Bouwmeester, T., Bauer, A., Ly-Hartig, N., Zhao, K., Chan, H., Gu, J., Gut, H., ... Thomä, N. H. (2011). Histone Methylation by PRC2 Is Inhibited by Active Chromatin Marks. *Molecular Cell*, *42*(3), 330–341. <https://doi.org/10.1016/j.molcel.2011.03.025>
- Schwartz, B. E., & Ahmad, K. (2005). Transcriptional activation triggers deposition and removal of the histone variant H3.3. *Genes and Development*, *19*(7), 804–814. <https://doi.org/10.1101/gad.1259805>
- Scott, I. M., Clarke, S. M., Wood, J. E., & Mur, L. A. J. (2004). Salicylate accumulation inhibits growth at chilling temperature in Arabidopsis. *Plant Physiology*, *135*(2), 1040–1049. <https://doi.org/10.1104/pp.104.041293>
- Seki, M., Ishida, J., Narusaka, M., Fujita, M., Nanjo, T., Umezawa, T., Kamiya, A., Nakajima, M., Enju, A., Sakurai, T., Satou, M., Akiyama, K., Yamaguchi-Shinozaki, K., Carninci, P., Kawai, J., Hayashizaki, Y., & Shinozaki, K. (2002). Monitoring the expression pattern of around 7,000 Arabidopsis genes under ABA treatments using a full-length cDNA microarray. *Functional and Integrative Genomics*, *2*(6), 282–291. <https://doi.org/10.1007/s10142-002-0070-6>
- Seneviratne, S. I., Nicholls, N., Easterling, D., Goodess, C. M., Kanae, S., Kossin, J., Luo, Y., Marengo, J., Mc Innes, K., Rahimi, M., Reichstein, M., Sorteberg, A., Vera, C., Zhang, X., Rusticucci, M., Semenov, V., Alexander, L. V., Allen, S., Benito, G., ... Zwiers, F. W. (2012). Changes in climate extremes and their impacts on the natural physical environment. *Managing the Risks of Extreme Events and Disasters to Advance Climate Change Adaptation: Special Report of the Intergovernmental Panel on Climate Change*, 9781107025, 109–230. <https://doi.org/10.1017/CBO9781139177245.006>
- Sequeira-Mendes, J., Araguez, I., Peiro, R., Mendez-Giraldez, R., Zhang, X., Jacobsen, S. E., Bastolla, U., & Gutierrez, C. (2014). The Functional Topography of the Arabidopsis Genome Is Organized in a Reduced Number of Linear Motifs of Chromatin States. *The Plant Cell*, *26*(6), 2351–2366. <https://doi.org/10.1105/tpc.114.124578>
- Shao, Z., Raible, F., Mollaaghababa, R., Guyon, J. R., Wu, C. T., Bender, W., & Kingston, R. E. (1999). Stabilization of chromatin structure by PRC1, a polycomb complex. *Cell*, *98*(1), 37–46. [https://doi.org/10.1016/S0092-8674\(00\)80604-2](https://doi.org/10.1016/S0092-8674(00)80604-2)
- Sheldon, C. C., Hills, M. J., Lister, C., Dean, C., Dennis, E. S., & Peacock, W. J. (2008). Resetting of FLOWERING LOCUS C expression after epigenetic repression by vernalization. *Proceedings of the National Academy of Sciences of the United States of America*, *105*(6), 2214–2219. <https://doi.org/10.1073/pnas.0711453105>
- Sheldon, C. C., Rouse, D. T., Finnegan, E. J., Peacock, W. J., & Dennis, E. S. (2000). The molecular

- basis of vernalization: The central role of FLOWERING LOCUS C (FLC). *Proceedings of the National Academy of Sciences of the United States of America*, 97(7), 3753–3758. <https://doi.org/10.1073/pnas.97.7.3753>
- Shen, L., Shao, N.-Y., Liu, X., Maze, I., Feng, J., & Nestler, E. J. (2013). diffReps: Detecting Differential Chromatin Modification Sites from ChIP-seq Data with Biological Replicates. *PLoS ONE*, 8(6), e65598. <https://doi.org/10.1371/journal.pone.0065598>
- Shi, Y., Ding, Y., & Yang, S. (2018). Molecular Regulation of CBF Signaling in Cold Acclimation. *Trends in Plant Science*, 23(7), 623–637. <https://doi.org/10.1016/j.tplants.2018.04.002>
- Shibasaki, K., Uemura, M., Tsurumi, S., & Rahman, A. (2009). Auxin response in Arabidopsis under cold stress: Underlying molecular mechanisms. *Plant Cell*, 21(12), 3823–3838. <https://doi.org/10.1105/tpc.109.069906>
- Shindo, C., Lister, C., Crevillen, P., Nordborg, M., & Dean, C. (2006). Variation in the epigenetic silencing of FLC contributes to natural variation in Arabidopsis vernalization response. *Genes and Development*, 20(22), 3079–3083. <https://doi.org/10.1101/gad.405306>
- Singh, P., Yekondi, S., Chen, P.-W., Tsai, C.-H., Yu, C.-W., Wu, K., & Zimmerli, L. (2014). Environmental History Modulates Arabidopsis Pattern-Triggered Immunity in a HISTONE ACETYLTRANSFERASE1-Dependent Manner. *The Plant Cell*, 26(6), 2676–2688. <https://doi.org/10.1105/tpc.114.123356>
- Sneppen, K., & Ringrose, L. (2019). Theoretical analysis of Polycomb-Trithorax systems predicts that poised chromatin is bistable and not bivalent. *Nature Communications*, 10(1), 1–18. <https://doi.org/10.1038/s41467-019-10130-2>
- Song, Z. T., Zhang, L. L., Han, J. J., Zhou, M., & Liu, J. X. (2021). Histone H3K4 methyltransferases SDG25 and ATX1 maintain heat-stress gene expression during recovery in Arabidopsis. *Plant Journal*, 105(5), 1326–1338. <https://doi.org/10.1111/tpj.15114>
- Stephens, M. (2017). False discovery rates: A new deal. *Biostatistics*, 18(2), 275–294. <https://doi.org/10.1093/biostatistics/kxw041>
- Steponkus, P. L., Uemura, M., Joseph, R. A., Gilmour, S. J., & Thomashow, M. F. (1998). Mode of action of the COR15a gene on the freezing tolerance of Arabidopsis thaliana. *Proceedings of the National Academy of Sciences of the United States of America*, 95(24), 14570–14575. <https://doi.org/10.1073/pnas.95.24.14570>
- Stewart-Morgan, K. R., Petryk, N., & Groth, A. (2020). Chromatin replication and epigenetic cell memory. *Nature Cell Biology*, 22(4), 361–371. <https://doi.org/10.1038/s41556-020-0487-y>
- Stewart-Morgan, K. R., Reverón-Gómez, N., & Groth, A. (2019). Transcription Restart Establishes Chromatin Accessibility after DNA Replication. *Molecular Cell*, 75(2), 284–297.e6. <https://doi.org/10.1016/j.molcel.2019.04.033>
- Stucki, M., Clapperton, J. A., Mohammad, D., Yaffe, M. B., Smerdon, S. J., & Jackson, S. P. (2005). MDC1 directly binds phosphorylated histone H2AX to regulate cellular responses to DNA double-strand breaks. *Cell*, 123(7), 1213–1226. <https://doi.org/10.1016/j.cell.2005.09.038>
- Sung, S., & Amasino, R. M. (2004). Vernalization in Arabidopsis thaliana is mediated by the PHD finger protein VIN3. *Nature*, 427(6970), 159–164. <https://doi.org/10.1038/nature02195>
- Sura, W., Kabza, M., Karłowski, W. M., Bieluszewski, T., Kus-Słowinska, M., Pawełszek, Ł., Sadowski, J., & Ziolkowski, P. A. (2017). Dual role of the histone variant H2A.Z in transcriptional regulation of stress-response genes. *Plant Cell*, 29(4), 791–807. <https://doi.org/10.1105/tpc.16.00573>
- Swindell, W. R. (2006). The Association Among Gene Expression Responses to Nine Abiotic Stress Treatments in Arabidopsis thaliana William. *Genetics*, 174(4), 1811–1824. <https://doi.org/10.1534/genetics.106.061374>
- Tähtiharju, S., Sangwan, V., Monroy, A. F., Dhindsa, R. S., & Borg, M. (1997). The induction of kin genes in cold-acclimating Arabidopsis thaliana. Evidence of a role for calcium. *Planta*, 203(4), 442–447. <https://doi.org/10.1007/s004250050212>

- Takahashi, D., Gorka, M., Erban, A., Graf, A., Kopka, J., Zuther, E., & Hinch, D. K. (2019). Both cold and sub-zero acclimation induce cell wall modification and changes in the extracellular proteome in *Arabidopsis thaliana*. *Scientific Reports*, *9*(1). <https://doi.org/10.1038/s41598-019-38688-3>
- Teige, M., Scheikl, E., Eulgem, T., Dóczi, R., Ichimura, K., Shinozaki, K., Dangl, J. L., & Hirt, H. (2004). The MKK2 pathway mediates cold and salt stress signaling in *Arabidopsis*. *Molecular Cell*, *15*(1), 141–152. <https://doi.org/10.1016/j.molcel.2004.06.023>
- The ENCODE Project Consortium. (2012). An Integrated Encyclopedia of DNA Elements in the Human Genome. *Nature*, *489*. <https://doi.org/10.1038/nature11247>
- Thomashow, M. F. (1999). Plant Cold Acclimation: Freezing Tolerance Genes and Regulatory Mechanisms. *Annual Review of Plant Physiology and Plant Molecular Biology*, *50*(1), 571–599. <https://doi.org/10.1146/annurev.arplant.50.1.571>
- Thomashow, M. F., Stockinger, E. J., Jaglo-Ottosen, K. R., Gilmour, S. J., & Zarka, D. G. (1997). Function and regulation of *Arabidopsis thaliana* COR (cold-regulated) genes. *Acta Physiologiae Plantarum*, *19*(4), 497–504.
- Thompson, J. D., Higgins, D. G., & Gibson, T. J. (1994). CLUSTAL W: Improving the sensitivity of progressive multiple sequence alignment through sequence weighting, position-specific gap penalties and weight matrix choice. *Nucleic Acids Research*, *22*(22), 4673–4680. <https://doi.org/10.1093/nar/22.22.4673>
- To, T. K., Nakaminami, K., Kim, J.-M., Morosawa, T., Ishida, J., Tanaka, M., Yokoyama, S., Shinozaki, K., & Seki, M. (2011). *Arabidopsis* HDA6 is required for freezing tolerance. *Biochemical and Biophysical Research Communications*, *406*(3), 414–419. <https://doi.org/10.1016/j.bbrc.2011.02.058>
- Townley, H. E., & Knight, M. R. (2002). Calmodulin as a potential negative regulator of *Arabidopsis* COR gene expression. *Plant Physiology*, *128*(4), 1169–1172. <https://doi.org/10.1104/pp.010814>
- Trapnell, C., Williams, B. A., Pertea, G., Mortazavi, A., Kwan, G., Van Baren, M. J., Salzberg, S. L., Wold, B. J., & Pachter, L. (2010). Transcript assembly and quantification by RNA-Seq reveals unannotated transcripts and isoform switching during cell differentiation. *Nature Biotechnology*, *28*(5), 511–515. <https://doi.org/10.1038/nbt.1621>
- Trojer, P., & Reinberg, D. (2007). Facultative Heterochromatin: Is There a Distinctive Molecular Signature? *Molecular Cell*, *28*(1), 1–13. <https://doi.org/10.1016/j.molcel.2007.09.011>
- Tsompana, M., & Buck, M. J. (2014). Chromatin accessibility: A window into the genome. *Epigenetics and Chromatin*, *7*(1), 1–16. <https://doi.org/10.1186/1756-8935-7-33>
- Uemura, M., Joseph, R. A., & Steponkus, P. L. (1995). Cold acclimation of *Arabidopsis thaliana*: Effect on plasma membrane lipid composition and freeze-induced lesions. *Plant Physiology*, *109*(1), 15–30. <https://doi.org/10.1104/pp.109.1.15>
- van Buer, J., Cvetkovic, J., & Baier, M. (2016). Cold regulation of plastid ascorbate peroxidases serves as a priming hub controlling ROS signaling in *Arabidopsis thaliana*. *BMC Plant Biology*, *16*(1), 163. <https://doi.org/10.1186/s12870-016-0856-7>
- Van Dijk, K., Ding, Y., Malkaram, S., Riethoven, J.-J., Liu, R., Yang, J. Y., Laczko, P., Chen, H., Xia, Y., Ladunga, I., Avramova, Z., & Fromm, M. (2010). Dynamic changes in genome-wide histone H3 lysine 4 methylation patterns in response to dehydration stress in *Arabidopsis thaliana*. *BMC Plant Biol*, *10*(lysine 4), 1–12. <https://doi.org/10.1186/1471-2229-10-238>
- Vlachonasios, K. E., Thomashow, M. F., & Triezenberg, S. J. (2003). Disruption mutations of ADA2b and GCN5 transcriptional adaptor genes dramatically affect *Arabidopsis* growth, development, and gene expression. *Plant Cell*, *15*(3), 626–638. <https://doi.org/10.1105/tpc.007922>
- Vogel, J. T., Zarka, D. G., Van Buskirk, H. A., Fowler, S. G., & Thomashow, M. F. (2005). Roles of the CBF2 and ZAT12 transcription factors in configuring the low temperature transcriptome of *Arabidopsis*. *Plant Journal*, *41*(2), 195–211. <https://doi.org/10.1111/j.1365-313X.2004.02288.x>
- Voigt, P., LeRoy, G., Drury, W. J., Zee, B. M., Son, J., Beck, D. B., Young, N. L., Garcia, B. A., & Reinberg, D. (2012). Asymmetrically modified nucleosomes. *Cell*, *151*(1), 181–193.

<https://doi.org/10.1016/j.cell.2012.09.002>

- Voigt, P., Tee, W. W., & Reinberg, D. (2013). A double take on bivalent promoters. *Genes and Development*, 27(12), 1318–1338. <https://doi.org/10.1101/gad.219626.113>
- Vyse, K., Faivre, L., Romich, M., Pagter, M., Schubert, D., Hinch, D. K., & Zuther, E. (2020). Transcriptional and Post-Transcriptional Regulation and Transcriptional Memory of Chromatin Regulators in Response to Low Temperature. *Frontiers in Plant Science*, 11(February), 1–18. <https://doi.org/10.3389/fpls.2020.00039>
- Waidmann, S., Kusenda, B., Mayerhofer, J., Mechtler, K., & Jonak, C. (2014). A DEK Domain-Containing protein modulates chromatin structure and function in Arabidopsis. *Plant Cell*, 26(11), 4328–4344. <https://doi.org/10.1105/tpc.114.129254>
- Waidmann, S., Petutschnig, E., Rozhon, W., Molnár, G., Popova, O., Mechtler, K., & Jonak, C. (2021). GSK3-mediated phosphorylation of DEK3 regulates chromatin accessibility and stress tolerance in Arabidopsis. *FEBS Journal*. <https://doi.org/10.1111/febs.16186>
- Wang, D. Z., Jin, Y. N., Ding, X. H., Wang, W. J., Zhai, S. S., Bai, L. P., & Guo, Z. F. (2017). Gene regulation and signal transduction in the ICE–CBF–COR signaling pathway during cold stress in plants. *Biochemistry (Moscow)*, 82(10), 1103–1117. <https://doi.org/10.1134/S0006297917100030>
- Wang, L., Sadeghnezhad, E., & Nick, P. (2020). Upstream of gene expression: What is the role of microtubules in cold signalling? *Journal of Experimental Botany*, 71(1), 36–48. <https://doi.org/10.1093/jxb/erz419>
- Wang, Y., Long, H., Yu, J., Dong, L., Wassef, M., Zhuo, B., Li, X., Zhao, J., Wang, M., Liu, C., Wen, Z., Chang, L., Chen, P., Wang, Q. fei, Xu, X., Margueron, R., & Li, G. (2018). Histone variants H2A.Z and H3.3 coordinately regulate PRC2-dependent H3K27me3 deposition and gene expression regulation in mES cells. *BMC Biology*, 16(1), 1–18. <https://doi.org/10.1186/s12915-018-0568-6>
- Weber, B., Zicola, J., Oka, R., & Stam, M. (2016). Plant Enhancers: A Call for Discovery. *Trends in Plant Science*, 21(11), 974–987. <https://doi.org/10.1016/j.tplants.2016.07.013>
- Wong, M. M., Cox, L. K., & Chrivia, J. C. (2007). The chromatin remodeling protein, SRCAP, is critical for deposition of the histone variant H2A.Z at promoters. *Journal of Biological Chemistry*, 282(36), 26132–26139. <https://doi.org/10.1074/jbc.M703418200>
- Xi, Y., Park, S. R., Kim, D. H., Kim, E. D., & Sung, S. (2020). Transcriptome and epigenome analyses of vernalization in Arabidopsis thaliana. *Plant Journal*, 103(4), 1490–1502. <https://doi.org/10.1111/tpj.14817>
- Yamaguchi-Shinozaki, K., & Shinozaki, K. (1994). A Novel cis-Acting Element in an Arabidopsis Gene is Involved in Responsiveness to Drought, Low-Temperature, or High-Salt Stress. *Plant Cell*, 6(2), 251–264. <https://doi.org/10.2307/3869643>
- Yamaguchi, N., Matsubara, S., Yoshimizu, K., Seki, M., Hamada, K., Kamitani, M., Kurita, Y., Inagaki, S., Suzuki, T., Gan, E. S., To, T., Kakutani, T., Nagano, A. J., Satake, A., & Ito, T. (2020). Removal of repressive histone marks creates epigenetic memory of recurring heat in Arabidopsis. *BioRxiv*, 1–36. <https://doi.org/10.1101/2020.05.10.086611>
- Yamaguchi, N., Matsubara, S., Yoshimizu, K., Seki, M., Hamada, K., Kamitani, M., Kurita, Y., Nomura, Y., Nagashima, K., Inagaki, S., Suzuki, T., Gan, E. S., To, T., Kakutani, T., Nagano, A. J., Satake, A., & Ito, T. (2021). H3K27me3 demethylases alter HSP22 and HSP17.6C expression in response to recurring heat in Arabidopsis. *Nature Communications*, 12(1), 1–16. <https://doi.org/10.1038/s41467-021-23766-w>
- Yamasu, K., & Senshn, T. (1990). Conservative segregation of tetrameric units of H3 and H4 histones during nucleosome replication. *Journal of Biochemistry*, 107(1), 15–20. <https://doi.org/10.1093/oxfordjournals.jbchem.a122999>
- Yan, A., Borg, M., Berger, F., & Chen, Z. (2020). The atypical histone variant H3.15 promotes callus formation in Arabidopsis thaliana. *Development (Cambridge)*, 147(11), 1–10. <https://doi.org/10.1242/DEV.184895>
- Yan, W., Chen, D., Smaczniak, C., Engelhorn, J., Liu, H., Yang, W., Graf, A., Carles, C. C., Zhou, D.-

- X., & Kaufmann, K. (2018). Dynamic and spatial restriction of Polycomb activity by plant histone demethylases. *Nature Plants*. <https://doi.org/10.1038/s41477-018-0219-5>
- Yang, H., Berry, S., Olsson, T. S. G., Hartley, M., Howard, M., & Dean, C. (2017). Distinct phases of Polycomb silencing to hold epigenetic memory of cold in Arabidopsis. *Science*, *357*(6356), 1142–1145. <https://doi.org/10.1126/science.aan1121>
- Yang, H., Han, Z., Cao, Y., Fan, D., Li, H., Mo, H., Feng, Y., Liu, L., Wang, Z., Yue, Y., Cui, S., Chen, S., Chai, J., & Ma, L. (2012). A companion cell-dominant and developmentally regulated H3K4 demethylase controls flowering time in Arabidopsis via the repression of FLC expression. *PLoS Genetics*, *8*(4). <https://doi.org/10.1371/journal.pgen.1002664>
- Yang, H., Mo, H., Fan, D., Cao, Y., Cui, S., & Ma, L. (2012). Overexpression of a histone H3K4 demethylase, JM15, accelerates flowering time in Arabidopsis. *Plant Cell Reports*, *31*(7), 1297–1308. <https://doi.org/10.1007/s00299-012-1249-5>
- Yang, R., Hong, Y., Ren, Z., Tang, K., Zhang, H., Zhu, J.-K., & Zhao, C. (2019). A Role for PICKLE in the Regulation of Cold and Salt Stress Tolerance in Arabidopsis. *Frontiers in Plant Science*, *10*, 900. <https://doi.org/10.3389/fpls.2019.00900>
- Yang, W., Jiang, D., Jiang, J., & He, Y. (2010). A plant-specific histone H3 lysine 4 demethylase represses the floral transition in Arabidopsis. *Plant Journal*, *62*(4), 663–673. <https://doi.org/10.1111/j.1365-313X.2010.04182.x>
- Yang, Z., Qian, S., Scheid, R. N., Lu, L., Chen, X., Liu, R., Du, X., Lv, X., Boersma, M. D., Scalf, M., Smith, L. M., Denu, J. M., Du, J., & Zhong, X. (2018). EBS is a bivalent histone reader that regulates floral phase transition in Arabidopsis. *Nature Genetics*, *50*(9), 1247–1253. <https://doi.org/10.1038/s41588-018-0187-8>
- Yelagandula, R., Stroud, H., Holec, S., Zhou, K., Feng, S., Zhong, X., Muthurajan, U. M., Nie, X., Kawashima, T., Groth, M., Luger, K., Jacobsen, S. E., & Berger, F. (2014). The histone variant H2A.W defines heterochromatin and promotes chromatin condensation in Arabidopsis. *Cell*, *158*(1), 98–109. <https://doi.org/10.1016/j.cell.2014.06.006>
- Yoo, S. Y., Kim, Y., Kim, S. Y., Lee, J. S., & Ahn, J. H. (2007). Control of flowering time and cold response by a NAC-domain protein in Arabidopsis. *PLoS ONE*, *2*(7). <https://doi.org/10.1371/journal.pone.0000642>
- Yu, G., Wang, L. G., & He, Q. Y. (2015). ChIP-seeker: An R/Bioconductor package for ChIP peak annotation, comparison and visualization. *Bioinformatics*, *31*(14), 2382–2383. <https://doi.org/10.1093/bioinformatics/btv145>
- Yuan, L., Liu, X., Luo, M., Yang, S., & Wu, K. (2013). Involvement of histone modifications in plant abiotic stress responses. *Journal of Integrative Plant Biology*, *55*(10), 892–901. <https://doi.org/10.1111/jipb.12060>
- Yuan, P., Yang, T., & Poovaiah, B. W. (2018). Calcium signaling-mediated plant response to cold stress. *International Journal of Molecular Sciences*, *19*(12), 1–11. <https://doi.org/10.3390/ijms19123896>
- Zarka, D. G., Vogel, J. T., Cook, D., & Thomashow, M. F. (2003). Cold Induction of Arabidopsis CBF Genes Involves Multiple ICE (Inducer of CBF Expression) Promoter Elements and a Cold-Regulatory Circuit That Is Desensitized by Low Temperature. *Plant Physiology*, *133*(2), 910–918. <https://doi.org/10.1104/pp.103.027169>
- Zeng, Z., Zhang, W., Marand, A. P., Zhu, B., Buell, C. R., & Jiang, J. (2019). Cold stress induces enhanced chromatin accessibility and bivalent histone modifications H3K4me3 and H3K27me3 of active genes in potato. *Genome Biology*, *20*(1), 1–17. <https://doi.org/10.1186/s13059-019-1731-2>
- Zhang, H., Bishop, B., Ringenberg, W., Muir, W. M., & Ogas, J. (2012). The CHD3 remodeler PICKLE associates with genes enriched for trimethylation of histone H3 lysine 27. *Plant Physiology*, *159*(1), 418–432. <https://doi.org/10.1104/pp.112.194878>
- Zhang, H., Rider, S. D., Henderson, J. T., Fountain, M., Chuang, K., Kandachar, V., Simons, A., Edenberg, H. J., Romero-Severson, J., Muir, W. M., & Ogas, J. (2008). The CHD3 remodeler PICKLE promotes trimethylation of histone H3 lysine 27. *Journal of Biological Chemistry*, *283*(33), 22637–22648. <https://doi.org/10.1074/jbc.M802129200>

- Zhang, X., Bernatavichute, Y. V., Cokus, S., Pellegrini, M., & Jacobsen, S. E. (2009). Genome-wide analysis of mono-, di- and trimethylation of histone H3 lysine 4 in *Arabidopsis thaliana*. *Genome Biology*, *10*(6), 1–14. <https://doi.org/10.1186/gb-2009-10-6-r62>
- Zhang, X., Clarenz, O., Cokus, S., Bernatavichute, Y. V., Pellegrini, M., Goodrich, J., & Jacobsen, S. E. (2007). Whole-genome analysis of histone H3 lysine 27 trimethylation in *Arabidopsis*. *PLoS Biology*, *5*(5), 1026–1035. <https://doi.org/10.1371/journal.pbio.0050129>
- Zhang, Y. Z., Yuan, J., Zhang, L., Chen, C., Wang, Y., Zhang, G., Peng, L., Xie, S. S., Jiang, J., Zhu, J. K., Du, J., & Duan, C. G. (2020). Coupling of H3K27me3 recognition with transcriptional repression through the BAH-PHD-CPL2 complex in *Arabidopsis*. *Nature Communications*, *11*(1). <https://doi.org/10.1038/s41467-020-20089-0>
- Zhao, C., Wang, P., Si, T., Hsu, C. C., Wang, L., Zayed, O., Yu, Z., Zhu, Y., Dong, J., Tao, W. A., & Zhu, J. K. (2017). MAP Kinase Cascades Regulate the Cold Response by Modulating ICE1 Protein Stability. *Developmental Cell*, *43*(5), 618–629.e5. <https://doi.org/10.1016/j.devcel.2017.09.024>
- Zhao, C., Zhang, Z., Xie, S., Si, T., Li, Y., & Zhu, J. K. (2016). Mutational evidence for the critical role of CBF transcription factors in cold acclimation in *Arabidopsis*. *Plant Physiology*, *171*(4), 2744–2759. <https://doi.org/10.1104/pp.16.00533>
- Zhao, K., Kong, D., Jin, B., Smolke, C. D., & Rhee, S. Y. (2021). A novel form of bivalent chromatin associates with rapid induction of camalexin biosynthesis genes in response to a pathogen signal in *Arabidopsis*. *ELife*, *10*, 1–15. <https://doi.org/10.7554/eLife.69508>
- Zhao, Y., & Garcia, B. A. (2015). Comprehensive catalog of currently documented histone modifications. *Cold Spring Harbor Perspectives in Biology*, *7*(9). <https://doi.org/10.1101/cshperspect.a025064>
- Zhen, Y., Dhakal, P., & Ungerer, M. C. (2011). *Fitness Benefits and Costs of Cold Acclimation in Arabidopsis thaliana*. *178*(1). <https://doi.org/10.1086/660282>
- Zheng, Y., Tipton, J. D., Thomas, P. M., Kelleher, N. L., & Sweet, S. M. M. (2014). Site-specific human histone H3 methylation stability: fast K4me3 turnover. *Proteomics*, *23*, 1–7. <https://doi.org/10.1002/pmic.201400060>. Site-specific
- Zhu, B., Zhang, W., Zhang, T., Liu, B., & Jiang, J. (2015). Genome-wide prediction and validation of intergenic enhancers in *Arabidopsis* using open chromatin signatures. *Plant Cell*, *27*(9), 2415–2426. <https://doi.org/10.1105/tpc.15.00537>
- Zhu, J., Shi, H., Lee, B. H., Damsz, B., Cheng, S., Stirm, V., Zhu, J. K., Hasegawa, P. M., & Bressan, R. A. (2004). An *Arabidopsis* homeodomain transcription factor gene, HOS9, mediates cold tolerance through a CBF-independent pathway. *Proceedings of the National Academy of Sciences of the United States of America*, *101*(26), 9873–9878. <https://doi.org/10.1073/pnas.0403166101>
- Zhu, L. J., Gazin, C., Lawson, N. D., Pagès, H., Lin, S. M., Lapointe, D. S., & Green, M. R. (2010). ChIPpeakAnno: A Bioconductor package to annotate ChIP-seq and ChIP-chip data. *BMC Bioinformatics*, *11*. <https://doi.org/10.1186/1471-2105-11-237>
- Zografos, B. R. (2013). *Mechanisms underlying vernalization-mediated VIN3 induction in Arabidopsis*. University of Texas.
- Zong, W., Zhao, B., Xi, Y., Bordiya, Y., Mun, H., Cerda, N. A., Kim, D. H., & Sung, S. (2021). DEK domain-containing proteins control flowering time in *Arabidopsis*. *New Phytologist*, *231*(1), 182–192. <https://doi.org/10.1111/nph.17366>
- Zrobek-Sokolnik, A. (2012). Temperature Stress and Responses of Plants. In *Environmental Adaptations and Stress Tolerance of Plants in the Era of Climate Change* (pp. 113–134). https://doi.org/10.1007/978-1-4614-0815-4_5
- Zuther, E., Juszczak, I., Ping Lee, Y., Baier, M., & Hinch, D. K. (2015). Time-dependent deacclimation after cold acclimation in *Arabidopsis thaliana* accessions. *Scientific Reports*, *5*, 12199. <https://doi.org/10.1038/srep12199>
- Zuther, E., Schaarschmidt, S., Fischer, A., Erban, A., Pagter, M., Mubeen, U., Giavalisco, P., Kopka, J., Sprenger, H., & Hinch, D. K. (2019). Molecular signatures associated with increased freezing tolerance due to low temperature memory in *Arabidopsis*. *Plant Cell and Environment*, *42*(3), 854–

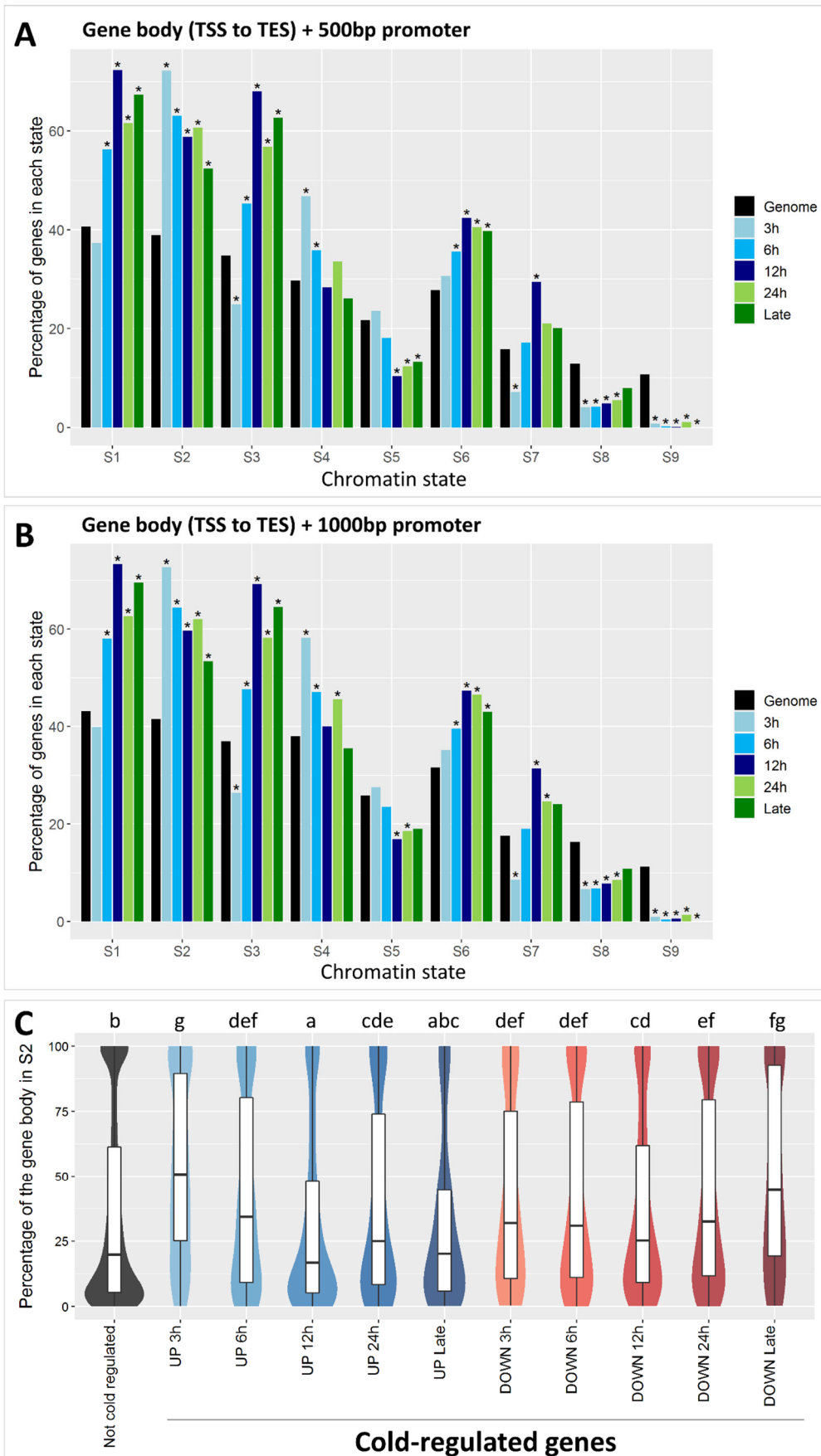
873. <https://doi.org/10.1111/pce.13502>

Divarci, R., *In Silico* and *in Vivo* Analysis of Cold-Regulated Trainable Genes in *Arabidopsis thaliana*, 2018 (BSc thesis submitted at Freie Universität Berlin)

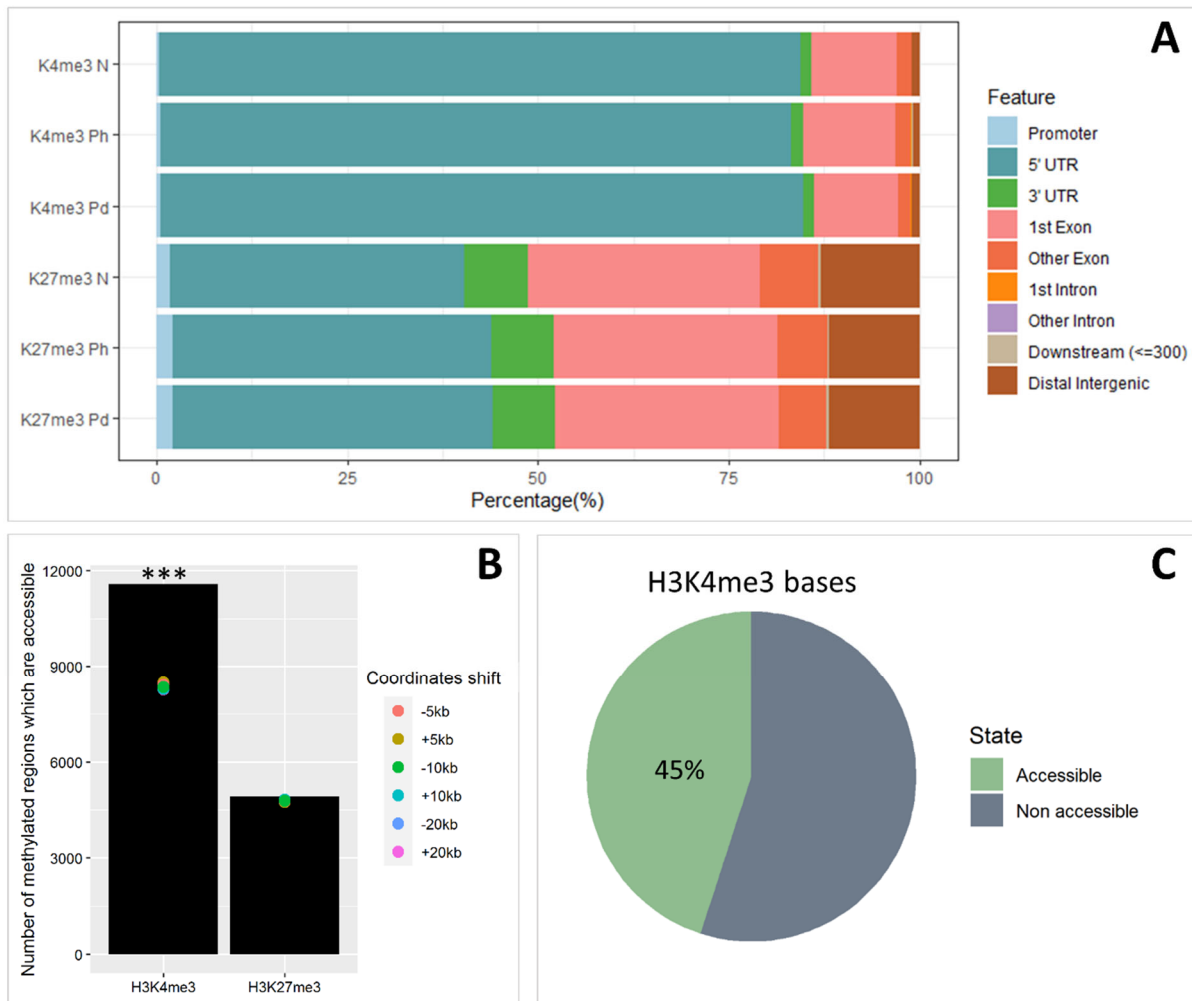
Lakowski, J., Investigation of the role of different epigenetic mutants in cold stress memory in *Arabidopsis thaliana*, 2017 (BSc thesis submitted at Freie Universität Berlin)

NIST/SEMATECH e-Handbook of Statistical Methods, <http://www.itl.nist.gov/div898/handbook/>, Section 7.4.7.4, accessed on June 2019

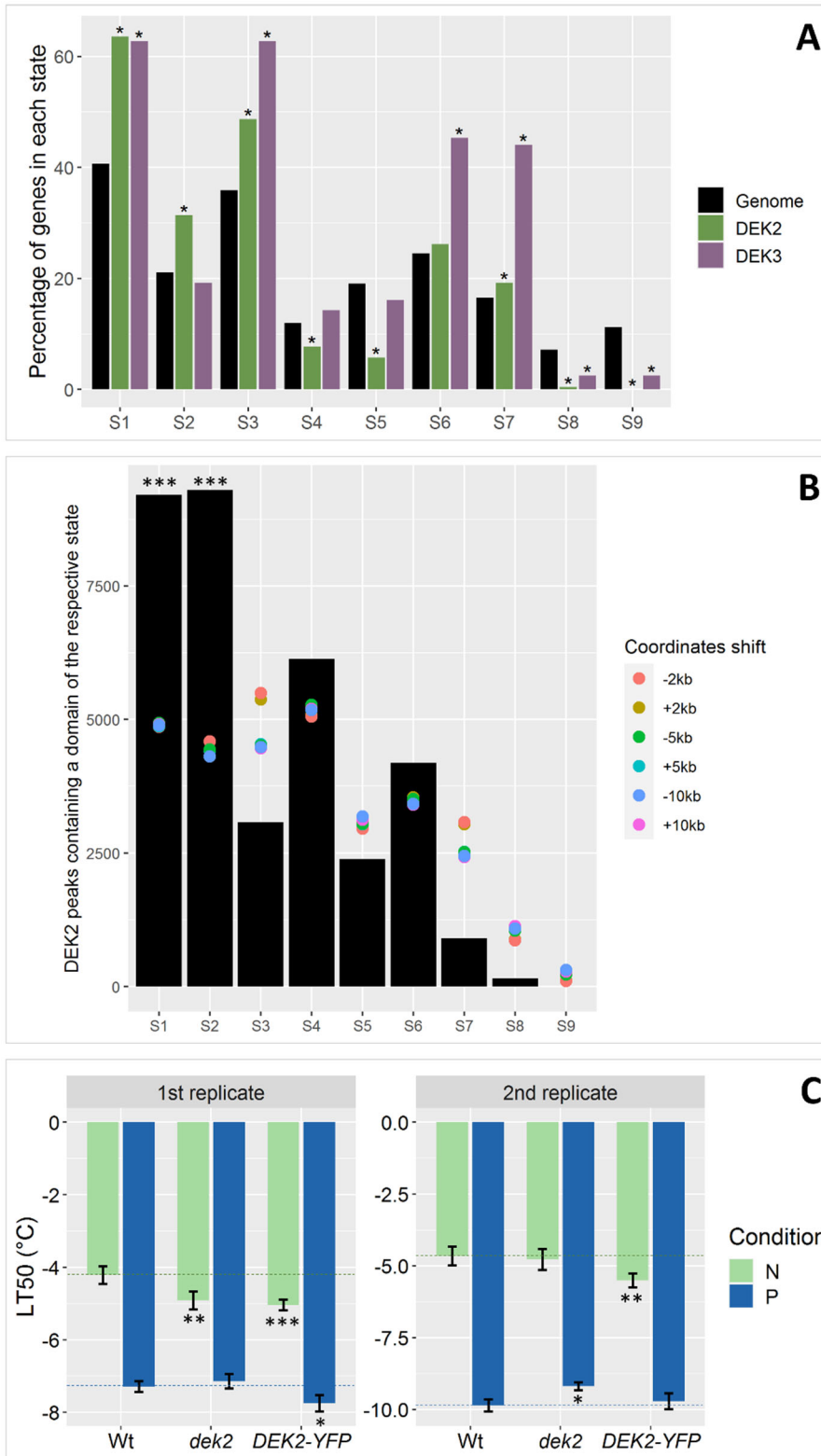
6 APPENDIX



Suppl. Figure 1: Impact of the promoter size on the chromatin state analysis. (A) and (B) Chromatin state analysis of genes induced at different time points during cold exposure, based on the RNA-seq data from Calixto et al. (2018). The chromatin states coordinates were obtained from Sequeira et al. (2014). * indicates significance compared to the genome, tested by Marascuilo procedure ($\alpha=0.05$). **(A)** Analysis performed on the gene body (TSS to TES) and an artificial 500 bp promoter **(B)** Analysis performed the gene body (TSS to TES) and an artificial 1 kb promoter. **(C)** Comparison of the percentage of the gene body in S2 state for S2 genes induced (UP) or repressed (DOWN) at various time points during cold exposure, based on the RNA-seq data from Calixto et al. (2018) and the S2 coordinates from Sequeira et al. (2014). The “Not cold-regulated list” contains S2 genes whose expression is not affected by cold. Significance was tested by Kruskal-Wallis test followed by a Dunn’s test with Benjamini Hochberg procedure ($\alpha=0.05$). Identical letters indicate no significant difference.

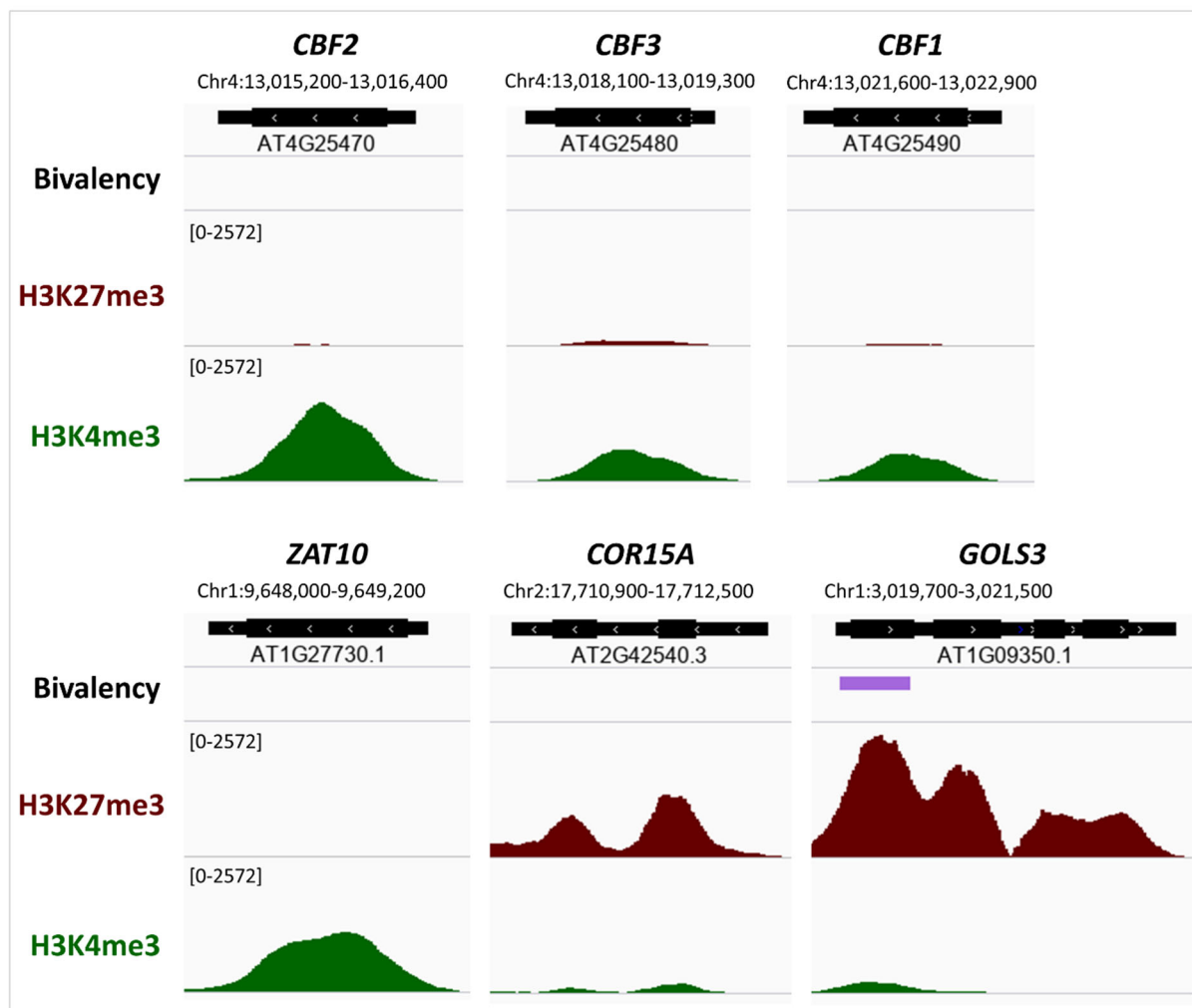


Suppl. Figure 2: Characterization of H3K4me3 and H3K27me3 domains. (A) Genomic feature distribution of the methylated domains in naive plants (N) or plants placed at 4°C for 3 h (Ph) or 3 d (Pd). The reproducible peaks were identified using MACS2 and IDR, and the attribution was performed by ChIPseeker. **(B)** Number of H3K4me3 or H3K27me3 domains overlapping with accessible regions. The accessible regions were obtained from Raxwal et al. (2020). The ± 5 kb, ± 10 kb and ± 20 kb are control sets where the coordinates of the methylated domains were shifted up- (+) or downstream (-) by the indicated number of bases. Significance was tested by permutation test, *** denotes p -value < 0.001 . **(C)** Pie charts showing the percentage of H3K4me3 bases identified as accessible in the data from Raxwal et al. (2020).

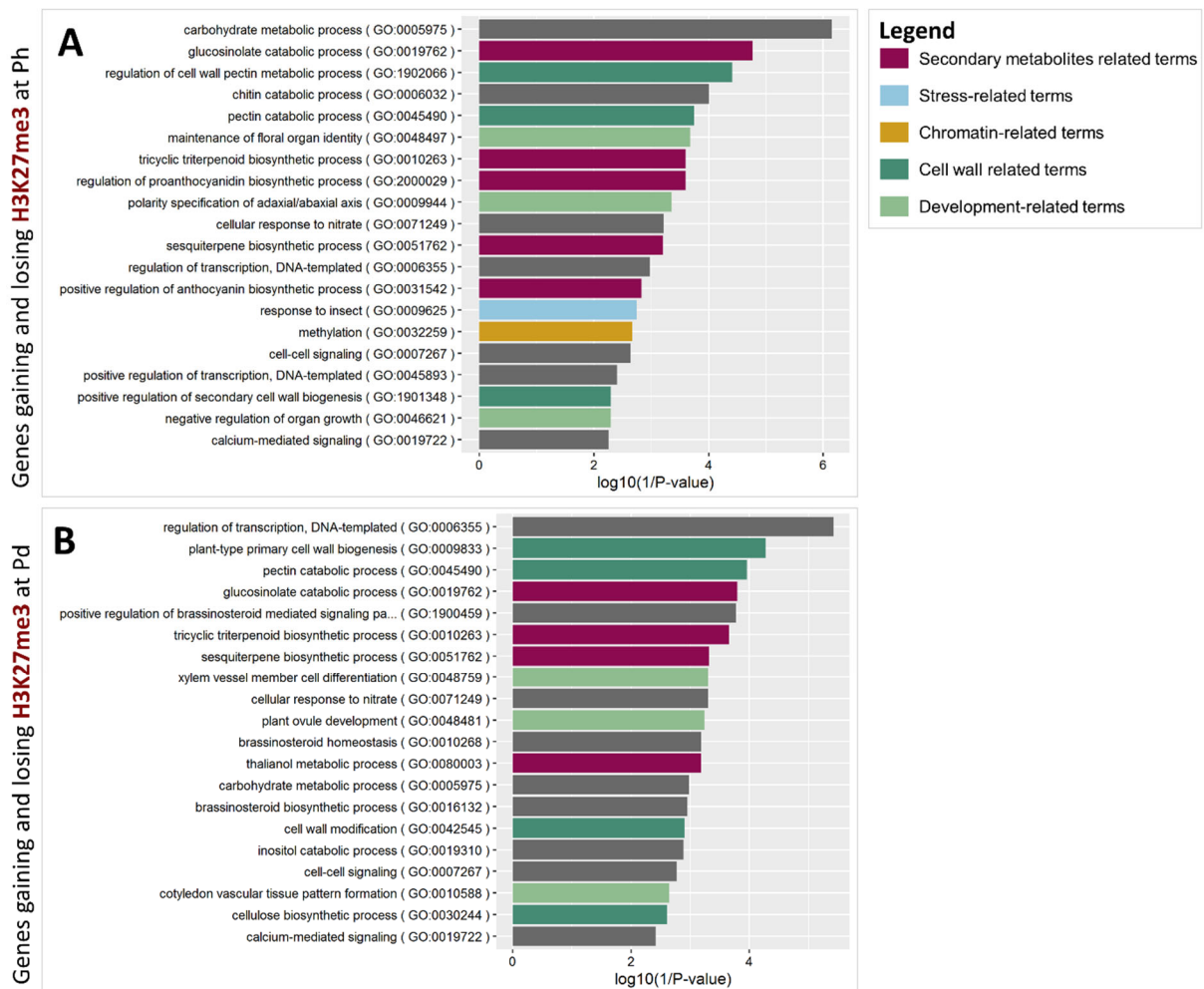


Suppl. Figure 3: Role of the putative bivalency readers DEK2 and DEK3 in the cold response. (A) Chromatin state analysis of the DEK2 and DEK3 target genes. The states coordinates were obtained from Sequeira et al. (2014), the DEK2 target genes were provided by Rayapuram et al. (2020, personal communication) and the DEK3 target genes were obtained from Waidmann et al. (2014). * indicates significance compared to the genome, tested by Marascuilo procedure ($\alpha=0.05$). **(B)** Number of DEK2 peaks containing a domain of each of the indicated states. The coordinates of DEK2 peaks were provided by Rayapuram et al. (2020, personal communication). The ± 2 kb, ± 5 kb and ± 10 kb are control sets where the coordinates of the DEK2 peaks were shifted up- (+) or downstream (-) by the indicated number of bases. Significance was tested by permutation test, *** indicate p -value ≤ 0.001 . **(C)** Freezing

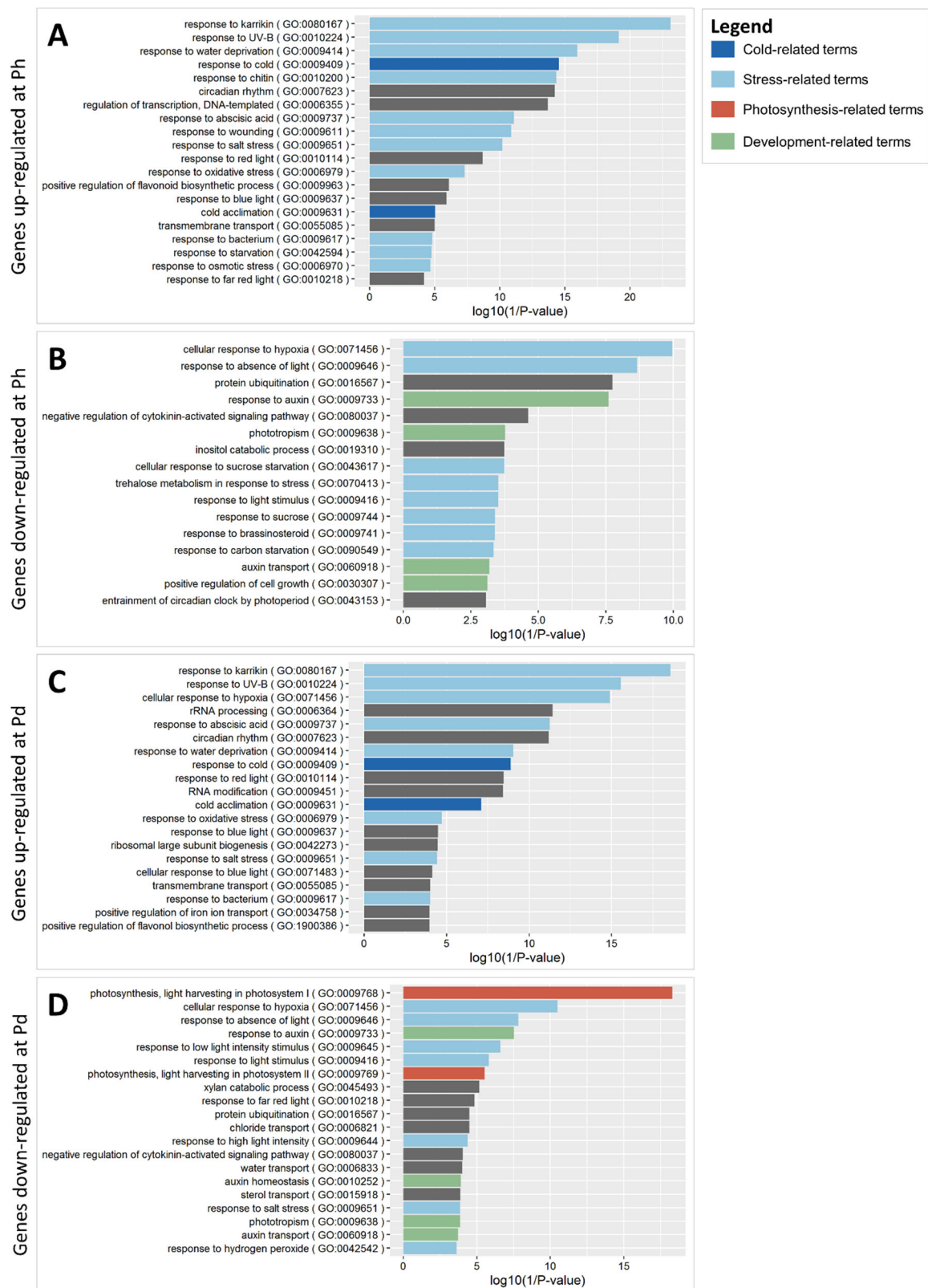
tolerance of *dek2* mutant and its complementation line *DEK2::DEK2-YFP*, before or after cold acclimation, measured by electrolyte leakage assay. Plants were grown for 21 days at 20°C (N) and then exposed to 4°C for three days (P), each replicate is plotted independently. Error bars represent the sem of three technical replicates. Statistical significance was assessed by 2-way ANOVA followed by a Dunnett post hoc test. The stars indicate a significant difference to the *Wt* in the same condition. *, ** and *** indicate respectively a p-value < 0.05, 0.01 and 0.001.



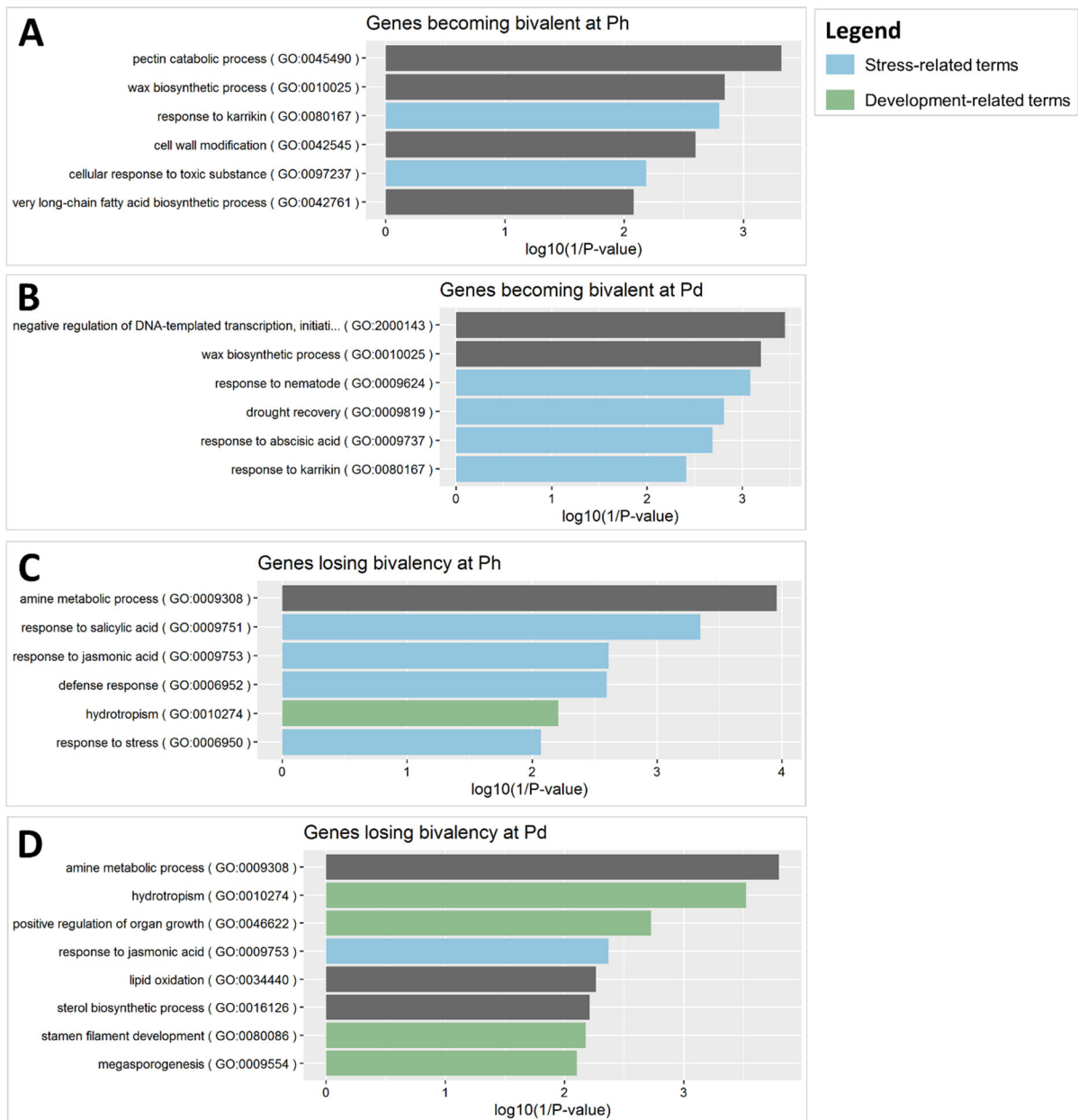
Suppl. Figure 4: H3K4me4 and H3K27me3 levels on selected cold-inducible genes. The ChIP-seq was performed on 21 day-old seedlings grown at 20°C. Bivalent domains represent windows of at least 150 bp where both H3K4me3 and H3K27me3 peaks were detected and are shown with purple bars. The tracks were obtained by merging two biological replicates and the numbers in brackets at the top of each track denote the scale of that track in RPKM.



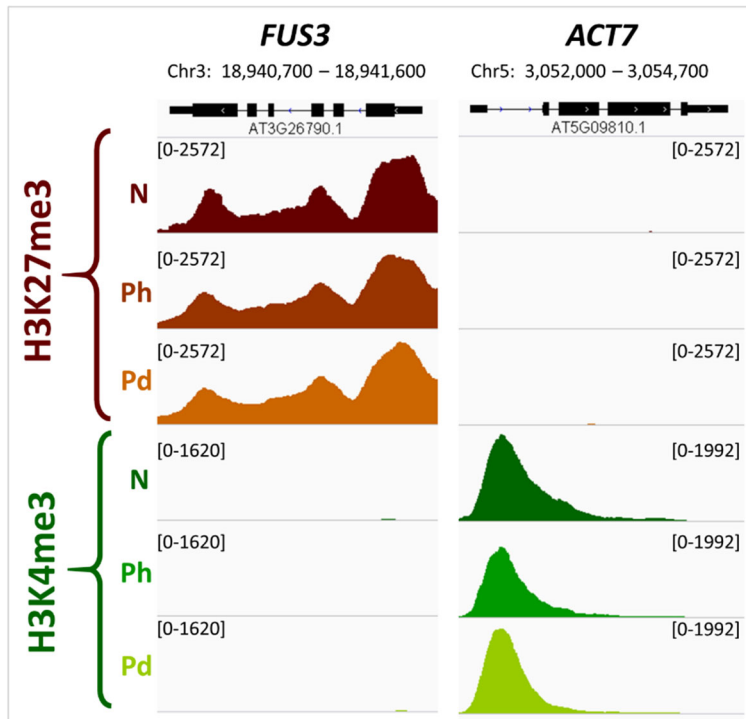
Suppl. Figure 5: GO biological process term enrichment analysis of genes showing both a gain and a loss of H3K27me3 upon cold exposure. (A) Genes gaining and losing H3K27me3 after 3 h at 4°C (B) Genes gaining and losing H3K27me3 after 3 d at 4°C. For both time points, the enrichment analysis was performed by topGO using the weight01 algorithm and significance was tested using Fisher's exact test comparing the list to all TAIR10 annotated genes. The 20 terms with the lowest p-values are displayed.



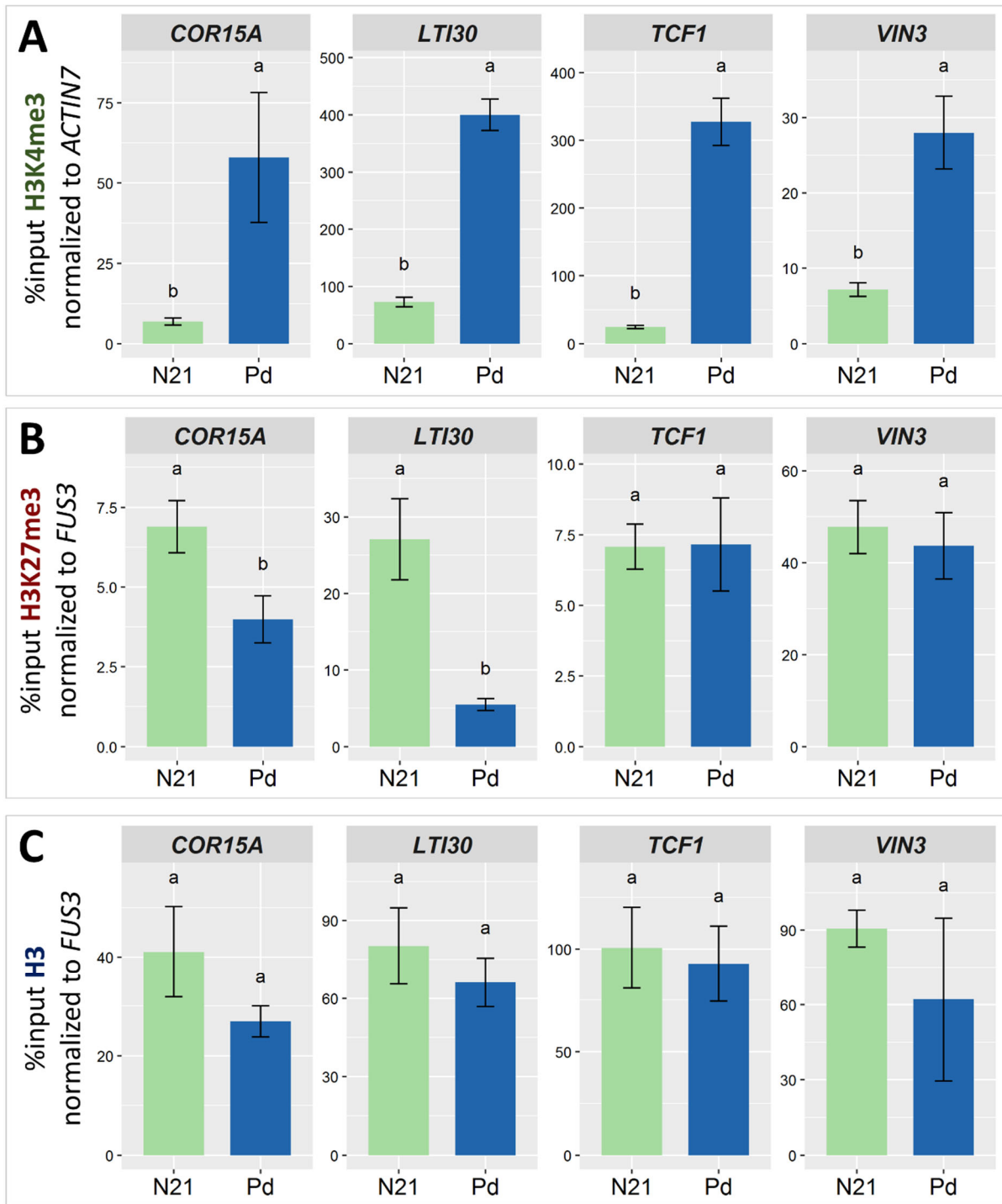
Suppl. Figure 6: GO biological process term enrichment analysis of genes showing differential expression during cold exposure. The enrichment analysis was performed by topGO using the weight01 algorithm and significance was tested using Fisher's exact test comparing the list to all TAIR10 annotated genes. The cold-regulated genes were identified from the RNA-seq experiment described in section 3.1.5. The 20 terms with the lowest p-values are displayed. **(A)** GO enrichment analysis of up-regulated genes after 3 h of cold exposure. **(B)** GO enrichment analysis down-regulated genes after 3 h of cold exposure. **(C)** GO enrichment analysis of up-regulated genes after three days of cold exposure **(D)** GO enrichment analysis of down-regulated genes after three days of cold exposure.



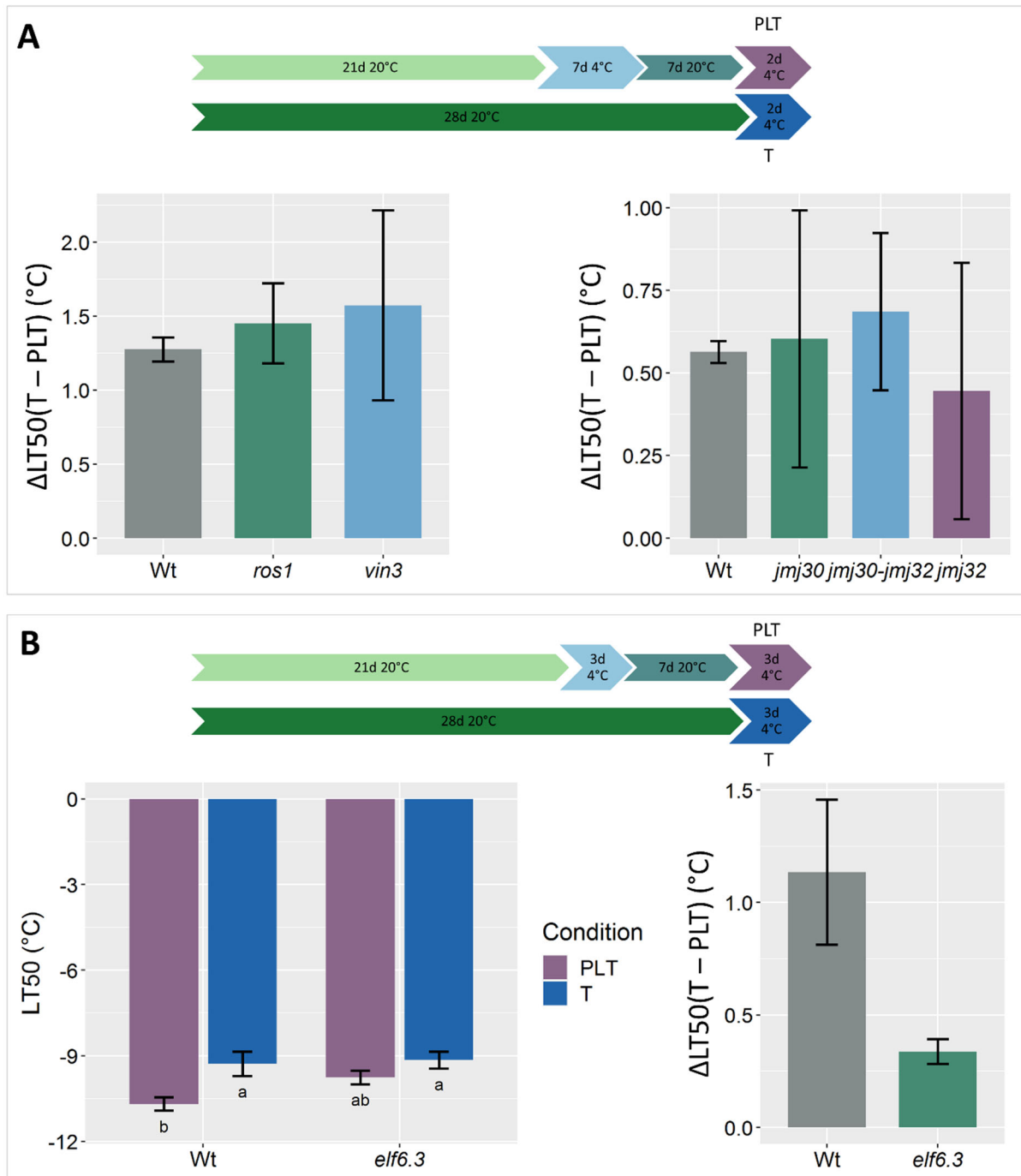
Suppl. Figure 7: GO biological process term enrichment analysis of genes gaining or losing bivalency upon cold exposure. The list of genes gaining or losing bivalency was obtained as explained in section 3.2.1.3. The enrichment analysis was performed by topGO using the weight01 algorithm and significance was tested using Fisher's exact test comparing the list to all TAIR10 annotated genes. The 20 terms with the lowest p-values are displayed. **(A)** GO enrichment analysis of genes gaining bivalency after 3 h of cold exposure. **(B)** GO enrichment analysis of genes gaining bivalency after three days of cold exposure. **(C)** GO enrichment analysis of genes losing bivalency after 3 h of cold exposure. **(D)** GO enrichment analysis of genes losing bivalency after three days of cold exposure.



Suppl. Figure 8: Genome browser views at genes used as controls in the ChIP-qPCR H3K27me3 and H3K4me3 ChIP-seq signals in 21 day-old naive plants (N) and plants exposed to cold for 3 h (Ph) or 3 d (Pd), from two merged biological replicates. The numbers in brackets at the top of each track denote the scale of that track in RPKM. FUS3 is used as a control for H3K27me3 and ACT7 as a control for H3K4me3.

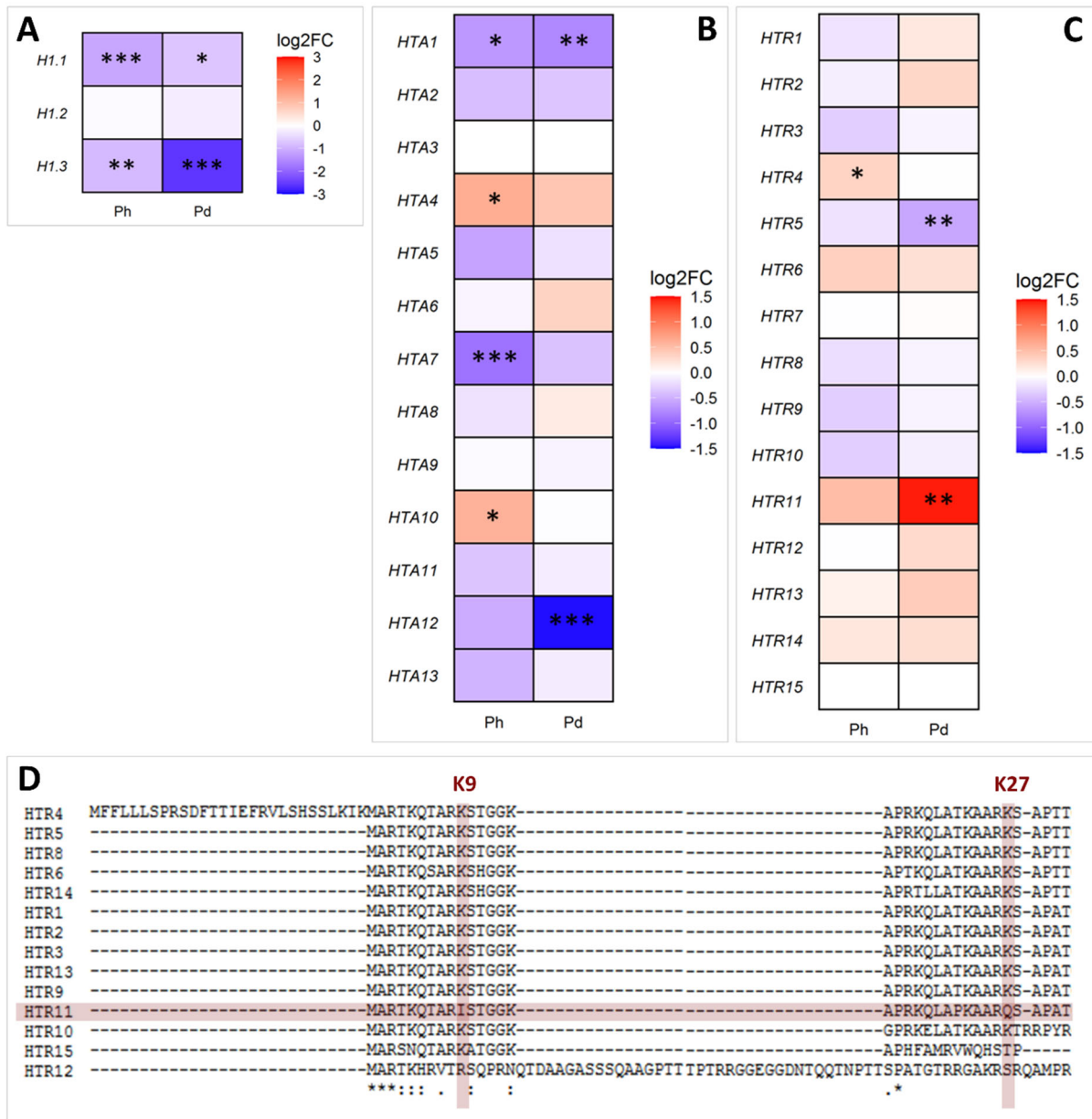


Suppl. Figure 9: Validation of the differential methylation analysis. (A) H3K4me3 levels after cold treatment, as %input normalized to ACTIN7. **(B)** H3K27me3 levels after cold treatment, as %input normalized to FUS3. **(C)** H3 levels after cold treatment, as %input normalized to FUS3. For all panels, plants were grown for 21 d (N21) and exposed to 4°C for three days (Pd). After cross-linking, the chromatin was extracted and immunoprecipitated using anti-H3K4me3, anti-H3K27me3 or anti-H3 antibodies. The purified DNA was amplified by qPCR. Error bars represent the sem of three to five biological replicates. Statistical significance was tested by one-way ANOVA followed by a Tukey post-hoc test ($\alpha = 0.05$). Identical letters indicate no significant difference.



Suppl. Figure 10: Complete results of the priming screening assays. (A) Plants were grown for 21 d at 20°C and then primed for 7 d at 4°C (P). They were then placed back at 20°C for seven days (PL) before being triggered at 4°C for two days (PLT). The control plants were grown 28 d at 20°C (N) and triggered at 4°C for two days (T). The freezing tolerance of the different mutants was assessed in the PLT and T conditions by an electrolyte leakage assay and the benefits of priming on the freezing tolerance is displayed as the difference in LT_{50} between T and PLT. Error bars represent the sem of at least two biological replicates. No significant difference was found when performing a one-way ANOVA followed by a Tukey post-hoc test ($\alpha = 0.05$). The left panel shows the results of the screening on *ros1* and *vin3* mutants while the right panel shows the results of the screening on *jmj30*, *jmj32* and *jmj30-jmj32* double mutants. **(B)** Assessment of the priming abilities of the *elf6.3* mutants in the shorter priming scheme. Plants were grown for 21 d at 20°C and then primed for 3 d at 4°C (P). They were then placed back at 20°C for seven days (PL) before being triggered at 4°C for three days (PLT). The control plants were grown 28 d at 20°C (N) and triggered at 4°C for three days (T). The freezing tolerance was assessed in the PLT and T conditions by an electrolyte leakage assay (left panel) and the benefits of priming on the freezing tolerance are displayed as the difference in LT_{50} between T and PLT (right

panel). Error bars represent the sem of three biological replicates. For the left panel, statistical significance was assessed by two-way ANOVA followed by a Tukey post hoc test ($\alpha = 0.05$). Identical letters indicate no significant difference. For the right panel, statistical significance was assessed by unpaired t-test but no difference was found.



Suppl. Figure 11: Cold-triggered changes in the expression of histone variants. (A), (B) and (C) Expression changes of genes encoding H1 (A), H2 (B) and H3 (C) variants according to the RNA-seq described in 3.1.5. Plants were exposed to cold for either 3 h (Ph) or 3 d (Pd). The color indicates the \log_2 fold change compared to non-cold-treated conditions. Stars show the adjusted p -value given by featureCounts: * p -adj < 0.05, ** p -adj < 0.01, *** p -adj < 0.001. (D) Multiple sequence alignment of the N-terminal part of the amino acid sequences of the H3 variants. As HTR7 is a pseudogene, it is absent from the figure. The alignment was performed with ClustalW. The red background shows the HTR11 variant and the positions where a lysine is substituted by another amino acid in this variant.

Suppl. Table 1: Genotyping primers

Primer name	Purpose	Primer sequence (5'-3')	Source
SALK_LB	Genotyping of SALK T-DNA insertion lines	TTGGGTGATGGTTCACGTAGTGGG	T-DNA Primer2
SAIL_LB	Genotyping of SAIL T-DNA insertion lines	GCCTTTTCAGAAATGGATAAATAGCCTTGCTTCC	T-DNA Primer2
GABI_LB	Genotyping of GABI T-DNA insertion lines	CTGGGAATGGCGAAATCAAGGCATC	T-DNA Primer2
FLAG_LB	Genotyping of FLAG T-DNA insertion lines	CGTGTGCCAGGTGCCCCACGGAATAGT	T-DNA Primer2
Wisc_LB	Genotyping of Wisconsin T-DNA insertion lines	CATTTTATAATAACGCTGCGGACATCTAC	T-DNA Primer2
atx1_2_LP atx1_2_RP	Genotyping of <i>atx1.2</i>	TGCCACATGGATGAGGTAAA CGCGACAAGAATTGTTTGAA	T-DNA Primer2
dek2_LP dek2_RP	Genotyping of <i>dek2</i>	ATTGCATTTATGGCCTCTGTG TTGGTTGGATTACCGTCATTC	T-DNA Primer2
ebs_LP ebs_RP	Genotyping of <i>ebs</i>	TGACATCGTCATCAGAACTGC ATGAAGTTTGTGTTTGGCTGG	T-DNA Primer2
elf6_FOR elf6_REV	Genotyping of <i>elf6</i> mutants	CCCGAATTGGTTTCAGATGT TTTGGTGAGCCAGTGTGAAG	T-DNA Primer2
jmj13_FOR jmj13_REV	Genotyping of <i>jmj13</i>	ATCTCCTTTGACAGCAACAGTTCCTACT ATCTCCTTTGACAGCAACAGTTCCTGCA	Primer3
jmj30_FOR jmj30_REV	Genotyping of <i>jmj30</i> mutants	AGAGATTGGTCCCGGAAGTT ACGATTTATTGGTCCGCATC	T-DNA Primer2
jmj32_FOR jmj32_REV	Genotyping of <i>jmj32</i> mutants	CCGTCACCGGAGATAGTGAT AACATGGTGAAACCACATGC	T-DNA Primer2
ref6c_FOR ref6c_REV	Genotyping of <i>ref6c</i>	GGTTGCTCCAGAGTTCAGACC CATGGTCTCCACATGCCAAGC	Yan et al., 2018
ros1_LB ros1_RB	Genotyping of <i>ros1</i>	CCAGTTAAGGACAGAACACCG TCGTCTTTTCGATCAAATCCAC	T-DNA Primer2
shl_LB shl_RB	Genotyping of <i>shl</i>	AGCTTACAATTGTTGGCAAGG GCGTTTGATCCTGACAGAGTC	T-DNA Primer2
vin3_LB vin3_RB	Genotyping of <i>vin3</i>	TCATGGGTTTCTTTGGTTG TTCCAAATGACAAGACGATCC	T-DNA Primer2

Suppl. Table 2: RT-qPCR primers

Gene		Primer sequence (5'-3')	Source
TIP41	Forward	GTGAAAACCTGTTGGAGAGAAGCAA	Primer3
	Reverse	TCAACTGGATACCCTTTTCGCA	
CBF1	Forward	GTCAACATGCGCCAAGGATA	Primer3
	Reverse	TCGGCATCCCAAACATTGTC	
CBF3	Forward	CCGAGTTTGTGGCTAATATGG	Primer3
	Reverse	GATACGTCGTCATCATCGCC	
COR15A	Forward	AGCTGTTCTCACTGGTATGG	Primer3
	Reverse	GAAGCTTTCTTTGTGGCCTC	
GOLS3	Forward	ACAGGCCAAGAAGGAAATATGG	Nishizawa et al., 2008

	Reverse	GATGGAGCTTTGGCACATTG	
LT130	Forward	TCCCGGTGGTCATCACTAGA	Primer3
	Reverse	AGCGACTCAATGAAAGAAAGCC	
TCF1	Forward	TTATGGACAGTGTGGCCAAGG	Primer 3
	Reverse	GGTCGTGTGCCATAGACCTG	
VIN3	Forward	AGAAGCTGTGTTCTCAGGCAATGG	Primer3
	Reverse	TCTTCGTCCTTCGACTTTTCGACAAA	
ZAT10	Forward	TCACAAGGCAAGCCACCGTAAG	Van Buer et al., 2016
	Reverse	TTGTCCGCGACGAGGTTGAATG	

Suppl. Table 3: ChIP and ReChIP-qPCR primers

Gene	Purpose	Primer sequence (5'-3')		Source
ACTIN7	H3K4me3	Forward	TAGTGAAAAATGGCCGATGG	Primer3
		Reverse	CCATTCCAGTTCATTGTCA	
FUS3	H3K27me3	Forward	GTGGCAAGTGTTGATCATGG	Kwon et al., 2009
		Reverse	AGTTGGCACGTGGGAAATAG	
COR15A	H3K4me3 & H3K27me3	Forward	CCGAGTTTCTGTTCGTTCTTT	Ding et al., 2012
		Reverse	CAATTCATGGCCGACCT	
LT130	H3K4me3 & H3K27me3	Forward	CTGGTACCGGTGGTGTTC	Primer3
		Reverse	ACCAGTGTTAGTAGTACCATAAGTT	
TCF1	H3K4me3 & H3K27me3	Forward	ACAGCTTGGATTGGGCTCTC	Primer3
		Reverse	GCCGCATTGCACTACTGAAC	
VIN3	H3K4me3 & H3K27me3	Forward	TTGAATGTAAGTGAAAGGAGAGAATTGATCC	Zografos, 2013
		Reverse	ATGAGCTTTGTTTTGTTAAGACCAGTG	
PERK10	ReChIP - control	Forward	TGCTCGTCCATTTCTATC	Sequeira et al., 2014
		Reverse	GGCATAGTGATTTGCCACA	
KAN2	ReChIP + control	Forward	TCTTCTCTGCCATGTCGATG	Sequeira et al., 2014
		Reverse	CATCTGTGAAACCGACTGA	
P1R1	ReChIP + control	Forward	CAACGGTTCTTCATCCGATT	Sequeira et al., 2014
		Reverse	CTGCTCGAAATGGCTCTACC	
EIF4A-III	ReChIP - control	Forward	TCGCGGTGTCTAGAATATGG	Primer3
		Reverse	AAGATCGGCATAACAGCCCT	
TIP41	ReChIP - control	Forward	GGAGGGTTTCGATCTCCCAG	Primer3
		Reverse	GCGATTCAGATGGAGACGGT	
ULT1	ReChIP Candidate	Forward	TGGCTAGTGGCAGGAAAAG	Primer3
		Reverse	GACCGAGTAGCTGTGCCATT	
WRKY48	ReChIP Candidate	Forward	AGCTAGGTTTTCGTTTCTGAC	Primer3
		Reverse	TGGCCGTATTTTCTCCACCTA	

Suppl. Table 4: Softwares

Software	Version	Purpose
Bowtie2	2.3.5.1	Mapping ChIP-seq reads
Cufflinks	2.2.1	RNA-seq workflow
DeepTools	3.3.1	Exploring sequencing data
diffReps	1.55.6	Differential methylation analysis
GraphPad Prism	7.0	Statistical analysis and figure generation
ImageJ	1.52i	Image treatment and analysis

Image Studio Lite	5.2	Western Blot images treatment and analysis
FastQC	0.11.7	Quality control of reads
Kallisto	0.46.2	Read count on transcripts
MACS2	2.2.5	Peak calling
MultiQC	1.9	Aggregating quality control reports
Qualimap	2.2.1	Assessing the quality of an alignment
R	4.0.3 & 3.6.2	Statistical analysis and figure generation
RStudio	1.2.5033	Statistical analysis and figure generation
Samtools	1.9	Manipulating alignment files
STAR	2.7.1	Mapping RNA-seq reads
Subread	2.0.1	Read aligner and counter

Suppl. Table 5: R packages

Package	Version
agricolae	1.3-5
Bioconductor	3.12
ChIPpeakAnno	3.26.0
ChIPseeker	1.28.3
DESeq2	1.32.0
dplyr	1.0.7
edgeR	3.34.0
GenomicFeatures	1.44.0
GenomicRanges	1.44.0
ggplot2	3.3.5
ggvenn	0.1.9
Org.At.tair.db	3.13.0
pheatmap	1.0.12
tidyverse	1.3.1
topGO	2.44.0
TxDb.Athaliana.BioMart.plantsmart28	3.2.2

Suppl. Table 6: Sources of reference data

Data type	Format	Source	Date of Download
TAIR10 full genomic sequence (toplevel)	fasta	ftp.ensemblgenomes.org	March 16th, 2021
TAIR10 transcript sequences (cdna.all)	fasta	ftp.ensemblgenomes.org	March 18th, 2021
TAIR10 annotation	gff3	www.arabidopsis.org	March 16th, 2021
TAIR10 Bowtie2 index	bt2	bowtie-bio.sourceforge.net/	January 15 th , 2021
Araport11 annotation	gff3	www.arabidopsis.org	March 30th, 2020
ChromDB		www.chromdb.org	July 30th, 2011

LIST OF PUBLICATIONS

Part of this work was published in the following article:

Vyse, K., **Faivre, L.**, Romich, M., Pagter, M., Schubert, D., Hinch, D. K., & Zuther, E. (2020). Transcriptional and post-transcriptional regulation and transcriptional memory of chromatin regulators in response to low temperature. *Frontiers in plant science*, *11*, 39.

Other article contributions:

Müller-Xing, R., Ardiansyah, R., Xing, Q., **Faivre, L.**, Tian, J., Wang, G., . & Goodrich, J. (2022). Polycomb Proteins Control Floral Determinacy by H3K27me3-mediated Repression of Pluripotency Genes in *Arabidopsis thaliana*. *Journal of experimental botany*.

Friedrich, T., **Faivre, L.**, Bäurle, I., & Schubert, D. (2019). Chromatin-based mechanisms of temperature memory in plants. *Plant, Cell & Environment*, *42*(3), 762-770.

ACKNOWLEDGEMENTS

First and foremost, I would like to thank Prof. Dr. Daniel Schubert for giving me the opportunity to work on this project, providing me not only with support and guidance for the last five years but also the trust and freedom to experiment by myself and to transform the initial idea into the work presented here. Thank you also for the many opportunities you gave me along the way, as well as fostering a lab with a wonderful atmosphere.

I would like to express my gratitude to Prof. Dr. Reinhart Kunze for also mentoring me and reviewing this work, as well as providing me with insightful ideas every time we met.

I am very grateful to the DFG and the CRC973 for the financial support given to this project. Being part of the CRC973 and the IRTG was a tremendous help to the completion of this work.

I also want to thank all the collaborators that contributed to this project: Prof. Dr. Kerstin Kaufmann and Dr. Jose Muinos for their invaluable expertise on ChIP-seq, Prof. Dr. Dirk Hinch, Dr. Ellen Zuther and Kora Vyse for their support on the cold memory experiments and finally Prof. Dr. Heribert Hirt and Dr. Naganand Rayapuram for including me in this exciting project that is DEK2.

To all current and past members of the best lab I could ever wish for: a massive thanks. I might not have finished this thesis if not for the constant support you provided me. To Melissa for your infinite trust in my abilities since day one. I am so glad to have been working at your side, sharing all the laughter and ugly cry of despair. To Kalyani, for all the illuminating discussions and relevant feedback you offered me. To Claire, your motivation helped me push through more times than you know. To Teresa, for being an example of determination and always knowing just what to say when I was down. Thank you to Ruth for the help with some experiments as well as the many advice and general lab support. To Ines, for answering all kind of stupid questions. We did not work together for long but you gave me very valuable lessons and tips that I will always remember. Many thanks also to Marina, Silke, Biswajit, Elise, Heni and Michael for all the support.

An extra special thanks to Claire, Melissa, Teresa and Elise for proofreading this work and ensuring that all those sentences actually made some kind of sense.

I would like to thank all the students I had the pleasure of supervising during my PhD: Josephin, Reyhan, Amos and Elodie. Your contributions to this project were precious and supervising you helped me become a better scientist. I wish you the best for your future career.

A massive thank you to Marlene, Constanze, Tino and Maren, the student helpers without whom I would have drown under genotyping PCRs. I would also like to extend a thank you to our gardeners Bernd and Helga for preparing hundreds of trays, as well as Nevin for all the invisible but invaluable work.

To all the DCPS PhD students, past and current: Raffaella, Bernadette, Kathi, Venja, Ishita, Manuel, Andras, Andreas, Aneth and Florencia: thank you for the support and understanding, for the suggestions and the advice. It was always a pleasure to meet and commiserate with you.

To the whole virtual coffee machine: without your support I would have probably quit a long time ago, or might not even have started a PhD in the first place. You are all such smart, funny, inspiring and wonderful women, the world probably does not deserve you. I'm so glad I found you and I can only hope that I provided you with even a tenth of the support and kindness you gave me in the past years. I wish you all the success and happiness you truly deserve.

To Gaelle and Clémence, for patiently listening to my never-ending complaints and for making me laugh daily, even from 800km away. You're the best.

To Lorenz, for believing in me more than myself, for patiently listening to the process of this work in all painstaking details and for all the rest. This thesis would not exist without you.

To Tino, for dragging me out of the lab, for the laughter, the music, the food and the sea. Thank you for reminding me that the most important and beautiful things in life are outside of the lab.

Enfin, un énorme merci à mes parents pour le support qu'ils m'ont apporté depuis le début de mes études, financier mais surtout émotionnel. Je ne serais jamais arrivée jusque là sans vous et votre infinie confiance en moi. Cette thèse vous est dédiée.